

**DEVELOPMENT AND VERIFICATION OF A SIMPLIFIED
BUILDING ENERGY MODEL**

A Thesis
Presented to
The Academic Faculty

By

Rachel Elizabeth Valade

In Partial Fulfillment
Of the Requirements for the Degree
Master of Science in the
School of Mechanical Engineering

Georgia Institute of Technology
May 2009

**DEVELOPMENT AND VERIFICATION OF A SIMPLIFIED
BUILDING ENERGY MODEL**

Approved by:

Dr. Sheldon Jeter, Advisor
School of Mechanical Engineering
Georgia Institute of Technology

Dr. Srinivas Garimella
School of Mechanical Engineering
Georgia Institute of Technology

Dr. Ruchi Choudhary
College of Architecture
Georgia Institute of Technology

Date Approved: December 8th, 2008

ACKNOWLEDGEMENTS

I would like to thank my faculty advisor, Dr. Sheldon M. Jeter, for his continued support, time, encouragement, guidance, references, and invaluable suggestions. Special thanks are also extended to my committee members, Drs. Srinivas Garimella and Ruchi Choudhary.

I would also like to thank the Georgia Tech Facilities Department, in particular Don Alexander, Brian Clarke, Steve Sywak, Scott Hitt, Onkar Auzla, and Ronnie Croy, for all of their help with Klaus related documentation and monitoring questions.

Finally, I am deeply and forever indebted to my family and friends for their constant love, support, and encouragement throughout my entire life.

TABLE OF CONTENTS

	Page
ACKNOWLEDGEMENTS	iii
LIST OF TABLES	vii
LIST OF FIGURES	x
LIST OF SYMBOLS	xiv
LIST OF GREEK SYMBOLS	xx
LIST OF ABBREVIATIONS	xxii
SUMMARY	xxv
1 INTRODUCTION	1
1.1 Background	2
1.1.1 Leadership in Energy and Environmental Design	3
1.1.2 ASHRAE Standard 90.1	4
1.1.3 Building Simulation	4
1.1.4 TMY Data	5
1.2 Scope	6
1.3 Thesis Organization	7
2 LITERATURE REVIEW	8
3 OVERVIEW OF THE EXAMPLE BUILDING	23
3.1 General Quantitative Data	23
3.2 Layout	24
3.3 Building Description	25
3.4 Occupancy	29
3.5 Original Detailed Building Model	29
3.5.1 Energy Saving Features	34
3.5.1.1 Roof Insulation	35
3.5.1.2 Exterior Wall Construction and Insulation	36
3.5.1.3 Window Glazing	37
3.5.1.4 Use of Shading Devices	38
3.5.1.5 Energy Efficient Lighting	39
3.5.1.6 Occupancy Sensor Lighting Controls	39
3.5.1.7 Use of Daylighting	40
3.5.1.8 Air Distribution System Type	40
3.5.1.9 Utilizing an Airside Economizer	40

3.5.1.10	Utilizing Heat Recovery	41
3.5.1.11	Chilled Water Temperature Difference	42
3.5.1.12	Hot Water Pump Control	42
4	MONITORING AN EXAMPLE BUILDING	44
4.1	Monitoring Principles	46
4.1.1	Raw Data Collection	46
4.1.1.1	Metasys Data	46
4.1.1.2	National Oceanic and Atmospheric Administration Data	49
4.1.1.3	The University of Georgia Data	50
4.1.2	Processing the Raw Data	50
4.1.3	Weather Data Comparisons	52
4.2	Clear Sky Model	57
4.3	Uncertainty Analysis	62
5	ANALYSIS AND MODELING OF EXAMPLE BUILDING	67
5.1	Load Calculations from Monitored Information	68
5.1.1	Heating Loads	68
5.1.2	Cooling Loads	71
5.1.3	Outside Air Loads	73
5.1.3.1	Air Handling Unit / Energy Recovery Unit Control Logic	78
5.1.3.2	Fan Curves Used to Determine Air Flow	80
5.1.3.3	Carbon Dioxide Concentrations Used to Determine Air Flow	87
5.1.4	Skin Loads	90
5.1.4.1	Solar Calculations	90
5.1.4.2	First Order Conduction Skin Loads	102
5.1.4.3	Transfer Function Conduction Skin Loads	108
5.1.4.4	Direct Solar Heat Gain Skin Loads	111
5.1.5	Internal Loads	112
5.1.5.1	Occupancy Loads	112
5.1.5.2	Electrical Loads	116
5.2	Models	117
5.2.1	Monitored Data	118
5.2.2	Combined Single-Zone Simplified Model	119
5.2.3	New eQUEST Model	125
5.2.3.1	Original DOE-2 Model	126
5.2.3.2	TMY Weather Data	127
6	MODEL COMPARISONS	129
6.1	Monitored Data vs. DOE-2 Predicted Model	139
6.2	eQUEST Model vs. DOE-2 Predicted Model	144
6.3	Monitored Data vs. eQUEST Model	150
6.4	Single-Zone Model Results and Discussion	155
6.4.1	Overall Temperature Change of the Building	156
6.4.2	Overall Performance of the Building	156
6.4.3	Predicted Heating vs. Cooling Load	157

6.4.4 Thermal Mass of the Building	164
7 CONCLUSIONS	166
8 RECOMMENDATIONS FOR FUTURE WORK	171
APPENDIX A: Heating Loads Code	174
APPENDIX B: Cooling Loads Code	176
APPENDIX C: Outside Air Loads Code	178
APPENDIX D: Outside Air Load Flow Calculations	183
APPENDIX E: Clear Sky Model Code	187
APPENDIX F: Combined Skin Load Code	190
APPENDIX G: Transfer Function Conduction Skin Loads Code	202
APPENDIX H: Electrical Loads Code	212
APPENDIX I: Metasys Sensor Identification Numbers	214
APPENDIX J: UGA Weather Data	216
APPENDIX K: Creating a Mock-TMY Data File	218
APPENDIX L: Directions for Metasys Data Collection	224
APPENDIX M: Directions for NOAA Data Collection	230
REFERENCES	236

LIST OF TABLES

	Page
Table 3.1: Proposed vs. Baseline Model Building Savings	32
Table 3.2: Actual vs. Proposed Building Savings	33
Table 3.3: Actual vs. Baseline Model Building Savings	33
Table 3.4: Roof Construction	35
Table 3.5: Glazed Aluminum Curtain Wall Construction	36
Table 3.6: Brick Wall Construction	37
Table 4.1: Data Samples Collected from KACB, Part 1	47
Table 4.2: Data Samples Collected from KACB, Part 2	48
Table 4.3: Extraterrestrial Solar Irradiation Constants (ASHRAE, 2001)	58
Table 4.4: Heating Load Error Propagation Analysis	63
Table 4.5: Cooling Load Error Propagation Analysis	64
Table 4.6: Outside Air Load Error Propagation Analysis	65
Table 5.1: Pressure Relationship Profile Components of Supply Fan	85
Table 5.2: Constants Used to Determine Supply Fan Static Pressure	86
Table 5.3: Surface Azimuth Angles	94
Table 5.4: $\beta_{CB}(i)$ Regression Coefficients	98
Table 5.5: $XO(i)$ Constants	98
Table 5.6: Brick Wall Construction	105
Table 5.7: Curtain Wall Construction	106
Table 5.8: Roof Construction	108
Table 5.9: Transfer Function Influence Coefficients for the Roof Construction	109

Table 5.10: Transfer Function Influence Coefficients for the Brick Wall Construction	109
Table 5.11: Transfer Function Influence Coefficients for the Glazed Aluminum Curtain Wall Construction	109
Table 5.12: Representative Rates at Which Heat and Moisture Are Given Off by Human Beings (ASHRAE, 2001)	113
Table 6.1: Model Names and Descriptions	129
Table 6.2: DOE-2 Predicted Model Loads Summary	130
Table 6.3: DOE-2 Baseline Model Loads Summary	131
Table 6.4: Percent Savings Overview of DOE-2 Predicted Model Compared to DOE-2 Baseline Model	131
Table 6.5: Monitored Loads Summary	132
Table 6.6: eQUEST Model Loads Summary	133
Table 6.7: Monitored Load Percent Savings to the Compared Simulation Models	133
Table 6.8: Percent Savings of Monitored Loads Compared to the DOE-2 Predicted Model	140
Table 6.9: Percent Savings Overview of the Monitored Loads Compared to DOE-2 Predicted Model	140
Table 6.10: Percent Savings of eQUEST Model Compared to the DOE-2 Predicted Model	145
Table 6.11: Percent Savings Overview of eQUEST Model Compared to DOE-2 Predicted Model	146
Table 6.12: Percent Savings of the Monitored Loads Compared to the eQUEST Model	151

Table 6.13: Percent Savings Overview of Monitored Loads Compared to eQUEST Model	151
Table 6.14: Single-Zone Model vs. Monitored Heating Load Comparison	157
Table 6.15: Single-Zone Model vs. Monitored Cooling Load Comparison	159
Table 6.16: Single-Zone Model vs. Monitored HVAC Load Comparison	161
Table 6.17: Single-Zone Model vs. Monitored Absolute HVAC Load Comparison	163

LIST OF FIGURES

	Page
Figure 3.1: The Klaus Building as Seen from Google Earth (Google, 2008)	24
Figure 3.2: Overall Layout of the Klaus Advanced Computing Building	25
Figure 3.3: Sample Air Handling Unit and Energy Recovery Unit Schematic	27
Figure 3.4: Chilled Water Cooling System Schematic	28
Figure 3.5: Steam Heating System Schematic	28
Figure 3.6: Climate Zones for the United States (ASHRAE, 2007)	34
Figure 3.7: Sample Air Handling Unit Working with the Energy Recovery Unit	41
Figure 4.1: Typical Energy Flows in a Control Volume Building	45
Figure 4.2: Outside Air Weather Station on the Roof of the Klaus Building	53
Figure 4.3: Location of Outside Air Weather Station on the Roof of the Klaus Building	53
Figure 4.4: Outside Air Weather Station Location on the Roof of the Klaus Building as Seen from Google Earth (Google, 2008).	53
Figure 4.5: Outside Air Temperature Comparisons for August 2007	55
Figure 4.6: Outside Air Relative Humidity Comparisons for August 2007	55
Figure 4.7: Humidity Ratio Comparisons for August 2007	57
Figure 4.8: Solar Radiation Comparison, January 1 st -7 th , 2007	60
Figure 4.9: Solar Radiation Comparison, April 1 st -7 th , 2007	60
Figure 4.10: Solar Radiation Comparison, July 1 st -7 th , 2007	61
Figure 4.11: Solar Radiation Comparison, October 1 st -7 th , 2007	61
Figure 5.1: Heating Load Energy Flow Diagram	69

Figure 5.2: Cooling Load Energy Flow Diagram	71
Figure 5.3: Air Handling Units 1, 2 and 4 Energy Flow Diagram	74
Figure 5.4: Air Handling Unit 3 Energy Flow Diagram	75
Figure 5.5: Air Handler Unit Flow Rate Diagram	75
Figure 5.6: Air Handler Unit Flow Rate Diagram	79
Figure 5.7: Fan Curve for Supply Fan 1	82
Figure 5.8: Fan Curve for Supply Fan 2	83
Figure 5.9: Fan Curve for Supply Fan 4	83
Figure 5.10: Pressure Relationship Profile of Supply Fan	85
Figure 5.11: Air Handler Unit Flow Rate Diagram	87
Figure 5.12: Outside Air Flow Rate Comparison	89
Figure 5.13: Solar Azimuth Angle and Solar Altitude Angle for January 1 st , 2008	93
Figure 5.14: Directional $\cos(\theta_B)$ on January 1 st , 2008	95
Figure 5.15: Transmittance vs. Incident Angle	96
Figure 5.16: Scatter Plot and Piecewise Regression of Clearness Index vs. Beam Transmittance Values (Balaras, 1988)	99
Figure 5.17: Clearness Index for January 1 st , 2008	100
Figure 5.18: Directional Solar Radiation for January 1 st , 2008	102
Figure 5.19: Brick Wall Thermal Resistance Network	105
Figure 5.20: Curtain Wall Thermal Resistance Network	106
Figure 5.21: Roof Thermal Resistance Network	107
Figure 5.22: Conduction Skin Load Comparison	110
Figure 5.23: Occupancy Comparison for March 3 rd , 2008	115

Figure 5.24: Occupancy Comparison for May 17 th , 2008	115
Figure 5.25: Regular Directional Octagon Schematic	122
Figure 5.26: Directional Octagon Schematic for the Klaus Building	122
Figure 6.1: Total Monthly Loads	134
Figure 6.2: Total Monthly Loads (without DOE-2 Baseline Model)	135
Figure 6.3: Monthly Electrical Load	136
Figure 6.4: Monthly Electrical Load (without DOE-2 Baseline Model)	136
Figure 6.5: Monthly Cooling Load	137
Figure 6.6: Monthly Cooling Load (without DOE-2 Baseline Model)	137
Figure 6.7: Monthly Heating Load	138
Figure 6.8: Monthly Heating Load (without DOE-2 Baseline Model)	138
Figure 6.9: DOE-2 Predicted Model vs. Monitored Total Load Comparison	141
Figure 6.10: DOE-2 Predicted Model vs. Monitored Electrical Load Comparison	142
Figure 6.11: DOE-2 Predicted Model vs. Monitored Cooling Load Comparison	143
Figure 6.12: DOE-2 Predicted Model vs. Monitored Heating Load Comparison	144
Figure 6.13: DOE-2 Predicted Model vs. eQUEST Model Total Load Comparison	147
Figure 6.14: DOE-2 Predicted Models vs. eQUEST Model Electrical Load Comparison	148
Figure 6.15: DOE-2 Predicted Model vs. eQUEST Model Cooling Load Comparison	149
Figure 6.16: DOE-2 Predicted Model vs. eQUEST Model Heating Load Comparison	150
Figure 6.17: eQUEST Model vs. Monitored Total Load Comparison	152
Figure 6.18: eQUEST Model vs. Monitored Electrical Load Comparison	153
Figure 6.19: eQUEST Model vs. Monitored Cooling Load Comparison	154

Figure 6.20: eQUEST Model vs. Monitored Heating Load Comparison	155
Figure 6.21: Single-Zone Model vs. Monitored Heating Load Comparison	158
Figure 6.22: Single-Zone Model vs. Monitored Cooling Load Comparison	159
Figure 6.23: Single-Zone Model vs. Monitored HVAC Load Comparison	161
Figure 6.24: Single-Zone Model vs. Monitored Absolute HVAC Load Comparison	164

LIST OF SYMBOLS

A	Area
A_{Brick}	Brick Wall Area
A_{GACW}	Glazed Aluminum Curtain Wall Area
A_{Roof}	Roof Area
A_{window}	Window Area
B	Variable for the Positioning of the Sun
B_{CS}	Solar Irradiation Constant
b_n	Transfer Function Coefficient
C_0	Quadratic Fit Intercept
C_1	Quadratic Fit Linear Coefficient
C_2	Quadratic Fit Quadratic Coefficient
C_C	Constant Conversion Factor
c_n	Transfer Function Coefficient
C_{OA}	Outside Air Carbon Dioxide Concentration
C_P	Specific Heat
$C_{\text{P,DA}}$	Specific Heat of Dry Air
$C_{\text{P,WV}}$	Specific Heat of Water Vapor
C_{RA}	Return Air Carbon Dioxide Concentration
C_{SA}	Supply Air Carbon Dioxide Concentration
CLF	Cooling Load Factor
∂	Partial Differential
dE/dt	Change of Energy With Respect to Change of Time
d_n	Transfer Function Coefficient

dT/dt	Change of Temperature With Respect to Change of Time
ET	Equation of Time
F_{CHW}	Chilled Water Flow
F_{CS}	Solar Irradiation Constant
G_{BN}	Beam Normal Radiation
$G_{BN,AM0}$	Solar Irradiation Beam Normal Constant
$G_{BN,calc}$	Calculated Beam Normal
G_{data}	Collected Solar Radiation Data
G_{SC}	Solar Constant
G_{SD}	Sky Dome Radiation
$G_{SD,calc}$	Calculated Sky Dome Radiation
G_T	Total Irradiation on a Tilted Surface
$G_{T,calc}$	Calculated Total irradiation on a Tilted Surface
H	Static Pressure
$H_{SF,i}$	Static Pressure for Variable i
h_{MA}	Mixed Air Enthalpy
h_{min}	Minimum Enthalpy
h_{MOA}	Minimum Outside Air Enthalpy
h_o	Coefficient of Heat Transfer by Long-Wave Radiation and Convection
h_{OA}	Outside Air Enthalpy
$h_{OA,i}$	Outside Air Enthalpy for Variable i
h_{RA}	Return Air Enthalpy
$h_{RA,i}$	Return Air Enthalpy for Variable i
h_{sl}	Saturated Liquid Enthalpy
h_{sv}	Saturated Vapor Enthalpy

$h_{WV@0°F}$	Enthalpy of Water Vapor at 0°F
i	Representative Variable Number
K_{DS}	Downstream Fan Constant
k_t	Clearness Index
K_{US}	Upstream Fan Constant
L_{lon}	Local Longitude
LTZ	Local Time Zone
m	Mass
\dot{m}	Mass Flow Rate
\dot{m}_{CHW}	Chilled Water Mass Flow Rate
\dot{m}_{CND}	Condensate Mass Flow Rate
\dot{m}_{EA}	Exhaust Air Mass Flow Rate
\dot{m}_{MA}	Mixed Air Mass Flow Rate
\dot{m}_{OA}	Outside Air Mass Flow Rate
$\dot{m}_{OA,i}$	Outside Air Mass Flow Rate for Variable i
\dot{m}_{RA}	Return Air Mass Flow Rate
\dot{m}_{SA}	Supply Air Mass Flow Rate
n	Numbered Day of the Year
N	Rotational Speed
N_{People}	Number of People
$P_{Controlled}$	Controlled Static Pressure
$P_{Downstream}$	Downstream Pressure
P_{Fan}	Static Pressure Across the Supply Fan
P_{Fixed}	Fixed Pressure

P_{reg}	Regulated Pressure
P_{ss}	Saturated Steam Pressure
P_{Upstream}	Upstream Pressure
\dot{Q}_{Brick}	Brick Skin Load
\dot{Q}_{C}	Cooling Load
\dot{Q}_{Cond}	Conduction Skin Load
$\dot{Q}_{\text{Cond},\tau}$	Conduction Skin Load (Transfer Function)
\dot{Q}_{GACW}	Glazed Aluminum Curtain Wall Skin Load
\dot{Q}_{H}	Heating Load
\dot{Q}_{HVAC}	Predicted Heating or Cooling Load
$\dot{Q}_{\text{HVAC,abs}}$	Absolute Predicted Heating or Cooling Load
$\dot{Q}_{\text{Internal}}$	Internal Load
$\dot{Q}_{\text{OA},i}$	Outside Air Load for Variable i
$\dot{Q}_{\text{OA,total}}$	Total Outside Air Load
\dot{Q}_{People}	People Load
\dot{Q}_{Roof}	Roof Skin Load
\dot{Q}_{SHG}	Solar Heat Gain Skin Load
\dot{Q}_{Skin}	Skin Load
R^2	Coefficient of Determination
R_v	Resistance Value
$R_{v,\text{Brick}}$	Brick Wall Resistance
$R_{v,\text{Brick},i}$	Brick Wall Resistance for Variable i

$R_{v,GACW}$	Glazed Aluminum Curtain Wall Resistance
$R_{v,CW,i}$	Glazed Aluminum Curtain Wall Resistance for Variable i
$R_{v,Roof}$	Roof Resistance
$R_{v,Roof,i}$	Roof Resistance for Variable i
SC	Shading Coefficient
ST	Local Solar Time
t	Time Step
T_H	High Temperature
THG	Total Heat Gain
T_{in}	Indoor Temperature
T_{IR}	Infrared Radiation Transfer of Sky Temperature
T_L	Low Temperature
T_{MA}	Mixed Air Temperature
T_{OA}	Outdoor Air Temperature
TOD	Time of Day
$T_{sol-air}$	Sol-Air Temperature
u	Uncertainty
\dot{V}	Volumetric Flow Rate
\dot{V}_{CHW}	Chilled Water Volumetric Flow Rate
\dot{V}_{CND}	Condensate Volumetric Flow Rate
\dot{V}_{CO_2}	Carbon Dioxide Generation Rate
\dot{V}_{MA}	Mixed Air Volumetric Flow Rate
\dot{V}_{CND}	Condensate Volumetric Flow Rate
\dot{V}_{OA}	Outside Air Volumetric Flow Rate

$\dot{V}_{OA,i}$	Outside Air Volumetric Flow Rate for Variable i
\dot{V}_{SA}	Supply Air Volumetric Flow Rate
$\dot{V}_{SF,i}$	Supply Fan Volumetric Flow Rate for Supply Fan i
\dot{W}_e	Electrical Load
$\dot{W}_{e,EB}$	Entire Building's Electrical Load (Including the Parking Garage)
$\dot{W}_{e,EPL}$	Emergency Power and Lights Electrical Load
$\dot{W}_{e,PL}$	Power and Lights Electrical Load
$\dot{W}_{e,MBA}$	Main Switchboard A Electrical Load
$\dot{W}_{e,MBB}$	Main Switchboard B Electrical Load
WV	Water Vapor
$XO(i)$	Band Coordinates
$YO(i)$	Band Coordinates

LIST OF GREEK SYMBOLS

α	Solar Altitude Angle
α_{abs}	Absorptivity
β	Tilt
$\beta_{\text{CB}}(i)$	Regression Coefficients
γ_{s}	Solar Azimuth Angle
γ_{sur}	Surface Azimuth Angle
$\gamma_{\text{sur,South}}$	Southern Surface Azimuth Angle
$\gamma_{\text{sur,South-West}}$	South-Western Surface Azimuth Angle
$\gamma_{\text{sur,West}}$	Western Surface Azimuth Angle
$\gamma_{\text{sur,North-West}}$	North-Western Surface Azimuth Angle
$\gamma_{\text{sur,North}}$	Northern Surface Azimuth Angle
$\gamma_{\text{sur,North-East}}$	North-Eastern Surface Azimuth Angle
$\gamma_{\text{sur,East}}$	Eastern Surface Azimuth Angle
$\gamma_{\text{sur,South-East}}$	South-Eastern Surface Azimuth Angle
δ	Declination Angle
ε	Energy Recovery Unit Effectiveness
θ_{B}	Incident Angle
$\theta_{\text{B,Roof}}$	Incident Angle of a Typical Roof
$\theta_{\text{B,Wall}}$	Incident Angle of a Typical Wall
θ_{Z}	Zenith Angle
ρ_{FG}	Foreground Reflectance
ρ_{liq}	Liquid Density

ρ_{OA}	Outside Air Density
$\rho_{OA,i}$	Outside Air Density for Variable i
ρ_{RA}	Return Air Density
ρ_{SA}	Supply Air Density
τ_b	Beam Transmittance
τ_{ref}	Transmittance
φ	Local Latitude Angle
ω	Solar Hour Angle
ω_{MA}	Mixed Air Humidity Ratio
ω_{OA}	Outside Air Humidity Ratio
ω_{RA}	Return Air Humidity Ratio

LIST OF ABBREVIATIONS

ACT	Advanced Computing and Technology
AHU	Air Handling Unit
ANSI	American National Standards Institute
ASHRAE	American Society of Heating, Refrigeration and Air-Conditioning Engineers
BDL	Building Description Language
BTU	British Thermal Unit
CFD	Computational Fluid Dynamics
CHW (or ChW)	Chilled Water
ChWR	Chilled Water Return
ChWS	Chilled Water Supply
CLF	Cooling Load Factor
CO ₂	Carbon Dioxide
CSM	Clear Sky Model
CW	Curtain Wall (Short for Glazed Aluminum Curtain Wall)
DOE	Department of Energy
DOE-2	Building Energy Use and Cost Analysis Tool
EA	Energy and Atmosphere
ECB	Energy Cost Budget
EES	Engineering Equation Solver
eQUEST	The <u>Q</u> uick <u>E</u> nergy <u>S</u> imulation <u>T</u> ool
ERU	Energy Recovery Unit
ERV	Energy Recovery Ventilation
EXA	Exhaust Air

GACW	Glazed Aluminum Curtain Wall
Georgia Tech	The Georgia Institute of Technology
GT	The Georgia Institute of Technology
HVAC	Heating, Ventilation and Air Conditioning
HW	Hot Water
HWR	Hot Water Return
HWS	Hot Water Supply
IESNA	Illuminating Engineering Society of North America
JCI	Johnson Controls Incorporated
KACB	Klaus Advanced Computing Building
Klaus	Klaus Advanced Computing Building
LBNL	Lawrence Berkeley National Laboratory
LEED	Leadership in Energy and Environmental Design
LHG	Latent Heat Gain
MA	Mixed Air
MAT	Mixed Air Temperature
MET	Meteorological Station
Min OA (or MOA)	Minimum Outside Air
NCDC	National Climatic Data Center
NOAA	National Oceanic and Atmospheric Administration
NREL	National Renewable Energy Laboratory
OA	Outside Air
RA	Return Air
RH	Relative Humidity
RLA	Relief Air

RReDC	Renewable Resource Data Center
RTD	Resistance Temperature Detectors
SA	Supply Air
SEAP	Simplified Energy Analysis Procedure
SF	Supply Fan
SHG	Sensible Heat Gain
SHGC	Solar Heat Gain Coefficient
SI	International System of Units
SZM	Single-Zone Model
T	Temperature
T&B	Test and Balance
THG	Total Heat Gain
TMY	Typical Meteorological Year
TRY	Test Reference Year
UGA	The University of Georgia
USGBC	United States Green Building Council
VAV	Variable Air Volume
VBA	Visual Basic for Applications
WBAN	Weather Bureau Army Navy

SUMMARY

The purpose of this research is to develop and verify a simplified and concise building simulation model suitable for high-level applications such as preliminary design or for embedding into adaptive control systems. An actual complex modern building and its energy system has been monitored. The monitored energy performance of this building has been compared with the empirical performance predicted by two simulation modeling programs and, alternatively, by a simplified single-zone model.

This project is composed of several related tasks. The first component is the monitoring of the energy consumption rates, pertinent environmental data, and load indicators of the new Klaus Advanced Computing Building on the Georgia Institute of Technology's Atlanta campus. The Klaus building was chosen because it represents a typical non-residential building. Subsequently, these findings have been compared with results from DOE-2 and eQUEST, well established energy simulation modeling programs. These comparisons allow for an empirical verification of the modeling program for Atlanta conditions. Finally, a simplified single-zone building model has been developed, and its predictions compared with the empirical data and with the results of the more complex programs. The results verify both the more complex programs and the single-zone model, and also demonstrate the use of a single-zone model for future work and predictions.

The work done to complete this research is presented in the following thesis. Detailed monitoring and load calculations are addressed, followed by the various modeling techniques which utilized the monitored data. Finally, comparisons, conclusions and recommendations for future work have been made.

1 INTRODUCTION

With the recent energy crisis and the rising price of energy in the United States, finding ways to lower the energy consumption of a building is very important. Many of today's existing buildings are not energy efficient, and consume more energy than is needed in order to make the working and living environments comfortable. Approximately 40% of total energy and more than half of electricity is consumed by the building sector (Tester et al., 2005).

Building designers today have available to them energy simulation programs that enable them to model proposed and existing buildings and facilitate the designers to optimize the design to reduce the heating and cooling loads of the building. There are also many benefits associated with reduced load designs such as improving air and water quality, reducing solid waste, reducing operating costs, enhancing occupant comfort and health, and most importantly, conservation of natural resources.

Detailed models may be helpful in predicting peak loads to help size the heating, ventilation and air conditioning (HVAC) system, design the air distribution system, and to indicate where corrective measures are needed. These detailed models might be accurate, but cannot be used early in the design phases when the important design decisions can really be influenced. Similarly, detailed design simulation programs cannot be embedded into a real-time controller or possibly embedded and later adapted to experience by an adaptive optimizing controller. Therefore, a verified simple model is very important and desirable because it can be used early in the design when the strategic decisions are made that determine the ultimate energy performance of the building.

1.1 Background

An existing building was needed to model and monitor. The building chosen for this research was the Klaus Advanced Computing Building located on the Georgia Institute of Technology's campus in Atlanta, GA. The Klaus building was chosen for a number of reasons, most important of which is because it is a typical, modern building. The Klaus building was not one which was built for studying. In fact, it has many features which make it awkward for studying, including its shape, orientation, an atrium, four air handling units (AHU), and two energy recovery units (ERU).

Typical buildings do not have outside air or solar radiation data taken onsite. Therefore, obtaining solar data was expected to be a problem. Originally, it was hoped that pyranometer data from a photovoltaic site on Georgia Tech's campus could be used, but it was ultimately not found possible to get data from these researchers due to the fact that their monitoring and upkeep of the recorded data seems to have ended in 2006. It was then expected that solar data would need to be modeled from simplistic weather observations. Fortunately, a professionally and conscientiously operated state-wide network not known to the HVAC community was found to exist and global radiation was actually available from a nearby site. This is a new and potentially very useful resource for HVAC and energy engineers since these weather data networks are readily available and are also more reliable than building instrumentation.

Additionally, the Klaus building includes a number of environmental and sustainable features which, in turn, has allowed the Klaus building to become LEED (Leadership in Energy and Environmental Design) Certified, as described next.

1.1.1 Leadership in Energy and Environmental Design

The Leadership in Energy and Environmental Design (LEED) Green Building Rating System was developed by the United State Green Building Council (USGBC) in 1998 (LEED, 2003). LEED is a voluntary, consensus-based national standard for developing high-performance, sustainable buildings. Members of USGBC, representing every component of the building industry, developed and continue to refine LEED.

LEED was created for many reasons, including, but not limited to: define the concept of a “green building” by establishing a standard of measurement, to promote integrated, whole-building design practices, to recognize environmental leadership in the building industry, to stimulate green competition, to raise consumer awareness of green building benefits, and to transform the building market.

LEED provides a complete framework for assessing building performance and meeting sustainability goals. Based on well-founded scientific standards, LEED emphasizes state-of-the-art strategies for sustainable site development, water savings, energy efficiency, materials selection and indoor environmental quality. LEED recognizes achievements and promotes expertise in green building through a comprehensive system of offering project certification, professional accreditation, training and practical resources.

There are approximately 70 points available for LEED Certification, up to ten of which can come from the Earth and Atmosphere (EA) Credit 1: Optimize Energy Performance. An additional point can be earned through EA Credit 3: Additional Commissioning. EA Credit 1 is earned by having components in the building which surpass ASHRAE Standard 90.1, which is described in the next section.

The research performed for this thesis shows that LEED guidelines do lead to reduced energy use without apparently compromising building performance, indoor air quality, or indoor environmental quality.

1.1.2 ASHRAE Standard 90.1

The American Society of Heating, Refrigeration, and Air-Conditioning Engineers (ASHRAE) publish many standards and guidelines. These standards typically refer to building codes. The standard of interest is ASHRAE Standard 90.1: Energy Standard for Buildings Except Low-Rise Residential Buildings.

The purpose of ASHRAE Standard 90.1 is to provide minimum requirements for the energy-efficient design of buildings (ASHRAE, 2007). In order to fully comply with LEED Certification requirements, a building must at least meet, if not exceed, the requirements provided by ASHRAE Standard 90.1.

This particular standard is jointly sponsored by the Illuminating Engineering Society of North America (IESNA) and the American National Standards Institute (ANSI). It is either referred to as ANSI/ASHRAE/IESNA Standard 90.1, ASHRAE/IESNA Standard 90.1, or simply ASHRAE Standard 90.1. Since this standard is continually revised, a year gets attached to the end of the title to establish which year the standard is referring to (i.e. ASHRAE Standard 90.1-1999 or ASHRAE Standard 90.1-2007).

1.1.3 Building Simulation

Building energy simulation is a useful tool for predicting heating, cooling, and electrical loads. The goal of building simulation is to predict the behavior of the modeled

system or establishment. There are currently many building energy use and cost analysis simulation software programs on the market either for purchase or as freeware. These building simulation tools can provide analytical power for the study and improvement of building performance. However, most of the available building simulation programs are very sophisticated and complex, perhaps excessively, such that they require a steep learning curve in order to produce useful results, not to mention the considerable amount of time it takes to fully construct and run a building simulation.

The Klaus building has been modeled twice during design using the DOE-2 computer simulation program. The first model depicts the building as it was intended to be built while the second model includes the bare minimum ASHRAE Standard 90.1-1999 requirements. Both DOE-2 models run during design use Typical Meteorological Year (TMY) weather data to simulate a typical year.

Next, the Klaus building was modeled with the eQUEST computer simulation program, a sister-program to DOE-2. However, the eQUEST model was simulated using a mock-TMY weather file which was created from actual weather data (in TMY format). The results presented herein show that simulations with the actual data do compare well with the measured results.

1.1.4 TMY Data

Typical Meteorological Year (TMY) weather data, mentioned above, is frequently used in building simulation to better assess the expected heating and cooling loads for the design of the building. TMY data is a composite of actual hourly long-term weather measurements for the area that reflects average temperature, humidity, wind, and solar conditions, to name a few. It is compiled of months selected from individual years which

are assembled to form a complete year. TMY data typically represents conditions characteristic of the past 30 years. Since the TMY weather data does not represent a typical year's data rather than the weather that actually occurred, a new weather file was needed and was created as part of this research for more realistic model comparisons. These comparisons verified the significant role weather data has on building energy.

1.2 Scope

The purpose of this research is to develop and verify a simplified and concise building simulation model suitable for high-level applications such as preliminary design or for embedding into adaptive control systems. An actual complex modern building and its energy system has been monitored. The monitored energy performance of this building has been compared with the empirical performance predicted by two simulation modeling programs and, alternatively, by a simplified single-zone model.

This project is composed of several related tasks. The first component is the monitoring of the energy consumption rates, pertinent environmental data, and load indicators of the new Klaus Advanced Computing Building on the Georgia Institute of Technology's Atlanta campus. The Klaus building was chosen because it represents a typical non-residential building. Subsequently, these findings have been compared with results from DOE-2 and eQUEST, well established energy simulation modeling programs. These comparisons allow for an empirical verification of the modeling program for Atlanta conditions. Finally, a simplified single-zone building model has been developed, and its predictions compared with the empirical data and with the results of the more complex programs. The results verify both the more complex programs and

the single-zone model, and also demonstrate the use of a single-zone model for future work and predictions.

The work done to complete this research is presented in the following thesis. Detailed monitoring and load calculations are addressed, followed by the various modeling techniques which utilized the monitored data. Finally, comparisons, conclusions and recommendations for future work are made.

1.3 Thesis Organization

The organization of this thesis is as follows:

- Chapter 2 provides a brief literature review on complex computer models and simplified models used for building simulation, comparisons, and the need for verification and validation of such models. Typical meteorological yearly weather data are also discussed.
- Chapter 3 describes the example building which was studied for this thesis: the Klaus Advanced Computing Building. This chapter also includes the building statistics, layout, description, occupancy and the original detailed building model.
- Chapter 4 discusses the monitoring of the example building.
- Chapter 5 portrays the analysis and modeling of the example building.
- Chapter 6 presents the results from comparing different models.
- Chapter 7 summarizes the important conclusions from this thesis.
- And, finally, Chapter 8 recommends future work which can be completed to further investigate building energy models.

2 LITERATURE REVIEW

Building energy simulation has become a useful tool for predicting cooling, heating and electrical loads for facilities. Simulation models have been validated throughout the years by comparing simulation results to actual measured values. The simulations have become more accurate as approaches were changed to be more comprehensive in their ability to model building features. These simulation models tend to require considerable experience in determining input parameters and large amounts of time to construct the models. As a result of the large number of man-hours required, simplified models have been sought and used. Simplified models are particularly useful for conducting preliminary assessments of energy conservation measures.

In commercial buildings, the heating and cooling systems are often the single largest user of energy. Determining the amount of energy these systems use is, therefore, important for many applications, including energy conservation. The amount of energy used for heating or cooling can be found with a number of methods. These methods include measuring the usage of each component of the system over a period of time, complex computer modeling, and simplified modeling. The first method is the most accurate, but measuring the energy used by each component is expensive and requires measurements over a long period of time. The second method is more uncertain and typically requires professional consultants a couple of weeks to model a typical commercial building. The simplified model method requires the shortest amount of time and is used for preliminary estimation purposes by energy surveyors. Unfortunately, the simple method is likely to be the least accurate method.

Simplified methods are generally used in initial screening studies, while more complex modeling is typically reserved for in-depth studies for determining energy usage and predicting savings through retrofits. It is desirable to have the simplest, yet acceptably accurate, model possible for an initial screening to determine if a more in-depth study is justified. A particular simplified model can be evaluated by comparison with a complex computer simulation and actual whole-building energy usage.

The energy usage in a building is dependent on construction, weather, and occupancy schedules as well as the individual systems that work to heat and cool the building. Models of energy usage must adequately reflect the influence of these factors. The following reviews literature related to modeling building energy usage with complex computer models as well as simplified techniques, followed by various comparisons and the need for verification and validation of such models. Finally, typical meteorological yearly (TMY) weather data are also discussed.

Complex computer model programs for building design and energy analysis have developed to become very sophisticated and precise, but in the process require a very steep learning curve and large amounts of data and time to produce useful results. Furthermore, detailed simulation models require a description of the building and its systems that is often unavailable at early design stage. Examples of complex computer modeling programs for building and energy analysis and simulation include, but are not limited to BLAST, DOE-2, Energy-10, EnergyPlus, eQUEST, ESP-r, FLOVENT, PowerDOE, TRNSYS, and so forth.

Since the programs used in this research are DOE-2 and eQUEST, two sister programs developed by EnerLogic and J.J. Hirsch and Associates in collaboration with

LBNL (EnerLogic et al., 2006, Hirsch et al., 1998, Hirsch et al., 2006a, and Hirsch et al., 2006b), only these complex programs will be reviewed.

A study of the DOE-2 simulation program was performed in the late 90's by Pasqualetto et al (1998). The approach used in this study used a multi-step process to investigate the validity of the DOE-2 program. The authors believe that the approach used in this study can also be applied to any other energy simulation software, and does not require any expensive monitoring of building or access to test cells. They also believe that the goal of any validation study should be to provide sufficient testing to ensure that the probability of failure is sufficiently low in order to be acceptable. This paper concludes that in this study, the majority of the results were satisfactory and therefore consistent with results from other validation studies of the DOE-2 program. Unfortunately, there were some discrepancies found mostly in the simulation of the HVAC system which implies that further validation needs to be done in this particular area (Pasqualetto et al., 1998).

An independent study by Carriere et al. (1999) was also performed in the late 90's which developed similar conclusions to those presented by Pasqualetto et al. For this paper, Carriere et al. describe a large five-story building which was intensely monitored over a one-year period. The results from the DOE-2 simulation program were then compared to the monitored performance (Carriere et al., 1999). Similarly to Pasqualetto et al., Carriere et al. concluded that the DOE-2 computer simulation was found to agree with the monitored performance to within a generally acceptable accuracy for modeling of this type, finding that the major discrepancies were from the steam energy

consumption (Carriere et al., 1999). Once again, this is part of the HVAC system which clearly indicates a need for improvement and further validation of the DOE-2 program.

In November 2001, Crawley attempted to promote the use of EnergyPlus as the future of building energy simulation by pointing out flaws in the BLAST and DOE-2 modeling programs. Crawley stated that “BLAST and DOE-2 are in many ways obsolete. Both of these hourly building energy-simulation programs were designed in the days of the mainframe computer, which has made expanding their capabilities time-consuming and expensive” (Crawley, 2001). He then went on to claim that the most serious deficiency of the two programs was their inaccurate space temperature prediction due to a lack of feedback from the HVAC module to the loads calculations. This, once again, is in line with the conclusions found by both Pasqualetto et al. and Carriere et al.

A study was performed at the Lawrence Berkley National Laboratory (LBNL) which documents many of the validation studies of the DOE-2 building energy analysis simulation program which have taken place since 1981 (Sullivan, 1998). This work was done as part of an effort related to continued development of the DOE-2 program. These validation studies compared calculated simulation data to measured data. Any discrepancies discovered during this study resulted in improvements in the simulation algorithms. This research concluded that the comparison of calculated and measured quantities resulted in a satisfactory level of confidence that is sufficient for continued use of the DOE-2 program, but that additional validation is also warranted, particularly at the component level to further improve the program.

Simplified models allow for quick analysis with minimal information in order to model building systems or even an entire building. There are multiple types of simplified

models, namely because any model which does not classify as a complex computer model can be lumped into the simplified model category.

Simplified models which use average monthly temperatures do calculations based on the premise that a straight line results when the difference between monthly heating and cooling loads are plotted as a function of average monthly temperature. This simplified method uses information including solar, internal, and design peak loads. In 1996, White found that this method could be applied to simple or complex buildings and is more accurate than standard calculation procedures that use heating and cooling degree days or temperature bins (White, 1996).

A study performed by Zhai and Chen (2005) combined typical building energy with a computational fluid dynamics (CFD) simulation. They found that, in general, a coupled simulation produces more accurate and detailed results due to the more precise information the CFD model reveals for the assessment of indoor air quality and thermal comfort. Additionally, this study did find that the empirical coefficient correlations used by typical complex energy simulation programs may significantly deviate from the real values, thus illustrating a further need for understanding and advancing the complex models.

Numerous studies have been performed and analyzed on the thermal mass of a building and its effects. In the mid 90's, Balaras (1996) reviewed and classified the work of many others regarding the factors affecting the performance of thermal mass, experimental studies which demonstrate the effectiveness of thermal mass, and a number of simplified design tools which account for thermal mass effects (Balaras, 1996). This paper concluded that the mass structure plays an essential part in the thermal response of

the building, creating a smaller interior air temperature variation with a high mass building as compared to a low mass building.

Yao et al. (2002) created a simplified single zone thermal resistance network model to be used as an integrated design tool. This model is driven by an annual weather file and then validated through comparisons with other programs. Simulation for over 150 cases relating to different orientations, building mass types and ventilation rates have been performed. This paper concludes that this simplified thermal resistance network model is a bit too simplistic since it represents more of a generic module rather than a representation of the whole building.

Wang and Xu have been working on numerous simplified thermal network models together (Wang and Xu, 2006a, Wang Xu, 2006b, and Xu and Wang, 2008). The first two papers discuss a study in which a building is described using two simplified thermal network models, one for the building envelope and one for the internal masses. A genetic algorithm estimator was developed to estimate the lumped internal thermal parameters using the operation data collected from site monitoring (Wang and Xu, 2006a). Next, the simplified dynamic building energy model was tested and validated in different weather conditions (Wang and Xu, 2006b). Both papers conclude that the thermal network model is thorough enough to predict the thermal performance of a building under different operating conditions by correctly capturing the dynamic characteristics within an average of about 10% error.

Two years later, Wang and Xu added a conduction transfer function component to their simplified thermal network model (Xu and Wang, 2008). This new model combines detailed physical models of building envelopes, calculated through a conduction transfer

function, and a thermal network model of building internal mass. Similarly to their previous results, this new model still predicted the cooling load within about 10% compared to the actual measurement. Even though the overall difference of 10% remained the same, this paper concludes that this new model with the addition of the conduction transfer function to the genetic algorithm for parameter identification can result in a more accurate performance than the original simplified model merging internal mass (Xu and Wang, 2008).

Building energy simulation is closely related to air conditioning design. One study by Hui and Cheung (Hui and Cheung, 1998) discusses the basic principles of building energy simulation and its relationship with air conditioning load and energy calculations and how to relate this application to air conditioning design. The paper concludes that a better understanding of building properties and design procedures must be found before improvements in building performance and simulation can be accomplished. Also, if better building energy efficiency is to be achieved, building energy simulation first needs to be further promoted in air conditioning design.

Comparing different types of systems with a simplified model can assist engineers in determining the best retrofit options or in estimating the energy benefits of different systems. One study by Katipamula and Claridge (Katipamula and Claridge, 1993) compares the post-retrofit energy savings for installing a VAV system to replace a Dual-Duct, Constant Volume distribution system when pre-retrofitted data was not available. The study compared values from a regression model for the VAV system with measured post-retrofit energy data and showed the comparison had an error of $\pm 7\%$ for daily values. Then, these results were shown to compare well with the savings predicted by a

simulated Dual-Duct, Constant Volume model compared to the measured post-retrofit VAV data. The paper concluded the use of its method for comparisons was promising for buildings lacking pre-retrofit data. However, the same methods can be applied to pre-retrofit options. Pre-retrofit buildings are usually the focus of an energy audit in which simplified models are needed.

A study was performed by Lee et al. to examine the use of the ASHRAE simplified energy analysis procedure (SEAP) for fault detection at the whole-building level (Lee et al., 2007) as well as to predict future consumptions using future weather data. Unfortunately, this paper concluded that the SEAP is an incomplete representation of any building, so it is important that a methodology be developed that can clearly and accurately define an error threshold to differentiate a true system fault from normal deviations between simulated and measured consumption caused by the imperfect simulation model (Lee et al., 2007).

There have been many studies performed to compare or validate various building energy models, each of which takes a slightly different approach. Some studies compare the models as a whole while others look at specific components. Either way, numerous comparison or validation studies have already been performed while still leaving room for future comparison and validation research. Irving put it best stating that “the development of tools for validation must be an ongoing process,” (Irving, 1988).

In the 80’s, research was performed at the Solar Energy Research Institute to investigate work related to validation of building energy analysis simulation programs (Judkoff, 1988). This work included a validation methodology, monitoring techniques used for empirical validation studies, and several analytical and empirical validation

studies. An overall conclusion from this study was that an absolute validation of the simulation programs for building energy analysis could never be achieved. However, the validation methods presented by Judkoff do prove very useful in weeding out large errors, pinpointing the sources of those errors, and establishing ranges of reasonable application for these computer programs (Judkoff, 1988).

Jensen believes that validation is a complex process which can be defined as a rigorous testing of a program comprising its theoretical basis, software implementation and user interface under a range of conditions typical for the expected use of the program (Jensen, 1995). Through his study, he concludes that in practice it is not possible to perform a complete validation of a program because there are too many interlinked factors and too many possible applications to test all combinations.

Research performed by Norford et al. states that computer models of building energy use, if calibrated with measured data, offer a means of assessing retrofit savings, optimizing HVAC operation, and presenting energy consumption feedback to building operators (Norford et al., 1994). This study also found that the calibration process itself can pinpoint differences between how a building was designed to perform and how it is actually functioning. Overall, this study found a large discrepancy between what the simulation software had predicted would happen and what actually occurred. Norford et al. believe that the nature of the occupants' business, including energy intensive facilities, the choices the occupants make about how to use lights and office equipment, and the manner in which the conditioning equipment is operated all have enormous impact on the actual loads of a building, thus causing the large discrepancies.

The predictions of the DOE-2 program for building energy analysis have been compared with the measurements in a couple of test houses in a study performed by Meldem et al. (1998). In all cases, DOE-2 agreed well with the actual measurements. However, this study, another case of verification in a very special building, concluded that the validation only applied to cases when the test houses were unoccupied and unconditioned, and therefore urged further research to test DOE-2's accuracy in modeling the effects of internal heat gains in occupied establishments.

Pan et al. (2007) presented a methodology for the calibration of building simulation models based on three different criteria. Among the steps of the calibration process, the authors performed several reevaluations of the internal loads in order to decrease the uncertainty of the simulations. They pointed out that those reevaluations are quite important to properly fit the models to the actual building profile. The authors also emphasized that the definition of operating schedules of the internal gains was one of the most challenging tasks due to its intrinsic randomness. However, in the end, this study concluded that only after several steps of calibration can an energy model accurately predict the actual energy usage of specific buildings (Pan et al., 2007).

In a study conducted by Neto et al., a comparison was made between a simple model based on an artificial neural network and a model that is based on physical principles as an auditing and predicting tool in order to forecast a building's energy consumption (Neto et al., 2008). Results from these comparisons show that both models are suitable for energy consumption forecasts. However, the complex computer simulation model, in this case EnergyPlus, presented an error range of $\pm 13\%$ for 80% of the tested data. Similar to the conclusions made by Norford et al., Meldem et al., and Pan

et al., these major uncertainties in the model predictions are mainly related to proper evaluation of lighting, equipment and occupancy schedules. Therefore, Neto et al. concludes that schedules of the internal loads must be periodically reevaluated to provide an updated description of the building usage and, therefore, a more accurate evaluation of the energy demand.

Salsbury and Diamond (2000) describe the concept of using simulation as a tool for performance validation and energy analysis of HVAC systems. The idea is to use simulation predictions as performance targets with which to compare monitored system outputs for performance validation and energy analysis (Salsbury and Diamond, 2000). This study believes that simulation represents the idealized behavior of the system and that, in practice, the ideal operation might not be achievable and therefore the simulation acts as the performance reference. Therefore, this study then concludes that by assuming the simulation represents the optimum level of performance, simulation can then be used to assess performance over an annual period and then predict potential improvements.

Another study was performed by Loutzenhiser and Maxwell (2006). to compare the daylighting and building energy predictions form DOE-2 with measured quantities from an actual building. For this research, the weather information was taken directly at the site and was used to create weather files for the simulations. Overall, this study concluded that the annual DOE-2 simulation predictions were at least twice as accurate as the hourly predictions.

In a study by Tronchin and Fabbri (2008), three different building energy software calculations have been analyzed and compared in order to quantify their differences with actual energy consumptions. Unfortunately, none of the programs were

able to provide the same results, nor comparable results of energy consumptions in the buildings. Thus, this study concluded that if a building were to have an energy audit or be modified, it would be better to use the same calculation model for all simulations due to inconsistent outputs between the various models.

And finally, a study performed by Waltz (1992) investigated achieving high level accuracy in energy simulations of existing buildings. Waltz believed that a high level of accuracy can only be achieved through optimization of three factors: (1) an intimate understanding of the simulation tool, (2) an intimate understanding of the building to be simulated, and (3) careful analysis and critique of the output data (Waltz, 1992). Waltz later declared that in order for a model to be considered “accurate,” the calculated total energy consumption would need to be within 5% of the building’s actual annual energy use (Waltz, 1992). Therefore, this thesis will show that the two models created and simulated specifically for this research (the eQUEST and the single-zone models) can be considered accurate.

Typical Meteorological Year (TMY) weather data are frequently used in building simulation to better assess the expected heating and cooling loads for the design of the building. TMY data are a composite of actual hourly long-term weather measurements for the area that reflects average temperature, humidity, wind, and solar conditions, to name a few. It is compiled of months selected from individual years which are assembled to form a complete year. TMY data typically represents conditions characteristic of the past 30 years.

A study performed in Athens, Greece by Argiriou et al. (1999) compared 17 different TMYs (or rather TRY, Test Reference Years, as it is referred to in Europe) and evaluated their differences. The results showed that as a whole, TMY data presents a better overall estimation compared to the use of only one, randomly selected year. However, these differences might be considered unimportant from the physical point of view, yet may lead to erroneous conclusions on the performance, sizing and feasibility assessment of energy systems (Argiriou et al., 1999). Nevertheless, even though TMY data may present a better overall estimation, each year does differ such that to accurately represent a particular year, typical TMY weather data are not the best bet.

Similarly, a study was conducted by Gugliermetti et al. (2004) to investigate the influence of the stochastic component of meteorological data in evaluating office building energy performance. This study showed that the climate data aspects can play a very important role in forecasting the energy consumption in office buildings. Gugliermetti et al. identified that the use of typical month day or annual weather data could induce an over or under estimation of building energy profiles, and thus preferred a mixture of the two to obtain the most accurate results.

Please note that the research presented in this thesis began its simplified model development around the same time that other groups also recognized the important need to further study and understand simplified building models. However, this thesis does illustrate some more sophisticated and accurate ways to calculate some of the building's features such as outside air loads, solar radiation affects, and conduction skin loads.

The simplified thermal resistance network model simulation study performed by Yao et al. (2002) did not utilize some important features which the single-zone model

presented in this thesis does. For example, Yao et al. made many assumptions regarding the solar effects on the envelope, especially for the solar heat gain through the windows, and they also utilized a simplified nodal analysis to calculate the conduction skin loads (Yao et al., 2002). This thesis will present a method to accurately calculate the solar effects on the envelope rather than relying on assumptions, as well as a conduction skin load which takes the thermal mass of the wall and a time lag into account.

Similarly, the first two papers by Wang and Xu (2006a and 2006b) discuss a study in which a building is described using two simplified thermal network models, one for the building envelope and one for the internal masses. For this study, a genetic algorithm estimator is developed to estimate the lumped internal thermal parameters using the operation data collected from site monitoring (Wang and Xu, 2006a, and Wang and Xu 2006b). However, two years later, Wang and Xu added a conduction transfer function component to their simplified thermal network model (Xu and Wang, 2008). The addition of Wang and Xu's conduction transfer function to their envelope load analysis was developed at approximately the same time in which the transfer function conduction skin load was used in the single-zone model presented in this thesis. On the other hand, this thesis does present a more accurate use of solar radiation (Wang and Xu simply use horizontal global solar radiation) as well as a sophisticatedly creative method to calculate the outside air load, thus allowing the single-zone model presented in this thesis to accurately model a building with minimal error.

As discussed above, even though there are numerous studies which have researched both complex and simple models as well as their comparisons and validation attempts, there is still room for future comparison and validation research. Therefore,

this thesis will bring together many of the ideas and techniques presented above in order to compare actual monitored data to both complex computer simulation programs and a simplified single-zone model while also creating an up-to-date mock-TMY weather file to produce more realistic and representative model results.

3 OVERVIEW OF THE EXAMPLE BUILDING

Verifying building performance is extremely important for educational, economical and environmental purposes. An existing building was needed to model and monitor. A new and important building, but not one especially designed for experimentation, was available. The building analyzed and discussed in this thesis is the Christopher W. Klaus Advanced Computing Building, better known as KACB or the Klaus Building from herein, located on the Georgia Institute of Technology campus in Atlanta, GA. It is important to note that this building was not built for studying but was chosen to better illustrate that the techniques used on this building can be used on any typical building, and not just on those designed to be monitored and studied. This research shows that it is possible and practical for governments and owners to reward designers and builders for actual performance even if there is no prior monitoring system in the building.

3.1 *General Quantitative Data*

The Klaus Advanced Computing Building is located on the campus of the Georgia Institute of Technology in Atlanta, Georgia at $33^{\circ} 46' 39.08''$ N (33.777524°) latitude and $84^{\circ} 23' 40.06''$ W (-84.394128°) longitude (Magnus, 2008). It is a three-story multi-use educational building and computer facility totaling approximately 210,000 square feet ($19,510 \text{ m}^2$). The mechanical equipment is located in the penthouse above the top floor, while a three-story underground parking garage sits beneath. This thesis will focus on the monitoring, modeling and evaluation of the main three-story building.

3.2 Layout

The Klaus building is home to part of both the College of Computing and the School of Electrical and Computer Engineering. The building consists of several laboratories, 8 computer class labs, 5 large classrooms and a 200-seat auditorium, study lounges, faculty offices, research laboratories, graduate student offices, conference rooms, common areas and an extensive atrium.

The building is oriented such that the majority of the open atrium faces south. The curved section with offices faces east while wrapping around to both the north east and south east. An aerial view of the Klaus building as seen from Google Earth (Google, 2008) is shown below in Figure 3.1.

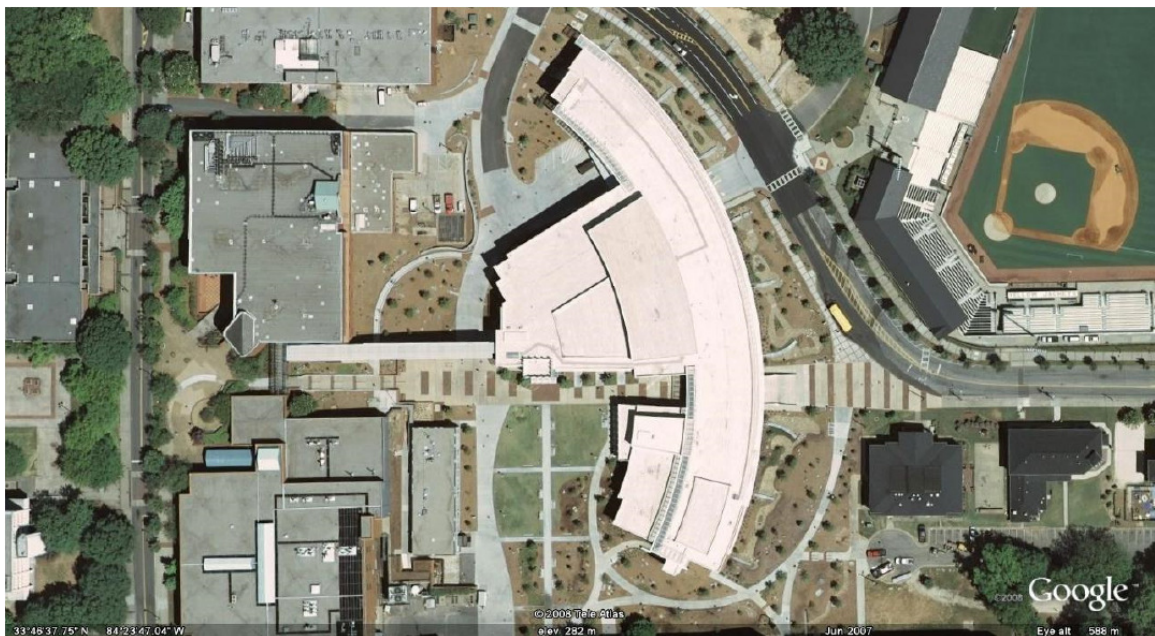


Figure 3.1: The Klaus Building as Seen from Google Earth (Google, 2008)

The overall outline of the first floor of the building which is separated into two sections is shown below in Figure 3.2. However, the second and third floors of the building are actually connected as one unit as illustrated by the dashed lines.



Figure 3.2: Overall Layout of the Klaus Advanced Computing Building

3.3 Building Description

The building envelope consists mainly of a glazed aluminum curtain wall construction, a brick wall construction, windows and a roof construction. The brick walls, roof and building as a whole are relatively massive, while the glazed aluminum curtain walls and the windows are relatively light. For more information regarding the wall, window and roof compositions, please refer to Section 5.1.4: Skin Loads.

The majority of the exterior walls of the building are of glazed aluminum curtain wall construction. The glazed aluminum curtain wall consists of approximately 35,5000 vertical square feet (3,298 m²). The curtain wall consists of spandrel glass on the exterior, an air layer, particle board underlay, mineral wool batt insulation, and gypsum board. The overall composite U-value for the glazed aluminum curtain wall construction is 0.0608 BTU/hr-ft²-°F (0.3452 W/m²-K, R-value = 16.44 hr-ft²-°F/BTU = 2.895 m²-K/W). Table 3.5: Glazed Aluminum Curtain Wall Construction provides a complete breakdown of the glazed aluminum curtain wall construction and relevant R-values.

A brick wall construction accounts for approximately 16,385 square feet (1,522 m²) of the exterior walls. The brick wall construction consists of common brick on the exterior, an air layer, a hollow light weight concrete block, expanded polyurethane insulation, and gypsum board. The overall composite U-value for the brick wall construction is 0.0434 BTU/hr-ft²-°F (0.2464 W/m²-K, R-value = 23.05 hr-ft²-°F/BTU = 4.059 m²-K/W). Table 3.6: Brick Wall Construction provides a complete breakdown of the brick wall construction and relevant R-values.

The horizontal roof area is approximately 60,600 square feet (5,630 m²). The roof construction is built-up roof on the exterior, two layers of expanded polyurethane insulation and light weight concrete. The overall composite U-value for the roof construction is 0.0186 BTU/hr-ft²-°F (0.1056 W/m²-K, R-value = 53.65 hr-ft²-°F/BTU = 9.448 m²-K/W). Table 3.4: Roof Construction provides a complete breakdown of the roof construction and relevant R-values.

Excluding the penthouse, windows occupy close to 38% of the exterior wall area, or approximately 31,355 square feet (2,913 m²). Section 5.1.4.4: Direct Solar Heat Gain Skin Loads provides more information regarding the windows and their load calculations.

The HVAC system consists of four main air handling systems, two of which work together in parallel. The heating and cooling for the building is provided by steam and chilled water from a central plant for the entire Georgia Tech campus. Also, there are two energy recovery units which provide pre-conditioned outside air to the air handlers based on the energy recovered from the exhaust air. There is a damper which is either fully opened or fully closed to determine if the air handlers are receiving direct outside air, or pre-conditioned minimum outside air.

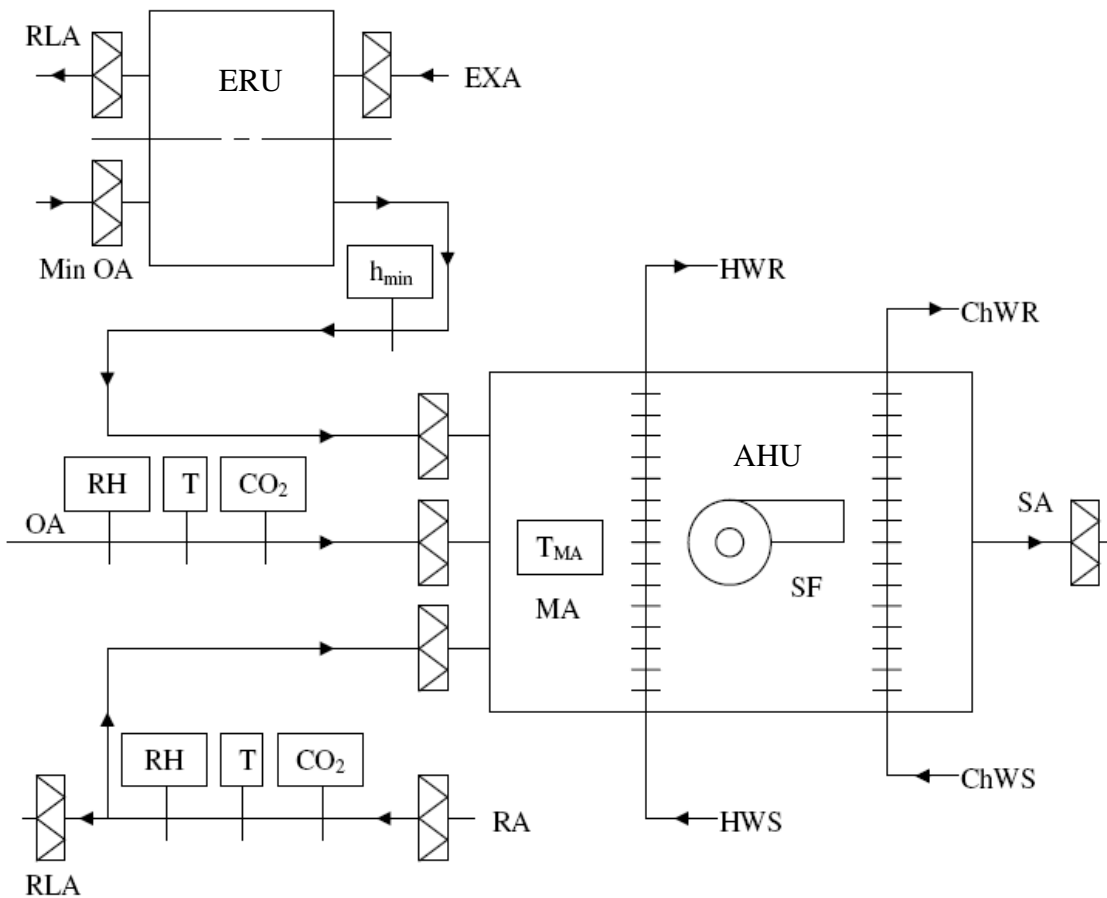


Figure 3.3: Sample Air Handling Unit and Energy Recovery Unit Schematic

Figure 3.3 is a sample illustration of the HVAC system used in the Klaus building. Similarly, an independent schematic of the chilled water cooling system and the steam heating system are illustrated in Figure 3.4 and Figure 3.5, respectively, before each subsystem connects to the overall HVAC system.

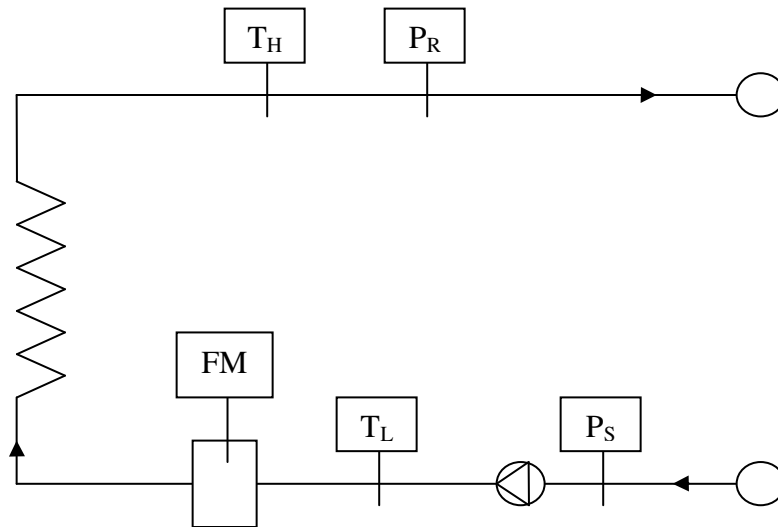


Figure 3.4: Chilled Water Cooling System Schematic

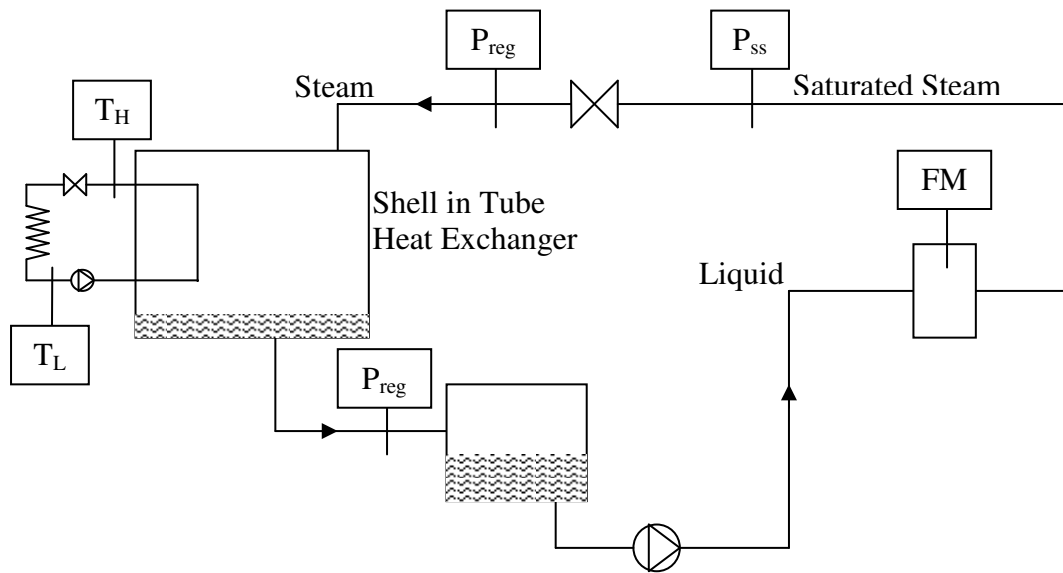


Figure 3.5: Steam Heating System Schematic

3.4 Occupancy

The occupants of KACB are assumed to be faculty, staff, undergraduate and graduate students. The number of people in the building at any given time has been estimated based on room utilization. For example, undergraduate students are assumed to occupy the classrooms during scheduled class times, while the graduate students occupy the laboratory spaces for extended hours. Also, the faculty/staff offices assume only one occupant for normal work hours, while the graduate student offices have four people per office for extended hours. These numbers have also been verified through the use of carbon dioxide concentration data and calculations. For more information on this comparison, please refer to Section 5.1.5.1: Occupancy Loads.

3.5 Original Detailed Building Model

Before the proposed Klaus Advanced Computing Building was built, it went through initial modeling and comparisons to determine how the building would perform and to determine possible energy saving features. This section will discuss the proposed building used for energy simulation and then continue on to discuss the proposed energy saving features.

The Klaus Advanced Computing Building is located on the campus of Georgia Tech in Atlanta, Georgia. It is a three-story (plus penthouse mechanical space) computer facility totaling approximately 210,000 square feet (19,510 m²) of floor area. It also includes three floors of below-grade parking. About 63,000 square feet (5,853 m²) of the floor area contains labs, 21,000 square feet (1,951 m²) contain classrooms and 54,000 square feet (5,017 m²) contain offices. The three-floor atrium comprises almost 12,000 square feet (1,115 m²) of floor area. The facility also houses conference rooms and

computer areas which total almost 8,000 square feet (743 m²). The remaining 52,000 square feet (4,831 m²) consists of “building core” functions, such as corridors, restrooms, storage areas, stairs and mechanical rooms (Poulos, 2003).

Before KACB was completed, the Georgia Institute of Technology Facilities Department applied for LEED credit and certification. It was proposed that KACB (a new building) would reduce the design energy cost compared to the energy cost budget for energy systems regulated by ASHRAE/IESNA Standard 90.1-1999 by at least 35% (Poulos, 2003). This thesis will verify that these predicted values accurately show the building’s current performance by comparing these predicted values to the actual values which will be calculated using monitored information collected directly from the Klaus building.

LEED EA Credit 1 (Optimize Energy Performance) offers from 1 to 10 points for designs that result in annual energy costs that are lower than the annual energy costs of the same building built to the minimum standards of ASHRAE 90.1-1999 (with minor adjustments). The annual energy costs of the proposed design and the minimum standards (referred to as the Baseline Model) were estimated through the use of the DOE-2 computer simulation program.

The Proposed Design model for the building was developed based on the construction document drawings dated 2/3/2003 and design information provided by the design team.

The Baseline Model was then developed that simulates the energy use of this building as if it were designed to meet the minimum requirements specified in ASHRAE 90.1- 1999. This Baseline Model is used as the benchmark for measuring the potential

Earth and Atmosphere (EA) credit points that can be achieved towards LEED certification. EA Credit 1 is to Optimize Energy Performance. The intent of this credit is to achieve increasing levels of energy performance in a building above what the current required standard to reduce environmental impacts associated with excessive energy use (LEED, 2003). A new building at least 35% more efficient than the Baseline Model can earn 4 points towards LEED certification.

Most of the building and system components needed to develop the two models were shown on the drawings and or other design documents. However, some of the information required to develop energy models is typically not shown on design documents. Values for this information have either been observed or estimated from reliable sources and set equal for both the Proposed Design and Baseline Models.

The weather used for this analysis was TMY (Typical Meteorological Year) hourly weather data for Atlanta, Georgia. TMY data is frequently used in building simulation to better assess the expected heating and cooling loads for the design of the building. TMY data is a composite of actual hourly long-term weather measurements for the area that reflects average temperature, humidity, wind, and solar conditions, to name a few. However, in this thesis, actual weather data which corresponds to the monitored data was used to calculate the actual loads on the building as well as to create a mock-TMY weather data file in order to best compare the predicted and actual building loads.

The Klaus building uses hot water for space heating and low pressure steam for humidification. Hot water is provided by a steam-to-hot water heat exchanger fueled by high pressure steam from one of the campus central steam plants. Low pressure steam for

humidification is provided by an unfired steam generator also fueled by the high pressure steam from the same steam plant. This steam plant has natural gas fired steam boilers.

Space cooling in the building is provided by chilled water (CHW) supplied by one of the campus central CHW plants.

The proposed design and baseline models were simulated using the DOE-2 building energy analysis program. For HVAC analysis, MBTU represents 1000 BTU, while MMBTU represents a million BTU. The proposed design model shows that the building as designed would consume 1,908,096 kWh (6,511 MMBTU) in electricity, 1,621 MMBTU (475,068 kWh) of steam and 5,827 MMBTU (1,707,725 kWh) of chilled water annually. The baseline model shows that the building as if it was designed to meet ASHRAE 90.1-1999 would consume 2,107,306 kWh (7,191 MMBTU) in electricity, 4,624 MMBTU (1,355k161 kWh) of steam and 10,931 MMBTU (3,203,560 kWh) of chilled water annually (Poulos, 2003). These data has been summarized below in Table 3.1:

Table 3.1: Proposed vs. Baseline Model Building Savings

	Proposed Building	Baseline Model	Savings
Electricity (MMBTU)	6,511	7,191	9.5%
Chilled Water (MMBTU)	5,827	10,931	46.7%
Steam (MMBTU)	1,621	4,624	64.9%
Total (MMBTU)	13,959	22,746	38.6%

The proposed building design numbers indicate the projected energy use of the building based on the actual design; whereas the baseline model’s building numbers indicate the minimum energy used of the building based solely on the ASHRAE standards. As illustrated above in Table 3.1, the proposed building design would allow

for a total savings of 39% as compared to the baseline model. These energy saving features for the proposed building are discussed in Section 3.5.1 below in more detail along with the ASHRAE/IESNA Standard 90.1-1999 (and ASHRAE/IESNA Standard 90.1-2007) requirements.

A summary of the actual energy results over the course of a year (September 2007 – August 2008) have been summarized and compared to the proposed building below in Table 3.2 and to the baseline building model in Table 3.3.

Table 3.2: Actual vs. Proposed Building Savings

	Actual Building	Proposed Building	Savings
Electricity (MMBTU)	5,495	6,511	15.6%
Chilled Water (MMBTU)	5,166	5,827	11.3%
Steam (MMBTU)	1,441	1,621	11.1%
Total	12,102	13,959	13.3%

Table 3.3: Actual vs. Baseline Model Building Savings

	Actual Building	Baseline Model	Savings
Electricity (MMBTU)	5,495	7,191	23.6%
Chilled Water (MMBTU)	5,166	10,931	52.7%
Steam (MMBTU)	1,441	4,624	68.8%
Total	12,102	22,746	46.8%

However, these DOE-2 simulation results for the proposed and baseline models were simulated using a regular TMY weather file rather than the actual weather which affected the actual building, thus causing some of the discrepancy between the actual building's load data and the modeled load data. These results and more are discussed through the remainder of this thesis.

3.5.1 Energy Saving Features

The proposed design, which is now the current building, incorporates the following energy saving features that improve on the minimum requirements prescribed by ASHRAE Standard 90.1-1999. Since the original energy modeling was performed, the latest ASHRAE Standard to be released is ASHRAE 90.1-2007 which has also been used for comparison in the coming sections. Building energy saving requirements, vary depending on where the building is located. Since Atlanta, Georgia is located in Climate Zone 3A (ASHRAE, 2007), as illustrated below in Figure 3.6, the energy saving requirements presented in the following sections are all for buildings located in this particular zone, Climate Zone 3A.

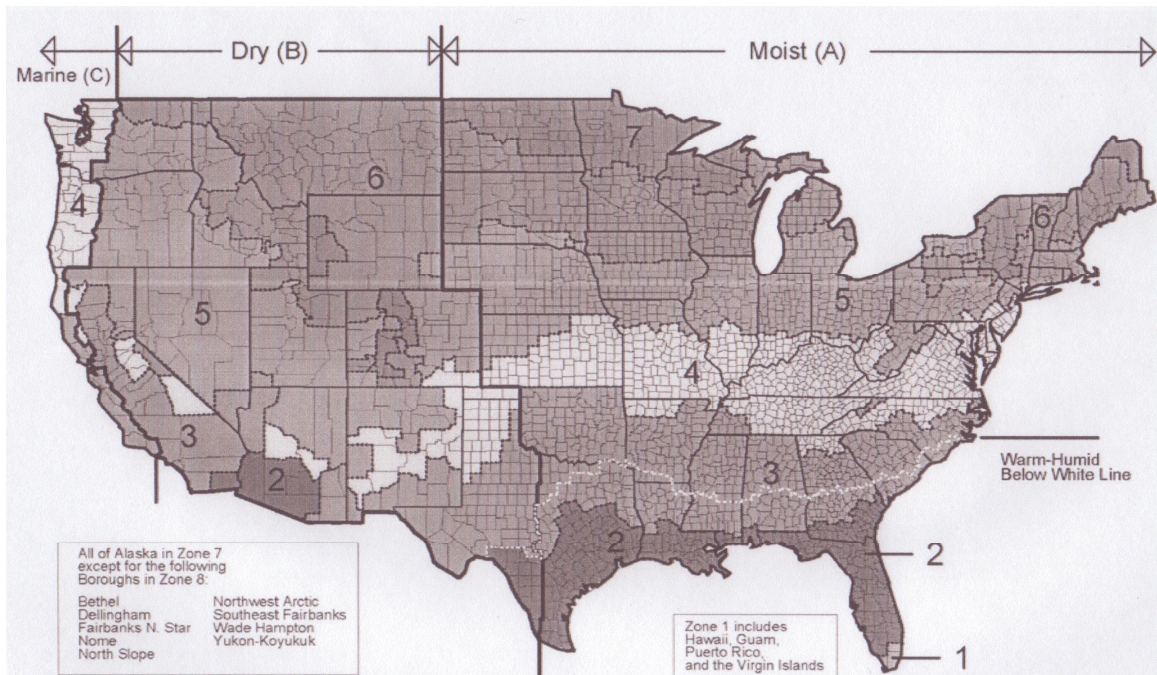


Figure 3.6: Climate Zones for the United States (ASHRAE, 2007)

3.5.1.1 Roof Insulation

ASHRAE 90.1-1999 requires that the roof have composite U-values of no more than 0.063 BTU/hr-ft²-°F (0.358 W/m²-K). This equates to an insulation level of approximately R-16. The roof insulation specified for this building includes R-30 insulation. This amount of insulation plus the other roof construction components presented in the proposed design details resulted in a U-value of 0.018 BTU/hr-ft²-°F (0.102 W/m²-K). The roof U-value of the proposed design is over 70% more efficient than the ASHRAE 90.1-1999 minimum requirement. Since the original energy modeling was performed, the latest ASHRAE Standard, ASHRAE 90.1-2007, now requires that the roof have composite U-values of no more than 0.48 BTU/hr-ft²-°F (2.73 W/m²-K) which equates to an insulation level of approximately R-21. This new U-value still leaves the proposed (now actual) building exactly 62.5% more efficient than the minimum ASHRAE requirement.

The design thickness and resistance values are illustrated below in Table 3.4 for the roof construction.

Table 3.4: Roof Construction

R_v	Construction	Thickness (inches)	Resistance (°F-hr-ft ² / BTU)
$R_{\text{Roof},1}$	Built-Up Roof	3/8	0.33
$R_{\text{Roof},2}$	Expanded Polyurethane Insulation	4	25.06
$R_{\text{Roof},3}$	Expanded Polyurethane Insulation	4	25.06
$R_{\text{Roof},4}$	Light Weight Concrete	8	3.20

3.5.1.2 Exterior Wall Construction and Insulation

ASHRAE 90.1-1999 requires that the exterior walls have composite U-values of no more than 0.151 BTU/hr-ft²-°F (0.857 W/m²-K). The construction components of the exterior walls presented in the proposed design details resulted in U-values ranging from 0.042 BTU/hr-ft²-°F (0.239 W/m²-K) for the brick wall constructions to 0.06 BTU/hr-ft²-°F (0.341 W/m²-K) for the glazed aluminum curtain wall constructions. The wall U-values of the proposed design are between 60% and 72% more efficient than the ASHRAE 90.1-1999 minimum requirement. Since the original energy modeling was performed, the latest ASHRAE Standard, ASHRAE 90.1-2007, now requires that the exterior walls have composite U-values of no more than 0.123 BTU/hr-ft²-°F (0.698 W/m²-K) which equates to an insulation level of approximately R-8. This new U-value still leaves the proposed (now actual) building between 51% and 66% more efficient than the minimum ASHRAE requirement.

The design thickness and resistance values are illustrated below in Table 3.5 for the glazed aluminum curtain wall construction and in Table 3.6 for the brick wall construction.

Table 3.5: Glazed Aluminum Curtain Wall Construction

R_v	Construction	Thickness (inches)	Resistance (°F-hr-ft ² / BTU)
$R_{CW,1}$	Spandrel Glass	1/4	1.70
$R_{CW,2}$	Air Layer	< 4	0.89
$R_{CW,3}$	Particle Board Underlay	5/8	0.29
$R_{CW,4}$	Mineral Wool Batt Insulation	4	13.00
$R_{CW,5}$	Gypsum Board	5/8	0.56

Table 3.6: Brick Wall Construction

R_v	Construction	Thickness (inches)	Resistance ($^{\circ}\text{F}\cdot\text{hr}\cdot\text{ft}^2 / \text{BTU}$)
$R_{\text{BW},1}$	Common Brick	4	0.80
$R_{\text{BW},2}$	Air Layer	< 4	0.89
$R_{\text{BW},3}$	Hollow Light Weight Concrete Block	8	2.00
$R_{\text{BW},4}$	Expanded Polyurethane Insulation	3	18.80
$R_{\text{BW},5}$	Gypsum Board	5/8	0.56

3.5.1.3 Window Glazing

ASHRAE 90.1-1999 requires that glazing have U-values of no more than 0.57 BTU/hr-ft²-°F (3.24 W/m²-K). The specifications of the proposed design show that there exist two distinct glazing types in this building; clear and fritted. The U-value for both glazing types is 0.29 BTU/hr-ft²-°F (1.65 W/m²-K). This U-value is 50% more efficient than the ASHRAE 90.1-1999 minimum requirement. Since the original energy modeling was performed, the latest ASHRAE Standard, ASHRAE 90.1-2007, requires that window glazings have U-values of no more than 0.6 BTU/hr-ft²-°F (3.41 W/m²-K). This new U-value is surprisingly higher than the previous requirements which in turn allows the proposed (now actual) building to be increase to 52% more efficient than the minimum ASHRAE requirement.

ASHRAE 90.1-1999 requires that glazing have solar heat gain coefficients (SHGC) of no more than 0.39. The SHGC value for the clear glass is 0.37 and for the fritted glass is 0.29. The fritted glass is the upper pane of multi-pane glazing in many, but not all, spaces throughout the building. These multi-pane glazing were input as single glazing with weighted average SHGCs based on the percentage of the glass that is fritted versus clear. Two different configurations exist in this building. In one configuration,

the total glazing height is approximately 9½ feet (2.896 m) with the upper 2½ feet (0.762 m, or 26%) being fritted and the rest clear. This configuration resulted in an average SHGC of 0.35. The second configuration has a total glazing height of 7 feet (2.134 m) with the upper 2½ feet (0.762m, or 36%) being fritted and the rest clear. This configuration resulted in an average SHGC of 0.34. The SHGC of the glazing in the proposed design range from 5% more efficient for clear glass to 15% more efficient for fritted glass compared to the ASHRAE 90.1-1999 minimum requirement. Since the original energy modeling was performed, the latest ASHRAE Standard, ASHRAE 90.1-2007, now requires that windows have a maximum SHGC of 0.25. Unfortunately, this new SHGC still no longer allows for the window glazing to be used as an energy saving feature. Luckily the building was completed before the latest ASHRAE Standard 90.1 was released. Otherwise, the Klaus building would range from 14% less efficient for fritted glass to 32% less efficient for clear glass than the minimum ASHRAE requirements and therefore need to be redesigned before construction.

3.5.1.4 Use of Shading Devices

ASHRAE 90.1-1999 does not require exterior shades, other than the structure of the building, to be included in the baseline model. The proposed design drawings show overhangs and horizontal “sunscreens” that provide shading for some of the glazing. These shading devices were included in the proposed design model but not included in the baseline model. As a result, space solar heat gain through glazing is reduced, and thus the overall energy consumption is reduced.

3.5.1.5 Energy Efficient Lighting

The building area method, as specified in ASHRAE 90.1-1999, was used to define lighting density in both the proposed design and baseline models for the building. “School / University” lighting power densities shown in Table 9.3.1.1 of ASHRAE 90.1-1999 were used in the baseline model. The average lighting density for the Baseline building is 1.5 W/ft². Actual lighting power density was obtained from the lighting drawings of the proposed design. The average lighting density of the proposed building is about 1.14 W/ft². The proposed design lighting density is about 24% more efficient than the ASHRAE 90.1-1999 minimum requirement. Since the original energy modeling was performed, the latest ASHRAE Standard, ASHRAE 90.1-2007, states that average “school / university” lighting power density is 1.2 W/ft². Although closer to the proposed (now actual), this new lighting density still leaves the building 5% more efficient than the minimum ASHRAE requirement.

3.5.1.6 Occupancy Sensor Lighting Controls

ASHRAE 90.1-1999 does not require interior lighting to be controlled by occupancy sensors. The proposed design specifies the lights in interior offices, all bathrooms and a total of five conference rooms be switched off by occupancy sensors when the spaces are unoccupied. These occupancy sensor lighting controls were included in the proposed design model but not included in the Baseline model. This reduced excess lighting energy, as well as space cooling load, which reduced annual energy consumption.

3.5.1.7 Use of Daylighting

ASHRAE 90.1-1999 does not require daylighting. The proposed design specifies dimmable ballasts with daylighting control for the lights in the exterior offices. These controls dim the lights when natural light enters the space. If the natural light provides all of the lighting needed, the daylight controls turn off the electric lights. These daylighting controls were included in the proposed design model but not included in the baseline model. This too reduced excess lighting energy, as well as space cooling load, which reduced annual energy consumption.

3.5.1.8 Air Distribution System Type

ASHRAE 90.1-1999 states that the baseline model's heating, ventilating and air-conditioning (HVAC) systems serving this building is simulated as variable air volume (VAV) systems with terminal reheat and with a minimum air flow rate of 0.4 cfm per square foot of floor area. The air system type of air handling units (AHU) AHU-1, 2 and 4 serving most of the areas in this building are VAV systems but they have parallel fan powered boxes serving perimeter zones. The minimum primary air flow rates of parallel fan powered boxes are typically less than terminal reheat boxes. As a result, overcooling and reheating energy is less in the proposed design building when compared with the baseline building.

3.5.1.9 Utilizing an Airside Economizer

ASHRAE 90.1-1999 does not require an airside economizer on HVAC systems in the Atlanta climatic region. The proposed design shows that AHU-1, 2 and 4 have an

airside economizer. An airside economizer reduces cooling energy during mild weather when outside air is cooler than return air.

3.5.1.10 Utilizing Heat Recovery

ASHRAE 90.1-1999 does not require heat recovery on HVAC systems in the Atlanta climatic region. The proposed building has AHU-1, 2 and 4 serving the majority of the areas in the building and utilizes energy recovery wheels.

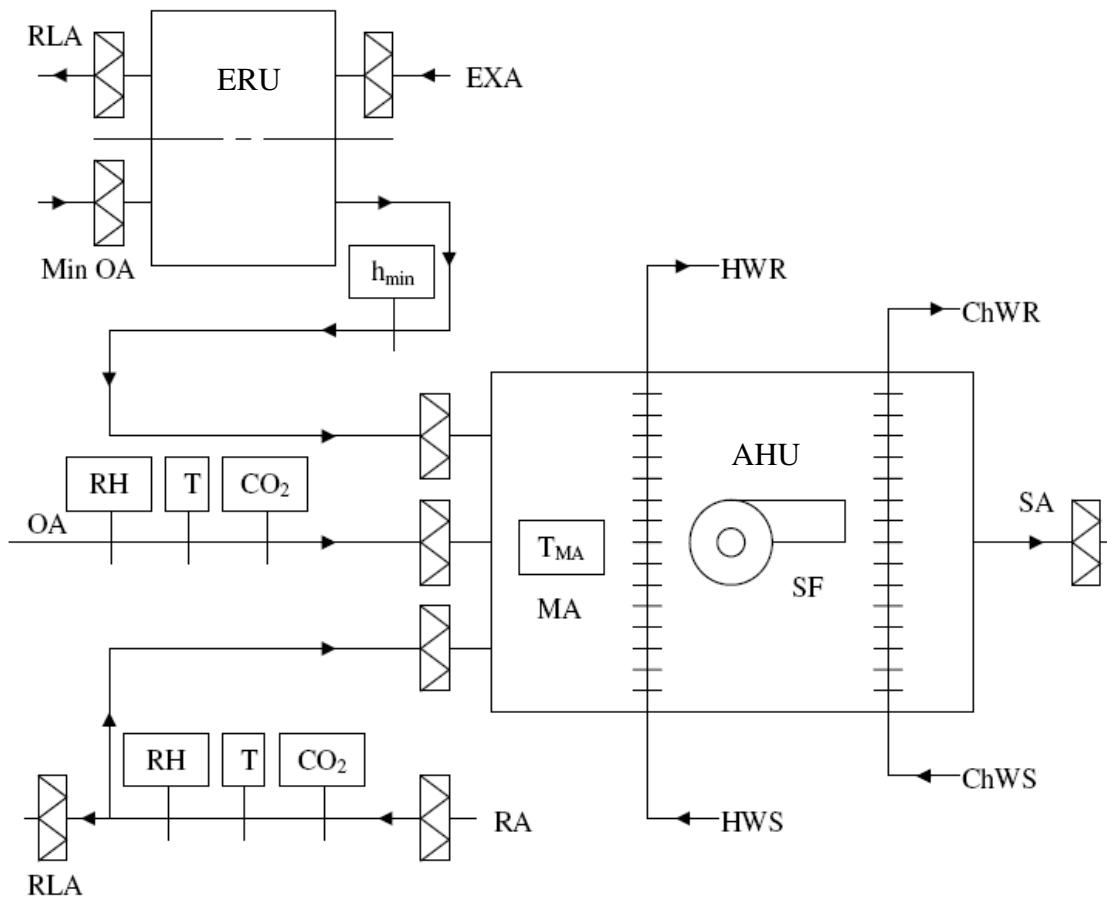


Figure 3.7: Sample Air Handling Unit Working with the Energy Recovery Unit

The energy recovery wheels recover sensible and latent energy from the relief air to heat or cool incoming outside air before introducing it to the AHUs. Depending on the season, the energy recovery wheels work to reduce the heating or cooling loads of the AHUs. As a result, the steam and chilled water consumption are reduced.

3.5.1.11 Chilled Water Temperature Difference

ASHRAE 90.1-1999 requires that the chilled water (CHW) temperature difference be 12°F (44°F supply and 56°F return). The proposed design specifies a 14°F temperature difference between CHW supply and return. The higher the CHW temperature difference is, the lower the CHW flow rate is required to be to deliver the same cooling capacity to the building AHUs. As a result, the proposed design has lower unit pumping power than the ASHRAE 90.1-1999 minimum requirement, and therefore consumes less energy.

3.5.1.12 Hot Water Pump Control

ASHRAE 90.1-1999 requires that the Baseline building hot water (HW) pumping system be modeled as primary only with continuous variable flow. It also states that the variable flow control be accomplished via variable speed drives for pumps that are greater than 50 horsepower (HP) and pump head exceeds 100 feet. Otherwise, pumps shall be modeled as a constant speed pump riding the pump curve. The building HW pump specified in the proposed design is 40 HP. As such, it was modeled as a constant speed pump riding the pump curve in the baseline model. The proposed design specifies a variable speed drive for the 40 HP HW pump. A pump with a variable speed drive is much more energy efficient than a pump riding on the pump curve. Therefore, the

proposed design HW pumping control is more energy efficient than the ASHRAE 90.1-1999 minimum requirements.

Now with the basic knowledge of the chosen example building, the next step is to monitor the pertinent weather and load data associated with the example building such that accurate models and calculations can be performed on said building.

4 MONITORING AN EXAMPLE BUILDING

In order to understand what is truly happening within a building, it must be monitored. Additionally, a building can also be modeled since a building simulation model's goal is to accurately represent the idealized behavior of the building as a whole. However, to best comprehend the loads within a building, a mixture of monitoring and modeling must be accomplished.

A building in its entirety acts as a control volume. Therefore, the first step before monitoring or modeling a building is to determine the energy sources which affect that control volume. There are eight energy sources which affect a typical building control volume. These energy flows are heating (\dot{Q}_H), cooling (\dot{Q}_C), outside air flow (\dot{Q}_{OA}), return air flow (\dot{Q}_{RA}), internal loads from people (\dot{Q}_{People}), lighting and equipment (\dot{W}_e), and skin loads from solar heat gain (\dot{Q}_{SG}) and conduction through walls (\dot{Q}_{Cond}). How these energy loads work can best be shown through the energy balance equation where

$$\frac{dE}{dt} = \dot{Q}_H - \dot{Q}_C + \dot{Q}_{OA, \text{total}} + \dot{Q}_{\text{Internal}} + \dot{Q}_{\text{Skin}} \quad (4.1)$$

The outside air energy flow on the right hand side of the above equation is actually a fluid enthalpy flow while the people part of the internal load is heat and fluid enthalpy; but the \dot{Q} symbol is used as a mere mnemonic. Also, please note that as usual the negligible (in energy terms) condensate flow is omitted. The typical energy flows discussed above which affect a building are illustrated below in Figure 4.1.

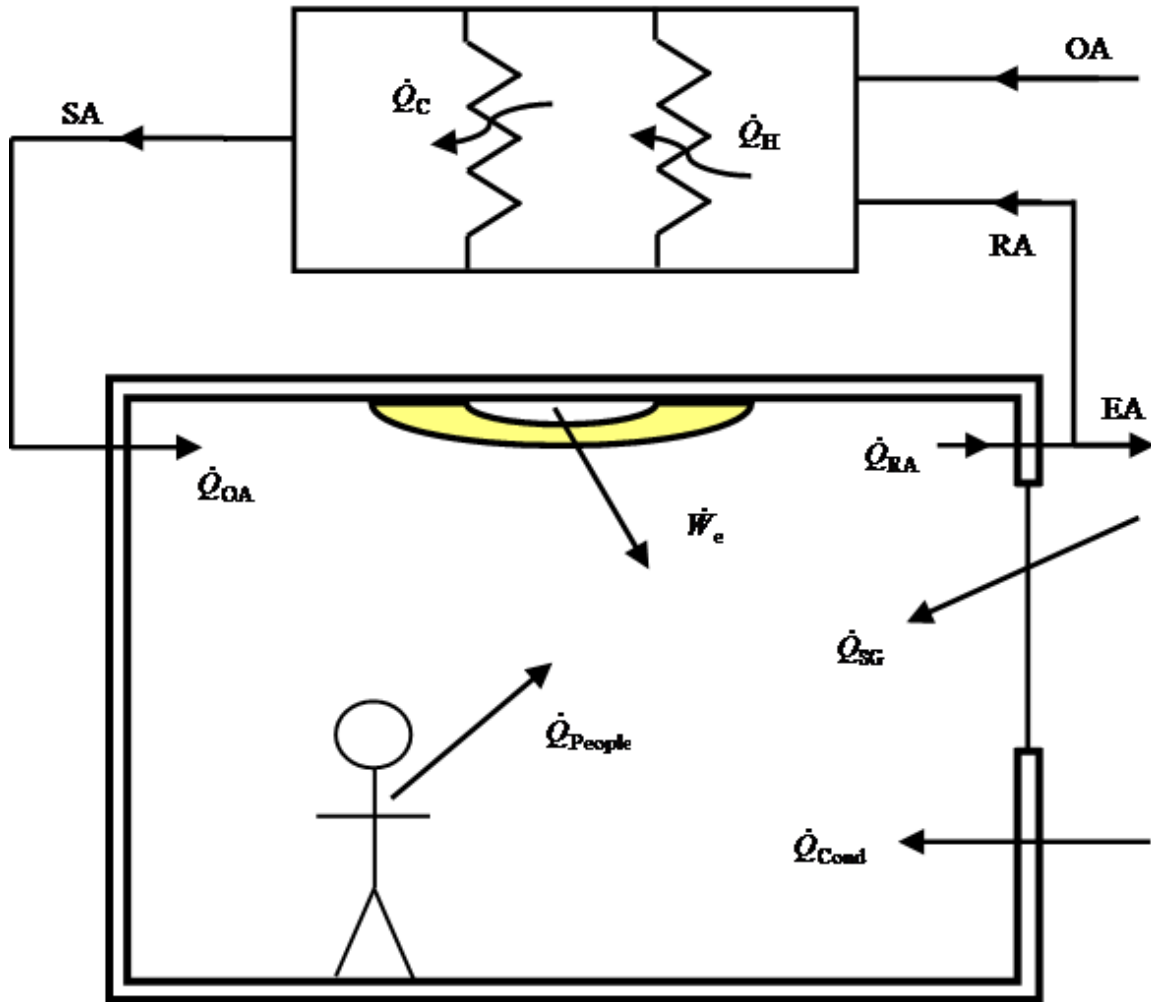


Figure 4.1: Typical Energy Flows in a Control Volume Building

Since the building is pressurized, it has been assumed that there is no infiltration load to consider. However, from the energy balance above, five major load components have been established: heating, cooling, outside air, internal and skin loads. Three of these loads, however, first need to be simplified for better understanding where

$$\frac{dE}{dt} = \dot{Q}_H - \dot{Q}_C + \dot{m}_{OA}(h_{OA} - h_{RA}) + (\dot{Q}_{Cond} + \dot{Q}_{SG}) + (\dot{Q}_{People} + \dot{W}_e) \quad (4.2)$$

The main elements of a building which needs to be monitored can be taken from the above energy balance. These loads have been monitored through three different

means, as presented below in Section 4.1: Monitoring Principles. After the data have been collected, each load must be calculated as discussed in the next chapter. And, finally, the calculated loads are then used in various models.

4.1 *Monitoring Principles*

In order to be able to model what is actually happening within the KACB, the energy consumption rates, pertinent environmental data, and load indicators have been monitored and collected. The energy consumption rates and load indicators have been collected daily through the Metasys, a program that allows users to view and collect data which has been provided and maintained by Johnson Controls Inc (JCI). The pertinent environmental data, however, has been collected and compared by three different sources: Metasys, the National Oceanic and Atmospheric Administration (NOAA), and the University of Georgia (UGA). Please refer to Section 4.1.3: Weather Data Comparisons for sample weather comparisons between the three data collection locations.

4.1.1 Raw Data Collection

The following three sections (Metasys, NOAA and UGA) will briefly describe the raw data collection associated with each system. However, for a more detailed look at how the data was collected and processed, please refer to the Appendices.

4.1.1.1 Metasys Data

In order to retrieve collected data from JCI's Metasys program for the Klaus Advanced Computing Building on Georgia Tech's campus, one either needs to be logged on to a Georgia Tech Facilities Department computer or virtually connect through the GT

Controls Network before even logging onto Metasys. Once Metasys has been opened, please refer to APPENDIX L: Directions for Metasys Data Collection, which goes through a sample step-by-step collection process for the Mixed Air Temperature 1 (MAT 1) of Air Handling Unit 1 (AHU 1). However, for the purposes of this thesis, the 41 data samples listed in Table 4.1 and Table 4.2 were collected, all using a similar collection process to that of the MAT 1 from AHU 1. The associated 95% expanded uncertainties are also given along with where the uncertainty information can be found.

For the complete Metasys sensor identification call numbers, please refer to APPENDIX I: Metasys Sensor Identification Numbers.

Table 4.1: Data Samples Collected from KACB, Part 1

	Sensor	Type	Uncertainty	Source
Electrical	Building Power	Watt Meter	1 W	Johnson Controls, 2007
	Building Power Demand	Watt Meter	1 W	
	Building Energy	Watt-Hour Meter	1 Wh	
	Emergency Power	Watt Meter	1 W	
	Emergency Power Demand	Watt Meter	1 W	
	Emergency Energy	Watt-Hour Meter	1 Wh	
	SWBD A Power	Watt Meter	0.1 kW	
	SWBD A Power Demand	Watt Meter	0.1 kW	
	SWBD A Energy	Watt-Hour Meter	0.1 kWh	
	SWBD B Power	Watt Meter	0.1 kW	
	SWBD B Power Demand	Watt Meter	0.1 kW	
	SWBD B Energy	Watt-Hour Meter	0.1 kWh	

Table 4.2: Data Samples Collected from KACB, Part 2

	Sensor	Type	Uncertainty	Source
Chilled Water	Building Flow	Ultrasonic	0.1 gpm	Taco, 2005
	Return Temperature	RTD	1 °F	
	Supply Temperature	RTD	1 °F	
	Return Pressure	Gauge	1 psi	
	Supply Pressure	Gauge	1 psi	
Hot Water / Steam / Condensate	Supply Temperature	RTD	1 °F	Taco, 2005
	Return Temperature	RTS	1 °F	
	Steam Pressure	Gauge	2.5 psi	
	Condensate Flow	Pulse	10 gal	
Outside Air Conditions	Temperature	RTD	1 °F	Taco, 2005
	Carbon Dioxide	Infrared	1 ppm	
	Relative Humidity	Hygrometer	1 %	
Return Air Conditions	AHU 1 & 2 Temperature	RTD	1 °F	Trane, 2004
	AHU 1 & 2 Relative Humidity	Hygrometer	1 %	
	AHU 1 & 2 Carbon Dioxide	Infrared	1 ppm	
	AHU 3 Temperature	RTD	1 °F	
	AHU 3 Relative Humidity	Hygrometer	1 %	
	AHU 3 Carbon Dioxide	Infrared	1 ppm	
	AHU 4 Temperature	RTD	1 °F	
	AHU 4 Relative Humidity	Hygrometer	1 %	
AHU 4 Carbon Dioxide	Infrared	1 ppm		
Mixed Air Conditions	AHU 1 Temperature	RTD	1 °F	Trane, 2004
	AHU 2 Temperature	RTD	1 °F	
	AHU 4 Temperature	RTD	1 °F	
Static Pressure	AHU 1 & 2	Differential	0.25 in wc	Trane, 2004
	AHU 4	Differential	0.25 in wc	
Fan Frequency	AHU 1	Multimeter	1.8 Hz	Trane, 2004
	AHU 2	Multimeter	1.8 Hz	
	AHU 4	Multimeter	1.8 Hz	

Not all of the above mentioned data was actually used in the KACB models. However, it was thought to be better safe than sorry and collect the additional data just in case it was later needed.

Even though outside air data is collected at the KACB through Metasys, pertinent weather data has also been collected through two other sources for comparison. The other two sources are the National Oceanic and Atmospheric Administration (NOAA) and the University of Georgia (UGA). The NOAA weather data is collected at the Hartsfield-Jackson Atlanta International Airport, while the UGA weather data is collected on the University of Atlanta campus located in Downtown Atlanta. Even though both the NOAA and UGA data are collected in Atlanta, neither is collected on the Georgia Tech campus. However, since the three weather stations (KACB, NOAA, and UGA) are all in Atlanta, it has been assumed (and then demonstrated in the next section) that they are considered close enough to be compared and used for any required calculations. Please refer to Section 4.1.3: Weather Data Comparisons for sample weather comparisons between the three data collection locations.

4.1.1.2 National Oceanic and Atmospheric Administration Data

First of all, in order to retrieve *free* weather data from NOAA, one needs to be connected to the internet from a .edu address or computer. Next, connect to following the National Climatic Data Center (NCDC), a subsidiary of NOAA website: <http://cdo.ncdc.noaa.gov/ulcd/ULCD> from which unedited local climatological data can be obtained. Once on the above mentioned website, please refer to APPENDIX M: Directions for NOAA Data Collection, which goes through a sample step-by-step collection process for hourly weather observations for May 2008. This NOAA weather data is collected at the Hartsfield-Jackson Atlanta International Airport. However, this data was never actually used for any required calculations, only weather data comparisons.

4.1.1.3 The University of Georgia Data

Unlike the free data collected from Metasys and NOAA, the data collected from the University of Georgia (UGA) has been purchased. Dr. Gerrit Hoogenboom, from the Department of Biological and Agricultural Engineering at UGA, is the person in charge of this data collection and distribution. Each month is available for purchase for a small fee of \$25/month. For logistical reasons, all of 2007 and all of 2008 (through September) have been purchased. Even though the UGA data provides much more data than is needed, the data which does get utilized are the temperature, relative humidity and solar radiation data for load calculations. Much of the other weather data collected through UGA was also used to create a mock-TMY weather file which is further discussed in Section 5.2.3.2: TMY Weather Data. Even though the UGA data is available in 15 minute increments, 30 minute increments will be used to best match up incrementally with the data collected from Metasys. Since this data was purchased, the processing was simplified once it was confirmed that there were no data gaps present. For the complete list of weather data collected from UGA, please refer to APPENDIX J: UGA Weather Data. The monitored location of the purchase UGA weather data is 33.74789° N, -84.41439° W which is very similar to the location of the Klaus building at 33.77752° N, -84.39413° W.

4.1.2 Processing the Raw Data

All of the data collected through Metasys, NOAA and UGA was, unfortunately, raw data which needed to be processed. Not only did each data source need its own form of processing, but many of the data sets collected from Metasys needed special attention.

However, since the UGA raw data was purchased, it had already been thoroughly processed before being obtained.

The main problem with the raw Metasys data was that there were extra erroneous data points continuously added throughout. These erroneous data points typically occurred at 29 or 59 minutes past the hour, whereas the accurate data would occur only on the hour and half hour. When the erroneous data did occur, the correct data typically would also appear. Therefore, these extra data points at 29 or 59 minutes past the hour would need to be removed as to eliminate superfluous data for calculations. Even though the majority of the inconsistent data occurred at 29 or 59 minutes past the hour, there were occasions for which erroneous data at other times also occurred. This data processing is particularly important as to maintain the correct number of hours (and half hours) throughout the year in their correct order as to not impede the accuracy of the model calculations.

This erroneous data problem was also prevalent with the collected NOAA weather data. However, unlike the Metasys data which was collected in half hour increments, the NOAA data is only collected hourly at 52 minutes past the hour. Therefore, the erroneous NOAA data processing needed to find all of the data which did not occur at 52 minutes past the hour. In any given month, there are typically between 100 and 200 extra recorded NOAA data points.

The data processing to find the extra data points from Metasys and NOAA took place both manually and through programming. Since there were so many exceptions to where/when the extra data points would occur, the programming would act as a good back up to the manual check, and vice versa. However, since the data was all collected

and placed into Excel documents, the processing was also done using Excel. Luckily, this was also found to be the easiest and best method for the data processing.

The final step to the data processing, more for the Metasys data than any of the other sources, was to verify that there was no missing data. For the Metasys data, there needed to be data present for every thirty minute increment on every hour and half hour in order to authenticate usable data. If, for some reason, there did happen to be a location or two in which there was data missing, a space would need to be added to indicate the absent time slot. This missing data point, or points, would be left blank as a reminder to have it later omitted during modeling. Fortunately, this rarely occurred. However, in a final effort to only utilize the accurate data, the final modeling code is instructed to skip any “empty” or “null” data cells to insure more accurate calculations. Please refer to the various Appendices for the exact code used for each specific load, within which “go to” statements were included to skip over the “empty” or “null” data cells.

4.1.3 Weather Data Comparisons

A typical building does not come equipped with a weather station. However, if a building is to be monitored or modeled correctly, the outside air and solar radiation data are needed. Weather data networks, however, are readily available and have been shown to be more reliable than an individual building’s instrumentation. For example, the outside air weather station on top of the Klaus building appears to be acceptable as illustrated below in Figure 4.2, Figure 4.3, and Figure 4.4.



Figure 4.2: Outside Air Weather Station on the Roof of the Klaus Building



Figure 4.3: Location of Outside Air Weather Station on the Roof of the Klaus Building

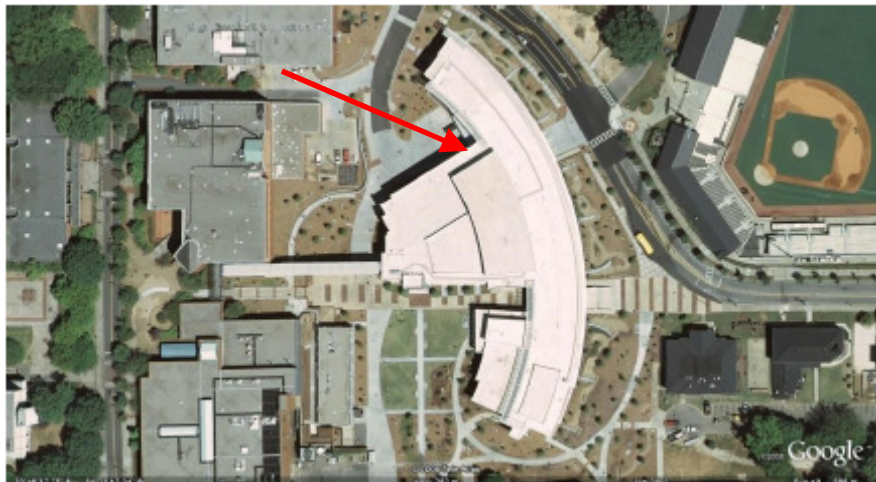


Figure 4.4: Outside Air Weather Station Location on the Roof of the Klaus Building as Seen from Google Earth (Google, 2008).

However, when data collection began for the Klaus building, the outside air temperature and relative humidity conditions did not seem to be quite right. In August 2007, the outdoor air temperature at the Klaus building consistently recorded days well above 100°F, while the relative humidity regularly jumped 70-80% in one day. As a third way to check the outdoor air conditions, the humidity ratio was calculated. If the data had been realistic, the humidity ratio would have stayed consistently around 0.015. Instead, there were large daily fluctuations.

Since the outside weather data being collected at the Klaus building through the Metasys program did not appear accurate enough, pertinent weather data was then collected through two other weather data network sources in Atlanta for comparison. The other two network sources are the National Oceanic and Atmospheric Administration (NOAA) and the University of Georgia (UGA).

The first two weather comparisons done between the three sites were for temperature and relative humidity throughout August 2007, and are illustrated below in Figure 4.5 and Figure 4.6:

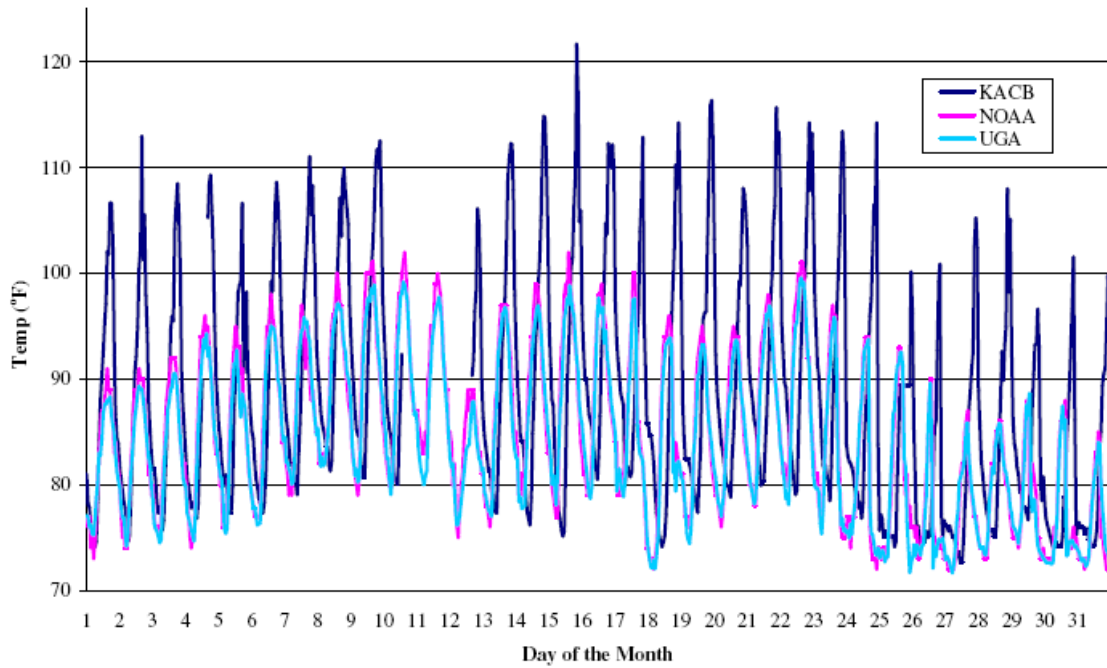


Figure 4.5: Outside Air Temperature Comparisons for August 2007

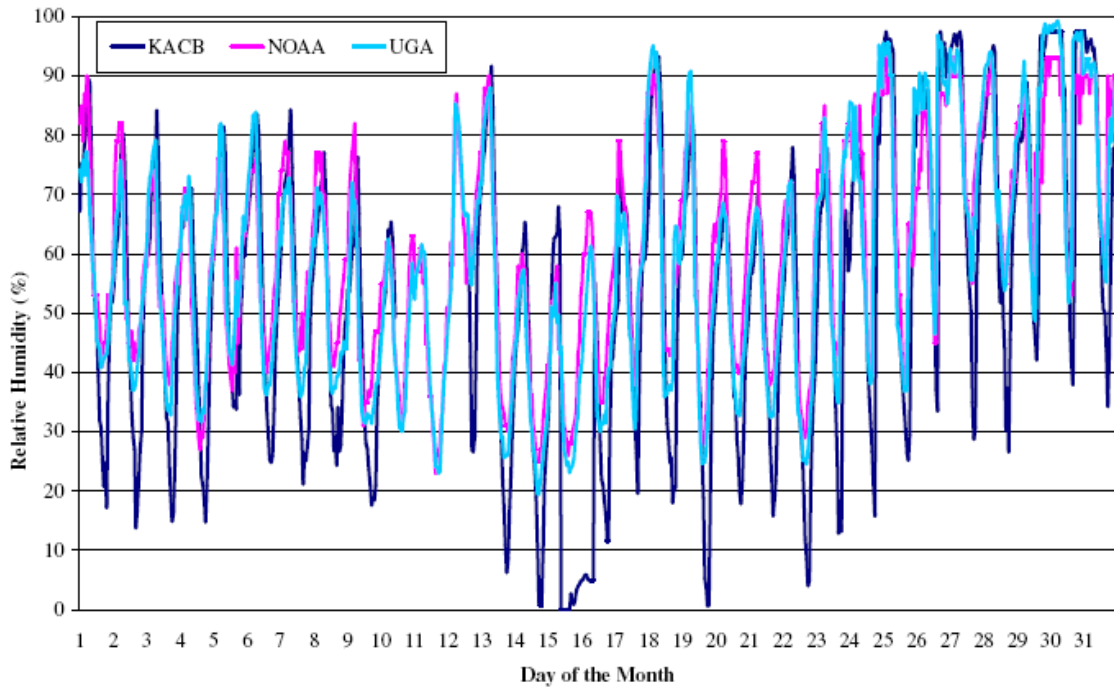


Figure 4.6: Outside Air Relative Humidity Comparisons for August 2007

As illustrated above, the temperature and relative humidity data collected at the Klaus building fluctuates much more than either of the other two sources, which leads one to believe that this data is not correct. This error is thought to be due to a “heat island” effect around where the temperature and relative humidity sensors are atop the Klaus building, even though the weather station set up (previously illustrated on page 53) appears to have been appropriately placed and installed.

However, the temperature and relative humidity weather data from both NOAA and UGA do appear to be in much more consistent and in better agreement. This correlation has been quantified through regression analysis which illustrates a great agreement between the NOAA and UGA data such that the temperature $R^2 = 0.96$ while the relative humidity $R^2 = 0.91$. Through a regression analysis, the uncertainty between the NOAA and UGA temperature data was found to be 0.172°F while the uncertainty between the NOAA and UGA relative humidity data was found to be $0.568\%RH$. This agreement is best noticed through the humidity ratio comparisons, once again for August 2007, as illustrated below in Figure 4.7:

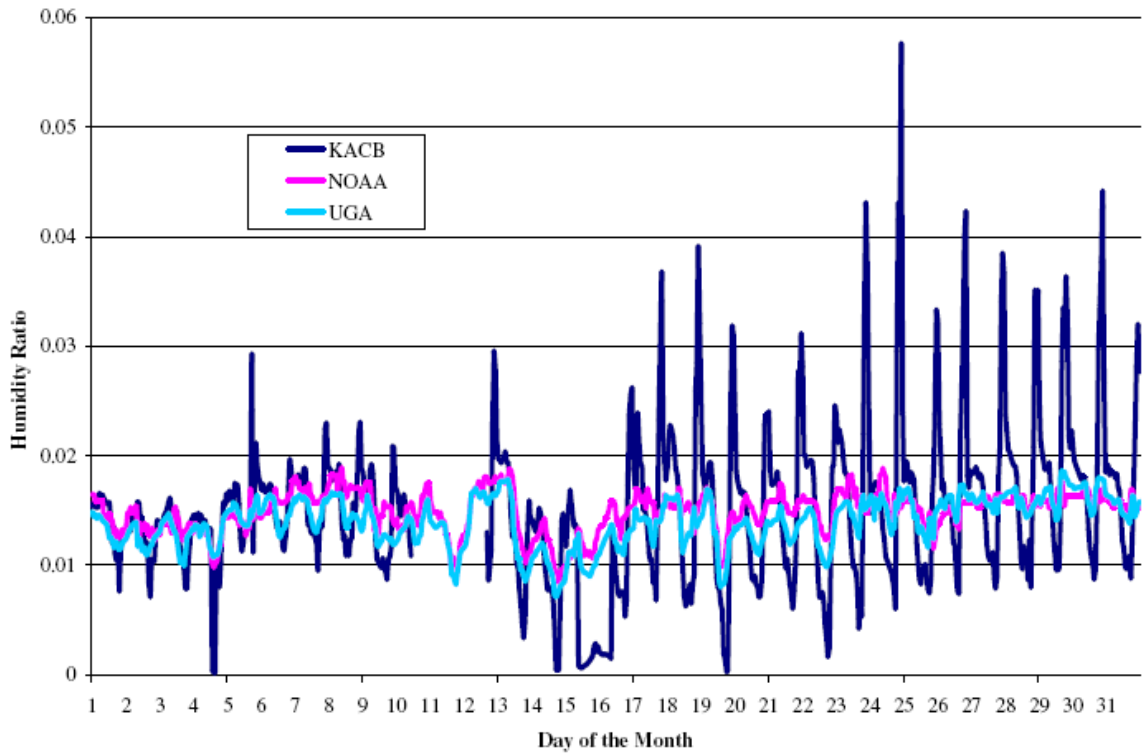


Figure 4.7: Humidity Ratio Comparisons for August 2007

Through a regression analysis, the uncertainty between the NOAA and UGA humidity ratio data was found to be 0.001. Since the NOAA and UGA data are in much better agreement than that of the outside weather data collected at the Klaus building, it has been assumed that either source would be suitable for use in future calculations.

4.2 Clear Sky Model

Now that the outside air conditions have been compared and confirmed, the next verification needed is for the solar radiation data, also collected from UGA. In order for this solar radiation data to be authenticated, a Clear Sky Model (CSM) has been developed. The purpose of the CSM is to establish how much solar radiation would be able to reach the Atlanta (more specifically, the Klaus building) at any given time throughout the year during ideally clear sky conditions.

In order to calculate the total radiation from the Clear Sky Model for Atlanta, first the beam normal radiation and sky dome radiation must be found

$$G_{\text{BN}} = G_{\text{BN,AM0}} \exp\left(\frac{-B_{\text{CS}}}{\sin \alpha}\right) \quad (4.3)$$

$$G_{\text{SD}} = F_{\text{CS}} G_{\text{BN}} \quad (4.4)$$

where $G_{\text{BN,AM0}}$ is the air mass zero apparent solar constant, B_{CS} is the atmospheric extinction coefficient, α is the solar altitude angle, and F_{CS} is the sky diffuse factor. The solar altitude angle is further discussed and calculated below in Section 5.1.4.1: Solar Calculations. However, $G_{\text{BN,AM0}}$, B_{CS} and F_{CS} are all constants which vary depending on the month. These values can be found below in Table 4.3 which is an excerpt from a table in the 2001 ASHRAE Fundamentals Handbook (ASHRAE, 2001).

Table 4.3: Extraterrestrial Solar Irradiation Constants (ASHRAE, 2001)

Month	$G_{\text{BN,AM0}}$ (BTU/hr-ft²)	B_{CS} (--)	F_{CS} (--)
January	390	0.142	0.058
February	385	0.144	0.060
March	376	0.156	0.071
April	360	0.180	0.097
May	350	0.196	0.121
June	345	0.205	0.134
July	344	0.207	0.136
August	351	0.201	0.122
September	365	0.177	0.092
October	378	0.160	0.073
November	387	0.149	0.063
December	391	0.142	0.057

Now that the beam normal radiation and the sky dome radiation have been calculated, the total irradiation on a tilted surface can be calculated as

$$G_T = G_{BN} \cos \theta_B + G_{SD} \left(\frac{1 + \cos \beta}{2} \right) + \rho_{FG} (G_{BN} \sin \alpha + G_{SD}) \left(\frac{1 - \cos \beta}{2} \right) \quad (4.5)$$

where θ_B is the incident angle, β is the tilt of a surface, ρ_{FG} is the foreground reflectance, α is the solar altitude angle, and G_{BN} and G_{SD} were calculated above. The incident angle, tilt and solar altitude angle are further discussed and calculated below in Section 5.1.4.1: Solar Calculations. However, a value of 0.2 is reasonable for the usual foreground reflectance and has been used for this Clear Sky Model.

Now that the Clear Sky Model has been calculated, the solar radiation data collected from UGA must be compared. The true test for accuracy is to verify that the UGA data not only follows the same pattern as the CSM, but that the UGA data never exceeds that of the CSM since the CSM illustrates the ideal data. This verification was accomplished using a “data movie” within Excel which allows weekly data to be viewed and compared where the x-axis represents the Julian day of the year. A sample of this data movie confirmation is provided below for the first week of January, April, July and October 2007 in Figure 4.8 - Figure 4.11:

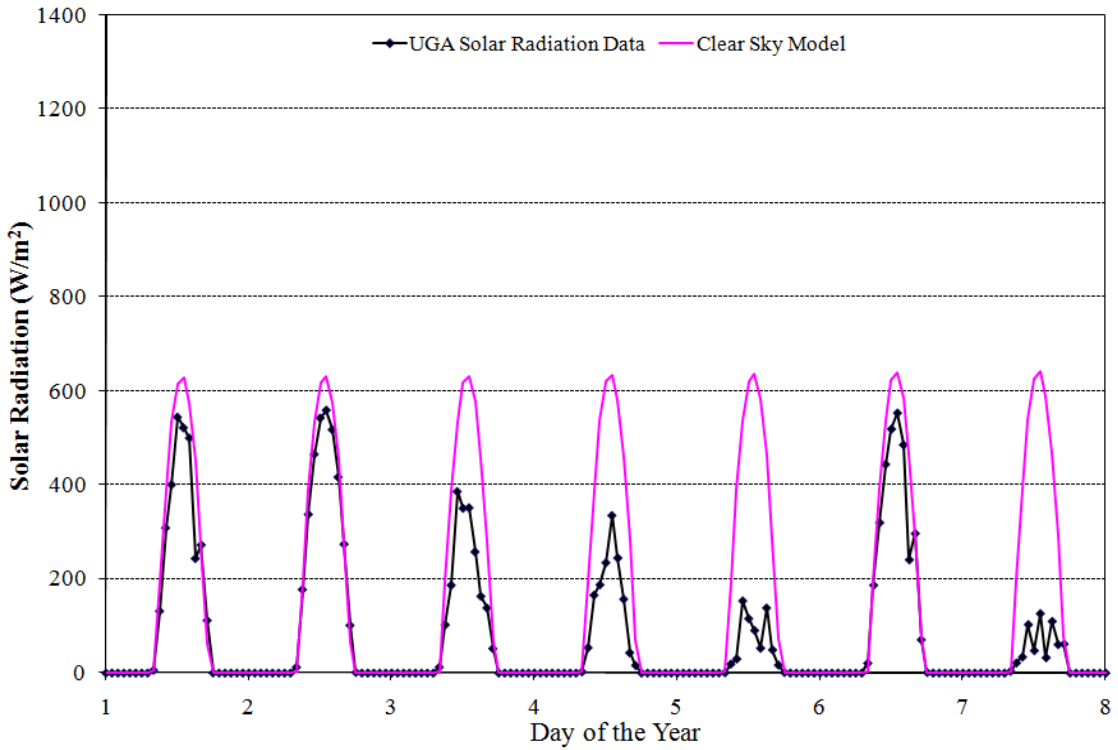


Figure 4.8: Solar Radiation Comparison, January 1st-7th, 2007

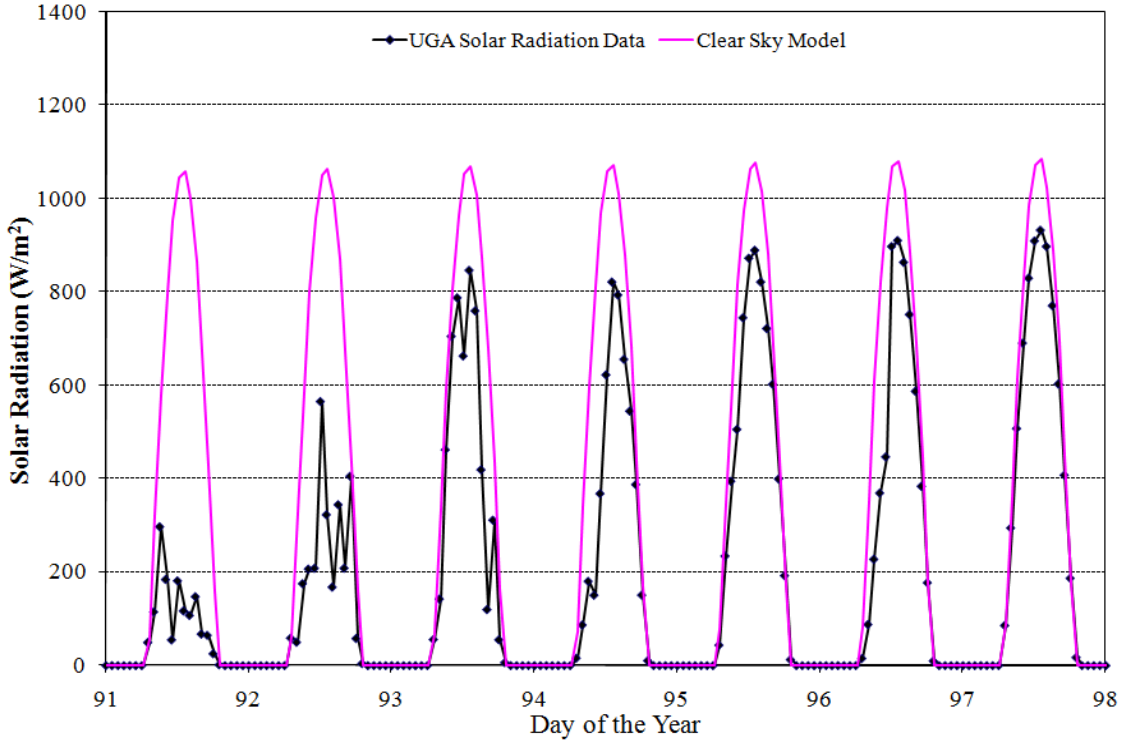


Figure 4.9: Solar Radiation Comparison, April 1st-7th, 2007

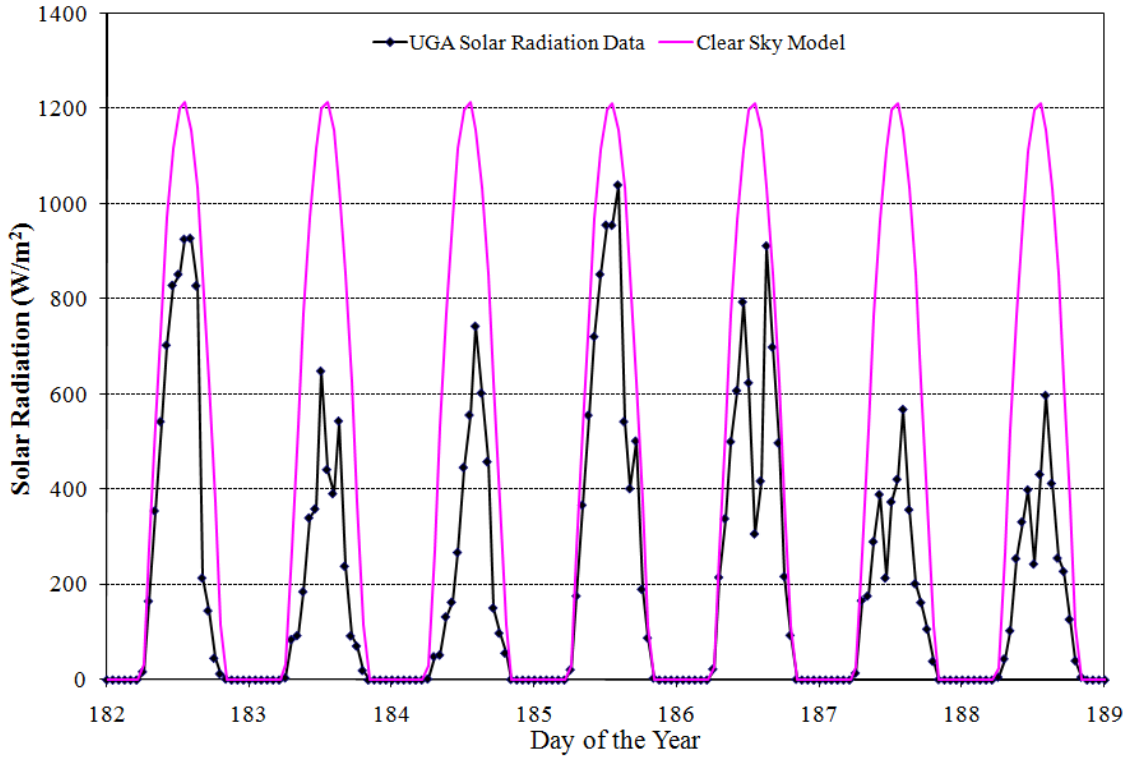


Figure 4.10: Solar Radiation Comparison, July 1st-7th, 2007

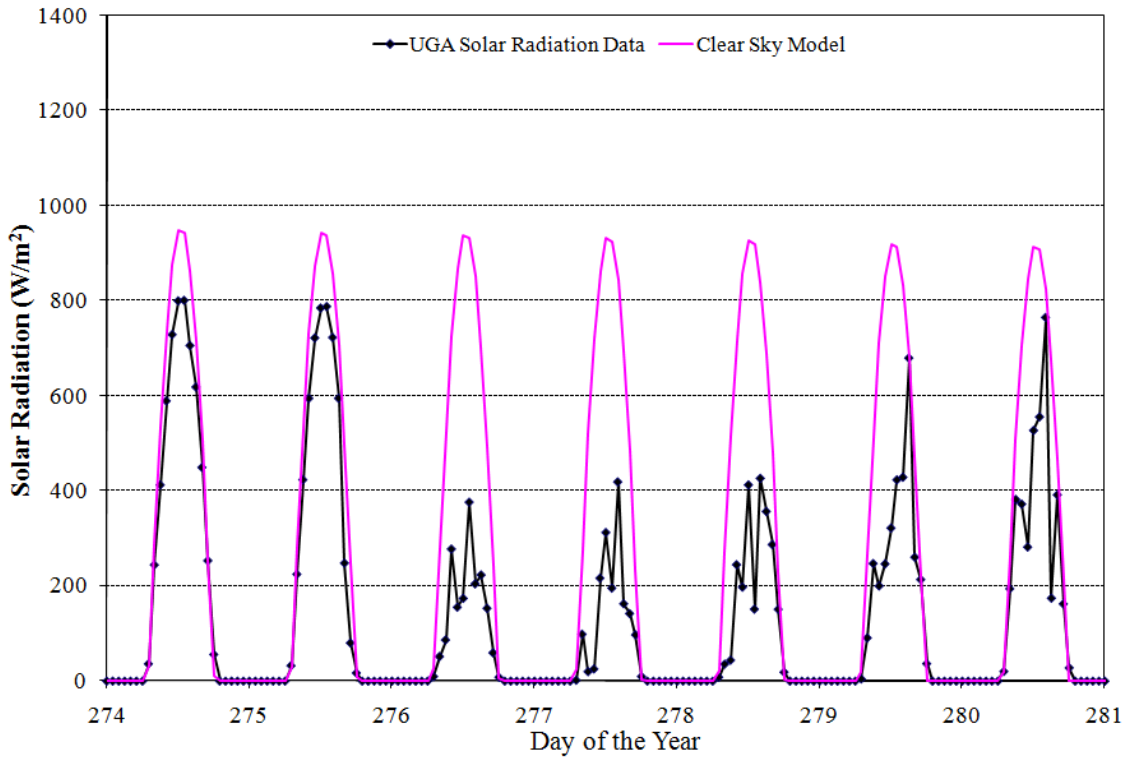


Figure 4.11: Solar Radiation Comparison, October 1st-7th, 2007

Not only does these figures illustrate excellent agreement between the CSM and the solar radiation data collected from UGA, but it also highlights cloudy days verses clear days. The similarities between the collected and CSM predicted solar radiation values validates that the solar radiation data collected from UGA is accurate enough to use for future calculations.

For the programming code which was used for the Clear Sky Model calculations within Excel's VBA, please refer to APPENDIX E: Clear Sky Model Code.

There is currently a new Meteorological (MET) Station being constructed on Georgia Tech's Atlanta campus. This MET station will also be equipped with a pyranometer array to collect necessary solar radiation data. This MET station will be used for future weather data and to confirm the UGA and NOAA data.

A typical pyranometer only collects total solar radiation data, but for accurate monitoring and modeling, beam normal and sky dome radiation data is also needed. Please refer to Section 5.1.4.1.3: Decomposition of Global Radiation Data into Beam Normal and Sky Dome Radiation, which explains how beam normal and sky dome radiation data can be obtained from only total solar radiation data. This method will also be verified once the new Georgia Tech MET station is completed.

4.3 *Uncertainty Analysis*

Some uncertainty exists in almost every measurement, and, therefore, also in any number calculated from that measurement. From the use of a truncated Taylor series expansion, partial derivatives and uncertainties, one can calculate the overall uncertainty of a calculated measurement through error propagation analysis. Error propagation

analysis is a technique to determine how uncertainties in multiple contributing direct measurements affect the overall uncertainty of a calculated measurement. Error propagation analyses for a set of typical data for each representative loads (heating, cooling, internal, outside air, and envelope) are discussed below along with calculated uncertainties for typical data.

For example, when the heating load of the Klaus building is calculated (further discussed in Chapter 5), there are three main components: the volumetric flow of the condensate, the density of the liquid, and the change in enthalpy. Therefore, the overall uncertainty for the heating load can be determined as

$$U_{\dot{Q}_H} = \sqrt{\left(\frac{\partial \dot{Q}_H}{\partial \dot{V}_{CND}} U_{\dot{V}_{CND}}\right)^2 + \left(\frac{\partial \dot{Q}_H}{\partial \rho_{liq}} U_{\rho_{liq}}\right)^2 + \left(\frac{\partial \dot{Q}_H}{\partial \Delta h} U_{\Delta h}\right)^2} \quad (4.6)$$

where the partial derivative of the heating load is taken with respect to each variable, multiplied by the uncertainty of that variable, squared is considered an influence coefficient. The overall uncertainty as determined by error propagation analysis is the square root of the sum of all of the influence coefficients. An error propagation analysis has been performed on a typical heating load

Table 4.4: Heating Load Error Propagation Analysis

Variable	Typical Data	Units	U_j	Units	$\left(\frac{\partial \dot{Q}_H}{\partial x_j} U_{x_j}\right)^2$
\dot{V}_{CND}	3	ft ³ /min	0.10	ft ³ /min	792
ρ_{liq}	60	lbs/ft ³	0.25	lbs/ft ³	110
Δh	991	BTU/lbs	0.01	BTU/lbs	0.27
\dot{Q}_H	26400	BTU	800	BTU	

which corresponds to approximately 3.0% error. For the heating load, the influence coefficient related to the volumetric flow of the condensate was the largest. This means that any uncertainty associated with the heating load is most affected by the volumetric flow.

Similarly, the overall uncertainty for the cooling load can be determined as

$$U_{\dot{Q}_C} = \sqrt{\left(\frac{\partial \dot{Q}_C}{\partial \dot{V}_{CHW}} U_{\dot{V}_{CHW}}\right)^2 + \left(\frac{\partial \dot{Q}_C}{\partial \rho_{liq}} U_{\rho_{liq}}\right)^2 + \left(\frac{\partial \dot{Q}_C}{\partial C_P} U_{C_P}\right)^2 + \left(\frac{\partial \dot{Q}_C}{\partial \Delta T} U_{\Delta T}\right)^2} \quad (4.7)$$

An error propagation analysis has also been performed on a typical cooling load

Table 4.5: Cooling Load Error Propagation Analysis

Variable	Typical Data	Units	U_j	Units	$\left(\frac{\partial \dot{Q}_C}{\partial x_j} U_{x_j}\right)^2$
\dot{V}_{CHW}	645	ft ³ /min	1.0	ft ³ /min	117
ρ_{liq}	62	lbs/ft ³	0.01	lbs/ft ³	12
C_P	1	BTU/(lbs-°F)	0.001	BTU/(lbs-°F)	75
ΔT	14	°F	0.50	°F	27000
\dot{Q}_C	75600	BTU	2700	BTU	

which corresponds to approximately 3.6% error. For the cooling load, the influence coefficient related to the temperature change was the largest. This means that any uncertainty associated with the cooling load is most affected by the temperatures changing.

The overall uncertainty for the internal load considers the electrical and equipment load as well as the occupancy load such that

$$U_{\dot{Q}_{\text{Internal}}} = \sqrt{\left(\frac{\partial \dot{Q}_{\text{Internal}}}{\partial \dot{W}_e} U_{\dot{W}_e}\right)^2 + \left(\frac{\partial \dot{Q}_{\text{Internal}}}{\partial \dot{Q}_{\text{People}}} U_{\dot{Q}_{\text{People}}}\right)^2} \quad (4.8)$$

However, since the electrical and equipment uncertainties are negligible, and the occupancy loads are determined through estimations, the overall uncertainty of the internal loads is based off the accuracy of the occupancy estimations. This number may not be reliable and therefore should not be accounted for.

The overall uncertainty for the outside air load can be determined as

$$U_{\dot{Q}_{\text{OA}}} = \sqrt{\left(\frac{\partial \dot{Q}_{\text{OA}}}{\partial \dot{V}_{\text{OA}}} U_{\dot{V}_{\text{OA}}}\right)^2 + \left(\frac{\partial \dot{Q}_{\text{OA}}}{\partial \rho_{\text{OA}}} U_{\rho_{\text{OA}}}\right)^2 + \left(\frac{\partial \dot{Q}_{\text{OA}}}{\partial \Delta h} U_{\Delta h}\right)^2} \quad (4.9)$$

An error propagation analysis has also been performed on a typical outside air load

Table 4.6: Outside Air Load Error Propagation Analysis

Variable	Typical Data	Units	U_j	Units	$\left(\frac{\partial \dot{Q}_{\text{OA}}}{\partial x_j} U_{x_j}\right)^2$
\dot{V}_{OA}	41360	ft ³ /min	1800	ft ³ /min	410
ρ_{OA}	0.071	lbs _{DA} /ft ³	0.001	lbs _{DA} /ft ³	130
Δh	3.24	BTU/lbs _{DA}	0.01	BTU/lbs _{DA}	29
\dot{Q}_{OA}	9400	BTU	430	BTU	

which corresponds to approximately 4.6% error. For the outside air load, the influence coefficient related to the volumetric flow of the outside air was the largest. This means that any uncertainty associated with the outside air load is most affected by the volumetric flow.

And, finally, the overall uncertainty for the envelope load can be determined as

$$U_{\dot{Q}_{\text{Skin}}} = \sqrt{\left(\frac{\partial \dot{Q}_{\text{Skin}}}{\partial \dot{Q}_{\text{Cond},\tau}} U_{\dot{Q}_{\text{Cond},\tau}}\right)^2 + \left(\frac{\partial \dot{Q}_{\text{Skin}}}{\partial \dot{Q}_{\text{SHG}}} U_{\dot{Q}_{\text{SHG}}}\right)^2} \quad (4.10)$$

An error propagation analysis has also been performed on a typical envelope load which estimates approximately 2.4% error for a typical skin load calculations. For the envelope load, the influence coefficient related to the solar heat gain load from the windows was the largest. This means that any uncertainty associated with the envelope load is most affected by the windows and not the walls, which is to be expected.

Now that the monitoring of the example building's data and its associated uncertainties has been discussed, the next step is to calculate the various loads and models.

5 ANALYSIS AND MODELING OF EXAMPLE BUILDING

After the example building has been monitored, the collected data can then be used in a variety of load calculations. These load calculations include heating, cooling, outside air, skin and internal loads which are described below in Section 5.1. After the various loads have been calculated, models can be created. Three new models are discussed below in Section 5.2, the monitored data, a single-zone model, and an eQUEST model.

The example building has been modeled multiple ways to allow for more comparisons. Having several comparisons allows for a better understanding of the strengths and weaknesses of each model which, in turn, allows for simpler models with greater accuracy. Therefore, how data is calculated and models are constructed and compared is extremely critical to not only this research, but also for the future of understanding and comparing building loads as well as creating predictive load models.

However, the outside air and skin load calculations typically present problems for load analysis models. This chapter specially focuses on two new and uniquely innovative methods to calculate the outside air loads from minimal monitored information, a technique to accurately determine directional beam normal and sky dome radiation components from only one horizontal total solar radiation measurement, and two comparative methods for calculating the conduction skin loads. The addition of these three load calculation components made this research not only complete and feasible, but also allowed the load calculations to be accurately incorporated into a simplified single-zone model.

5.1 Load Calculations from Monitored Information

The Klaus building was modeled using the real time data which was collected during the monitoring process. The monitored data was then used to help determine the heating loads, cooling loads, outside air loads, skin loads, people loads and electrical loads. The load totals were then combined to determine the overall performance of the Klaus building. All of these calculations were completed in Excel using VBA code. The calculations were completed for each 30 minute increment which corresponds to the collected real time data. The total load calculations as well as the yearly estimates were found by summing the appropriate data. Each load type is discussed in more detail in each of the following sections.

5.1.1 Heating Loads

The heating load can be determined from the real time hot water/steam data. The saturated steam which entered the KACB came from the campus supply. There was, however, a flow meter which helped to determine how much of the campus steam passed through the Klaus building. The energy flow diagram for the heating loads is illustrated below in Figure 5.1:

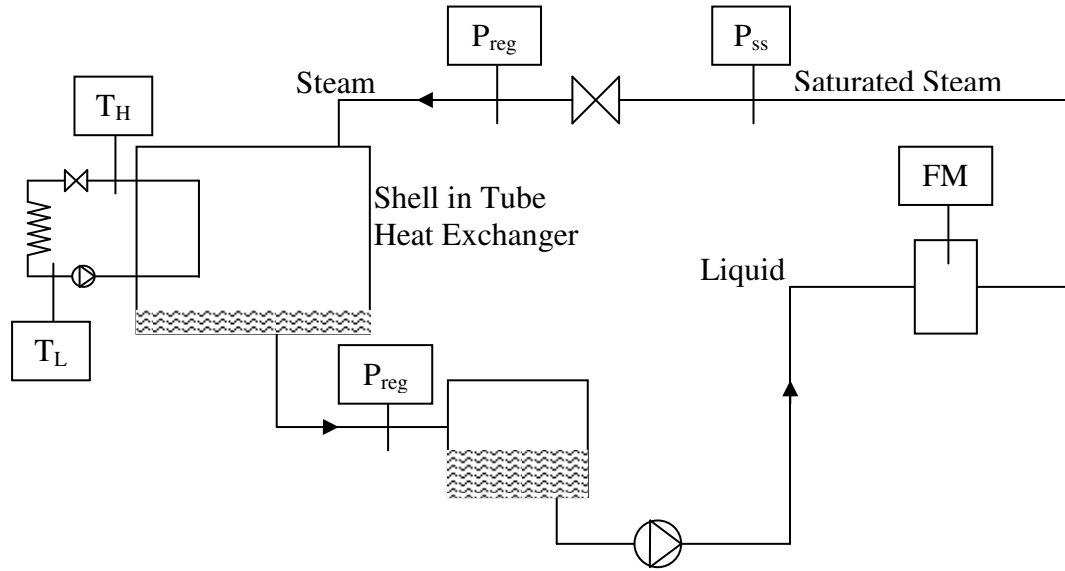


Figure 5.1: Heating Load Energy Flow Diagram

From the energy flow diagram, the heating load equation can be defined as

$$\dot{Q}_H = \dot{m}_{CND} (h_{sv} - h_{sl}) \quad (5.1)$$

where the condensate mass flow rate is taken from the flow meter (labeled FM in Figure 5.1) which has an uncertainty of 10 gallons. The flow meter actually measures the total flow of the condensate as it passes through the building, which then needs to be manipulated to determine the actual volumetric flow rate based on the necessary increment of time

$$\dot{V}_{CND} = \frac{F_{CND}}{\Delta t} \quad (5.2)$$

Once the volumetric flow is determined, it is then multiplied by the density of the liquid to figure out the mass flow rate of the condensate

$$\dot{m}_{CND} = \dot{V}_{CND} \rho_{liq} \quad (5.3)$$

In order to actually find the density of the liquid, an Excel Add-In for property evaluation, SteamTab (ChemicaLogic, 1998), was used. This particular Excel Add-In found the liquid density as a function of the regulated pressure

$$\rho_{\text{liq}}(P_{\text{reg}}) \quad (5.4)$$

Next, the enthalpies of the saturated vapor and the saturated liquid were determined. These enthalpies were also found using the Excel Add-In. As shown below, the enthalpy of the saturated vapor was found as a function of the saturated steam pressure, while the enthalpy of the saturated liquid was found as a function of the regulated pressure

$$h_{\text{sv}}(P_{\text{ss}}) \quad (5.5)$$

$$h_{\text{sl}}(P_{\text{reg}}) \quad (5.6)$$

The final step to determine the heating load of the Klaus building was to make sure that all of the units matched up or canceled out. Since the real time monitored data for the heating load was collected in English units, the calculated heating load would then appear in BTU/min. However, the volumetric flow measured at the flow station was collected in gallons per minute. Therefore, the gallons first needed to be converted to cubic feet. Then, the final equation used to determine the heating load within the Klaus building is

$$\dot{Q}_H = C_C \dot{V}_{\text{CND}} \rho_{\text{liq}} (h_{\text{sv}} - h_{\text{sl}}) \quad (5.7)$$

where the conversion factor, C_C , is equal to 0.1336806 ft³/gal to account for the gallon to cubic feet unit conversion.

Since the Klaus building is instrumented with what amounts to revenue meters, the heating load can be determined, as explained above. However, in a typical building, some fuel consumption data might be available, but such data would be inaccurate because of unknown combustion efficiency and would not have the time resolution

needed to properly evaluate the heating loads. Also, there is no resistance heating is used in the Klaus building.

For the programming code which was used for the heating load calculations within Excel's VBA, please refer to APPENDIX A: Heating Loads Code.

5.1.2 Cooling Loads

Similar to the heating load, the cooling load can also be determined from the real time chilled water data. There is an advantage of steam for heating and chilled water for cooling due to the fact that they are available simultaneously. Whereas an older two pipe system would need to switch from heating to cooling and vice-versa.

The chilled water which entered the KACB also came directly from the campus supply. There was, however, a building flow meter which helped to determine exactly how much of the campus chilled water partook in the cooling of the Klaus building. The energy flow diagram for the cooling loads is illustrated below in Figure 5.2:

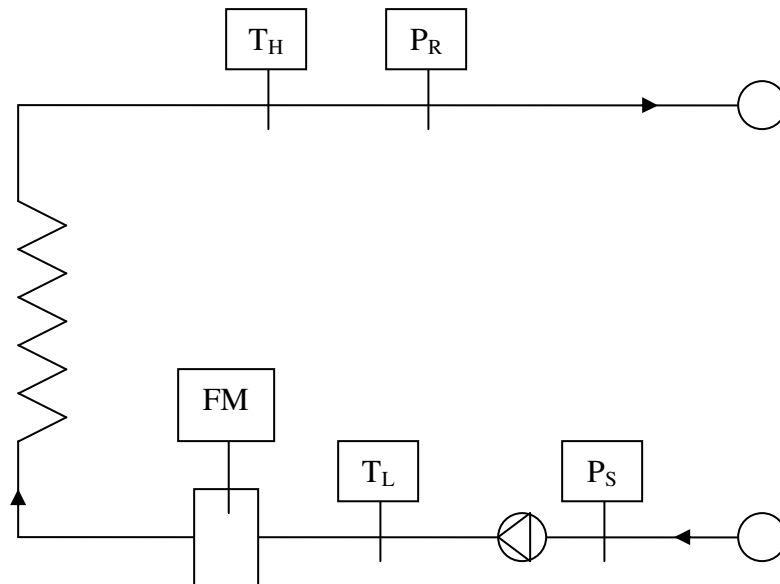


Figure 5.2: Cooling Load Energy Flow Diagram

From the energy flow diagram, the cooling load equation can be defined as

$$\dot{Q}_C = \dot{m}_{\text{CHW}} C_P (T_H - T_L) \quad (5.8)$$

where the chilled water mass flow rate is taken from the flow meter (labeled FM in Figure 5.2) with an uncertainty of 0.1 gpm. The flow meter actually measures the volumetric flow of the chilled water as it passes through, and is then multiplied by the density of the liquid

$$\dot{m}_{\text{CHW}} = \dot{V}_{\text{CHW}} \rho_{\text{liq}} \quad (5.9)$$

In order to actually find the density and specific heat of the chilled water, the same Excel Add-In which was used with the heating loads was used. However for the chilled water, the density and specific heat were found as functions of temperature. Since the flow meter is located on the supply side of the heat exchanger, the supply (or lower) temperature was used to determine both the density and the specific heat

$$\rho_{\text{liq}}(T_L) \quad (5.10)$$

$$C_P(T_L) \quad (5.11)$$

The final step to determine the cooling load of the Klaus building was to make sure that all of the units matched up or canceled out. Since the real time monitored data for the cooling load was collected in English units, the calculated cooling load would then appear in BTU/min. However, the flow data was collected in gallons. Therefore, the gallons needed to be converted to cubic feet. The gallon to cubic feet conversion used for the cooling loads was the same as for the heating loads as mentioned above where $C_C = 0.1336806 \text{ ft}^3/\text{gal}$. Therefore, the final equation used to determine the cooling load within the Klaus building is

$$\dot{Q}_C = C_C \dot{V}_{\text{CHW}} \rho_{\text{liq}} C_P (T_H - T_L) \quad (5.12)$$

For the programming code which was used for the cooling load calculations within Excel's VBA, please refer to APPENDIX B: Cooling Loads Code.

5.1.3 Outside Air Loads

Outside air loads are extremely important for determining overall building loads. In order to correctly calculate outside air loads, the outside air flow must be known. Unfortunately, there is typically no attempt to measure the outside air flow, or even the supply and return air flows in a building. Outside air is hard to measure reliably because an anemometer is easy to contaminate. However, a good estimate of outside air flow is hugely important to determine so that outside air loads can be calculated. Therefore, an innovative way of finding the outside air flow was established.

The mixed air temperature in the air handling units was available and monitored. This temperature is needed not for control purposes, but for safety reasons as to monitor for and avoid freezing a finned coil. Similarly, the supply fan frequency, pressure and fan curve data were also available and monitored to help determine the unknown flow rate ratio. Therefore, a successful method was determined to estimate the outside air flow from the supply air flow and some already available psychrometric measurements.

Two different approaches were used and then compared in order to determine what the actual outside air loads were. Although both methods utilized systems of psychrometric equations, fan curves and fan laws based on the fan frequencies, the first also took into account minimum outdoor air requirements obtained through the energy recovery unit (ERU) analysis while the second stemmed from carbon dioxide (CO₂) concentrations.

In the Klaus building, there are four air handler units (AHU), two of which (AHU 1 and AHU 2) work together in parallel, and two ERUs which service three (AHU 1, AHU 2 and AHU 4) of the AHUs. Since AHUs 1, 2 and 4 all work alongside an ERU, Figure 5.3 is a basic schematic which illustrates how the ERU and AHU work together, while Figure 5.4 illustrates AHU 3 by itself.

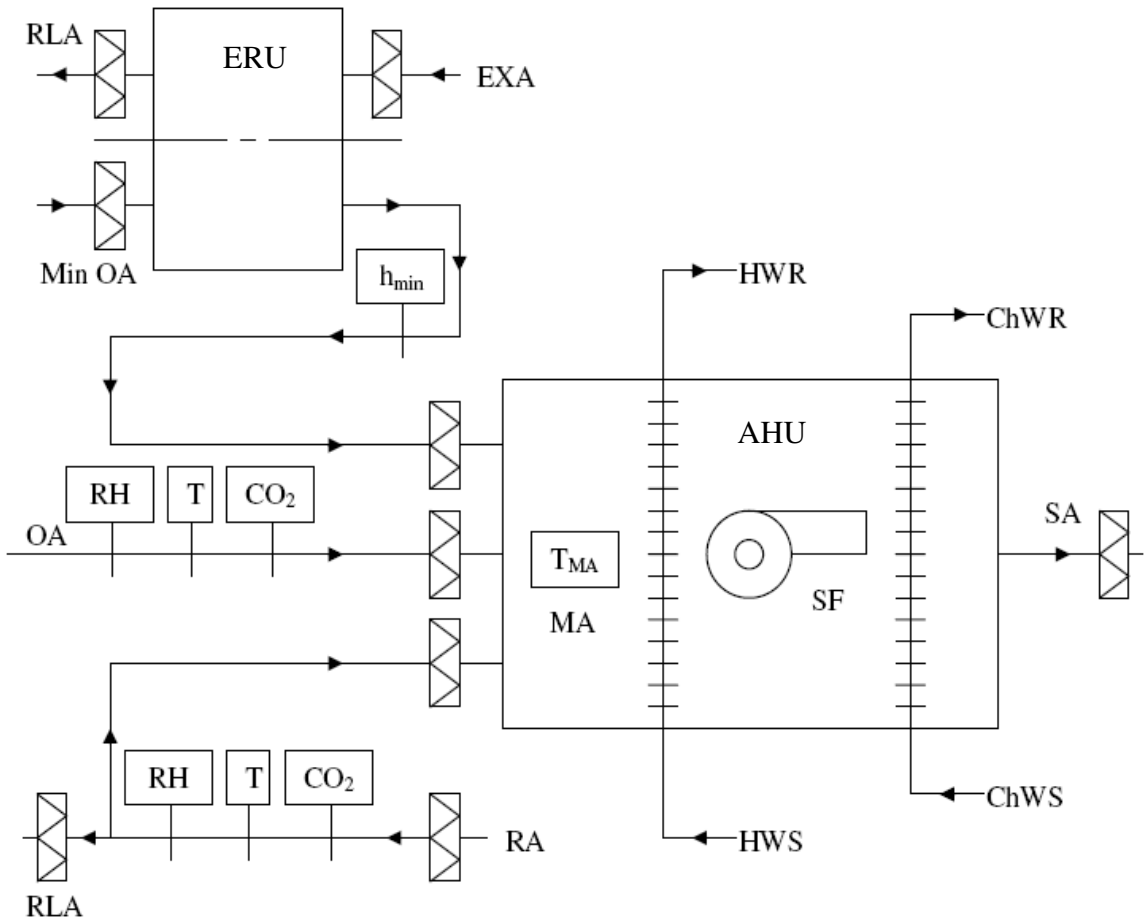


Figure 5.3: Air Handling Units 1, 2 and 4 Energy Flow Diagram

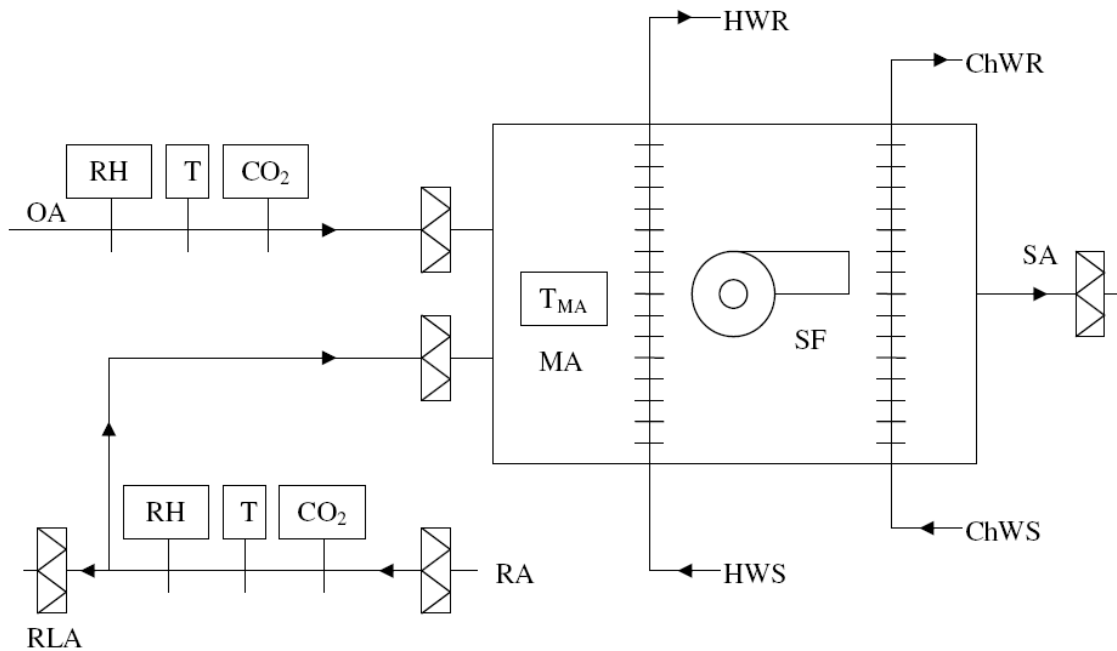


Figure 5.4: Air Handling Unit 3 Energy Flow Diagram

In Figure 5.5, below, a simpler diagram illustrates where the indicated psychrometric data points and mass flow rates are defined for the adiabatic mixing within the air handling units



Figure 5.5: Air Handler Unit Flow Rate Diagram

For the first approach, the following method was used for the three AHUs which work alongside the ERUs to determine the mass flow rate (and consequently volumetric flow rate) of outside air on the building. Start with a system of four equilibrium based equations where

$$\dot{m}_{OA} + \dot{m}_{RA} = \dot{m}_{MA} \quad (5.13)$$

is the mass conservation,

$$\dot{m}_{OA} h_{OA} + \dot{m}_{RA} h_{RA} = \dot{m}_{MA} h_{MA} \quad (5.14)$$

is the energy conservation,

$$\dot{m}_{OA} \omega_{OA} + \dot{m}_{RA} \omega_{RA} = \dot{m}_{MA} \omega_{MA} \quad (5.15)$$

is the moisture conservation, and

$$h_{MA} = C_{P,DA} T_{MA} + \omega_{MA} (C_{P,WV} T_{MA} + h_{WV@0^\circ F}) \quad (5.16)$$

is the enthalpy property equation where $C_{P,DA} = 0.240$ BTU/lbm_{MA}°F, $C_{P,WV} = 0.444$ BTU/lbm_{WV}°F, $h_{WV@0^\circ F} = 1061$ BTU/lbm_{WV} at 0°F, and the temperatures are relative temperatures. Since this system of four equations has four unknowns (\dot{m}_{OA} , \dot{m}_{RA} , h_{MA} and ω_{MA}) and the other necessary numbers can be calculated from monitored data, one can solve for the needed outside air mass flow rate

$$\dot{m}_{OA} = \frac{\dot{m}_{MA} \left(\left(\frac{C_{P,DA} T_{MA}}{C_{P,WV} T_{MA} + h_{WV@0^\circ F}} + \omega_{RA} \right) (h_{OA} - h_{RA}) + h_{RA} (\omega_{RA} - \omega_{OA}) \right)}{\left(\frac{h_{OA} - h_{RA}}{C_{P,WV} T_{MA} + h_{WV@0^\circ F}} + \omega_{RA} - \omega_{OA} \right) (h_{OA} - h_{RA})} \quad (5.17)$$

this ultimately also gives the outside air volumetric flow rate

$$\dot{V}_{OA} = \frac{\dot{V}_{MA} \left(\frac{\rho_{OA}}{\rho_{MA}} \right) \left(\left(\frac{C_{P,DA} T_{MA}}{C_{P,WV} T_{MA} + h_{WV@0^{\circ}F}} + \omega_{RA} \right) (h_{OA} - h_{RA}) + h_{RA} (\omega_{RA} - \omega_{OA}) \right)}{\left(\frac{h_{OA} - h_{RA}}{C_{P,WV} T_{MA} + h_{WV@0^{\circ}F}} + \omega_{RA} - \omega_{OA} \right) - h_{RA}} \quad (5.18)$$

Due to this very complicated result, the step-by-step algebraic proof is presented below in APPENDIX D: Outside Air Load Flow Calculations. Also, these equations have been checked and verified using the Engineering Equation Solver (EES) program which solves equations simultaneously. A sample of the EES code is also presented in APPENDIX D: Outside Air Load Flow Calculations.

Although this method for determining the outside air flow has been mathematically verified, further testing and experimentation is also desirable, as discussed in Chapter 8. However, due to the mathematical verification and comparisons, this method has been considered to be an accurate enough estimate which is extremely important and has made the rest of this research feasible.

Since there are four AHUs which have to be accounted for, the total outdoor air load has to take into account all four such that

$$\dot{Q}_{OA,total} = \dot{Q}_{OA,1} + \dot{Q}_{OA,2} + \dot{Q}_{OA,3} + \dot{Q}_{OA,4} \quad (5.19)$$

where each the load for each AHU is simply

$$\dot{Q}_{OA,i} = \dot{m}_{OA,i} (h_{OA,i} - h_{RA,i}) = \dot{V}_{OA,i} \rho_{OA,i} (h_{OA,i} - h_{RA,i}) \quad (5.20)$$

Unfortunately, only the calculations for AHU 3 are this simple. Since AHU 3 does not work with an ERU and has a constant volume supply fan, the above equation can be utilized to find the outside air load ($\dot{Q}_{OA,3}$) associated with AHU 3. The remaining

three AHUs, however, need to utilize two new variants: control logic and fan curves which are further discussed in Sections 5.1.3.1 and 5.1.3.2, where the control logic is part of the programming code which decides whether or not the energy recovery unit will run. The basis for the control logic used in the Klaus building depends on the return air and outdoor air enthalpies.

For the programming code which was used for the outdoor air load calculations within Excel's VBA, please refer to APPENDIX C: Outside Air Loads Code.

5.1.3.1 Air Handling Unit / Energy Recovery Unit Control Logic

Air Handlers 1, 2 and 4 all utilize the benefits of an Energy Recovery Unit. Energy recovery ventilation is the process of using the energy contained in a normally exhausted building to pre-treat the incoming outdoor ventilation air. The benefits of using an ERU include meeting ventilation and energy standards, improving indoor air quality, and reducing the total HVAC equipment capacity. The ERUs used in the Klaus building are air-to-air enthalpy heat exchangers which transfer both sensible and latent heat.

Since the ERUs in the Klaus building are not always in use, a control logic must be developed in order to best calculate the outdoor air loads. The control logic used for the ERUs in the Klaus building is determined based on the return air and outdoor air enthalpies. As illustrated above in Figure 5.3: Air Handling Units 1, 2 and 4 Energy Flow Diagram, there are plenty of dampers present before and after the ERU and AHU. These dampers determine where the air flow into the AHU comes from. For the Klaus building, the AHUs get their entire air supply either directly from outside or from the ERU. This means that the damper is either completely opened or completely closed. If

the air supply comes directly from outside, it is simply known as the outdoor air (OA), whereas if the air supply comes from the ERU, it is known as the minimum outdoor air (MOA).

The control logic that alters when the dampers are open or closed is based on the outdoor air and return air enthalpies. Whenever the ERU is on and the dampers are fully open, the minimum outdoor air needs to be determined. This can be found through the use of the ERUs effectiveness such that

$$\varepsilon = \frac{\dot{m}_{OA}(h_{OA} - h_{MOA})}{\dot{m}_{EA}(h_{OA} - h_{RA})} \quad (5.21)$$

where ε is the ERU effectiveness. Then solving for h_{MOA}

$$h_{MOA} = h_{OA} - \frac{\dot{m}_{OA}}{\dot{m}_{EA}} \varepsilon (h_{OA} - h_{RA}) \quad (5.22)$$

For both ERUs, the effectiveness is known to be $\varepsilon = 0.8$, while the \dot{m}_{OA} to \dot{m}_{EA} ratio for both ERUs has been found to be approximately 0.9. Therefore,

$$h_{MOA} = h_{OA} - 0.72(h_{OA} - h_{RA}) \quad (5.23)$$

Now that the minimum outdoor air has been established, one needs to recall the outdoor air volumetric flow equation where



Figure 5.6: Air Handler Unit Flow Rate Diagram

and

$$\dot{V}_{OA} = \frac{\dot{V}_{MA} \left(\frac{\rho_{OA}}{\rho_{MA}} \right) \left(\left(\frac{C_{P,DA} T_{MA}}{C_{P,WV} T_{MA} + h_{WV@0^{\circ}F}} + \omega_{RA} \right) (h_{OA} - h_{RA}) + h_{RA} (\omega_{RA} - \omega_{OA}) \right)}{\left(\frac{h_{OA} - h_{RA}}{C_{P,WV} T_{MA} + h_{WV@0^{\circ}F}} + \omega_{RA} - \omega_{OA} \right) (h_{OA} - h_{RA})} - h_{RA} \quad (5.24)$$

In this equation, any time the ERU is in use, the h_{OA} needs to be replaced by h_{MOA} . Once again, this is only the case for AHUs 1, 2 and 4 since AHU 3 does not use an ERU.

For the programming code which was used for the outdoor air load control logic calculations within Excel's VBA, please refer to APPENDIX C: Outside Air Loads Code.

5.1.3.2 Fan Curves Used to Determine Air Flow

The volumetric flow of mixed air within the Klaus building is needed to help determine the volumetric flow of outdoor air. In order to find the volumetric flow of the mixed air, general and very reliable laws called the fan laws are used in application and fan curves were employed.

The most simplistic fan law is that volumetric flow (cfm) varies directly with rotational speed (rpm) such that

$$\frac{\dot{V}_2}{\dot{V}_1} = \frac{N_2}{N_1} \quad (5.25)$$

where \dot{V} is the volumetric flow and N is the rotational speed. The other useful fan law for the purpose of the Klaus building is that the static pressure varies with the square of the rotational speed

$$\frac{H_2}{H_1} = \left(\frac{N_2}{N_1} \right)^2 \quad (5.26)$$

where H is the static pressure. Thus, using these two fan laws for dynamic simulation, the static pressure, volumetric flow and rotational speed are all found to be proportional to one another

$$\frac{H_2}{H_1} \propto \left(\frac{\dot{V}_2}{\dot{V}_1} \right)^2 \propto \left(\frac{N_2}{N_1} \right)^2 \quad (5.27)$$

This relationship allows one to assume that the relationship is quadratic.

Air handlers 1, 2 and 4 all utilize these fan laws along with their individual fan curve for the supply fan in the AHU. From the specified speed, test and balance (T&B) report speed, T&B datum point, and system curve a fan curve has been created for each supply fan. According to most turbo-machinery textbooks, the ideal fan curve is a downward sloping straight line where friction and leakage introduce a roughly quadratic correction (Dixon, 1998). Therefore, a quadratic curve should work. So, from each fan curve, a unique quadratic fit has been made to relate the volumetric flow to the static pressure

$$H_1 = C_0 + C_1 \dot{V}_1 + C_2 \dot{V}_1^2 \quad (5.28)$$

The fan curve for supply fan 1 which is located in AHU 1 is illustrated below in Figure 5.7

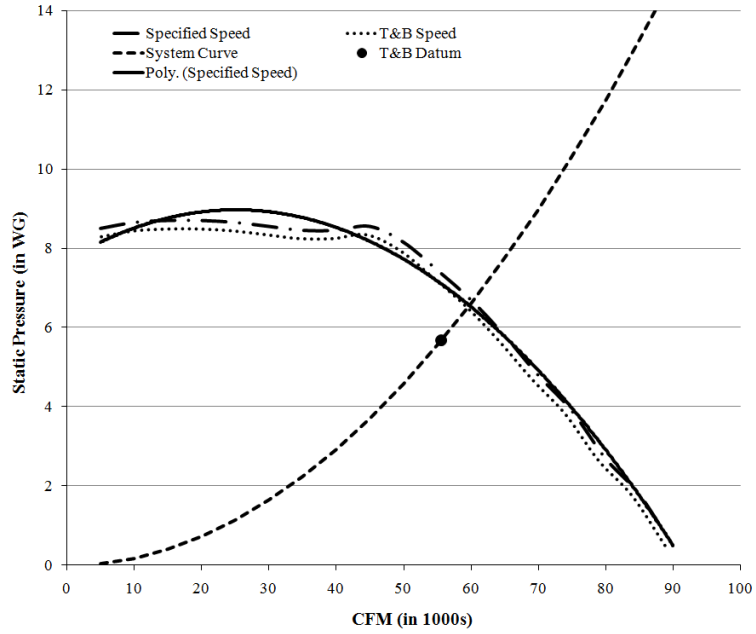


Figure 5.7: Fan Curve for Supply Fan 1

where the quadratic fit is

$$H_{SF1} = 7.6989 + 0.1011\dot{V}_{SF1} - 0.002\dot{V}_{SF1}^2 \quad (5.29)$$

Regression results show good representation, especially near the normal operating point.

Similarly to supply fan 1, the fan curve for supply fan 2 which is located in AHU 2 is illustrated below in Figure 5.8

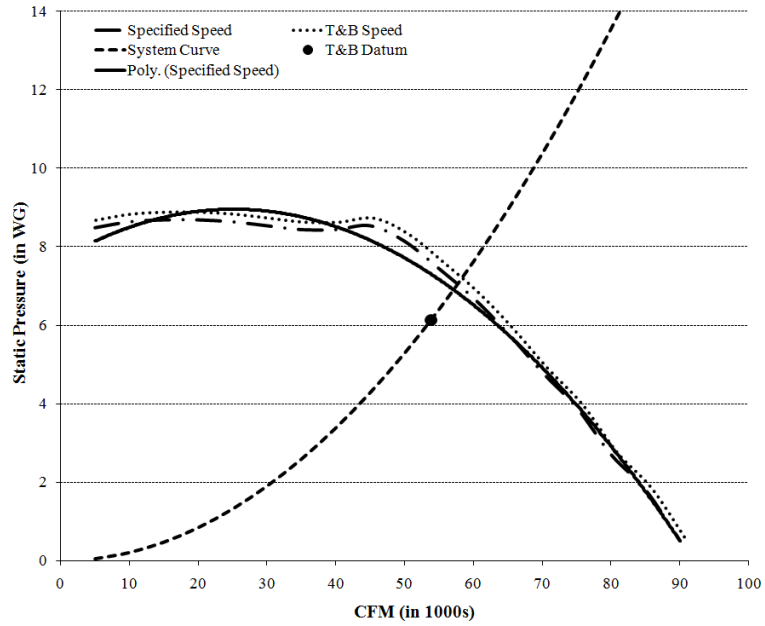


Figure 5.8: Fan Curve for Supply Fan 2

where the quadratic fit is

$$H_{SF2} = 7.6989 + 0.1011\dot{V}_{SF2} - 0.002\dot{V}_{SF2}^2 \quad (5.30)$$

Finally, the fan curve for supply fan 4 which is located in AHU 4 is illustrated below in Figure 5.9

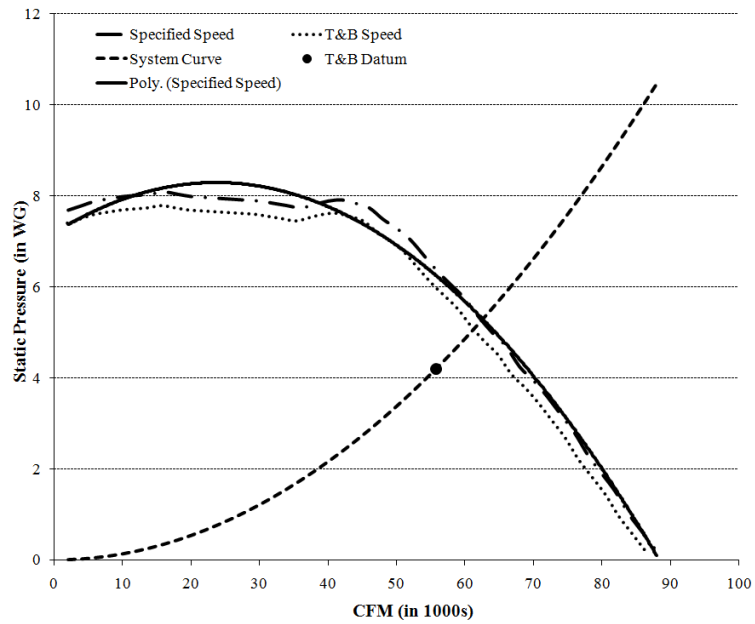


Figure 5.9: Fan Curve for Supply Fan 4

where the quadratic fit is

$$H_{\text{SF4}} = 7.1891 + 0.0934\dot{V}_{\text{SF4}} - 0.002\dot{V}_{\text{SF4}}^2 \quad (5.31)$$

For all three supply fans, the quadratic curve fits appear to be reasonable due to the high $R^2 = 0.922$ value which is very close to the desired correlation unity of 1.

Now that the relationship between volumetric flow and static pressure is assumed to be reasonable, the next step is to solve for a new volumetric flow through equation manipulation and use of the fan laws. To begin, find the new static pressure

$$H_2 = H_1 \left(\frac{N_2}{N_1} \right)^2 \quad (5.32)$$

this then manipulates the original quadratic relationship to be

$$H_2 = \left(\frac{N_2}{N_1} \right)^2 (C_0 + C_1\dot{V}_1 + C_2\dot{V}_1^2) \quad (5.33)$$

However, the new volumetric flow can also be found as

$$\dot{V}_1 = \dot{V}_2 \left(\frac{N_2}{N_1} \right) \quad (5.34)$$

which then also manipulates the quadratic relationship to be

$$H_2 = \left(\frac{N_2}{N_1} \right)^2 \left(C_0 + C_1 \left(\frac{N_1}{N_2} \right) \dot{V}_2 + C_2 \left(\frac{N_1}{N_2} \right)^2 \dot{V}_2^2 \right) \quad (5.35)$$

which simplifies to

$$H_2 = \left(\frac{N_2}{N_1} \right)^2 C_0 + \left(\frac{N_2}{N_1} \right) C_1 \dot{V}_2 + C_2 \dot{V}_2^2 \quad (5.36)$$

Now, solving for \dot{V}_2 ,

$$\dot{V}_2 = \frac{-C_1 \left(\frac{N_2}{N_1} \right) \pm \sqrt{\left(C_1 \left(\frac{N_2}{N_1} \right) \right)^2 - 4C_2 \left(\left(\frac{N_2}{N_1} \right)^2 C_0 - H_2 \right)}}{2C_2} \quad (5.37)$$

where C_0 , C_1 and C_2 are unique to the specified fan curve and H_2 is the supply fan static pressure. In order to get the desired positive volumetric flow, the “-” answer (subtracting the square root) must be used.

However, obtaining the supply fan static pressure requires a little effort. Figure 5.10, below, illustrates the pressure relationship of a supply fan inside of the air handler.

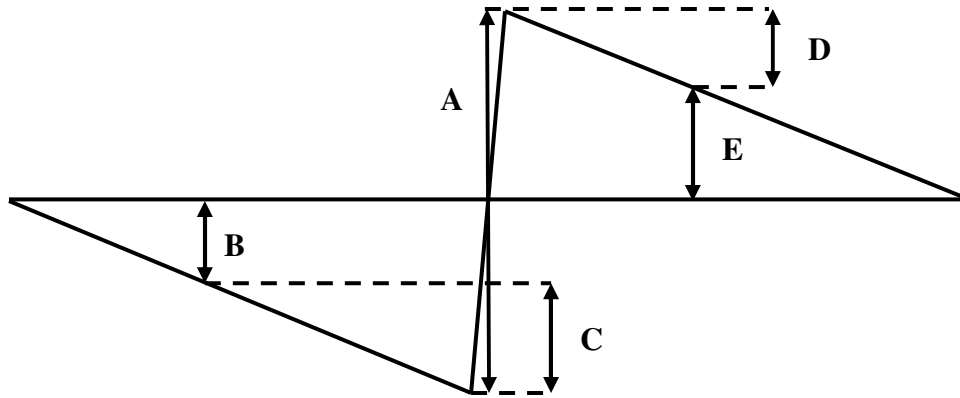


Figure 5.10: Pressure Relationship Profile of Supply Fan

where

Table 5.1: Pressure Relationship Profile Components of Supply Fan

A	ΔP_{Fan}
B	P_{Fixed}
C	$\Delta P_{\text{Upstream}}$
D	$\Delta P_{\text{Downstream}}$
E	$P_{\text{Controlled}}$

such that

$$\Delta P_{\text{Fan}} = P_{\text{Fixed}} + \Delta P_{\text{Upstream}} + \Delta P_{\text{Downstream}} + P_{\text{Controlled}} \quad (5.38)$$

Each of the above pressures differs for each supply fan. P_{Fixed} , a negative pressure, is the pressure at the entrance to the air handler. This pressure must remain constant (hence P_{Fixed}) in order to maintain the minimum outdoor air flow. Next, $\Delta P_{\text{Upstream}}$, also a negative pressure, is the pressure difference between the entrance to the air handler and the pressure at the inlet of the supply fan. After the supply fan, $\Delta P_{\text{Downstream}}$, a positive pressure, is the pressure difference between the outlet of the supply fan and the supply air's static pressure. These two pressure differences vary depending on the volumetric flow of air through the air handler (discussed below). And, finally, $P_{\text{Controlled}}$, a positive pressure, is the supply air's static pressure which is controlled to be a constant.

Therefore, in order to determine ΔP_{Fan} , the supply fan static pressure, $\Delta P_{\text{Upstream}}$ and $\Delta P_{\text{Downstream}}$ must first be found. Both of these pressure differences vary depending on the volumetric flow of air through the air handler where

$$\Delta P_{\text{Upstream}} = K_{\text{US}} \dot{V}^2 \quad (5.39)$$

and

$$\Delta P_{\text{Downstream}} = K_{\text{DS}} \dot{V}^2 \quad (5.40)$$

where K_{US} is the upstream constant and K_{DS} is the downstream constant. However, both constants vary for each air handler. These constant have been calculated and are illustrated below

Table 5.2: Constants Used to Determine Supply Fan Static Pressure

	AHU 1	AHU 2	AHU 4
K_{US}	-2.00E-05	-1.90E-05	-1.44E-05
K_{DS}	8.82E-06	6.13E-06	1.79E-05

Now that $\Delta P_{\text{Upstream}}$ and $\Delta P_{\text{Downstream}}$ have been established, and P_{Fixed} and $P_{\text{Controlled}}$ are also known, ΔP_{Fan} can be determined, and then, ultimately, the volumetric flow of the mixed supply air. The upstream and downstream pressure drops are caused by the usual filters and coils which are in air handling units.

The adjusted fan curve method described above was used to calculate the volumetric flow of mixed supply air knowing only the supply fan frequency and being able to calculate the static pressure across the supply fan. Once this volumetric flow was obtained, the outside air volumetric flow could then also be found.

For the programming code which was used for the fan curves to determine the volumetric flow and outside air load calculations within Excel's VBA, please refer to APPENDIX C: Outside Air Loads Code.

5.1.3.3 Carbon Dioxide Concentrations Used to Determine Air Flow

The second method to compare the outside air volumetric flow rates uses air density and CO₂ concentrations. Where



Figure 5.11: Air Handler Unit Flow Rate Diagram

Once again, start with the mass conservation equation

$$\dot{m}_{\text{RA}} + \dot{m}_{\text{OA}} = \dot{m}_{\text{SA}} \quad (5.41)$$

and the carbon dioxide concentration conservation equation

$$\dot{m}_{\text{RA}} C_{\text{RA}} + \dot{m}_{\text{OA}} C_{\text{OA}} = \dot{m}_{\text{SA}} C_{\text{SA}} \quad (5.42)$$

where C is the concentration of carbon dioxide at each air location. Then, one can solve for the needed outside air mass flow rate given the densities and the mass flow rate ratios such that

$$\dot{m}_{OA} = \frac{\rho_{OA} \rho_{RA} \dot{V}_{SA}}{\left(\rho_{OA} \frac{(C_{SA} - C_{OA})}{(C_{RA} - C_{SA})} + \rho_{RA} \right)} \quad (5.43)$$

which ultimately also gives the outside air volumetric flow rate

$$\dot{V}_{OA} = \frac{\rho_{RA} \dot{V}_{SA}}{\left(\rho_{OA} \frac{(C_{SA} - C_{OA})}{(C_{RA} - C_{SA})} + \rho_{RA} \right)} \quad (5.44)$$

This method for determining the volumetric flow of outside air as a function of carbon dioxide concentrations has been used to verify the accuracy of the first method which uses control logic based on the ERU, temperature, enthalpies and humidity ratios. A sample of this relationship is illustrated below in Figure 5.12 which compares the outside air flow rates determined by control logic and carbon dioxide concentrations.

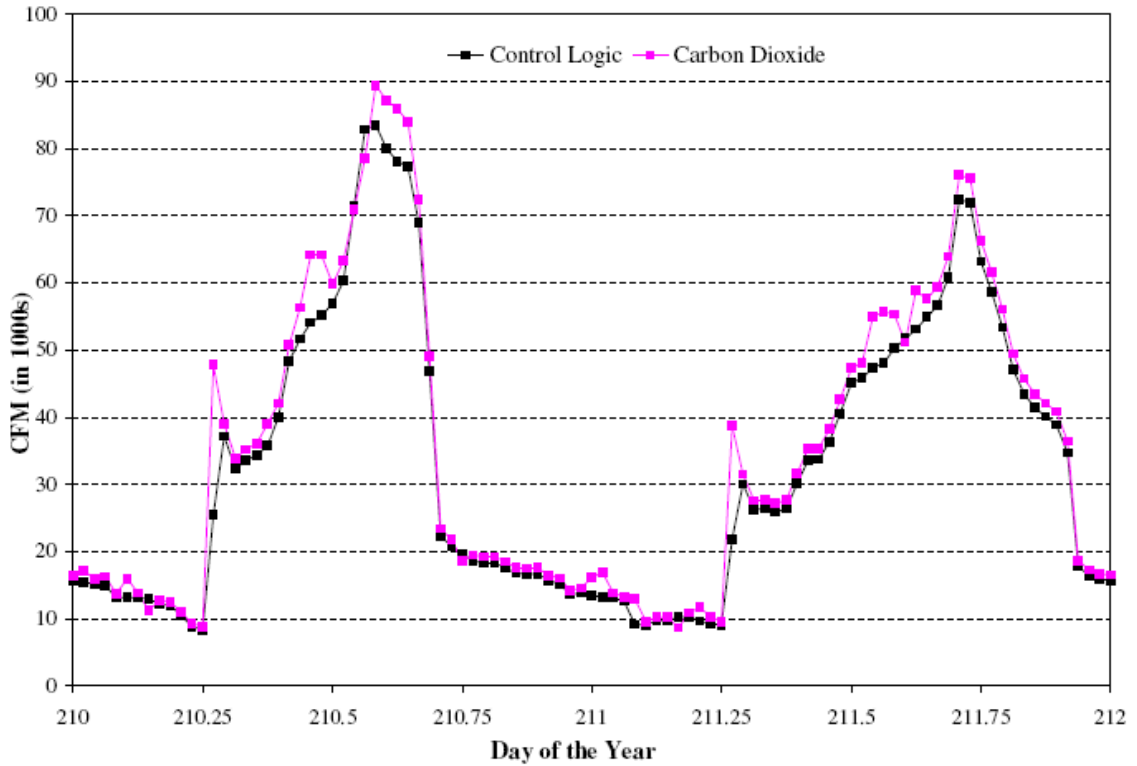


Figure 5.12: Outside Air Flow Rate Comparison

where the x-axis represents the Julian day of the year and time (hour) fraction of the day (e.g. .25 would be 6am, .5 would be 12 noon, and .75 would be 6pm) and the y-axis represents the volumetric air flow in thousands. This comparison correlates to an $R^2 = 0.928$ which represents a very reasonable correlation between the two methods.

As illustrated above, the outside air flow rate as determined from the system's control logic closely mimics the outside air flow rate calculated from the carbon dioxide concentrations. However, during the two sample days (July 29-30th, 2008), the outside air calculated using the carbon dioxide concentrations appears to be slightly more sensitive to changes.

The carbon dioxide concentration data has also be used to infer the number of people in the building. The information discussed below in Section 5.1.5.1: Occupancy

Loads uses the estimated number of people in the building based on expected occupancy schedules. Additionally, the carbon dioxide concentration data has been used to verify the number of people by using the known rate of outside air to determine the amount of carbon dioxide which has been added to the building.

5.1.4 Skin Loads

The skin load calculations for any building need to consider the loads for the various wall and roof constructions as well as the load associated with the direct solar heat gain through the fenestration. The load related to the wall and roof constructions will be referred to as the conduction skin load (Sections 5.1.4.2 and 5.1.4.3) while the load related to the fenestration will be the direct solar heat gain skin load (Section 5.1.4.4). However, before either skin load can be determined, the outside air conditions and the sun's position have to be taken into account and are discussed below in Section 5.1.4.1: Solar Calculations.

5.1.4.1 Solar Calculations

Solar radiation flux onto the Earth varies at different times of the year due to the annual elliptical pattern of the Earth's orbit around the Sun. The distance between the Earth and the Sun continuously changes throughout the year, the minimum being 1.471×10^{11} meters during the winter solstice (December 21) and the maximum being 1.521×10^{11} meters during the summer solstice (June 21), (Goswami, 2000). Therefore, the amount of solar radiation intercepted by the Earth varies throughout the year. The equations used to determine the positioning of the Sun can be found in Section 5.1.4.1.1, while the equations used to determine the solar angles and how much solar radiation falls

on various surface angles can be found in Section 5.1.4.1.2, and, finally, the equations used to estimate sky dome radiation can be found in Section 5.1.4.1.3.

5.1.4.1.1 Positioning of the Sun

The following equations and calculations are fairly straightforward; however they are not familiar to all readers, so they have been included to assure completeness.

The axis of the Earth's daily rotation around itself is at an angle of 23.45° to the axis of its ecliptic orbital plane around the sun. This tilt is the major cause of the seasonal variation of the solar radiation available at any location on the Earth. The angle between the Earth-Sun line (through their centers) and the plane through the equator is called the solar declination angle, δ , which varies between -23.45° and $+23.45^\circ$ and is estimated as

$$\delta = 23.45 \sin\left(\frac{360(284 + n)}{365}\right) \quad (5.45)$$

where n is the day number during a year, starting with January 1st as $n = 1$.

The solar hour angle, ω , is based on the nominal time of 24 hours which is required for the sun to move 360° around the Earth which really means 15° per hour. Therefore, the solar hour angle is defined as

$$\omega = 15(ST - 12) \quad (5.46)$$

Next, the sun angles at a particular location can be obtained from the local solar time, which differs from the local standard time. The equation for local solar time is

$$ST = \frac{TOD + ET + 4(LTZ - L_{lon})}{60} \quad (5.47)$$

Local solar time depends on the time of day (TOD) in minutes, the equation of time (ET), the local time zone (LTZ), and the local longitude (L_{lon}). The local longitude for the Klaus building is approximately 88.4° West, while the LTZ is 75° West since the Klaus building is in Atlanta which is in the Eastern Time Zone. The equation of time can be obtained through

$$ET = 9.87 \sin(2B) - 7.53 \cos B - 1.5 \sin B \quad (5.48)$$

which depends solely on B ,

$$B = \frac{360(n - 81)}{364} \quad (5.49)$$

which varies with the day of the year.

5.1.4.1.2 Solar Angles and Calculations Based on Wall, Window and Roof Positions

The solar altitude angle (α) is the angle from the horizon to the sun in a vertical plane which can be defined as

$$\sin \alpha = \sin \varphi \sin \delta + \cos \delta \cos \omega \cos \varphi = \cos \theta_z \quad (5.50)$$

where δ is the declination angle, ω is the solar hour angle, and φ is the local latitude angle. φ for the Klaus building is approximately 33.8° North. The zenith angle (θ_z) is the angle between the site to the sun line and the vertical at the site which is the complement of the solar altitude angle

$$\theta_z = 90 - \alpha \quad (5.51)$$

The solar azimuth angle (γ_s) is the angle toward the vertical plane of the sun while measured in the horizontal plane.

$$\sin \gamma_s = \frac{\cos \delta \sin \omega}{\cos \alpha} \quad (5.52)$$

$$\cos \gamma_s = \frac{\cos \delta \cos \omega \sin \varphi - \sin \delta \cos \varphi}{\cos \alpha} \quad (5.53)$$

Both the sine and the cosine of the solar azimuth angle are needed so that the two-argument tangent can be used to position the azimuth in the proper quadrant where

$$\gamma_s = \arctan(\cos \gamma_s, \sin \gamma_s) \quad (5.54)$$

The solar azimuth angle and the solar altitude angle both continuously vary depending on the time of day and the day of the year. Figure 5.13 below illustrates the specific changes in both angles over the course of January 1st, 2008 in Atlanta, Georgia.

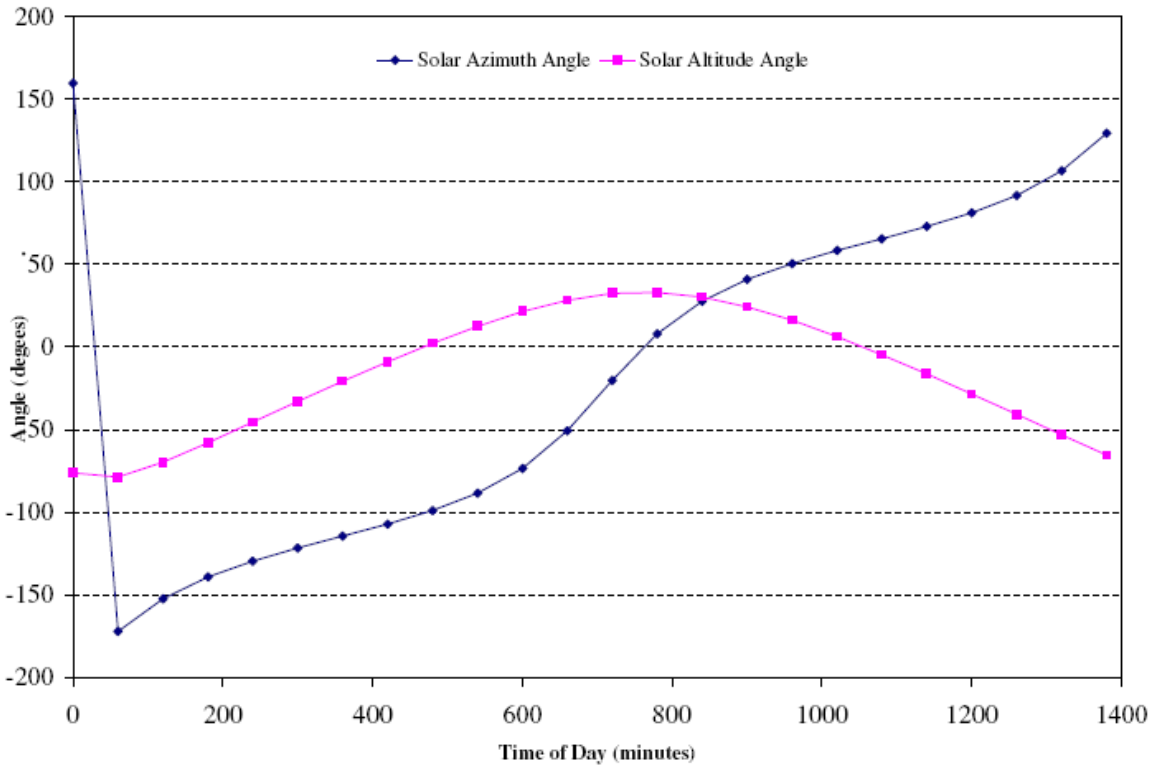


Figure 5.13: Solar Azimuth Angle and Solar Altitude Angle for January 1st, 2008

The orientation of a plane is defined by its tilt, β , from the horizontal and its surface azimuth angle, γ_{sur} . β is 0° for horizontal surfaces, such as roofs, and 90° for

vertical surfaces, which is typically most structural walls. The surface azimuth angle is measured west from due south in the horizontal plane.

Table 5.3: Surface Azimuth Angles

γ_{sur} Wall Direction	Angle (degrees)
$\gamma_{\text{sur, South}}$	0
$\gamma_{\text{sur, South-West}}$	45
$\gamma_{\text{sur, West}}$	90
$\gamma_{\text{sur, North-West}}$	135
$\gamma_{\text{sur, North}}$	180
$\gamma_{\text{sur, North-East}}$	225
$\gamma_{\text{sur, East}}$	270
$\gamma_{\text{sur, South-East}}$	315

The incident angle (θ_B) is the angle at which the sun's light approaches a surface.

The incident angle for beam radiation can be defined as

$$\cos \theta_B = \sin \beta \sin \gamma_{\text{sur}} \cos \alpha \sin \gamma_s + \sin \beta \cos \gamma_{\text{sur}} \cos \alpha \cos \gamma_s + \cos \beta \sin \alpha \quad (5.55)$$

Alternatively, one can eliminate the solar altitude and solar azimuth angles and rewrite the incident angle in terms of latitude, declination angle and solar hour angles as

$$\begin{aligned} \cos \theta_B = \sin \beta \sin \gamma_{\text{sur}} (\cos \delta \sin \omega) + \sin \beta \cos \gamma_{\text{sur}} (\cos \delta \cos \omega \sin \varphi - \sin \delta \cos \varphi) + \\ \cos \beta (\cos \delta \cos \omega \cos \varphi + \sin \delta \sin \varphi) \end{aligned} \quad (5.56)$$

Either of the above incident angle equations can be used to calculate the beam radiation on a tilted surface. There are, however, two special cases which can simplify the incident angle equations. The first special case is for horizontal surfaces such as flat roofs since $\beta = 0^\circ$ and the incident angle can simplify to

$$\cos \theta_{B, \text{Roof}} = \sin \alpha \quad (5.57)$$

The second special case is for vertical surfaces such as most building walls since $\beta = 90^\circ$ and the incident angle can simplify to

$$\cos \theta_{B,Wall} = \sin \gamma_{sur} \cos \alpha \sin \gamma_s + \cos \gamma_{sur} \cos \alpha \cos \gamma_s = \cos \alpha \cos(\gamma_{sur} - \gamma_s) \quad (5.58)$$

Since the incidence angle varies not only with the time of day or the day of the year, but also directionally, Figure 5.14 clearly illustrates this effect the incidence angle has on walls facing each of the eight typical directions on January 1st, 2008 in Atlanta, Georgia. An incident cosine of zero indicates that the wall is not lit by beam radiation.

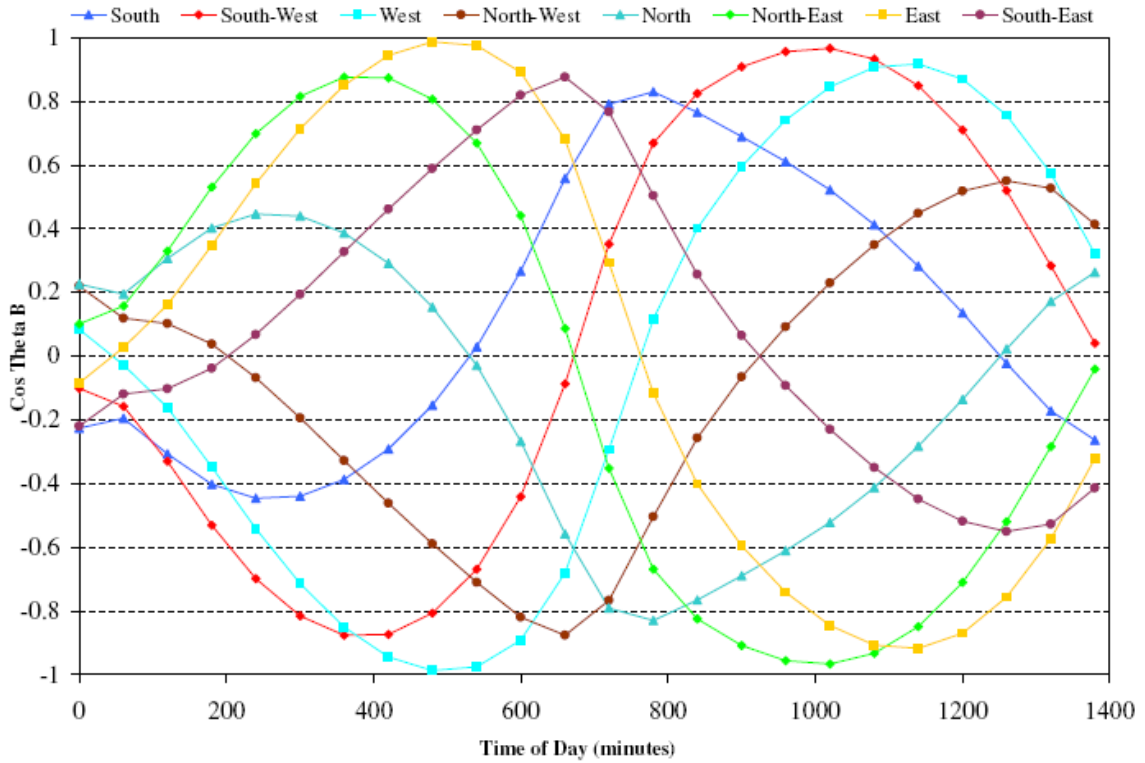


Figure 5.14: Directional $\cos(\theta_B)$ on January 1st, 2008

Finally, the transmittance, τ_{ref} , of the windows on the Klaus building vary as a function with the incident angle

$$\tau_{ref}(\theta_B) \quad (5.59)$$

which is a generalized transmittance function as defined by ASHRAE in the *Fundamentals Handbook* (ASHRAE, 1997). This relationship is best represented graphically as illustrated below in Figure 5.15:

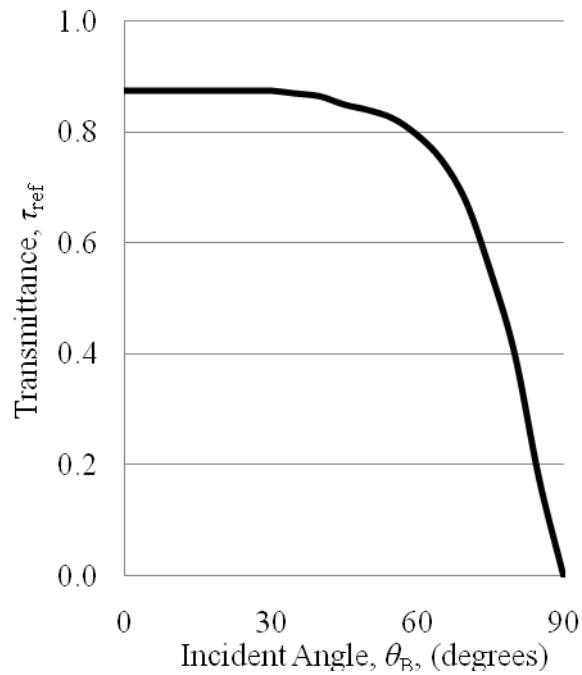


Figure 5.15: Transmittance vs. Incident Angle

This transmittance is for simple fenestration, but as is typical, this trend is used to show the normal variation for all types. This relationship illustrating transmittance as a function of incident angle was used to determine the transmittance for the solar heat gain load calculations in Section 5.1.4.4 at various incident angles throughout the day as the sun passed through the sky.

5.1.4.1.3 Decomposition of Global Radiation Data into Beam Normal and Sky Dome Radiation Components

The solar radiation data provided by UGA is the overall global solar radiation data. Unfortunately, this number cannot be used as is. Instead, it must be broken down into its sky dome and beam normal components.

To begin this break-down process, the clearness index, k_t , must be found

$$k_t = \frac{G_{\text{data}}}{G_{\text{SC}} \sin \alpha} \quad (5.60)$$

where G_{data} is the collected solar radiation data, G_{SC} is the solar constant, and α is the solar altitude angle.

The next step is to somehow relate the beam transmittance, τ_b , to the clearness index, k_t ,

$$\tau_b(k_t) \quad (5.61)$$

The method used in this thesis to relate the beam transmittance, τ_b , to the clearness index, k_t , follows the technique presented in Dr. Constantinos Balaras' PhD dissertation (Balaras, 1988). This relationship is

$$\tau_b = YO(i) + (k_t - XO(i)) \beta_{\text{CB}}(i) \quad (5.62)$$

where $\beta_{\text{CB}}(i)$ are regression coefficients, and $XO(i)$ and $YO(i)$ are coordinates for each band. $YO(i)$ is a function of both $\beta_{\text{CB}}(i)$ and $XO(i)$

$$YO(i) = YO(i-1) + \beta_{\text{CB}}(i-1)(XO(i) - XO(i-1)) \quad (5.63)$$

and

$$YO(1) = 0 \quad (5.64)$$

Both $\beta_{CB}(i)$ and $XO(i)$ are constants for the piece-wise linear fit to the solar radiation correlation which is needed due to the slight “S” shape dependence actually observed in the data (please refer to Figure 5.16). These constants can be found below in the following two tables:

Table 5.4: $\beta_{CB}(i)$ Regression Coefficients

$\beta_{CB}(i)$:	Coefficient Value:
$\beta_{CB}(1)$	0.000000000000000000
$\beta_{CB}(2)$	0.0007178049038916
$\beta_{CB}(3)$	0.0297251792001800
$\beta_{CB}(4)$	0.2490303701482000
$\beta_{CB}(5)$	0.9466134865964000
$\beta_{CB}(6)$	1.4771915943150000
$\beta_{CB}(7)$	1.5680115400000000
$\beta_{CB}(8)$	2.0773194934010000
$\beta_{CB}(9)$	1.3778101387490000

Table 5.5: $XO(i)$ Constants

$XO(i)$:	Constant Value:
$XO(1)$	0.00
$XO(2)$	0.05
$XO(3)$	0.15
$XO(4)$	0.25
$XO(5)$	0.35
$XO(6)$	0.45
$XO(7)$	0.55
$XO(8)$	0.65
$XO(9)$	0.75
$XO(10)$	0.85

While the number of significant digits for the $\beta_{CB}(i)$ Regression Coefficients might seem excessive, they are all necessary to avoid unnecessary round off errors during intermediate calculations.

The relationship of these equations, coefficients and constants is best illustrated below in Figure 5.16, taken from Dr. Constantinos Balaras' PhD dissertation (Balaras, 1988), which demonstrates the piecewise regression relating the clearness index to the beam transmittance for a scatter plot of data which was collected over a five year period.

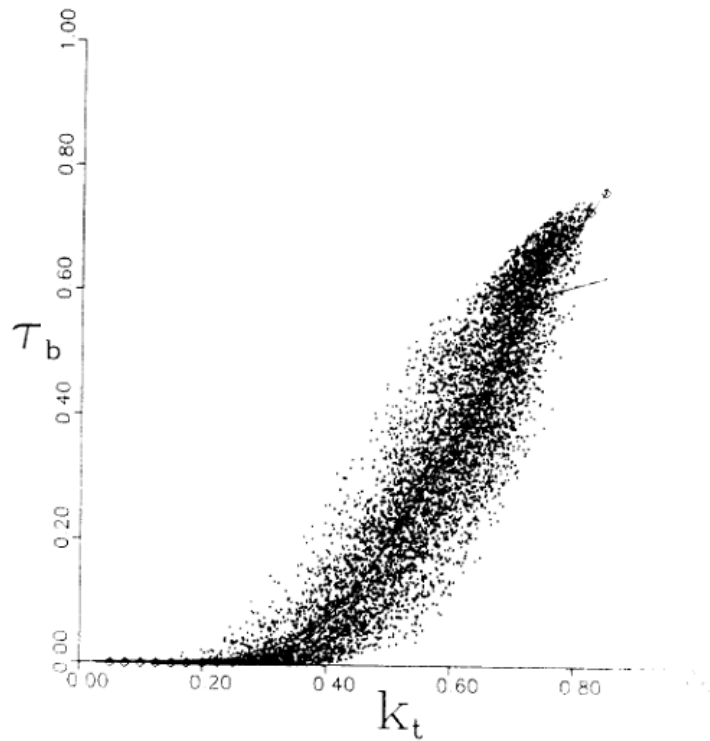


Figure 5.16: Scatter Plot and Piecewise Regression of Clearness Index vs. Beam Transmittance Values (Balaras, 1988)

The clearness index has been calculated for Atlanta, Georgia using the method described by Balaras (Balaras, 1998). The clearness index is illustrated below in Figure 5.17 for January 1st, 2008 in Atlanta, Georgia. As expected, the clearness index is at its highest during day and zero at night.

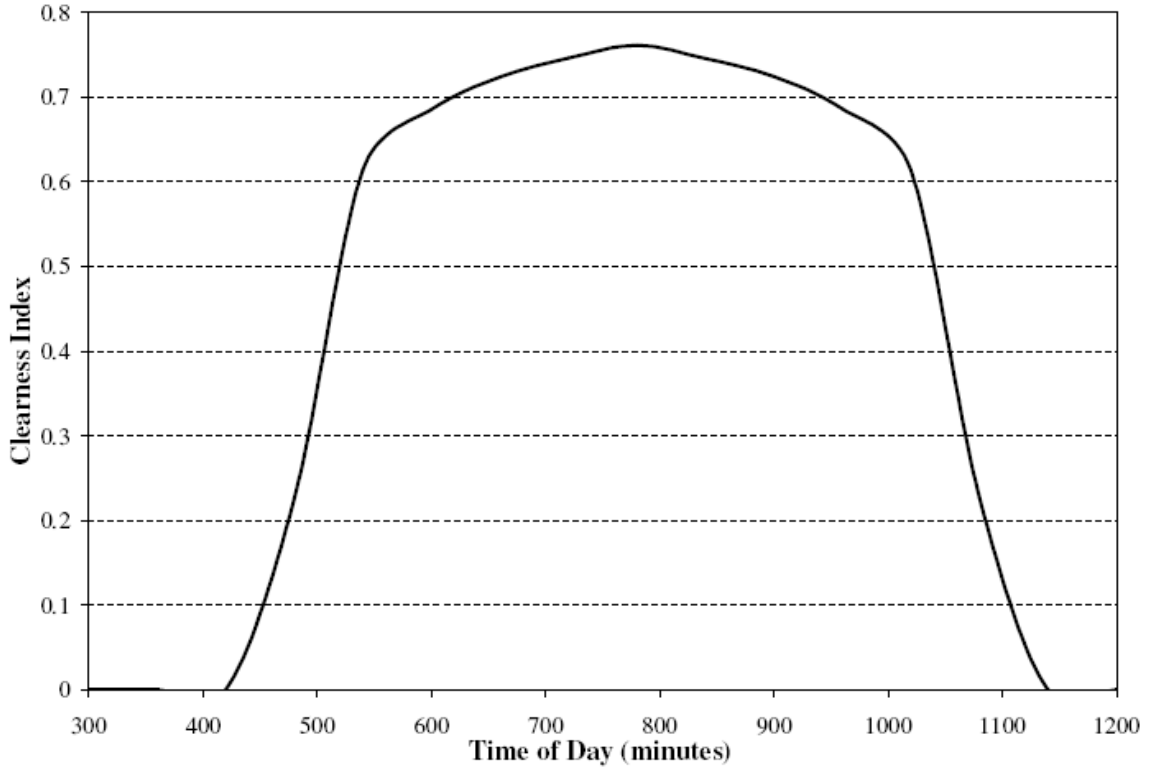


Figure 5.17: Clearness Index for January 1st, 2008

Now that the relationship between the beam transmittance and the clearness index has been found, the next step is to calculate the beam normal radiation from the beam transmittance and the solar constant

$$G_{\text{BN,calc}} = \tau_b G_{\text{SC}} \quad (5.65)$$

The collected solar radiation data is a function of the sky dome radiation, the beam normal radiation, and either the solar altitude angle or the zenith angle such that

$$G_{\text{data}} = G_{\text{SD,calc}} + G_{\text{BN,calc}} \sin \alpha = G_{\text{SD,calc}} + G_{\text{BN,calc}} \cos \theta_z \quad (5.66)$$

where all of the variables are known except for the sky dome radiation. Therefore the equation can be rearranged to give

$$G_{\text{SD,calc}} = G_{\text{data}} - G_{\text{BN,calc}} \sin \alpha \quad (5.67)$$

Now that the beam normal radiation and sky dome radiation components have been found given the overall global radiation, the total irradiation on a tilted surface can be found through

$$G_{T,calc} = G_{BN,calc} \cos \theta_B + G_{SD,calc} \left(\frac{1 + \cos \beta}{2} \right) + \rho_{FG} (G_{BN,calc} \sin \alpha + G_{SD,calc}) \left(\frac{1 - \cos \beta}{2} \right) \quad (5.68)$$

where $G_{BN,calc}$ and $G_{SD,calc}$ have been calculated through the above equations in this section, θ_B is the incident angle and α is the solar altitude angle, both of which constantly vary throughout the day as the sun's light approaches each surface, ρ_{FG} is the foreground reflectance, and β is the tilt of the surface. For the Klaus building, the foreground reflectance is assumed to be $\rho_{FG} = 0.2$, the tilt for the roof is $\beta = 0^\circ$, and the tilt for all of the walls is $\beta = 90^\circ$.

Since the incidence angle has directional variations, the total irradiation on a tilted surface in each of the eight directions also varies. This is best illustrated below in Figure 5.18 which shows the predicted clear sky model radiation, the global solar radiation, and the total irradiation on a tilted plane in all eight typical directions for a sunny day (January 1st, 2008) in Atlanta, Georgia.

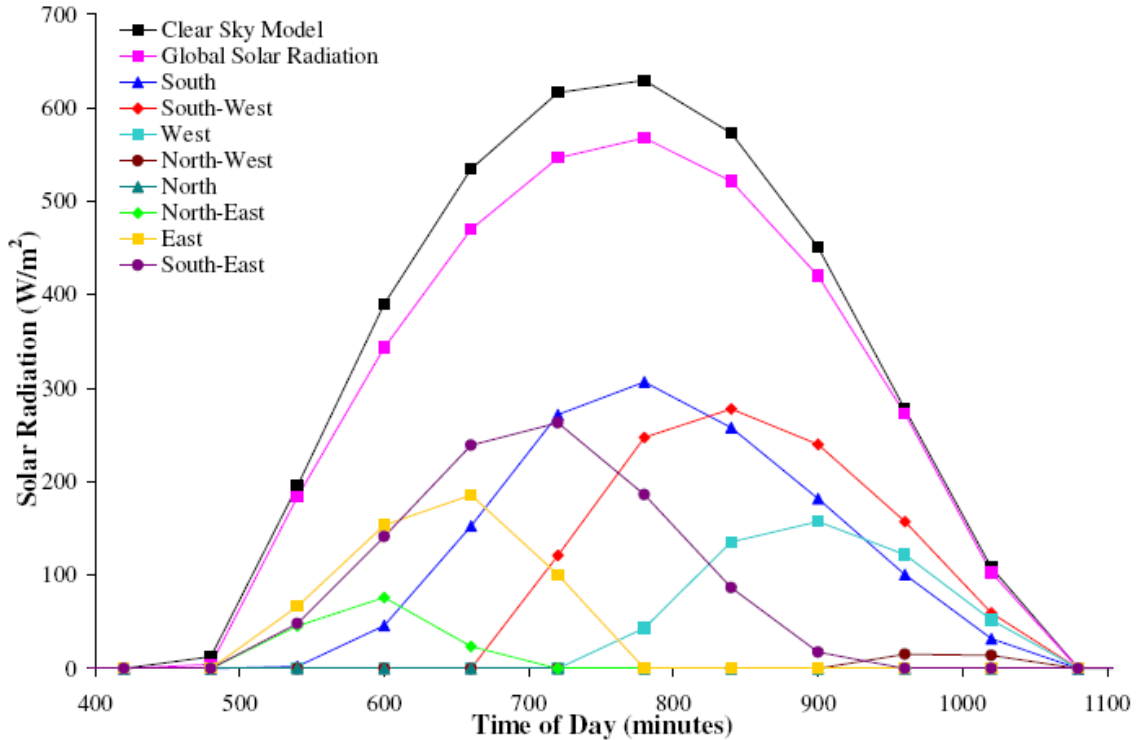


Figure 5.18: Directional Solar Radiation for January 1st, 2008

The sun rises in the east and sets in the west. Figure 5.18 clearly demonstrates this expected trend with the East, South-East and North-East directional surfaces capturing more solar radiation in the morning, then the South-East, South and South-West directional surfaces receiving the majority of the midday solar radiations, and finally the South, South-West, West and (a little) North-West getting more solar radiation in the afternoon.

5.1.4.2 First Order Conduction Skin Loads

The heat gain by conduction through the wall and roofs at a specific time depends on the sol-air temperature, the overall conductance of the structure, and the heat capacity, which creates the time lag in the wall or roof. However, this method used to calculate the conduction skin load does not take into account the heat capacity time lag. Instead, a

simple first order conduction skin load model is described here, while a more complex skin load calculation which utilizes the heat capacity time lag and influence coefficients is discussed below in Section 5.1.4.3 on page 108.

The simple first order conduction skin load can be defined as

$$\dot{Q}_{\text{Cond}} = \frac{A}{R_v} (T_{\text{sol-air}} - T_{\text{in}}) \quad (5.69)$$

where A is the total area associated with each wall or roof construction, R_v is the resistance of the wall or roof construction, $T_{\text{sol-air}}$ is the sol-air temperature, and T_{in} is the zone temperature inside of the building.

The sol-air temperature is the temperature of the outdoor air that, in the absence of all radiation changes, gives the same rate of heat entry into the surface as would the combination of incident solar radiation, radiant energy exchange with the sky and other outdoor surroundings, and convective heat exchange with the outdoor air (ASHRAE, 1993). Sol-air temperature is defined as

$$T_{\text{sol-air}} = T_{\text{OA}} + \frac{\alpha_{\text{abs}} G_T}{h_o} - \Delta T_{\text{IR}} \quad (5.70)$$

where T_{OA} is the outdoor air temperature, α_{abs} is the absorptance of a surface, G_T is the total solar radiation incident on the surface, h_o is the coefficient of heat transfer by long-wave radiation and convection at the outer surface, and ΔT_{IR} is the infrared radiation transfer of sky temperature to the surface.

The total solar radiation, G_T , used for the skin load calculations is from the collected solar radiation data from UGA which is then modified based on the directional orientation of the wall (South, South-West, West, North-West, North, North-East, East, and South-East) by where the sun is in the sky.

Absorptance, α_{abs} , varies by surface depending on how light or dark the facade is. For a light surface, $\alpha_{\text{abs}} \approx 0.45$, while for a dark surface $\alpha_{\text{abs}} \approx 0.90$. For these conduction skin load calculations, the brick wall construction assumes $\alpha_{\text{abs}} = 0.90$, while the glazed aluminum curtain wall and roof constructions assume $\alpha_{\text{abs}} = 0.45$.

The coefficient of heat transfer by long-wave radiation and convection at the outer surface is a constant for $T_{\text{sol-air}}$ calculations, such that $h_o = 3 \text{ BTU} / (\text{hr-ft}^2\text{-}^\circ\text{F})$.

The infrared radiation transfer of sky temperature to the surface, ΔT_{IR} , varies based on the position of the surface/wall. For vertical surfaces $\Delta T_{\text{IR}} = 0^\circ\text{F}$, and for horizontal surfaces $\Delta T_{\text{IR}} = 7^\circ\text{F}$. For these conduction skin load calculations, all of the walls have $\Delta T_{\text{IR}} = 7^\circ\text{F}$, and the roof has $\Delta T_{\text{IR}} = 0^\circ\text{F}$.

Based on the exterior construction of the Klaus building, there are three different assemblies which have been considered for the conduction skin load: the brick wall construction, the glazed aluminum curtain wall construction and the roof construction. The exterior walls, which account for approximately 62.3% of the Klaus building's outer surface, are either brick wall or glazed aluminum curtain wall construction. The other 37.7% of the exterior are windows (or fenestration) which will also be taken into account in Section 5.1.4.4: Direct Solar Heat Gain Skin Loads. The brick wall covers approximately 31.6% of the non-window building exterior, while the glazed aluminum curtain wall covers the remaining 68.4%. The roof construction, on the other hand, is considered to be consistent for the entire roof of the building.

Since there are four constructions taken into account for the conduction skin load, they all need to be considered separately and then combined such that

$$\dot{Q}_{\text{Cond}} = \dot{Q}_{\text{Brick}} + \dot{Q}_{\text{GACW}} + \dot{Q}_{\text{Roof}} + \dot{Q}_{\text{Window}} \quad (5.71)$$

Given the four components of the above equation, each construction needs its unique area and resistance to be taken into account.

Each construction will be discussed further in the following three sections. For the programming code which was used for the conduction skin load calculations within Excel's VBA, please refer to APPENDIX F: Combined Skin Load Code.

5.1.4.2.1 Brick Wall Construction

The Klaus building's vertical exterior consists of approximately 19.7% (16,385 square feet) brick wall construction. The brick wall construction consists of five components, common brick on the exterior, an air layer, a hollow light weight concrete block, expanded polyurethane insulation, and gypsum board. The thermal resistance network for the brick wall construction is illustrated below in Figure 5.19:

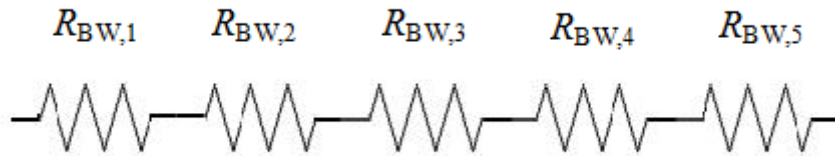


Figure 5.19: Brick Wall Thermal Resistance Network

where

Table 5.6: Brick Wall Construction

R_v	Construction	Thickness (inches)	Resistance ($^{\circ}\text{F}\cdot\text{hr}\cdot\text{ft}^2 / \text{BTU}$)
$R_{BW,1}$	Common Brick	4	0.80
$R_{BW,2}$	Air Layer	< 4	0.89
$R_{BW,3}$	Hollow Light Weight Concrete Block	8	2.00
$R_{BW,4}$	Expanded Polyurethane Insulation	3	18.80
$R_{BW,5}$	Gypsum Board	5/8	0.56

Since the thermal resistance network for the brick wall construction is all in series, the total thermal resistance value can be determined by simply adding all five components

$$R_{v,Brick} = R_{BW,1} + R_{BW,2} + R_{BW,3} + R_{BW,4} + R_{BW,5} \quad (5.72)$$

which gives a total $R_{v,Brick}$ thermal resistance value of 23.05 °F-hr-ft²/BTU for the brick wall construction conduction load calculations.

5.1.4.2.2 Glazed Aluminum Curtain Wall Construction

The Klaus building's vertical exterior consists of approximately 42.6% (35,500 square feet) glazed aluminum curtain wall construction. The curtain wall construction consists of five components, spandrel glass on the exterior, an air layer, particle board underlay, mineral wool batt insulation, and gypsum board. The thermal resistance network for the curtain wall construction is illustrated below in Figure 5.20:

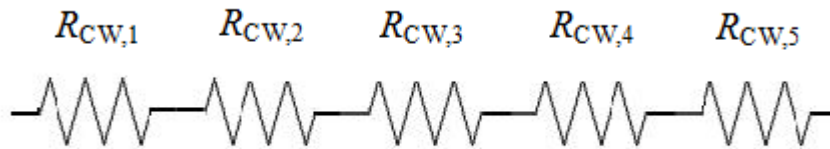


Figure 5.20: Curtain Wall Thermal Resistance Network

where

Table 5.7: Curtain Wall Construction

R_v	Construction	Thickness (inches)	Resistance (°F-hr-ft ² / BTU)
$R_{CW,1}$	Spandrel Glass	1/4	1.70
$R_{CW,2}$	Air Layer	< 4	0.89
$R_{CW,3}$	Particle Board Underlay	5/8	0.29
$R_{CW,4}$	Mineral Wool Batt Insulation	4	13.00
$R_{CW,5}$	Gypsum Board	5/8	0.56

Since the thermal resistance network for the curtain wall construction is all in series, the total thermal resistance value can be determined by simply adding all five components

$$R_{v,GACW} = R_{CW,1} + R_{CW,2} + R_{CW,3} + R_{CW,4} + R_{CW,5} \quad (5.73)$$

which gives a total $R_{v,GACW}$ thermal resistance value of 16.44 °F-hr-ft²/BTU for the curtain wall construction conduction load calculations.

5.1.4.2.3 Roof Construction

The horizontal roof area is approximately 60,600 square feet. The roof construction is built-up roof on the exterior, two layers of expanded polyurethane insulation and light weight concrete.

The Klaus building's horizontal exterior is all considered the roof construction which is approximately 60,600 square feet. The roof construction consists of four components, built-up roof on the exterior, two layers of expanded polyurethane insulation and light weight concrete. The thermal resistance network for the roof construction is illustrated below in Figure 5.21:

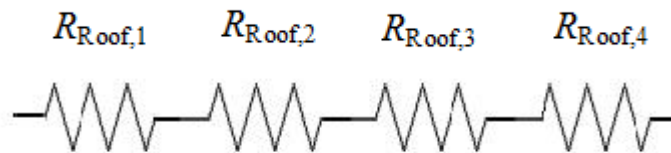


Figure 5.21: Roof Thermal Resistance Network

where

Table 5.8: Roof Construction

R_v	Construction	Thickness (inches)	Resistance (°F-hr-ft ² / BTU)
$R_{\text{Roof},1}$	Built-Up Roof	3/8	0.33
$R_{\text{Roof},2}$	Expanded Polyurethane Insulation	4	25.06
$R_{\text{Roof},3}$	Expanded Polyurethane Insulation	4	25.06
$R_{\text{Roof},4}$	Light Weight Concrete	8	3.20

Since the thermal resistance network for the roof construction is all in series, the total thermal resistance value can be determined by simply adding all four components

$$R_{v,\text{Roof}} = R_{\text{Roof},1} + R_{\text{Roof},2} + R_{\text{Roof},3} + R_{\text{Roof},4} \quad (5.74)$$

which gives a total $R_{v,\text{Roof}}$ thermal resistance value of 53.65 °F-hr-ft²/BTU for the roof construction conduction load calculations.

Overall, the calculated R values of the roof and the two wall compositions agree quite well with the original calculations performed by the design engineers and architects.

5.1.4.3 Transfer Function Conduction Skin Loads

The heat gain by conduction through the walls and roof at a specific time depends on the sol-air temperature, the overall conductance of the structure, and the heat capacity, which creates the time lag in the wall or roof. The first method used to calculate the skin load was the first order conduction skin load discussed above in Section 5.1.4.2. This second method is a more complex skin load calculation which utilizes the heat capacity time lag and influence coefficients.

The transfer function conduction skin load can be defined as

$$\dot{Q}_{\text{Cond},\tau} = A \left[\sum_{n=0} b_n T_{\text{sol-air}} - \sum_{n=1} d_n \frac{\dot{Q}_{\text{Cond},\tau-\Delta t}}{A} - T_{\text{in}} \sum_{n=0} c_n \right] \quad (5.75)$$

where A is the surface area of a roof or wall, $T_{\text{sol-air}}$ is the sol-air temperature, $\dot{Q}_{\text{Cond},\tau-\Delta t}$ is the conduction skin load at the prior time increment, T_{in} is the constant indoor air temperature, and b_n , d_n , and c_n are the influence coefficients which vary depending on the wall or roof construction. These transfer function influence coefficient values for the Klaus building can be found below. Table 5.9 contains the coefficients for the roof construction; Table 5.10 contains the coefficients for the brick wall construction; and Table 5.11 contains the coefficients for the glazed aluminum curtain wall construction. These values have been modified from the *1977 ASHRAE Handbook* (ASHRAE, 1977) for the corrected U-values for each wall construction

Table 5.9: Transfer Function Influence Coefficients for the Roof Construction

Coefficient	n = 0	n = 1	n = 2	n = 3	n = 4	n = 5
b_n (BTU/(hr-ft ² -°F))	0.00000	0.00003	0.00035	0.00056	0.00018	0.00015
c_n (BTU/(hr-ft ² -°F))	0.00114	-	-	-	-	-
d_n (unit less)	-	-0.24424	0.12954	-0.02560	0.00170	-0.00003

Table 5.10: Transfer Function Influence Coefficients for the Brick Wall Construction

Coefficient	n = 0	n = 1	n = 2	n = 3	n = 4
b_n (BTU/(hr-ft ² -°F))	0.00000	0.00056	0.00208	0.00104	0.00009
c_n (BTU/(hr-ft ² -°F))	0.00378	-	-	-	-
d_n (unit less)	-	-0.25101	0.10210	-0.01258	0.00041

Table 5.11: Transfer Function Influence Coefficients for the Glazed Aluminum Curtain Wall Construction

Coefficient	n = 0	n = 1	n = 2	n = 3
b_n (BTU/(hr-ft ² -°F))	0.00382	0.01985	0.00629	0.00008
c_n (BTU/(hr-ft ² -°F))	0.03003	-	-	-
d_n (unit less)	-	-0.44738	0.06573	-0.00002

The combined conduction skin load data (roof, brick wall and glazed aluminum curtain wall) has been calculated two ways: through the first order conduction skin load equation discussed in Section 5.1.4.2 and through the transfer function conduction skin load equation discussed above. This comparison is best illustrated below in Figure 5.22

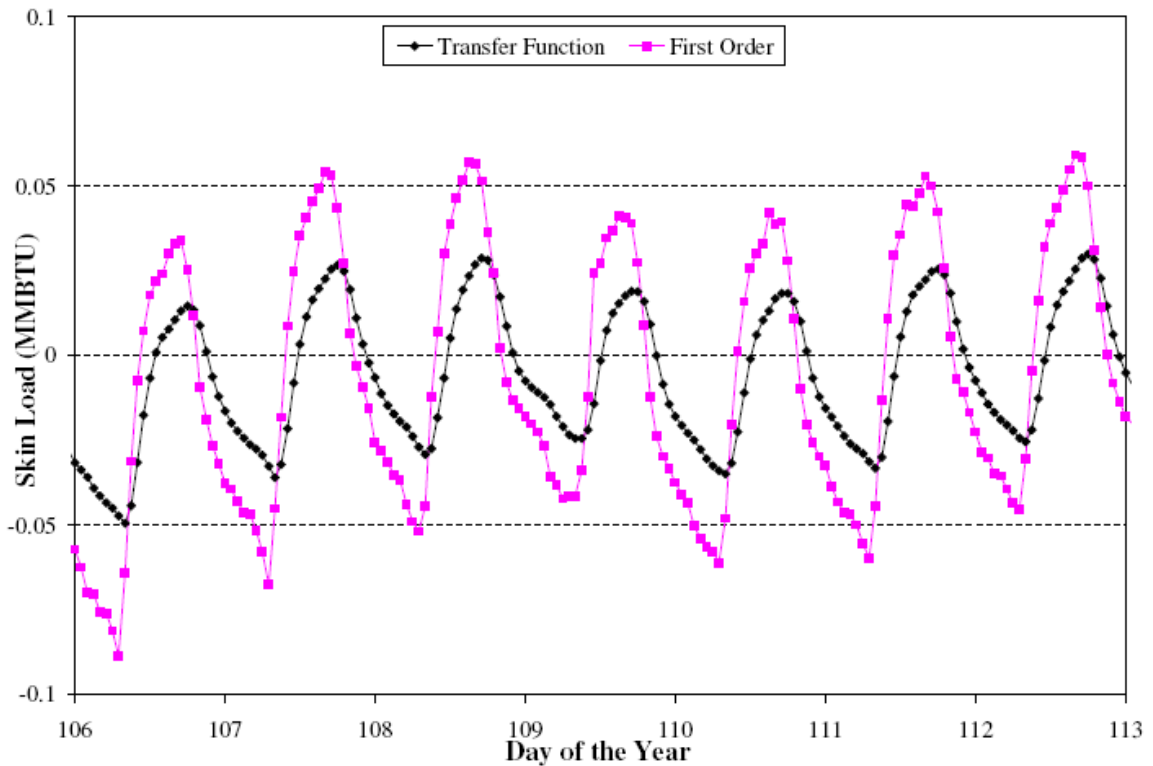


Figure 5.22: Conduction Skin Load Comparison

As illustrated above, the two conduction skin loads follow the same trend (shown for April 16th - 22nd, 2008 which is equal to Julian day 106-113). The transfer function conduction skin load is much less affected by the changing environmental conditions (temperature and solar radiation) due to the heat capacity and time lag built into its equation. However, over the course of the year (September 2007 – August 2008), the difference between these two conduction loads is approximately 3 MMBTUs, or 2.5% of the total annual conduction skin load, which is small enough to be considered negligible.

In a general purpose single-zone model for engineers to use in preliminary design, a few wall types (light, medium, heavy) could be cataloged, adjustments made for actual U-values, and then applied for a wide range of actual wall types. For the programming code which was used for the transfer function conduction skin load calculations within Excel's VBA, please refer to APPENDIX G: Transfer Function Conduction Skin Loads Code.

5.1.4.4 Direct Solar Heat Gain Skin Loads

The direct solar heat gain by through windows at a specific time depends on the transmittance of the window, the incident angle of the sun, the shading coefficient, directional solar radiation and the absorptivity of the glass. Therefore, the solar heat gain skin load can be defined as

$$\dot{Q}_{\text{SHG}} = \alpha_{\text{abs}} SC \tau_{\text{ref}}(\theta_{\text{B}}) G_{\text{T}} A \quad (5.76)$$

where α_{abs} is the absorptivity of the windows, SC is the shading coefficient, τ_{ref} is the transmittance which is a function of the incident angle θ_{B} , G_{T} is the total solar radiation incident to the surface, and A is the amount of area covered by windows (per direction). The total solar radiation (G_{T}) used for the skin load calculations is from the collected solar radiation data from UGA which is then modified based on the directional orientation of the wall (South, South-West, West, North-West, North, North-East, East, and South-East) by where the sun is in the sky. τ_{ref} , and θ_{B} are discussed above in Section 5.1.4.1: Solar Calculations.

The absorptivity of the windows in the Klaus building has been estimated to be 0.9 while the shading coefficient has been estimated to be 0.43 based on Klaus construction documents.

For the programming code which was used for the solar heat gain skin load calculations within Excel's VBA, please refer to APPENDIX F: Combined Skin Load Code.

5.1.5 Internal Loads

For any building, there are three internal loads which have to be considered: People, Lighting and Equipment. For the Klaus building, the loads from people are determined based on estimated occupancy schedules while the electrical loads from the lighting and equipment can be determined from the real time electrical data collected through Metasys.

5.1.5.1 Occupancy Loads

The people loads, sometimes referred to as occupancy loads, can be defined as

$$\dot{Q}_{\text{People}} = N_{\text{People}} \cdot THG \cdot CLF \quad (5.77)$$

where N_{People} is the estimated number of people in the building, THG is the total heat gain and CLF is the cooling load factor. The THG in the Klaus building takes into account both sensible heat gain (SHG) and latent heat gain (LHG). Since the Klaus building has a high person density and there are variable space temperatures, the CLF is assumed to be one. However, the effect of people is different for heating vs. cooling loads because cooling loads include the latent heat gain whereas the heating loads do not.

Sensible heat gain is added directly to the space by conduction, convection and/or radiation. Latent heat gain occurs when moisture is added to the space (from occupants or equipment). The conversion of sensible heat gain from people to the space cooling load is affected by the thermal storage characteristics of that space since some percentage of the sensible load is radiant energy. On the other hand, latent heat gains are considered to be instantaneous. The representative heat gain rates used for the Klaus building occupancy load calculations are shown in Table 5.12 which is an excerpt from the full table provided in the *ASHRAE Handbook* (ASHRAE, 2001) to better illustrate the specific heat gains used for a building like Klaus.

Table 5.12: Representative Rates at Which Heat and Moisture Are Given Off by Human Beings (ASHRAE, 2001)

Degree of Activity	Location	Sensible Heat Gain	Latent Heat Gain	Total Heat Gain
Moderately Active Office Work	Offices, Hotels, Apartments, etc.	250 BTU/h	200 BTU/h	450 BTU/h

The number of people in the Klaus building has been estimated based on occupancy schedules, and then verified through carbon dioxide calculations. Occupancy schedules can be subdivided into three categories: daily schedules, weekly schedules, and annual schedules. The daily schedules vary depending on the day of the week (weekdays, Saturdays, or Sundays and Holidays) and the time of the year (regular, summer, or break). The weekly schedules also vary based on the time of the year (regular, summer, break, or month). For all three schedule types, the building occupancy is estimated based on predicted fractions of the total occupancy.

The building's construction documents estimated a maximum of 1824 business people in the building and a maximum of 625 people in the classrooms (and

auditoriums). Together this estimates that a maximum of 2449 people will ever be in the Klaus building at any given time. However, since this is the maximum allowed occupancy, the occupancy schedule fractions are rarely (if ever) documented as one which means that N_{People} will always be well under 2449, but will continually change depending on the day of the week, month of the year, school schedule, and so forth.

Carbon dioxide measurements have been used to verify the occupancy estimations. The average person generates carbon dioxide at a rate of approximately 0.31 L/min (ASHRAE, 2002). Therefore, the number of people in the building can be determined as

$$N_{\text{People}} = \frac{\dot{V}_{\text{OA}} (C_{\text{RA}} - C_{\text{OA}})}{\dot{V}_{\text{CO}_2}} \quad (5.78)$$

where \dot{V}_{OA} is the volumetric flow of outside air entering the building, C_{RA} is the carbon dioxide concentration of return air, C_{OA} is the carbon dioxide concentration of outside air, and \dot{V}_{CO_2} is the carbon dioxide generation rate (0.31 L/min).

The estimated number of the people in the building has been compared to the number of people calculated through the use of the carbon dioxide measurements. This comparison is illustrated below for a typical school year day (March 3rd, 2008) and a typical summer day (May 17th, 2008).

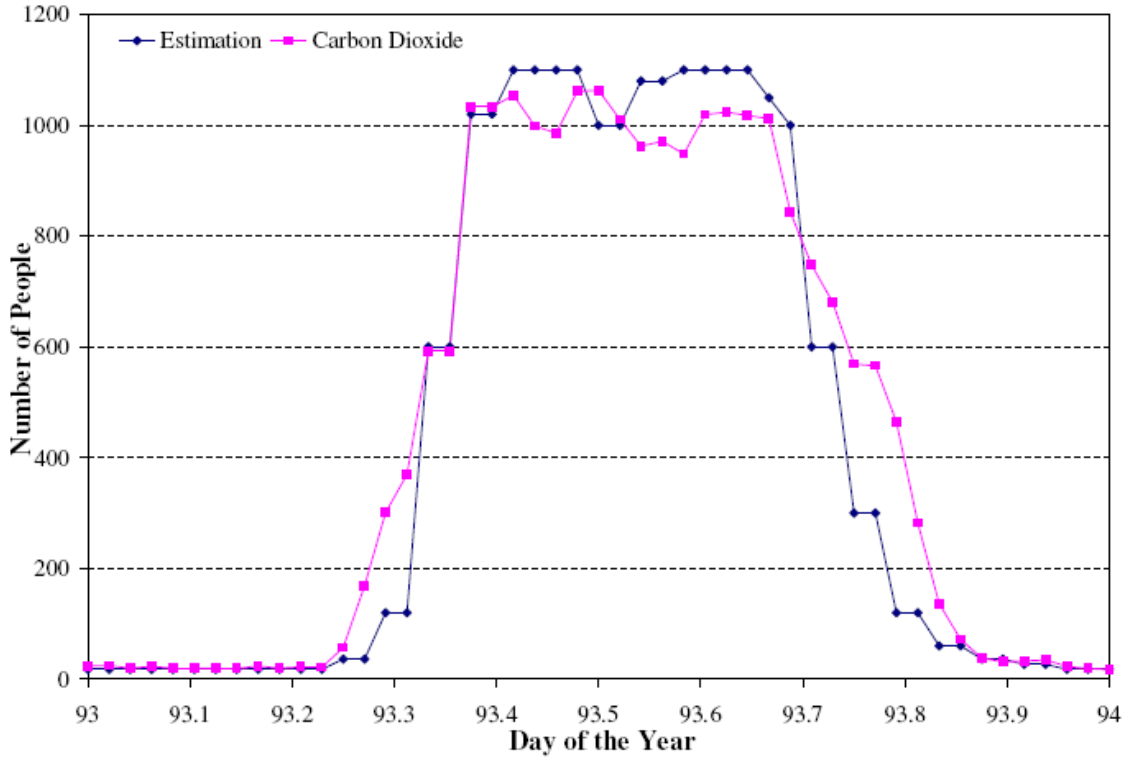


Figure 5.23: Occupancy Comparison for March 3rd, 2008

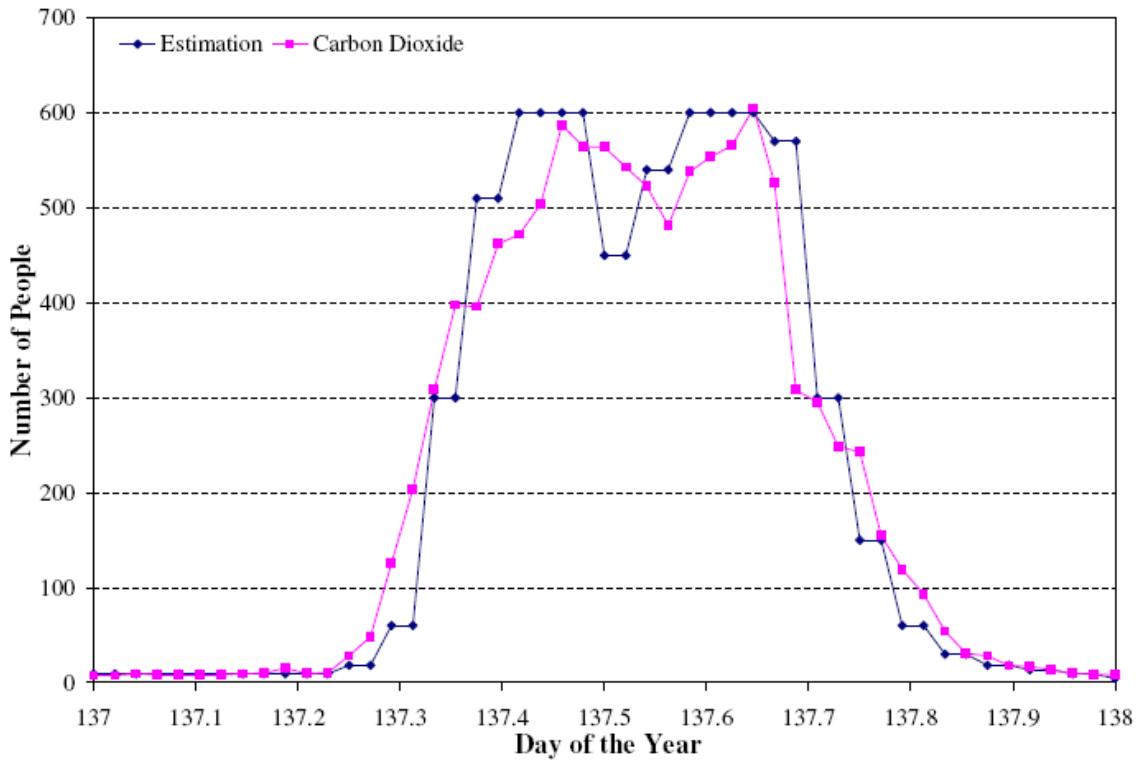


Figure 5.24: Occupancy Comparison for May 17th, 2008

where the x-axis represents the day of the year and time (hour) fraction of the day (e.g. .5 would be 12 noon) and the y-axis represents the number of people in the building.

As illustrated in the two figures above, the estimated building occupancy closely mimics the number of people in the building as determined from the carbon dioxide concentrations. Figure 5.23 portrays March 3rd, 2008 which was chosen as a sample week day during the typical school year. Next, Figure 5.24 portrays May 17th, 2008 which was chosen as a sample week day during the summer. One thing of note between the two figures is that the summer occupancy schedule has far fewer people in the building.

5.1.5.2 Electrical Loads

The electrical loads for the Klaus building include data for both the equipment and the lighting. This data can be determined from the real time electrical data collected with Metasys which have then been combined to be

$$\dot{W}_e = \dot{W}_{e,PL} + \dot{W}_{e,EPL} \quad (5.79)$$

where \dot{W}_e is the total electrical load, $\dot{W}_{e,PL}$ is the electrical load from the power and lights within the building, and $\dot{W}_{e,EPL}$ is the emergency power and lights load.

Since the parking deck attached to the Klaus building is not being considered in the overall load analysis, the above equation can be used to find the overall electrical load for the Klaus building not including the parking deck. If the parking deck were to be included, a different equation would need to be used which would also take into account the power and lighting needed for the parking deck. This equation would be

$$\dot{W}_{e,EB} = \dot{W}_{e,MBA} + \dot{W}_{e,MBB} \quad (5.80)$$

where $\dot{W}_{e,EB}$ is the electrical load for the entire building (including the parking deck), $\dot{W}_{e,MBA}$ is the Main Breaker A on the switchboard, and $\dot{W}_{e,MBB}$ is the Main Breaker B on the switchboard, both of which measure basically half of the total building load.

Since only the building, not the parking deck, is being analyzed, the original \dot{W}_e equation has been used for calculations. For the programming code which was used for the both the building and the building plus the parking deck electrical load calculations within Excel's VBA, please refer to APPENDIX H: Electrical Loads Code.

Finally, the electrical load data and calculations were completed using SI units while all of the other calculations have utilized English units. Therefore, the electrical load units of kWh have been converted to MBTUs for overall energy use comparisons and percent savings as a whole. However, the DOE and eQUEST output summaries also record their energy loads in SI units. Therefore, only direct electrical energy load comparisons will use SI units.

5.2 Models

In order to thoroughly understand what the original DOE-2 model predicted for the Klaus building, three additional model variations were completed. The first model is composed of only three load components: heating, cooling, and electrical and is discussed below in Section 5.2.1: Monitored Data . The second model was created to treat the Klaus building as one unit in a simplified single-zone model which takes into consideration all of the typical loads on a building. This second model is discussed below in Section 5.2.2: Combined Single-Zone Simplified Model. The third, and final, model is another complex computer-based building simulation model, eQUEST.

Although this model is very similar to the original DOE-2 model, the major variation of note is the updated weather file. This final model is discussed below in Section 5.2.3: New eQUEST Model.

5.2.1 Monitored Data

The monitored data model was created based on the three major loads within a building: heating, cooling, and electrical. This energy balance is illustrated below as

$$\frac{dE}{dt} = \dot{Q}_H + \dot{Q}_C + \dot{W}_e \quad (5.81)$$

where \dot{Q}_H is the heating load, \dot{Q}_C is the cooling load, and \dot{W}_e is the electrical load. The calculations of these monitored loads have been discussed in detail above in Sections 5.1.1, 5.1.2, and 5.1.5.2, respectively.

This model is referred to as the monitored data model since all three loads represent the actual load which occurred in the Klaus building over the September 2007 – August 2008 time frame. These three loads were selected for comparison since the energy predictions from the original DOE-2 model which was created before the building was built focused on electricity, natural gas, chilled water and steam. However, the Klaus building does not utilize any natural gas.

Modeling only the heating, cooling, and electrical loads allows for quick comparisons, verifications and validations between the predicted DOE-2 model and the actual monitored data. Overall, the monitored heating, cooling, and electrical loads within the Klaus building were within 13.3% of those predicted by the original DOE-2 model. These comparisons are detailed below in Chapter 6.

5.2.2 Combined Single-Zone Simplified Model

There are seven energy sources which affect a typical building control volume. These energy flows are heating (\dot{Q}_H), cooling (\dot{Q}_C), outside air flow ($\dot{Q}_{OA,total}$), internal loads from people (\dot{Q}_{People}), lighting and equipment (\dot{W}_e), and skin loads from solar heat gain (\dot{Q}_{SG}) and conduction through walls (\dot{Q}_{Cond}). How these energy loads work can best be shown through the energy balance equation where

$$\frac{dE}{dt} = \dot{Q}_H - \dot{Q}_C + \dot{Q}_{OA,total} + \dot{Q}_{Internal} + \dot{Q}_{Skin} \quad (5.82)$$

From the energy balance above, five major load components have been established: heating, cooling, outside air, internal and skin loads. Three of these loads, however, first need to be simplified for better understanding where

$$\frac{dE}{dt} = \dot{Q}_H - \dot{Q}_C + (\dot{Q}_{OA} - \dot{Q}_{RA}) + (\dot{Q}_{Cond} + \dot{Q}_{SG}) + (\dot{Q}_{People} + \dot{W}_e) \quad (5.83)$$

The right hand side of the above equation illustrates all of the loads acting on a building. These loads can also be compared to the thermal mass time-lag model for the building where

$$\frac{dE}{dt} = mC \frac{dT}{dt} = \dot{Q}_H - \dot{Q}_C + \dot{m}_{OA} (h_{OA} - h_{RA}) + \dot{Q}_{Cond} + \dot{Q}_{SG} + \dot{Q}_{People} + \dot{W}_e \quad (5.84)$$

where mC is the thermal mass of the building and $\frac{dT}{dt}$ is the changing temperature rate.

This temperature rate is determined from the return air temperature through numerical differentiation where

$$\frac{dT}{dt} = \lim_{t \rightarrow 0} \frac{-T(t + 2\Delta t) + 8T(t + \Delta t) - 8T(t - \Delta t) + T(t - 2\Delta t)}{12\Delta t} \quad (5.85)$$

where T is the return air temperature and Δt is the time step (0.5 hours). However, there are four exceptions, the first and last data points, and the second and second to last data points. Therefore,

$$\frac{dT}{dt} = \lim_{t \rightarrow 0} \frac{T(t + \Delta t) - T}{\Delta t} \quad (5.86)$$

can be used for the first and last data points and

$$\frac{dT}{dt} = \lim_{t \rightarrow 0} \frac{T(t + \Delta t) - T(t - \Delta t)}{2\Delta t} \quad (5.87)$$

can be used to determine the second and second to last data points.

Inspection of the temperature derivative reveals that the indoor temperature and consequently the indoor energy hardly changes over the year. This minimal change in temperature indicates that, as desired, the building indoor state remains almost exactly constant and well-controlled.

The next step is to then determine the thermal mass of the building based on the building's energy loads and the temperature rate. Once the thermal mass for the building is determined, this information can then be used to help predict how the building will continue to operate. Unfortunately, determining the building's thermal mass is not as simple as it appears due to the constant load fluctuations within the building. Therefore, a different approach was used. Also, however, since the building construction is tight and the building is kept pressurized, the effect of the thermal mass on the building is minimal.

This new approach utilizes the fact that the simplest single-zone model would have no building heat capacity. This model incorporates all of the loads which can be

calculated from commonly available information to then predict the necessary heating or cooling load of the building.

Given this behavior of a precisely controlled building means that in the simplest single-zone model, the building dynamics can be ignored and it can be assumed that at any instant the building HVAC system almost exactly meets the load. This assumption is equivalent to assuming constant controlled indoor conditions. Since this response is desired in contemporary HVAC design, this simplified single-zone model is actually suitable for most existing buildings. This limited model is not adequate for supporting more advanced HVAC controls wherein the indoor air state may be allowed to drift somewhat to reduce energy during peak periods.

For this simplified single-zone model, the basic shape of the building has been modeled as an octagon (as illustrated below as a regular octagon in Figure 5.25 and as the actual Klaus octagonal overview in Figure 5.26) with the eight typical directions (North, North-East, East, South-East, South, South-West, West, and North-West) with a flat roof for solar heat gain.

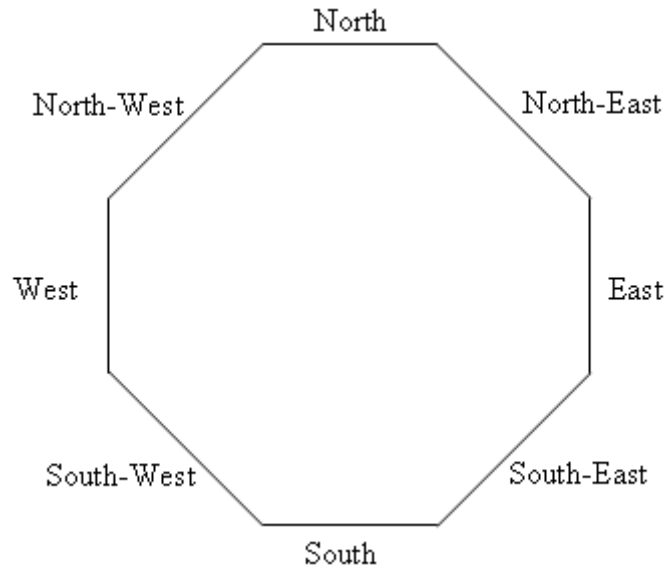


Figure 5.25: Regular Directional Octagon Schematic

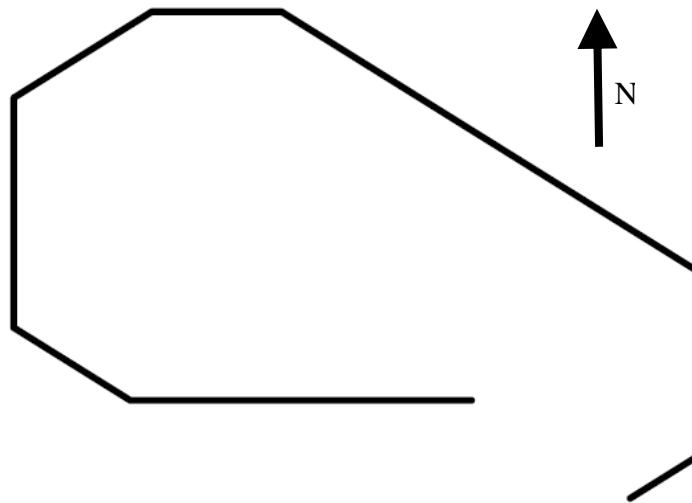


Figure 5.26: Directional Octagon Schematic for the Klaus Building

The actual building walls are assigned to one of the eight directions. Every wall can have fenestration with basic transmittance as function of incident angle and adjustable normal incidence transmittance. Each wall can consist of fenestration, light wall (in this case the glazed aluminum curtain wall construction), and heavy wall (in this

case the brick wall construction) for conduction loads. More wall types can be added, but may not really be needed.

The envelope loads have been determined through the transfer function model for conduction through the walls and the solar heat gain model for the load from the windows. The transfer function conduction skin load model will be used instead of the first order conduction skin load since the transfer function model takes into account the thermal time lag within the walls, and, therefore, will indicate a more accurate conduction envelope load at specified times. The transfer function coefficients can be adjusted for actual conductance (but in the future, a wall heat capacity can be modeled so that the transfer function coefficients will not be needed.) The solar heat gain model is of particular interest due to the fact that it utilizes collected solar radiation data which is only available as the global solar radiation data which has then been broken down into its sky dome and beam normal components. It is likely that future buildings would be able to use these envelope models due to the fact that global solar radiation data is more readily available than its individual components, yet these models also are able to accurately break down the global solar radiation data into its various components. Next, the building's internal loads can be determined through accurate measurements or occupancy schedules. For example, the occupancy can be determined by the method which utilizes the outside air and return air carbon dioxide concentrations while the electrical loads are determined through the building's breaker switchboards.

The envelope conduction loads are calculated from simple and well established heat transfer models, and the solar heat gain is calculated from somewhat more complex solar decomposition and transmittance-absorptance models. Therefore, these two loads

as well as the internal loads are expected to be precisely determined. In contrast, the outside air load requires a somewhat complex thermodynamic and fluid mechanical calculation.

The outdoor air load is proportional to the occupancy since the building actually has demand control ventilation. In an alternative design, the building could have constant outdoor air supply switching on enthalpy control to maximum outdoor air flow for free cooling. Even though the outside air loads have been verified using both the carbon dioxide concentrations and the control logic from the air handlers and energy recovery units, both of these calculations are determined through fan laws, fan curves and equilibrium equations. Therefore, the outside air load should be an acceptable estimate to be used in this single-zone model.

Finally, the simplified single-zone model will determine the necessary heating or cooling load (\dot{Q}_{HVAC}) on the building by ignoring the rate of energy accumulation or reduction in the building. The HVAC load is assumed to instantaneously meet the imposed loads, so

$$\dot{Q}_{\text{HVAC}} = \dot{m}_{\text{OA}}(h_{\text{OA}} - h_{\text{RA}}) + \dot{Q}_{\text{Cond}} + \dot{Q}_{\text{SG}} + \dot{Q}_{\text{People}} + \dot{W}_e \quad (5.88)$$

where \dot{Q}_{HVAC} is determined as the needed heating load or cooling load, whichever is needed to help the building level off again. For now, the HVAC system is assumed to instantaneously meet the load. In future work, the building's interior state can be allowed to drift dynamically.

To determine the actual accuracy of the simplified single-zone model to predicted the heating and cooling loads, these calculated heating and cooling loads have been compared to the actual heating and cooling loads which were measured within the

example building. These results and further discussion of this single-zone model can be found in Section 6.4.

5.2.3 New eQUEST Model

A complex computer simulation modeling program, DOE-2, was used for hour-by-hour load predictions for how the Klaus building would operate before it was built. In order to best compare the predicted DOE-2 model to the actual monitored data was to recreate an updated DOE-2 model. This was done using another complex building simulation program, eQUEST. Both DOE-2 and eQUEST are developed by J. J. Hirsch and Associates in collaboration with the Lawrence Berkeley National Laboratory (LBNL), and partially funded by the United States Department of Energy (DOE).

DOE-2 and eQUEST programs are both available as freeware. However eQUEST is the more user friendly version of DOE-2. eQUEST is a sophisticated, yet easy to use program once the building design is complete and the building is fully described. It not only offers a detailed graphical user interface to assist with inputs, but it also provides a graphical display of the HVAC equipment and the modeled building geometry. DOE-2, on the other hand, is only composed of code in text form.

In order to accurately compare the monitored load data with the computer model's simulation, a new simulation was performed on the Klaus building using eQUEST. The majority of the building inputs were kept the same between the original DOE-2 model and the new eQUEST model to assure consistency between the results. The inputs used in the original DOE-2 model are discussed in more detail below in Section 5.2.3.1. The only significant input which differs between the original DOE-2 model and the new

eQUEST model is the weather data which is discussed in more detail below in Section 5.2.3.2.

Even though eQUEST is more user friendly than the DOE-2 program, there are still many aspects which complicate the program, especially the sheer number of inputs which are required to adequately run the simulation. The simplified single-zone model needs basic information as inputs which can easily be updated as the building design progresses while the eQUEST (and DOE-2) program requires exact details on the sizing, spacing, orientation, interaction and so forth of almost every necessary input. For example, the single-zone model uses the overall wall area (as a combination of heavy wall, light wall and fenestration) in each of the eight typical directions while the eQUEST program inputs require each window and wall segment to be individually entered before the outer structure can be complete. Similarly, the eQUEST model requires the specific floor plan of the building while the single-zone model considers the interior as one entity. Therefore, even though the eQUEST program is available as freeware and is more user friendly than the DOE-2 program, the simplified single-zone model is still faster to create, can be created before the building is finalized, and allows for quick changes as the building's design progresses.

5.2.3.1 Original DOE-2 Model

In order to be the most compatible for comparisons, all of the inputs for the new eQUEST model are exactly the same as those used for the original DOE-2 model, except for the weather data. An overview of the original DOE-2 inputs is provided below.

The original DOE-2 model (and subsequently the new eQUEST model) of the Klaus building was comprised of 106 zones: 82 exterior and 24 interior zones. The

building is cooled through the campus (Georgia Tech's) chilled water supply and heated through the campus steam supply. Electrical loads are also accounted for. There are four air handler units, and two energy recovery units. The equipment, lighting and occupancy schedules vary dependant on the time of day, day of the week, month of the year, and various holidays and school vacations.

The building's structure within the DOE-2 model consists of three-conditioned floors, with a penthouse above and a three-story parking deck below the main building. The outside wall constructions include brick wall compositions, glazed aluminum curtain wall compositions, clear glass windows, fritted glass windows, doors, a roof and sun-screens. The modeled building's structure is consistent with that presented above in Sections 3.5.1.1 - 3.5.1.4, 5.1.4.2.1 - 5.1.4.2.3, and 5.1.4.4.

The coding language used for DOE-2 is called Building Description Language (BDL), (Hirsch, 2006a). The BDL code consists solely of text. The input file for the Klaus building from the original DOE-2 simulation model includes 8,102 lines of unique BDL code.

5.2.3.2 TMY Weather Data

The weather used for the original DOE-2 analysis was TMY (Typical Meteorological Year) hourly weather data for Atlanta, Georgia. TMY data is frequently used in building simulation to better assess the expected heating and cooling loads for the design of the building. TMY data is a composite of actual hourly long-term weather measurements for the area that reflects average temperature, humidity, wind, and solar conditions, to name a few.

TMY data is a set of standard hourly weather values for a one-year period. It is compiled of months selected from individual years which are assembled to form a complete year. TMY data typically represents conditions characteristic of the past 30 years. Since the TMY weather data does represent a typical year's data rather than the weather that actual occurred, a new weather file was created for the new eQUEST simulation.

Accurate weather data is necessary in order to truly compare and validate the collected data to that predicted with the computer simulation software. Therefore, a new weather file needed to be created using the actual weather which occurred over the time period in which the Klaus building was monitored. This new weather file was created using the same format as a typical TMY data file so that the eQUEST program would still be able to run properly. The weather data that was purchased from UGA was used along with some supplemental weather data in order to adequately create a new mock-TMY data file.

Since TMY stands for "Typical Meteorological Year," the new weather file is referred to as a mock-TMY as to eliminate any misunderstandings related to a typical year's weather data verses the actual weather data for that year. For more information about how the mock-TMY file was created, please refer to APPENDIX K: Creating a Mock-TMY Data File.

The results and comparisons of the various models presented above in this chapter are further discussed and evaluated in the next chapter, Chapter 6: MODEL COMPARISONS.

6 MODEL COMPARISONS

Before most building are constructed, a computer simulation model is often developed which attempts to predict how that building will actually perform once it is built. The Klaus building is no exception. There were two DOE-2 models created to predict the yearly loads within the Klaus building: one uses the actual components (DOE-2 Predicted Model) and the other (DOE-2 Baseline Model) uses the minimum requirements as defined by *ASHRAE Standard 90.1-1999* (ASHRAE, 1999). These models were created to indicate a representative year, not a specific year.

There are four models discussed in this chapter as well as the actual load results. These models are the DOE-2 Predicted Model, the DOE-2 Baseline Model, the eQUEST Model and the Single-Zone Model (SZM) where

Table 6.1: Model Names and Descriptions

Model Name	Model Description
DOE-2 Predicted	This model was created before the Klaus building was built to illustrate how the building should ideally operate in a typical year using TMY weather data.
DOE-2 Baseline	This model was created before the Klaus building was built to simulate how the building would operate for a typical year using TMY weather data if only the minimum <i>ASHRAE Standard 90.1</i> requirements were met.
eQUEST	This model was simulated for the September 2007 - August 2008 time period for which the actual load data was also calculated. This model uses an actual weather data file in TMY format in order to accurately portray the actual weather during the monitored time period.
Single-Zone	This simplified model predicts the heating or cooling load in the building based on the other imposed loads which directly affect the building.
Actual Load Data	The actual load data was calculated using the monitored information from September 2007 - August 2008.

The predicted load summaries for the two DOE-2 models are condensed below in Table 6.2 and Table 6.3. Please note that for HVAC analysis, MBTU represents a thousand BTU, while MMBTU represents a million BTU. For simplified conversion to SI, recall that a BTU is approximately one kJ (1,000 BTU = 1.055 kJ); therefore a thousand BTUs (an MBTU in HVAC style) is approximately one MJ, and a million BTUs (or MMBTU in HVAC style) is about one GJ.

Table 6.2: DOE-2 Predicted Model Loads Summary

Month	Electrical (kWh)	CHW (MMBTU)	Steam (MMBTU)
September	192,305	966	1
October	188,120	577	30
November	169,294	235	123
December	116,413	93	450
January	185,355	114	364
February	167,886	154	287
March	166,995	221	192
April	172,004	468	70
May	113,741	618	37
June	132,849	764	18
July	143,229	796	22
August	159,905	820	27
Total	1,908,096	5,826	1,621

Table 6.3: DOE-2 Baseline Model Loads Summary

Month	Electrical (kWh)	CHW (MMBTU)	Steam (MMBTU)
September	194,568	1,168	23
October	206,997	837	170
November	189,586	591	378
December	117,335	303	755
January	211,519	555	808
February	190,563	535	619
March	190,151	604	467
April	194,716	771	240
May	149,003	1,147	362
June	149,379	1,305	276
July	150,968	1,624	305
August	162,577	1,490	221
Total	2,107,362	10,930	4,624

Through the use of energy saving features previously discussed in Section 3.5.1, the loads calculated in the DOE-2 Predicted Model all allowed for yearly savings as compared to the DOE-2 Baseline Model. These savings are summarized below

Table 6.4: Percent Savings Overview of DOE-2 Predicted Model Compared to DOE-2 Baseline Model

	DOE-2 Predicted	DOE-2 Baseline	Savings
Electrical (MMBTU)	6,511	7,191	9.5%
Cooling (MMBTU)	5,827	10,931	46.7%
Heating (MMBTU)	1,621	4,624	64.9%
Total	13,959	22,746	38.6%

The DOE-2 Predicted Model anticipated the Klaus building to save approximately 39% of its yearly electrical, heating, and cooling energy consumption. For LEED certification, Earth and Atmosphere (EA) Credit-1 points are awarded for projected model savings. For a projected savings of 39%, the Klaus building was able to earn 4 EA Credit-1 points towards LEED certification.

Unlike the two DOE-2 models, the actual monitored loads for the Klaus building have been calculated for a specific time period, September 2007 – August 2008. The load summaries of calculations from the actual monitored data is presented in Table 6.5

Table 6.5: Monitored Loads Summary

Month	Electrical (kWh)	CHW (MMBTU)	Steam (MMBTU)
September	131,570	690	9
October	144,885	696	34
November	150,865	250	119
December	121,441	166	281
January	126,372	112	327
February	158,387	148	283
March	160,027	141	214
April	169,701	166	72
May	111,826	513	45
June	120,759	755	16
July	105,448	839	20
August	109,074	691	21
Total	1,610,352	5,166	1,441

Since the two DOE-2 Models represent a typical year and not the actual year in which the monitored data was created for, another computer simulation model was created using eQUEST, a sister program to DOE-2. The eQUEST Model utilizes a file created directly from the September 2007 – August 2008 weather conditions for Atlanta, Georgia instead of employing TMY (Typical Meteorological Year) Data which was used for the DOE-2 Models. This new weather file was created to represent the actual weather conditions as for the specified year as opposed to using the assumed typical weather, but still followed the necessary file format so that the model would still run properly. Please refer to APPENDIX K: Creating a Mock-TMY Data File for a detailed description as to

how to create a mock-TMY weather file. The load summaries for the eQUEST Model is condensed below in Table 6.6

Table 6.6: eQUEST Model Loads Summary

Month	Electrical (kWh)	CHW (MMBTU)	Steam (MMBTU)
September	154,098	720	4
October	156,951	676	37
November	153,691	274	122
December	115,779	152	319
January	148,100	101	336
February	167,809	148	296
March	166,500	152	204
April	171,909	188	70
May	113,325	520	42
June	121,101	822	20
July	115,097	820	19
August	128,552	721	30
Total	1,712,912	5,294	1,499

The monitored loads over the course of September 2007 – August 2008 were lower than the three computer simulation models. The percent savings from the actual monitored load data compared to the three simulation models is presented below in Table 6.7

Table 6.7: Monitored Load Percent Savings to the Compared Simulation Models

eQUEST	4.2%
DOE-2 Predicted	13.3%
DOE-2 Baseline	46.8%

As expected, the eQUEST Model best represents the actual monitored load data as shown through the 4.2% difference in the September 2007 – August 2008 building loads.

A graphical representation of the load data provided in the above tables for the DOE-2 Predicted Model, the DOE-2 Baseline Model, the Actual monitored data, and the eQUEST Model are illustrated below in Figure 6.1 – Figure 6.8. Please refer back to Table 6.1 for model descriptions.

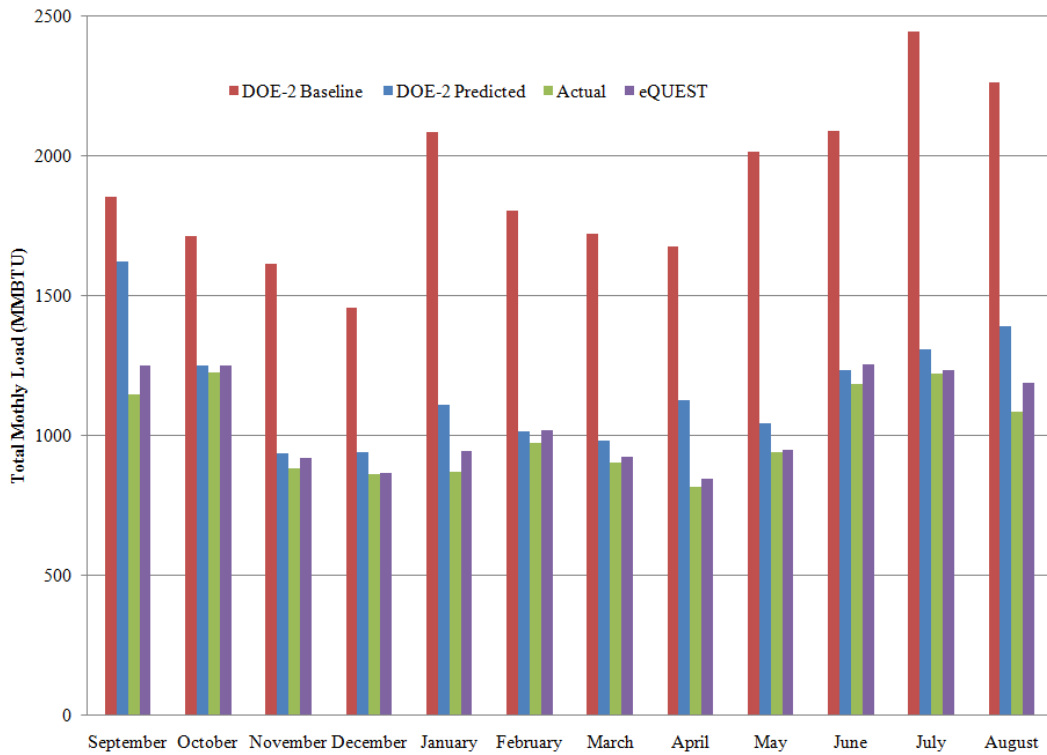


Figure 6.1: Total Monthly Loads

Figure 6.1 compares the total monthly loads for the four sets of data, while Figure 6.2 eliminates the DOE-2 Baseline Model, which was created based on the minimum requirements from *ASHRAE Standard 90.1* (ASHRAE, 2001) for a building in Atlanta, to focus on the more representative data.

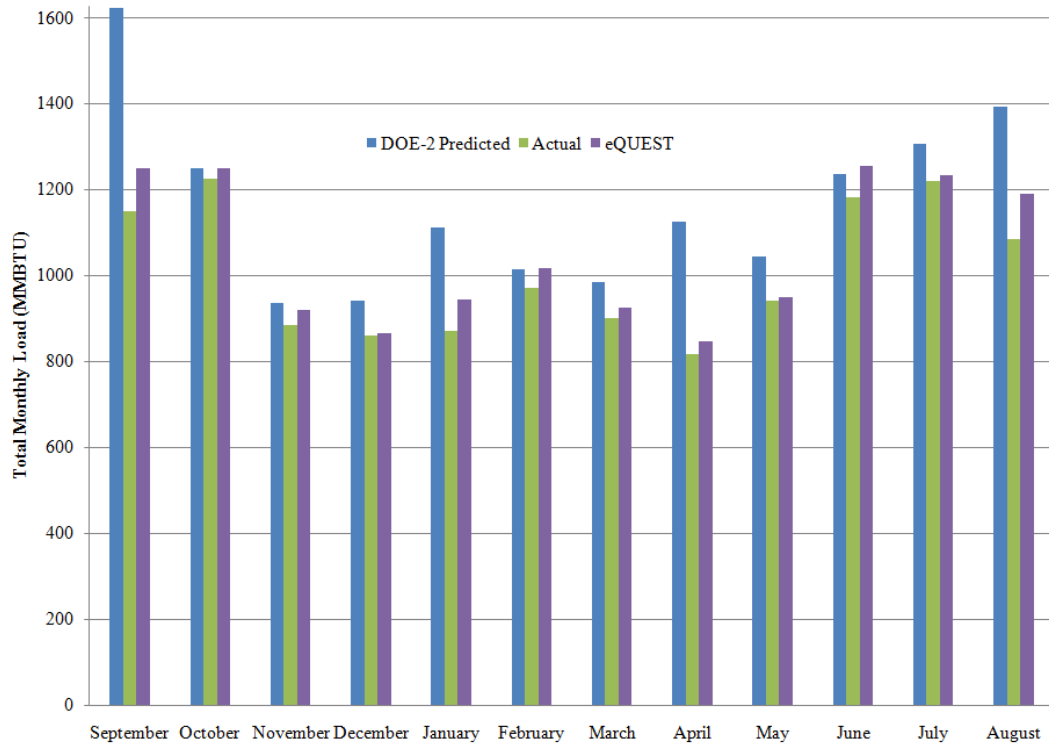


Figure 6.2: Total Monthly Loads (without DOE-2 Baseline Model)

Next, these loads are broken down into the three main components: Electrical Loads, Cooling Loads, and Heating Loads. Each load (electrical, cooling, and heating) has two figures: one with all four loads (DOE-2 Predicted Model, DOE-2 Baseline Model, the Actual monitored data, and the eQUEST Model) represented, and the other without the DOE-2 Baseline Model.

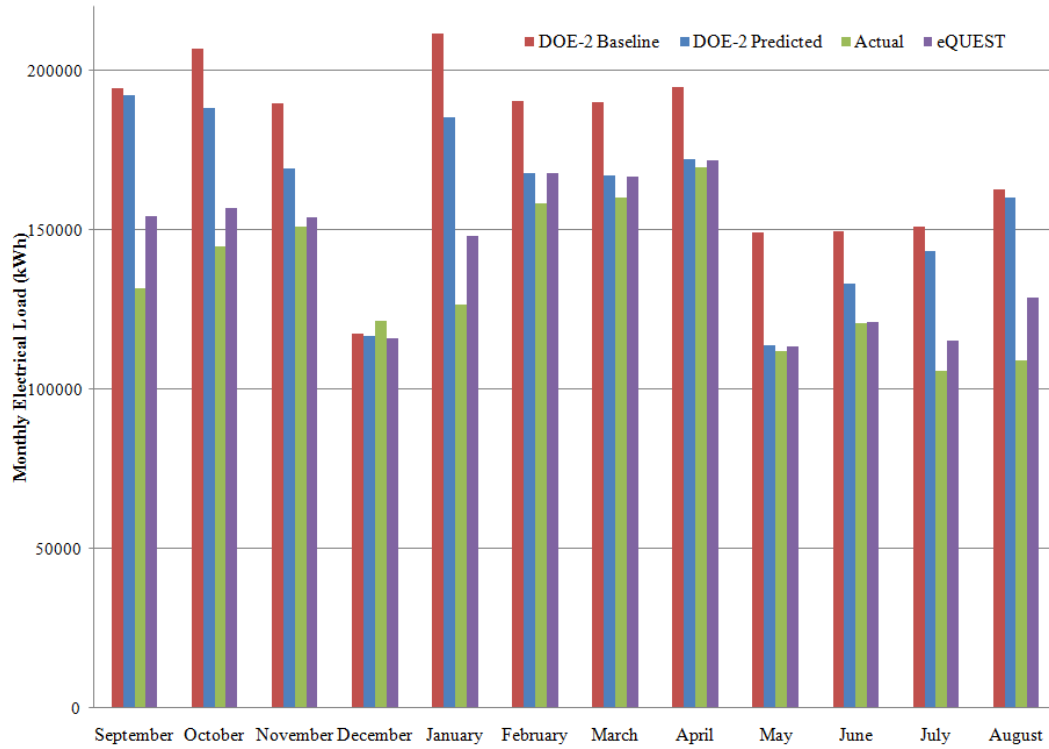


Figure 6.3: Monthly Electrical Load

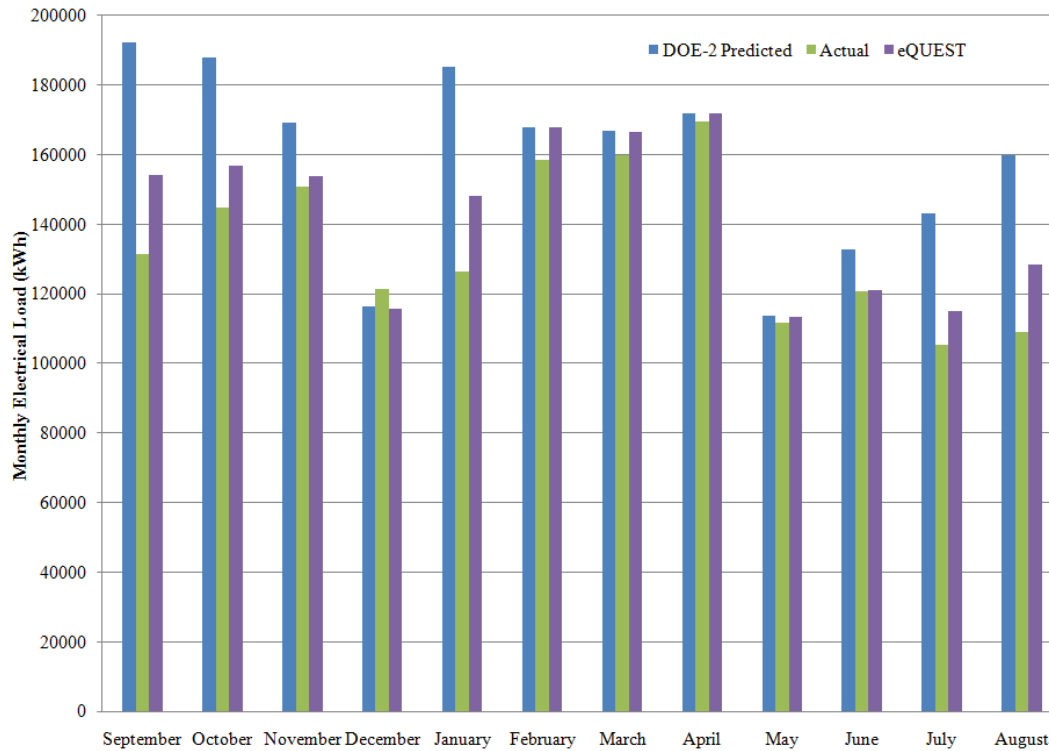


Figure 6.4: Monthly Electrical Load (without DOE-2 Baseline Model)

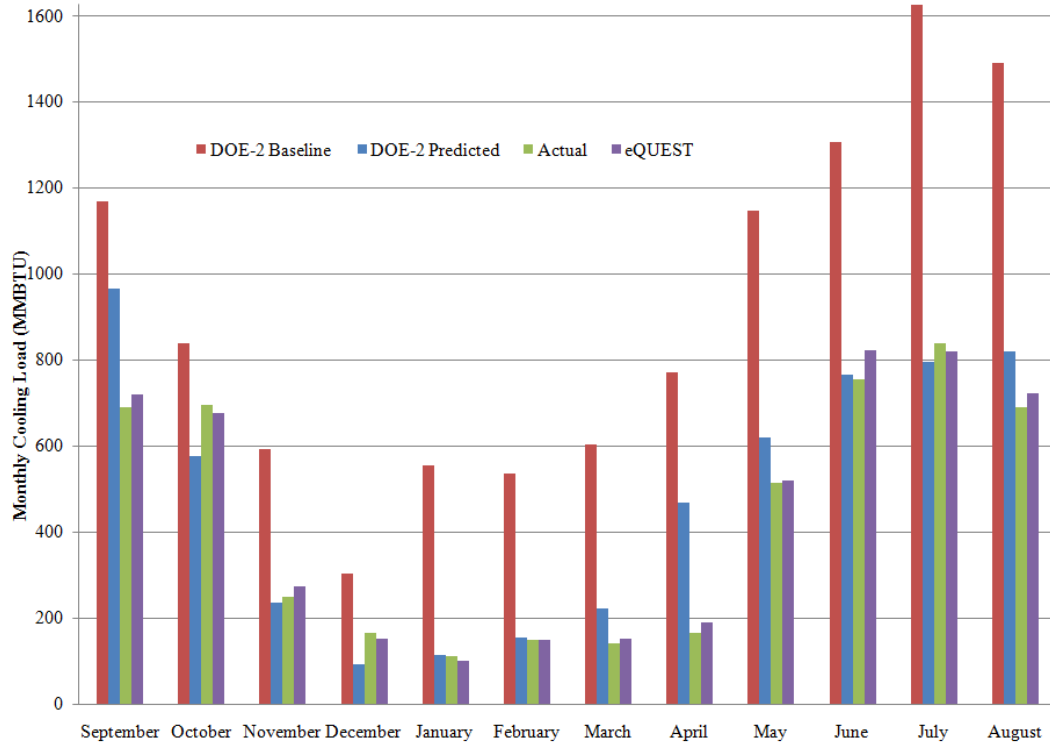


Figure 6.5: Monthly Cooling Load

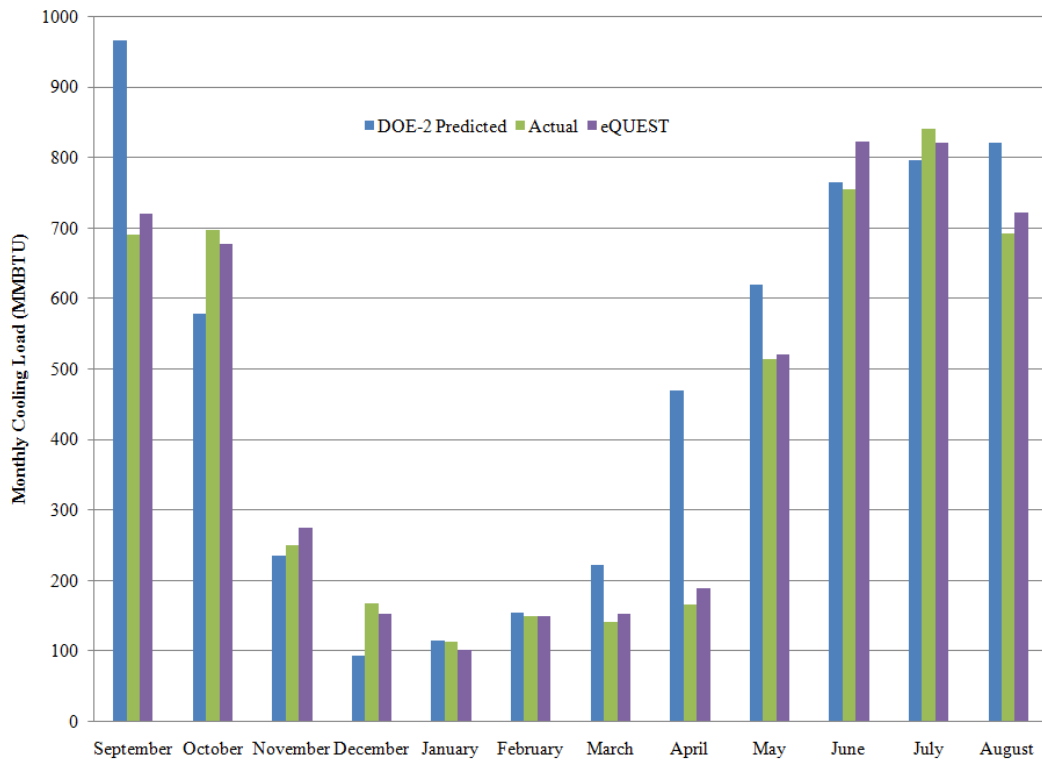


Figure 6.6: Monthly Cooling Load (without DOE-2 Baseline Model)

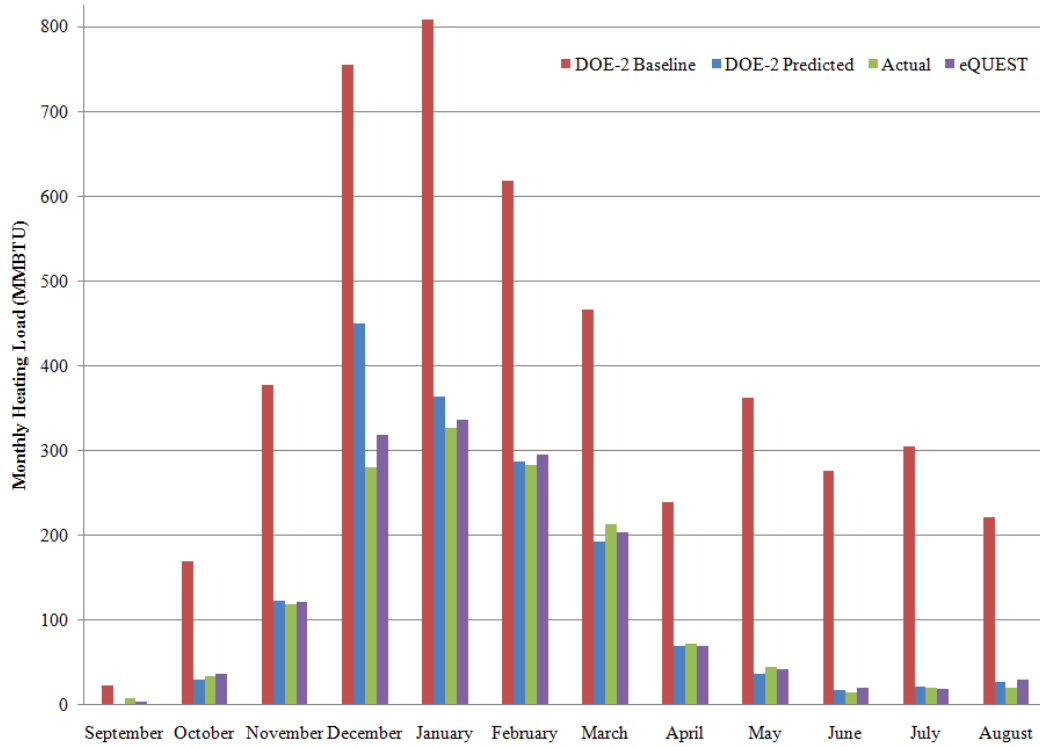


Figure 6.7: Monthly Heating Load

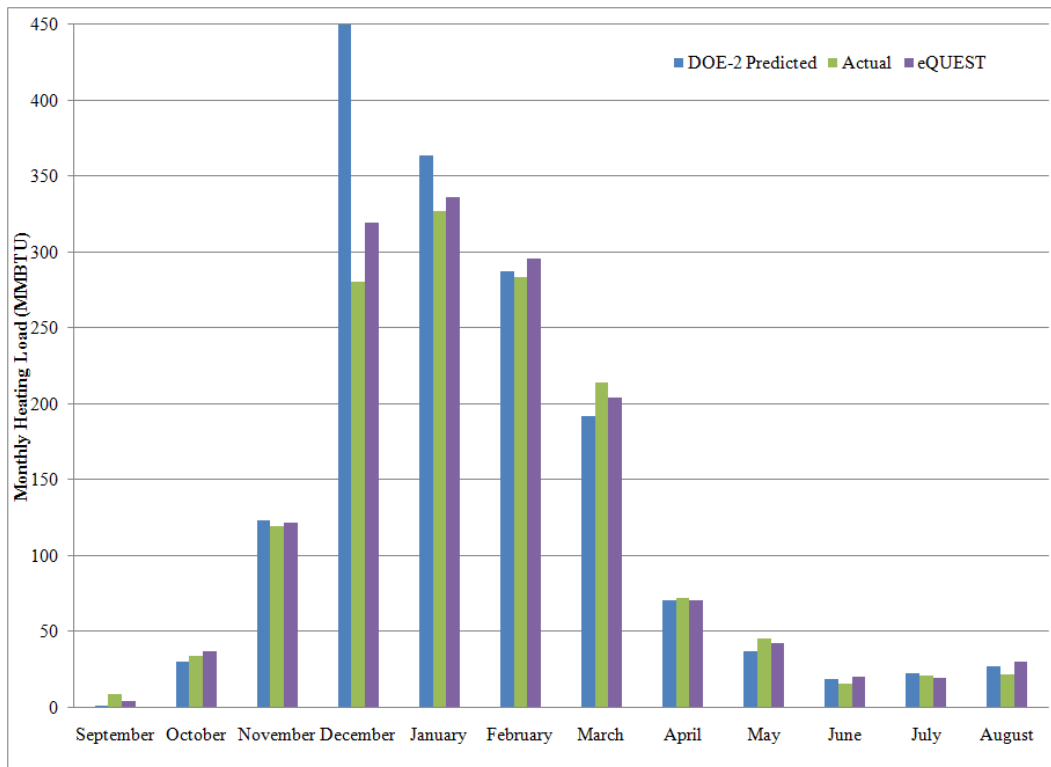


Figure 6.8: Monthly Heating Load (without DOE-2 Baseline Model)

The basic relationships between the DOE-2 Predicted Model, the DOE-2 Baseline Model, the Actual Monitored Data, and the eQUEST Model have been illustrated above. Now, Section 6.1 will directly compare the Monitored Data to the DOE-2 Predicted Model, Section 6.2 will compare the DOE-2 Predicted Model with the eQUEST Model, Section 6.3 will compare the Monitored Data to the eQUEST Model, and, finally, Section 6.4 will discuss the Single-Zone Model.

6.1 Monitored Data vs. DOE-2 Predicted Model

Before most buildings are constructed, there is a computer simulation model created which attempts to predict how that building will actually perform once it is built. The Klaus building is no exception. The DOE-2 computer simulation program was used to create the predicted model. However, this model was created to indicate a representative year, not a specific year. Now that the Klaus building has been completed and closely monitored for over a year, the DOE-2 Predicted Model can be compared to the Actual Monitored Data to determine how accurate its predictions were.

The load data for the DOE-2 Predicted Model and the Actual Monitored Data were previously presented in Table 6.2 and Table 6.5, respectively. The percent savings of what actually happened within the Klaus building to the DOE-2 Predicted Model are summarized below

Table 6.8: Percent Savings of Monitored Loads Compared to the DOE-2 Predicted Model

Month	Electrical (%)	Cooling (%)	Heating (%)
September	31.6	28.5	- 752.0
October	23.0	- 20.6	- 12.6
November	10.9	- 6.3	3.3
December	- 4.3	- 78.5	37.7
January	31.8	2.1	10.1
February	5.7	3.8	1.3
March	4.2	36.4	- 11.3
April	1.3	64.6	- 3.1
May	1.7	17.0	- 22.5
June	9.1	1.2	13.0
July	26.4	- 5.4	7.0
August	31.8	15.8	21.9

Even though the DOE-2 Predicted Model sometimes over estimated and sometimes under estimated its load predictions, overall the Klaus building used less energy than the predicted model calculated. These savings have been condensed for the entire year's data below in Table 6.9

Table 6.9: Percent Savings Overview of the Monitored Loads Compared to DOE-2 Predicted Model

	Actual	DOE-2 Predicted	Savings
Electrical (MMBTU)	5,495	6,511	15.6%
Cooling (MMBTU)	5,166	5,827	11.3%
Heating (MMBTU)	1,441	1,621	11.1%
Total	12,102	13,959	13.3%

Overall, the Klaus building consumed 13.3% less energy than the DOE-2 model had predicted. There are a number of possible reasons for this difference. The most plausible reason is due to the fact that the DOE-2 model simulated a typical year with the hope of representing an average year. However, in terms of weather, no two years are

ever the same. Therefore, an average year will not produce the same energy needs as an exact year. However, further monitoring may help resolve this question.

The majority of the time, at least for September 2007 – August 2008 data, the DOE-2 model appears to have overestimated the loads which would ultimately affect the Klaus building. This is best represented below in Figure 6.9

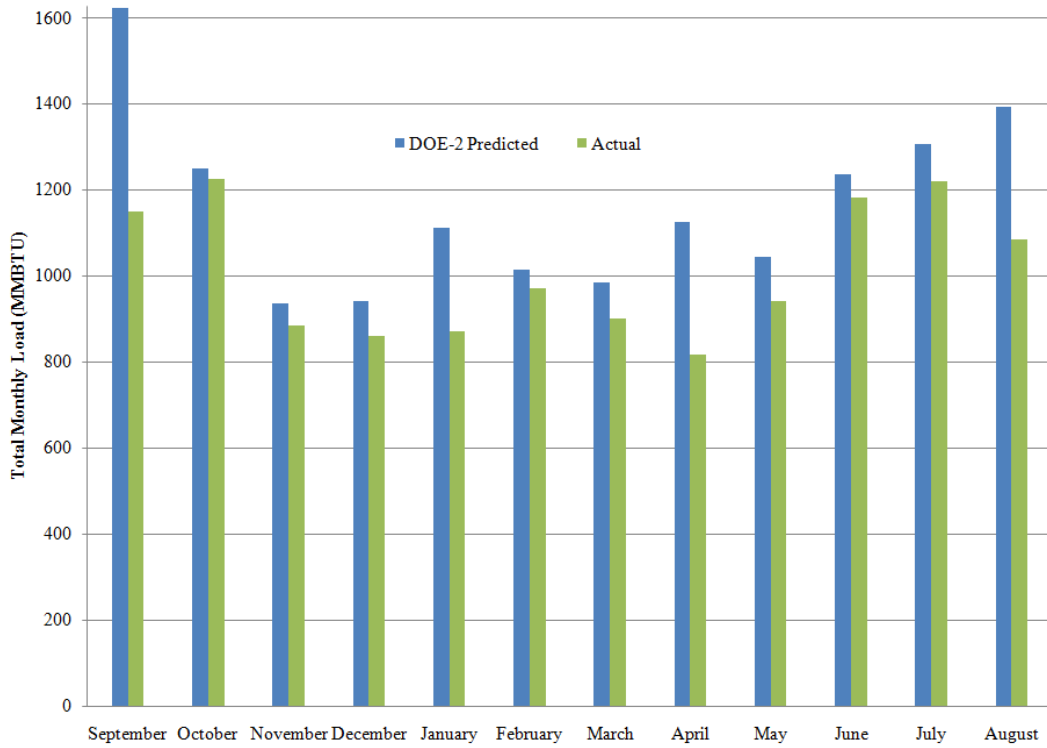


Figure 6.9: DOE-2 Predicted Model vs. Monitored Total Load Comparison

To better understand what exactly is happening to the each total monthly load, Figure 6.9 has been broken down into the main three load components: Electrical, Cooling, and Heating.

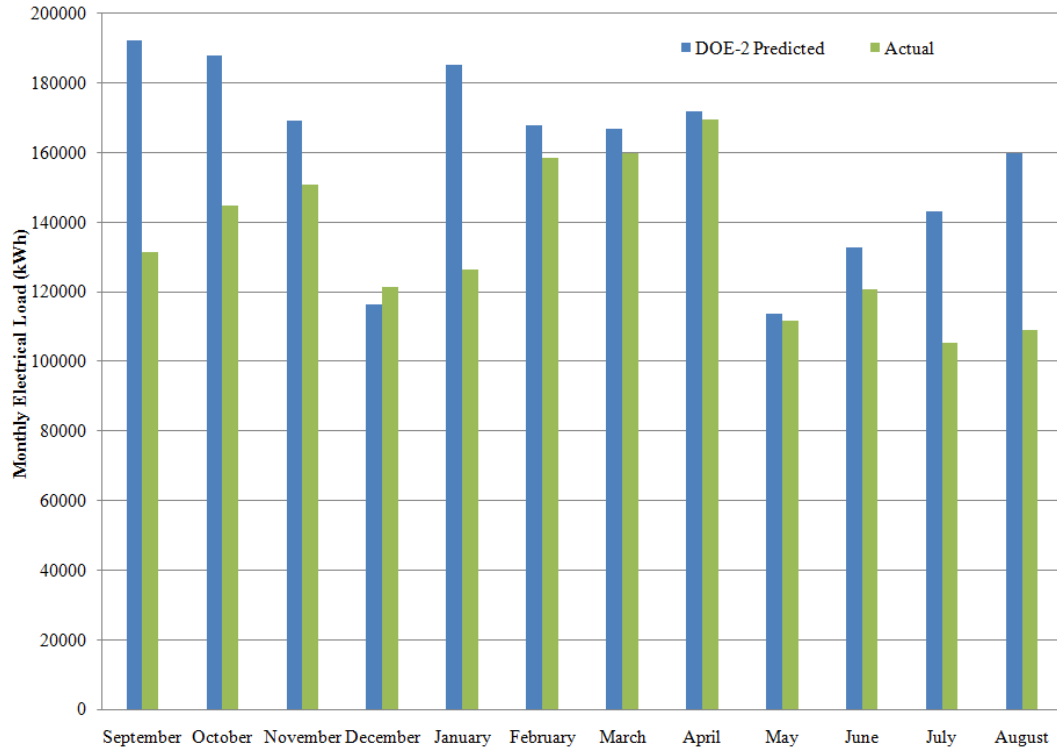


Figure 6.10: DOE-2 Predicted Model vs. Monitored Electrical Load Comparison

Figure 6.10 displays the monthly electrical load comparison. As illustrated above, the DOE-2 model overestimates the monthly electrical load for every month except for December. A possible reason is that university buildings are often occupied during off scheduled hours.

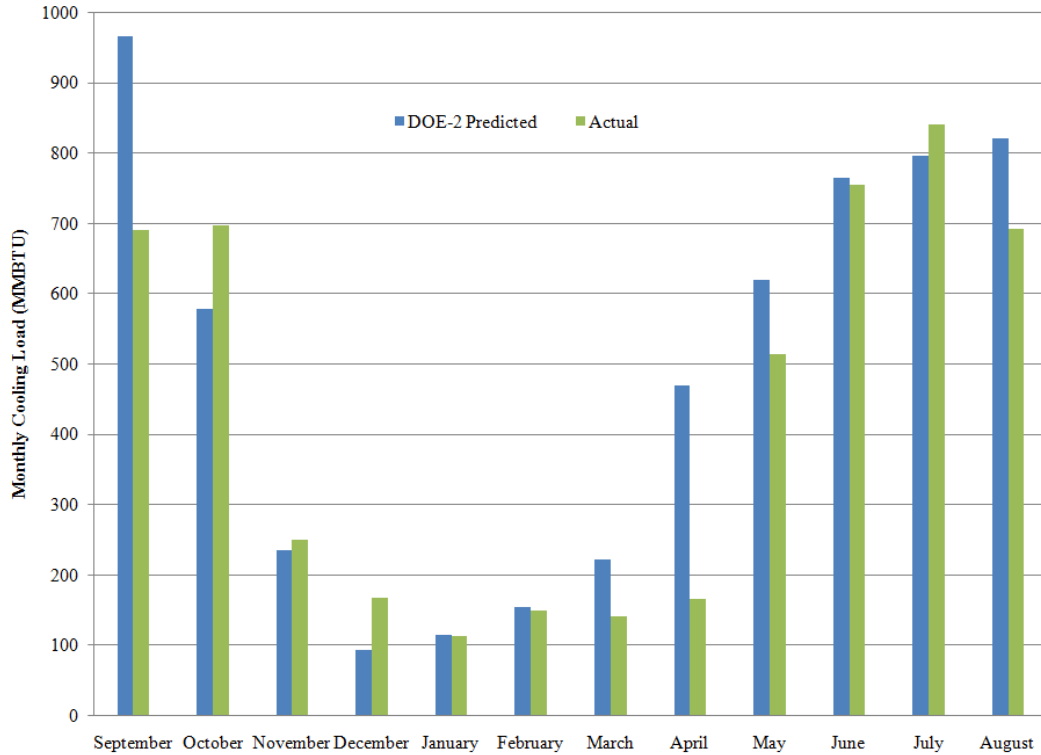


Figure 6.11: DOE-2 Predicted Model vs. Monitored Cooling Load Comparison

Figure 6.11 displays the monthly cooling load comparison. As illustrated above, both the actual data and the DOE-2 model follow a similar month-to-month trend. However, if there is a drastic difference, it typically is from an overestimation of the DOE-2 model. Also, one month of note is April where the DOE-2 model simulates the cooling load to be similar to May while the actual load appears to be much more similar to March. Similarly, September is another month of note where the DOE-2 model simulate the cooling load to be greater than the rest of the year whereas the actual load appears to be right in line with the August and October, the two months surrounding it. These discrepancies are most likely due to the DOE-2 model using typical weather data opposed to the actual weather data.

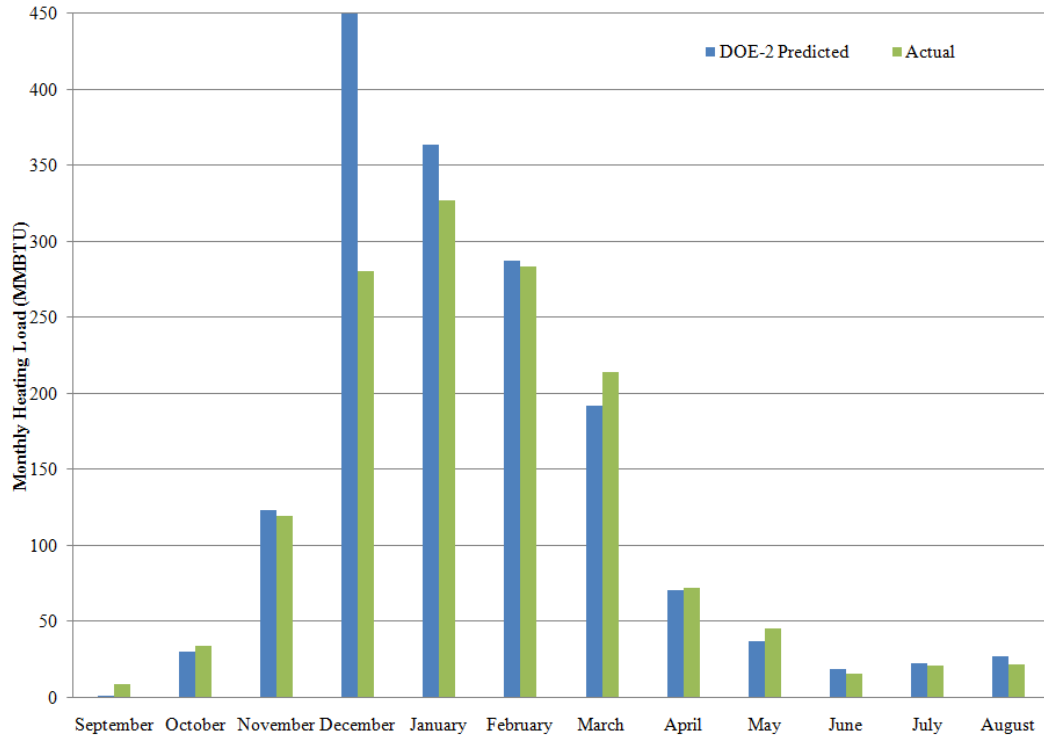


Figure 6.12: DOE-2 Predicted Model vs. Monitored Heating Load Comparison

Figure 6.12 displays the monthly heating load comparison. Once again, as illustrated above, both the actual data and the DOE-2 model follow a similar month-to-month trend. The only drastic difference of note is the dramatic increase in heating loads during the month of December. This is most likely due to similar reasoning to the electrical load increase in December.

6.2 eQUEST Model vs. DOE-2 Predicted Model

eQUEST and DOE-2 are sister programs. They have both been developed by J.J. Hirsch and Associates. The main difference of note between the models run in these two simulation programs is the weather data. The weather data used for the DOE-2 Predicted Model is TMY (Typical Meteorological Year) data which takes the average weather over many years to determine what the typical weather at any given time on any given day

should be. On the other hand, the weather data used for the eQUEST Model was compiled using the actual weather data from the September 2007 – August 2008 timeframe. All of the other inputs into the two simulation programs, aside from the weather files, were kept constant to assure a more accurate comparison.

The load data for the DOE-2 Predicted Model and the eQUEST Model were previously presented in Table 6.2 and Table 6.6, respectively. The percent savings of the eQUEST Model to the DOE-2 Predicted Model are summarized below

Table 6.10: Percent Savings of eQUEST Model Compared to the DOE-2 Predicted Model

Month	Electrical (%)	Cooling (%)	Heating (%)
September	19.9	25.5	- 300.0
October	16.6	- 17.2	- 23.3
November	9.2	- 16.6	1.0
December	0.5	- 63.7	29.1
January	20.1	11.4	7.7
February	0.0	3.9	- 3.1
March	0.3	31.4	- 6.3
April	0.1	59.8	0.0
May	0.4	15.9	- 13.5
June	8.8	- 7.6	- 11.1
July	19.6	- 3.0	13.6
August	19.6	12.1	- 11.1

Even though the DOE-2 Predicted Model sometimes over estimated and sometimes under estimated its load predictions, overall the eQUEST Model calculated a slightly lower yearly energy than the DOE-2 Predicted Model calculated. These savings have been condensed for the entire year's data below in Table 6.11

Table 6.11: Percent Savings Overview of eQUEST Model Compared to DOE-2 Predicted Model

	eQUEST	DOE-2 Predicted	Savings
Electrical (MMBTU)	5,845	6,511	10.2%
Cooling (MMBTU)	5,294	6,149	13.9%
Heating (MMBTU)	1,499	1,625	7.8%
Total	12,638	14,285	11.5%

Overall, the eQUEST Model calculated the Klaus building to consume 11.5% less energy than the DOE-2 model had predicted. Due to the fact that all of the inputs were kept constant except for the input weather files, this large difference must be due to the actual vs. predicted weather. This noticeable discrepancy, due solely to the weather data, clearly illustrates the true importance of accurate weather information for precise modeling.

The majority of the time, at least for September 2007 – August 2008 data, the DOE-2 model appears to have overestimated the loads, most likely due to a milder year weather wise than normal. This is best represented below in Figure 6.13

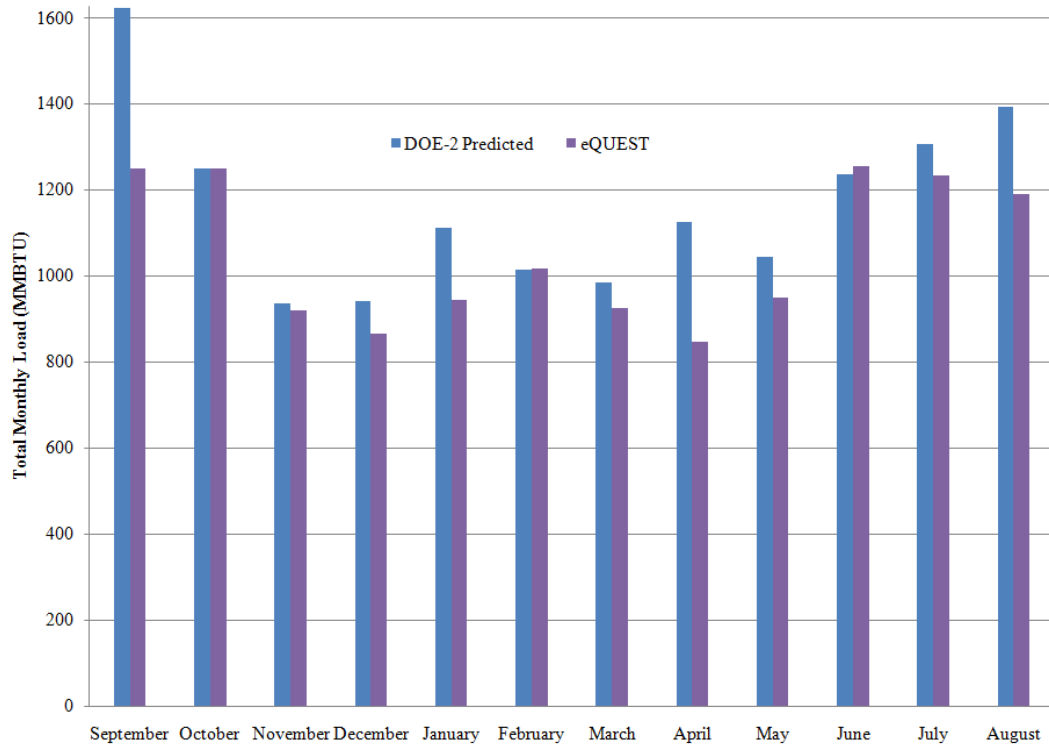


Figure 6.13: DOE-2 Predicted Model vs. eQUEST Model Total Load Comparison

To better understand what exactly is happening to the each total monthly load, Figure 6.13 has been broken down into the main three load components: Electrical, Cooling, and Heating.

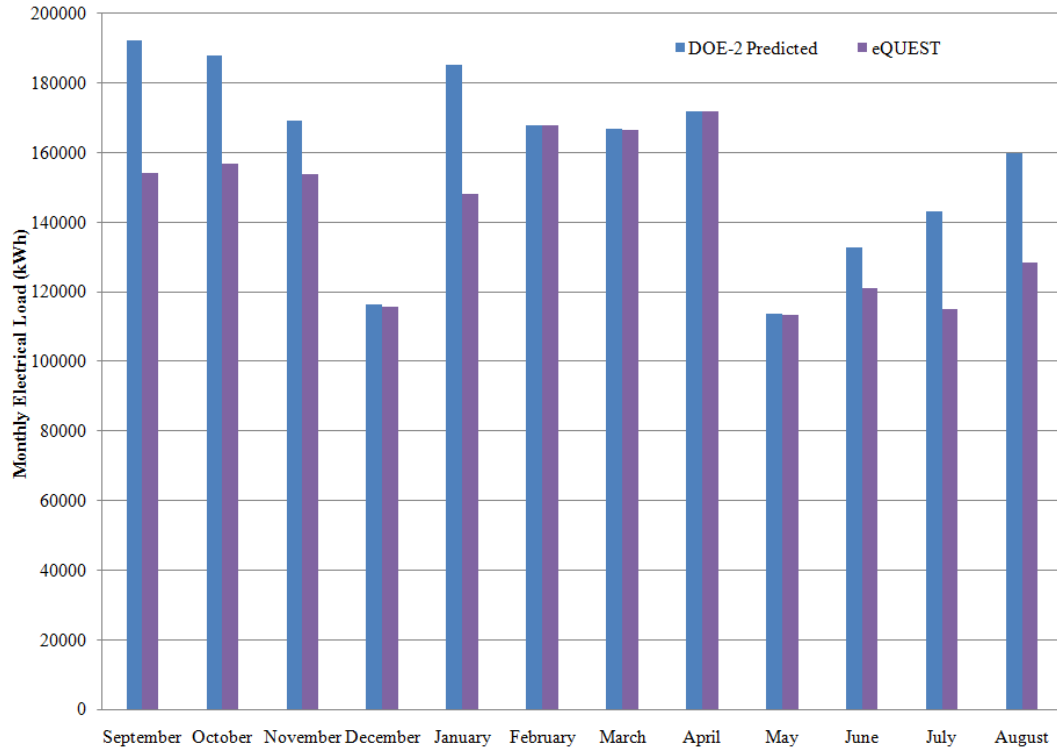


Figure 6.14: DOE-2 Predicted Models vs. eQUEST Model Electrical Load Comparison

Figure 6.14 displays the monthly electrical load comparison. As illustrated above, the DOE-2 model overestimates just over half of the monthly electrical loads while the others are all in great agreement. The electrical load is mainly determined from the equipment and the lighting, which appear to have very well defined schedules.

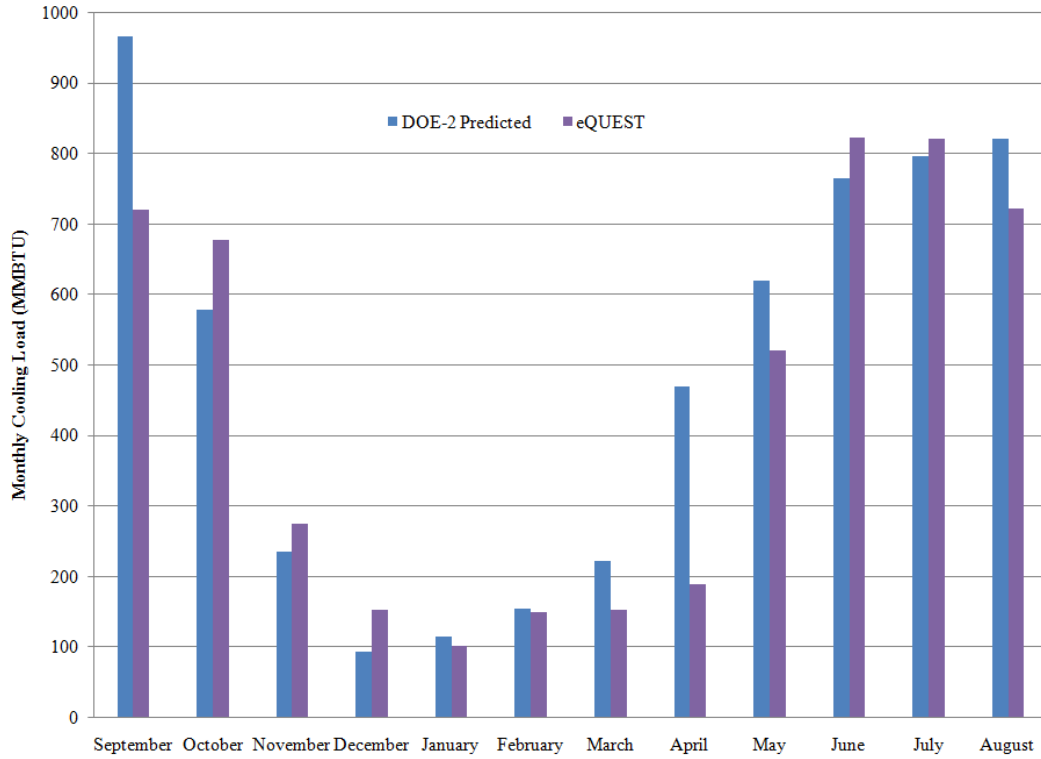


Figure 6.15: DOE-2 Predicted Model vs. eQUEST Model Cooling Load Comparison

Figure 6.15 displays the monthly cooling load comparison. As illustrated above, both models follow a similar month-to-month trend. Unlike other data which shows an overestimation from the DOE-2 Predicted Model, the cooling load fluctuates between the two models as to which is an over vs. under estimation.

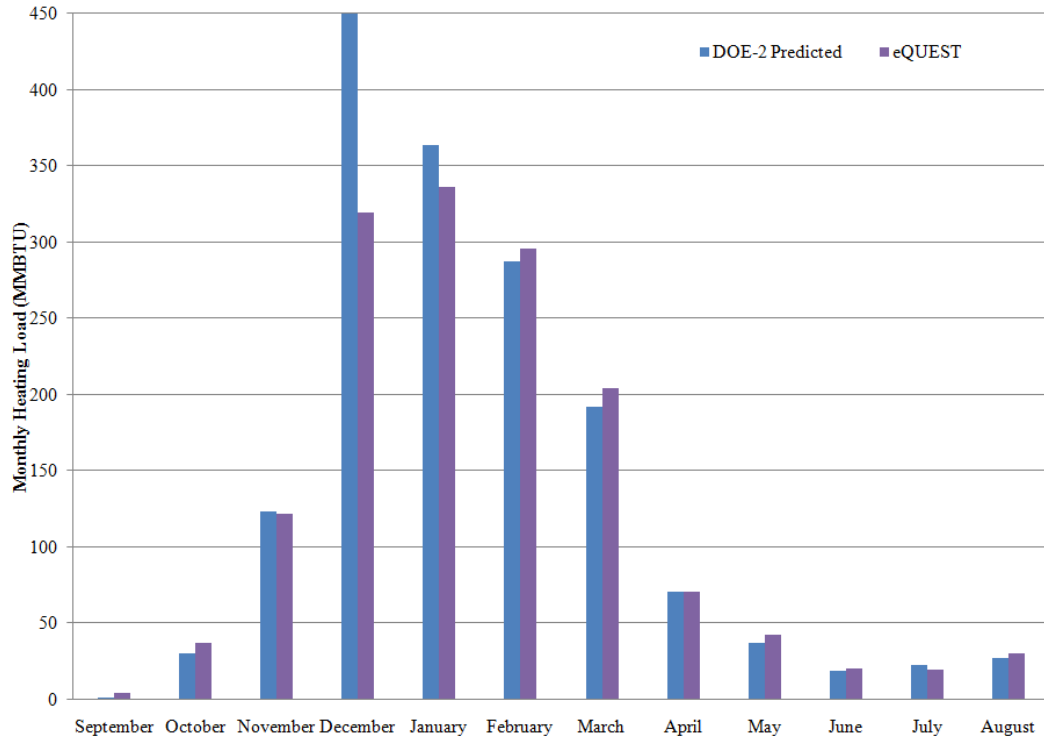


Figure 6.16: DOE-2 Predicted Model vs. eQUEST Model Heating Load Comparison

Figure 6.16 displays the monthly heating load comparison. Once again, as illustrated above, both models follow a similar month-to-month trend. The only drastic difference of note is the dramatic increase in the DOE-2 Predicted Model heating loads during the month of December.

6.3 Monitored Data vs. eQUEST Model

The Actual Monitored Data and the eQUEST Model should present very similar results due to the fact that they both utilized the same time frame (September 2007 – August 2008) and weather data. The load data for the Actual Monitored Data and the eQUEST Model were previously presented in Table 6.5 and Table 6.6, respectively. The percent savings of what actually happened within the Klaus building to the eQUEST Model are summarized below

Table 6.12: Percent Savings of the Monitored Loads Compared to the eQUEST Model

Month	Electrical (%)	Cooling (%)	Heating (%)
September	14.6	4.1	- 113.0
October	7.7	- 2.9	8.7
November	1.8	8.8	2.3
December	- 4.9	- 9.0	12.1
January	14.7	- 10.5	2.6
February	5.6	- 0.1	4.3
March	3.9	7.2	- 4.8
April	1.3	12.1	- 3.1
May	1.3	1.3	- 7.9
June	0.3	8.2	21.7
July	8.4	- 2.3	- 7.6
August	15.2	4.2	29.7

Even though the eQUEST Model sometimes slightly over estimated and sometimes slightly under estimated its load predictions, overall the Klaus building still used less energy than the predicted model calculated. These savings have been condensed for the entire year’s data below in Table 6.13

Table 6.13: Percent Savings Overview of Monitored Loads Compared to eQUEST Model

	Actual	eQUEST	Savings
Electrical (MMBTU)	5,495	5,845	6.0%
Cooling (MMBTU)	5,166	5,294	2.4%
Heating (MMBTU)	1,441	1,499	3.9%
Total	12,102	12,638	4.2%

Overall, the Klaus building consumed 4.2% less energy than the eQUEST Model calculated. Even though this difference is so minimal, there are still a number of possible reasons for the variations. The most plausible reason is due to the fact that the eQUEST

Model simulated the ideal circumstances within the Klaus building, while the actual data shows what actually happened.

The majority of the time where there are discrepancies, the eQUEST Model appears to have overestimated the loads. This is best represented below in Figure 6.17



Figure 6.17: eQUEST Model vs. Monitored Total Load Comparison

To better understand what exactly is happening to the each total monthly load, Figure 6.18 has been broken down into the main three load components: Electrical, Cooling, and Heating.

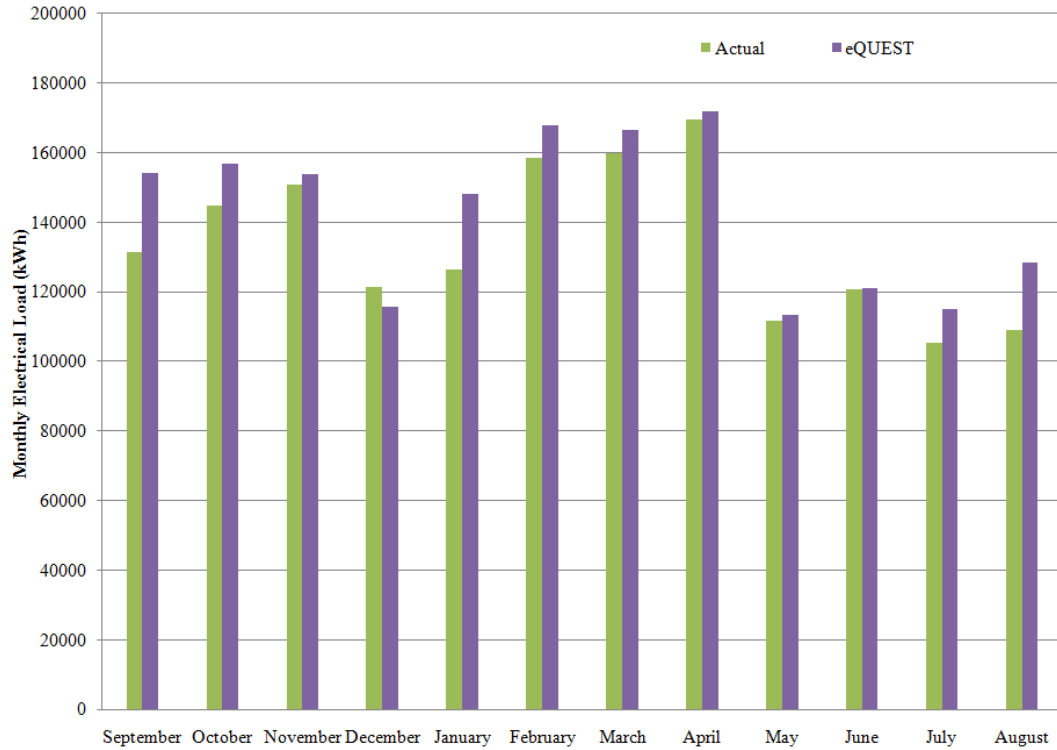


Figure 6.18: eQUEST Model vs. Monitored Electrical Load Comparison

Figure 6.18 displays the monthly electrical load comparison. As illustrated above, the eQUEST Model tends to slightly overestimate the monthly electrical loads.

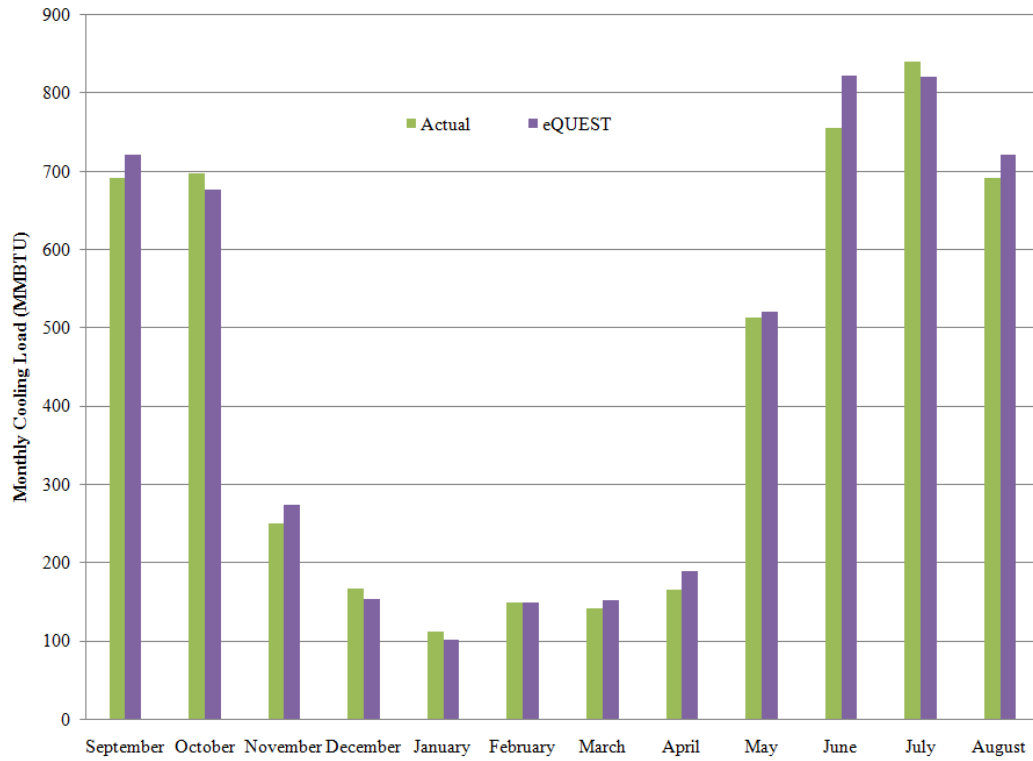


Figure 6.19: eQUEST Model vs. Monitored Cooling Load Comparison

Figure 6.19 displays the monthly cooling load comparison. As illustrated above, both the actual data and the eQUEST Model follow a very similar month-to-month trend without any drastic differences.

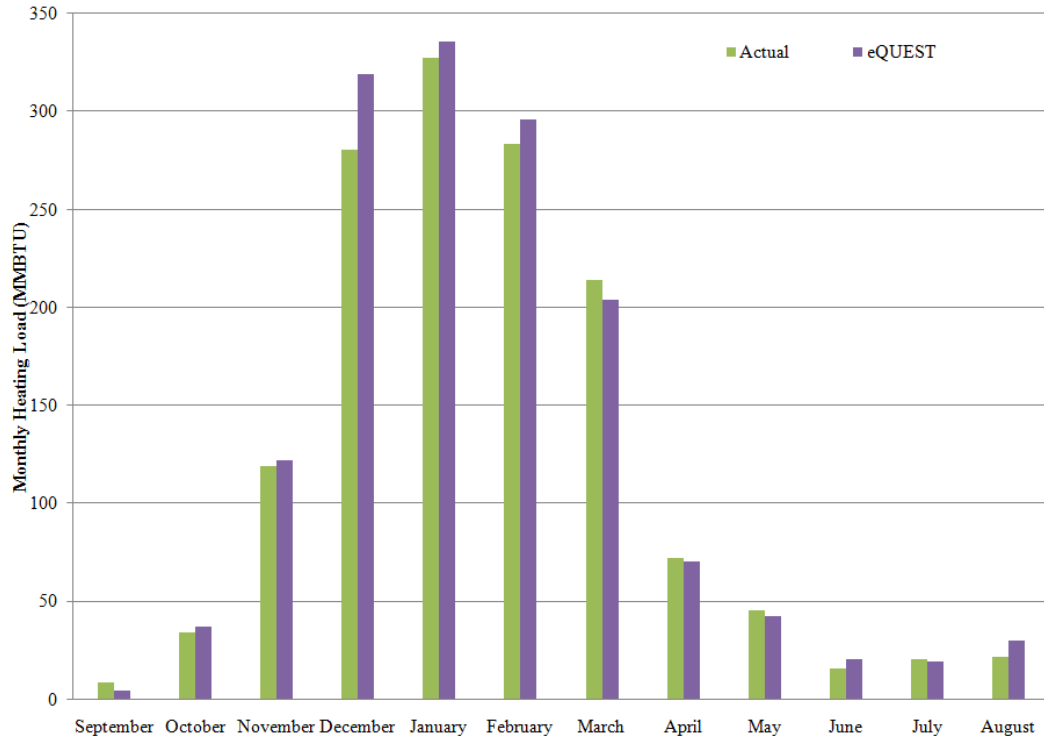


Figure 6.20: eQUEST Model vs. Monitored Heating Load Comparison

Figure 6.20 displays the monthly heating load comparison. As illustrated above, both the actual data and the eQUEST Model once again follow a very similar month-to-month trend without any drastic differences.

6.4 Single-Zone Model Results and Discussion

There are multiple aspects to the single-zone model described in Section 5.2.2: Combined Single-Zone Simplified Model, including the thermal mass of the building, the temperature rate within the building, the overall performance of the building, and the predicted heating and cooling loads of the building. These results are presented and discussed in the following sections.

6.4.1 Overall Temperature Change of the Building

The overall temperature change of the building is determined from the return air temperature through numerical differentiation. This number represents how the temperature in the building fluctuates over time. In order to determine how the building changes in the course of a year, sum all of the temperatures for that given year to determine the overall change in temperature per year. For the chosen example building, the Klaus building, during the studied year, September 2007 – August 2008, the overall temperature change was found to be 2.49°F annually. This means that over the course of the sample year, the return temperature of the building increased 2.49°F. The overall temperature in a building is expected to stay pretty consistent throughout the course of a year, resulting in no overall temperature change. Therefore, a minimal change of 2.49°F (very close to 0°F) is considered not only reasonable, but extremely realistic.

6.4.2 Overall Performance of the Building

The overall performance of the building is determined very similarly to the annual temperature change, by summing all of the loads over the course of a year. All of the loads which affect a building were considered in order to find the overall performance of the building, including heating, cooling, outside air, internal and envelope loads. The overall performance of a building is expected to be zero for an entire year which indicates a perfect energy balance within the building. For the chosen example building the Klaus building, during the studied year, September 2007 – August 2008, the overall error of the building was found to be approximately -4.48 MMBTUs which is approximately 0.1% of the total building load over the course of the sample year. Therefore, the building's

overall performance over the course of the sample year is extremely close to what was to be expected.

6.4.3 Predicted Heating vs. Cooling Load

The predicted heating and cooling loads were determined through the single-zone model calculations which utilized readily available information such that future buildings would also be able to predict such loads. Please refer back to Section 5.2.2: Combined Single-Zone Simplified Model for the complete description. From the single-zone model inputs, the outputs were either the necessary heating load or the necessary cooling load for the given time steps, in this case 30 minutes (0.5 hours). These loads have been summarized monthly for the single-zone model (SZM) compared to the actual monitored data as presented below for the heating loads (Table 6.14 and Figure 6.21) and the cooling loads (Table 6.15 and Figure 6.22).

Table 6.14: Single-Zone Model vs. Monitored Heating Load Comparison

Month	SZM (MMBTU)	Actual (MMBTU)
September	99.7	8.5
October	60.1	33.8
November	141.8	118.9
December	309.7	280.6
January	410.9	327.3
February	288.9	283.3
March	230.5	213.7
April	211.1	72.2
May	64.0	45.3
June	89.9	15.7
July	39.4	20.5
August	21.0	21.1

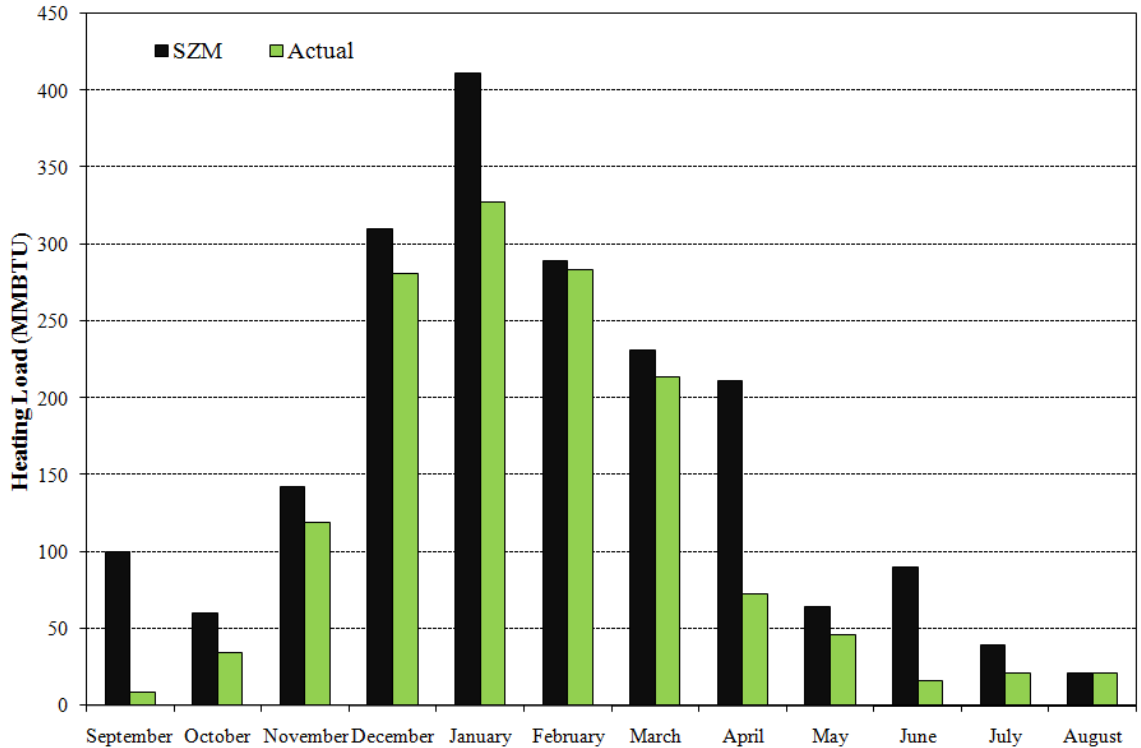


Figure 6.21: Single-Zone Model vs. Monitored Heating Load Comparison

As illustrated above, even though the exact numbers do not perfectly match, the single-zone model does accurately depict the monthly heating load trend which was observed in the example building over the examined time frame of September 2007 – August 2008. Figure 6.21 clearly shows that the single-zone model calculates a higher heating load than what the actual monitored data load was. A possible reason for this discrepancy between the two heating loads could be due to the fact that the single-zone model only determines how the building should react to various conditions (especially weather conditions) whereas the monitored data represents what actually happened, even if it does not perfectly follow environmental changes. In addition, the extra heating loads could be due to cool air at night which the building mass would fix.

Table 6.15: Single-Zone Model vs. Monitored Cooling Load Comparison

Month	SZM (MMBTU)	Actual (MMBTU)
September	704.8	690.3
October	636.6	695.8
November	433.7	249.9
December	271.7	166.0
January	143.5	111.6
February	157.9	148.1
March	178.0	140.6
April	226.7	165.6
May	590.8	513.1
June	772.8	754.9
July	825.8	839.3
August	744.5	690.6

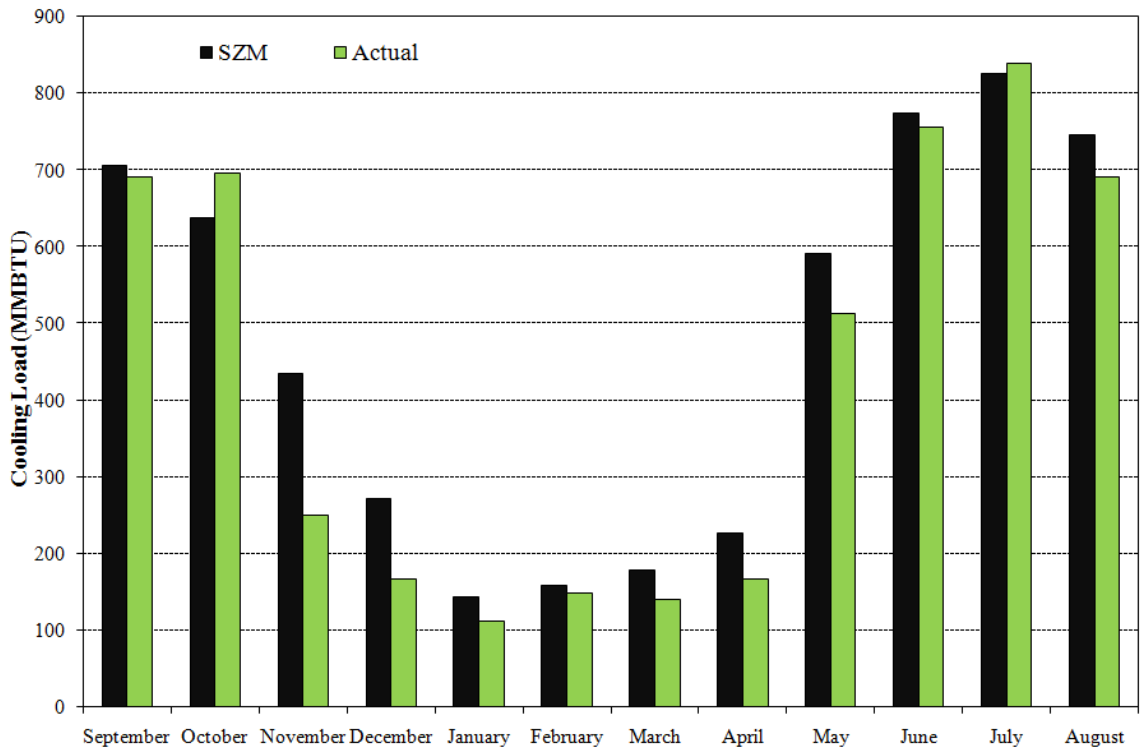


Figure 6.22: Single-Zone Model vs. Monitored Cooling Load Comparison

Similarly to the heating loads, even though the exact cooling load numbers do not perfectly match, the single-zone model does accurately depict the monthly cooling load trend which was observed in the example building over the examined time frame of September 2007 – August 2008. A possible reason for this discrepancy between the two cooling loads could be due to the fact that the single-zone model only determines how the building should react to various conditions (especially weather conditions) whereas the monitored data represents what actually happened.

To best understand what the calculated heating and cooling loads mean, they need to be compared together. In order to do so, the overall HVAC load is computed as

$$\dot{Q}_{\text{HVAC}} = \dot{Q}_{\text{H}} - \dot{Q}_{\text{C}} \quad (6.1)$$

where the cooling load is subtracted from the heating load. The single-zone model HVAC load calculation has been compared to the actual monitored HVAC load. This information has been summarized monthly in Table 6.16 and Figure 6.23. If the total monthly HVAC load is positive, it represents a heating load, whereas if the total monthly HVAC load is negative, it represents a cooling load.

Table 6.16: Single-Zone Model vs. Monitored HVAC Load Comparison

Month	SZM (MMBTU)	Actual (MMBTU)
September	- 605.1	- 681.8
October	- 576.5	- 662.0
November	- 291.8	- 131.0
December	38.0	114.6
January	267.4	215.7
February	131.0	135.3
March	52.5	73.2
April	- 15.5	- 93.4
May	- 526.8	- 467.8
June	- 682.9	- 739.3
July	- 786.4	- 818.8
August	- 723.5	- 669.5
Total	- 3719.7	- 3724.9

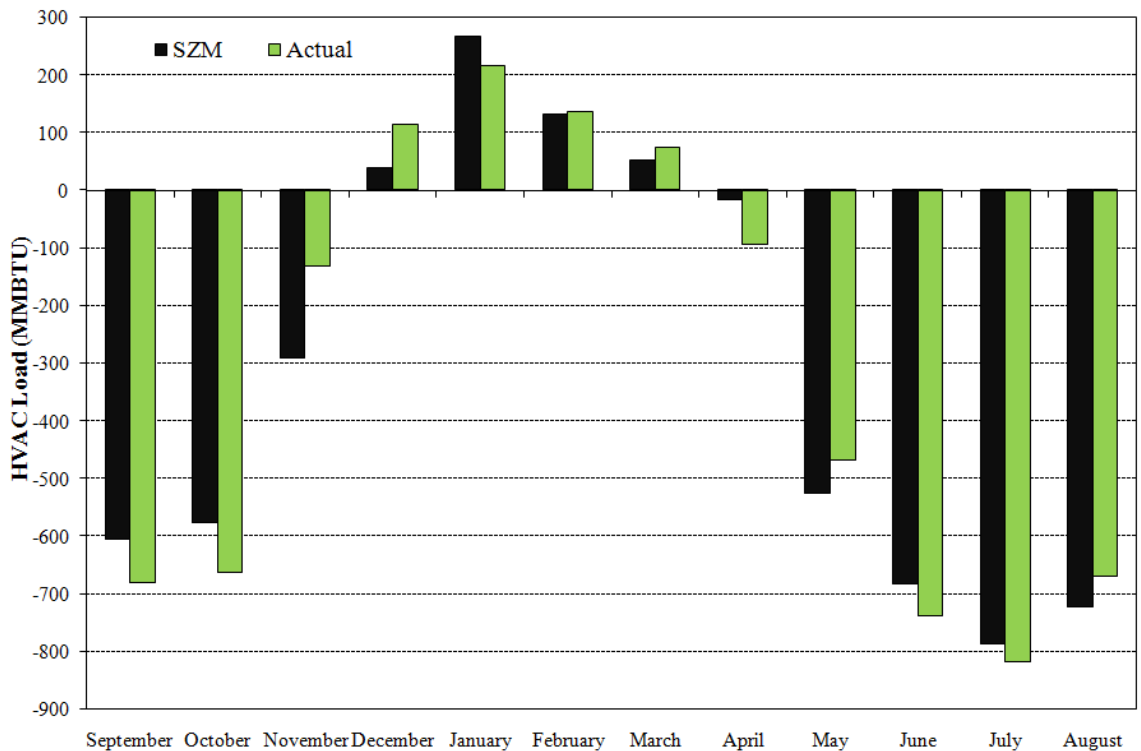


Figure 6.23: Single-Zone Model vs. Monitored HVAC Load Comparison

As illustrated above, even though the exact numbers do not perfectly match, the single-zone model does accurately depict the monthly HVAC load trend which was observed in the example building over the examined time frame of September 2007 – August 2008. Note how the building experiences greater heating loads during the winter months (December, January, February and March) while the rest of the year (September – November and April – August) experiences a higher cooling load.

Over the course of the year, there were 2,980 hours in which the building was heated, and the remaining 5,780 hours the building was cooled. This results in 34% heating and 66% cooling which is very similar to the 4 months (33%) with greater heating loads and 8 months (67%) with greater cooling loads.

Another statistic of note is the overall accuracy of the single-zone model's HVAC load summary for the entire year. The bottom row of Table 6.16 indicates the total HVAC load summary over the course of the examined year (September 2007 – August 2008). This row states that the single-zone model's total HVAC load is -3719.7 MMBTUs while the actual monitored total HVAC load is -3724.9 MMBTUs. Not only do both of these represent a large overall cooling load within the building, but they also indicate a very minimal yearly difference of 0.14%. Therefore, even though the single-zone model's monthly load calculations are not exactly what the actual monitored load data was, when looked at on the larger scale of a year, the single-zone model is able to accurately depict the building's necessary HVAC loads.

Another reason for the minimal difference between the monitored data and the single-zone model could be that the uncertainties of the heating and cooling loads are cancelling each other out. Therefore, the absolute HVAC load was considered as

$$\dot{Q}_{\text{HVAC,abs}} = \dot{Q}_{\text{H}} + \dot{Q}_{\text{C}} \quad (6.2)$$

where the heating and cooling loads are added rather than subtracted. The single-zone model absolute HVAC load calculation has been compared to the actual monitored absolute HVAC load. This information has been summarized monthly in Table 6.17 and Figure 6.24 below.

Table 6.17: Single-Zone Model vs. Monitored Absolute HVAC Load Comparison

Month	SZM (MMBTU)	Actual (MMBTU)
September	804.5	698.8
October	696.7	729.6
November	575.5	368.8
December	581.4	446.5
January	554.3	438.9
February	446.8	431.4
March	408.5	354.3
April	437.8	237.7
May	654.8	558.4
June	862.7	770.6
July	865.2	859.7
August	765.5	711.7
Total	7653.9	6606.6

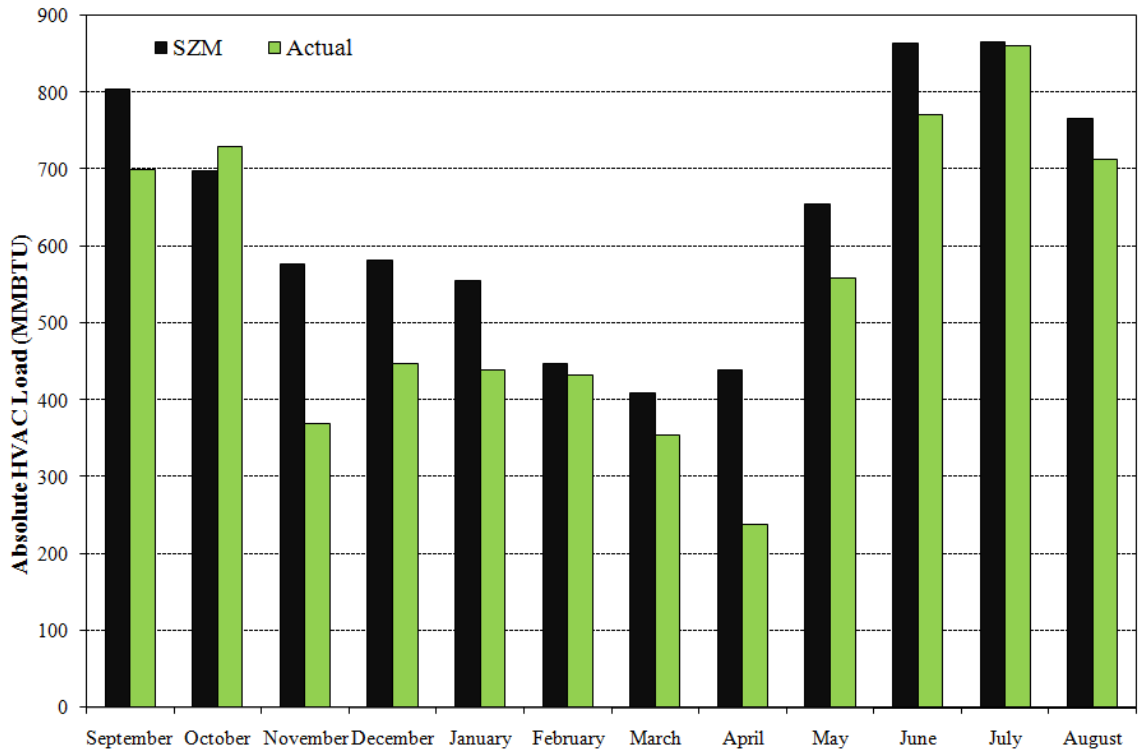


Figure 6.24: Single-Zone Model vs. Monitored Absolute HVAC Load Comparison

From the absolute HVAC method, the annual absolute HVAC load from the single-zone model was found to be nearly 14% (13.68% to be exact) different than the annual monitored absolute HVAC load. This difference clearly shows that some of the cooling error was cancelled out by the heating error, and vice-versa.

It should be noted that the single-zone model only takes a few minutes to define and then only a few more minutes to run, compared with the huge amount of time and data that must be assembled which is required to run a detailed model. Additionally, the accuracy of the detailed model is hardly better.

6.4.4 Thermal Mass of the Building

To determine the thermal mass of a building requires a fairly complicated dynamic model. From the observed inputs and outputs, one needs to infer the dynamic

parameters of the model, in particular the effective thermal capacity. Therefore, the thermal mass of the building was not able to be determined through the research conducted for this thesis. Instead, a more sophisticated parameterization study would need to be conducted. The output from the dynamical systems would then allow for the parameters to be inferred. From these inferred parameters, a more accurate account of what the thermal mass of a building is can then be determined. Please refer to Chapter 8: RECOMMENDATIONS FOR FUTURE WORK for more information regarding this parameterization study. However, finding the thermal mass of the building was attempted and hoped to have been completed during this research, but it was never explicitly proposed. Ultimately, the time consumed with data collection, especially of solar and outdoor air data did not allow for an adequate study of this issue. Overall, however, in this well controlled building, energy capacity modeling does not appear to be critical to the overall energy budget. In contrast, it may become economically desirable or even necessary in the future to minimize the peak demand for power to drive the HVAC cooling or even heating system. In this case, some modeling of the building dynamics and some measure of the thermal mass are needed. A more advanced topic is furthermore modeling the humidity capacity of the building, but both of these topics, while worthwhile, are well beyond the present scope.

As discussed above, the DOE-2 Model, the eQUEST Model and the Single-Zone Model were all able to accurately predict the building's annual and monthly loads for the given September 2007 – August 2008 timeframe.

7 CONCLUSIONS

The purpose of this work was to develop and verify a simplified and concise building simulation model suitable for high-level applications such as preliminary design or for embedding into adaptive control systems. An actual complex modern building and its energy system has been monitored. The monitored energy performance of this building has been compared with the empirical performance predicted by a two simulation modeling programs and, alternatively, by a simplified single-zone model.

This project was composed of several related tasks. The first component was the monitoring of the energy consumption rates, pertinent environmental data, and load indicators of the new Klaus Advanced Computing Building on the Georgia Institute of Technology's Atlanta campus. The Klaus building was chosen because it represents a typical non-residential building. Subsequently, these findings were compared with results from DOE-2 and eQUEST, well established energy simulation modeling programs. These comparisons allow for an empirical verification of the modeling program for Atlanta conditions. Finally, a simplified single-zone building model was developed, and its predictions compared with the empirical data and with the results of the more complex programs. The results verify both the more complex programs and single-zone model, and also demonstrate the use of a single-zone model for future work and predictions.

In order to calculate the actual measured loads on the Klaus building, the data first had to be monitored. From the monitored data, heating, cooling, outside air, envelop and internal loads were calculated. The heating load was easily determined from the

building's steam, while the cooling load was easily determined from the building's chilled water. The other loads, however, were not as straightforward.

Even though the outside air load presented numerous problems, the Klaus building was still ideal since most buildings not meant for studying also would not have flow meters available in the air handling units. Since there were no flow meters, alternative methods to determine the outside air flow and ultimately the outside air loads were found. These methods included using fan laws and fan curves to determine how much air flowed through the units, control logic to determine whether or not the energy recovery ventilators were in use, and then comparing one set of results to those found through the use of carbon dioxide concentrations to verify the validity.

Next, the walls have to be considered separately than the windows for the envelope loads calculations. Solar heat gain loads were considered for the windows. In order to accurately calculate the window (or the wall) loads, directional solar radiation data is needed. Unfortunately, solar radiation data is typically collected solely as the overall global solar radiation. Therefore, a method for taking solar radiation data and breaking it down into directional solar radiation was found. From this directional solar radiation data, the solar heat gain loads on the windows could be determined.

Conduction skin loads were considered for the walls. In fact, two conduction skin load approaches were used, first order and transfer function conduction skin loads. These two conduction skin load methods illustrated extremely close annual loads, whereas the first order method fluctuated a lot more daily in reaction to not taking the heat capacity or time lag of the walls into consideration. Both conduction skin loads also took into account the directional solar radiation data.

The final step to determine the actual loads on the Klaus building was to consider the internal loads. These internal loads were broken down into two categories: electrical and people. The electrical load took into account both the lighting and the equipment loads and was determined through the main breaker system in the building. The people load, on the other hand, was first estimated based on daily, weekly, and annual occupancy schedules. The occupancy estimates which were originally used were then verified through the use of carbon dioxide concentrations.

Once the actual monitored load data was completed and compiled for the Klaus building, the other models were investigated and then compared to the actual data.

First, two sister computer energy load simulation model programs were investigated. These two programs were DOE-2 and eQUEST. Even though these complex programs have been found to be extremely complicated and time consuming, they have proven to be fairly accurate.

The DOE-2 program contained the model and simulation of the Klaus building before it was built to predict how it would perform during a typical year using a TMY weather file. After actually monitoring the building for a year, the predictions made through the DOE-2 simulation model were found to be within 13.3% of what actually happened.

eQUEST was later used to model the Klaus building for the exact same time period in which the monitored data was collected. For consistency purposes, the eQUEST model used all of the same building inputs as the DOE-2 model used, except for the weather data. For the eQUEST model, a mock-TMY weather file was created which contained the actual weather information for the monitored year. Once the eQUEST

simulation model was run using the new mock-TMY weather file, the building's modeled loads were found to be within 4.2% of what actually occurred.

The fact that both the DOE-2 model and the eQUEST model used identical building inputs, except for the weather file, clearly emphasizes the importance of the weather data. Not only does the weather affect whether the building is heating or cooling, but it also influences the outside air loads, the envelope loads and the building's equipment. In the case of the monitored year (September 2007 – August 2008), weather alone caused an 11.5% difference between the DOE-2 model and the eQUEST model.

Finally, a simplified single-zone model was investigated. This model was created straightforward enough such that it could not only be used for almost any other building, but also for it to be quick and easy to use. Over the course of the modeled year, the building temperature increased 2.49°F while the overall performance of the building was found to be roughly -4.48 MMBTUs which is approximately 0.1% of the total building load, both of which are extremely close to the expected values.

The last aspect of the single-zone model focused on the predicted heating vs. cooling load of the building, or, more importantly, the HVAC load. The single-zone model's total HVAC load is -3719.7 MMBTUs while the actual monitored total HVAC load is -3724.9 MMBTUs. Not only do both of these represent a large overall cooling load within the building, but they also indicate a very minimal yearly difference of 0.14%. Therefore, the single-zone model is able to very accurately depict the building's necessary HVAC loads.

According to Waltz, in order for a model to be considered "accurate," the calculated total energy consumption would need to be within 5% of the building's actual

annual energy use (Watzl, 1992). Therefore, the results from the eQUEST and the single-zone models are both less than the required 5%, and therefore can be considered accurate.

In conclusion, out of the three models which were compared to the monitored data of what actually occurred in the Klaus building over the September 2007 – August 2008 timeframe, the single-zone model was able to best predict the necessary annual loads at a difference of 0.14%, followed by the eQUEST model and its precise weather data with a difference of 4.2%, and, finally, by the original DOE-2 model with a difference of 13.3%. Therefore, due to the accuracy, easy and quickness of the single-zone model as compared to the more complex computer simulation programs, engineers, architects and designers in the future can hope to utilize faster and more user-friendly programs during the design and monitoring phases of a building.

8 RECOMMENDATIONS FOR FUTURE WORK

Although quite a bit of hard work and plenty of time went into this research, there is always more which can be done, both directly and indirectly related. Similarly, the conclusions gathered and accuracy of the various models should encourage future work and endless possibilities for building occupants, designers, engineers, and architects alike.

To begin, small steps can be taken such as recalibrating sensors and inserting flow meters into the air handling units. Sensors need to be recalibrated quite often to assure that the measurements they are recording are as precise as they could be. Also, by recalibrating the sensors, the loads calculated within the Klaus building, or any building for that matter, will be as accurate as possible. Likewise, if there were flow meters installed in the air handlers, the outside air load calculations which were originally calculated through on fan curves, control logic and carbon dioxide concentrations can all be verified. Although flow sensors are desirable to check the flow calculation methods, hopefully this verification will help to show that they are not really necessary.

On a related note, if someone were to conduct future work directly on this research, the next step would be to determine the thermal mass of the building. In order to determine this thermal mass, a dynamical system parameterization study must be done. This would require various regression models and parameter isolations based on the transient activities of the building's loads. For example, a rigorous statistical time series analysis is especially needed since real-time on-line parameter determination is actually very necessary in the field.

Similarly, the single-zone model performed on the Klaus building was found to be extremely accurate. Since a single-zone model was already quite accurate, just think of how much more accuracy could be gained by simply increasing the single-zone model to be a two-zone model. A short coming of the single-zone model was that it could only account for heating or cooling at any given time, not both. This is not realistic due to the fact that heating and cooling within a building can occur simultaneously, especially for a building the size of the Klaus building which utilizes four air handlers. There are a couple of ways in which these two-zones could be determined, the simplest and most logical of which would be an internal zone and an external zone. Due to how much of an influence the weather data had on a building, as illustrated through the differences in the DOE-2 and the eQUEST models, the external zone will more than likely be much more affected by weather changes than the internal zone.

Due to the fact that the single-zone model was so simple yet was able to better model the HVAC loads within the Klaus building, a major recommendation for future work is to create simpler computer energy simulation models which do not require as much time or such intricate details, yet are still able to provide accurate building load predictions. While the more complex energy simulation programs can still be used, these simplified load simulation models could be used for preliminary design, evaluating existing buildings, and embedded controls.

And, finally, once the building's thermal mass and single-zone, or two-zone, models are complete, a new model can be created which combines the two. This new model would then be able to be embedded into a building's control system in order to create adaptive controls. These adaptive controls would be able to predict the necessary

loads on a building before they are actually necessary due to its prior knowledge of the building's thermal mass, how it has performed in the past, and any necessary weather data.

APPENDIX A: Heating Loads Code

Sub Calc_Heat_Loads ()

Dim fd(12), ld(12)

```
fd(1) = 1          'January
ld(1) = fd(1) + 30
fd(2) = ld(1) + 1  'February
ld(2) = fd(2) + 27
fd(3) = ld(2) + 1  'March
ld(3) = fd(3) + 30
fd(4) = ld(3) + 1  'April
ld(4) = fd(4) + 29
fd(5) = ld(4) + 1  'May
ld(5) = fd(5) + 30
fd(6) = ld(5) + 1  'June
ld(6) = fd(6) + 29
fd(7) = ld(6) + 1  'July
ld(7) = fd(7) + 30
fd(8) = ld(7) + 1  'August
ld(8) = fd(8) + 30
fd(9) = ld(8) + 1  'September
ld(9) = fd(9) + 29
fd(10) = ld(9) + 1 'October
ld(10) = fd(10) + 30
fd(11) = ld(10) + 1 'November
ld(11) = fd(11) + 29
fd(12) = ld(11) + 1 'December
ld(12) = fd(12) + 30
```

convert_gal_ft = 0.1336806 'Conversion: 1 gallon to 0.1336806 cubic feet

row_num = 1

For days = fd(1) To ld(12)

For ToD_2hrs = 1 To 48

ToD = (ToD_2hrs - 1) / 2

'Heating:

Flow_H = Worksheets("Heating").Cells(row_num + 1, 3)

P_reg = 15 'psi

P_ss = Worksheets("Heating").Cells(row_num + 1, 4) 'psi

qual_sv = 0 'Quality of Saturated Vapor

qual_sl = 1 'Quality of Saturated Liquid

rho_H = stpsat(P_reg, qual_sv, 3, 1)

P_ss_val = Worksheets("Heating").Cells(row_num + 1, 4)

```
Rem Debug.Print(P_ss_val)
  If P_ss_val = Empty Then GoTo 11
  h_sv = stpsat(P_ss, qual_sl, 8, 1)
  h_sl = stpsat(P_reg, qual_sv, 8, 1)
  h_dif = h_sv - h_sl

  Heating_Load = convert_gal_ft * Flow_H * rho_H * h_dif
```

11 Rem skip to here when data is missing

```
row_num = row_num + 1
```

```
'Column Headings:
```

```
Worksheets("Heating").Cells(1, 6).Value = "Heating Load (BTU/min)"
```

```
'Load Values to fill in Loads Tab Columns:
```

```
Worksheets("Heating").Cells(row_num, 6).Value = Heating_Load
```

```
Next ToD_2hrs
```

```
Next days
```

```
End Sub
```


APPENDIX B: Cooling Loads Code

Sub Calc_Cool_Loads()

Dim fd(12), ld(12)

```
fd(1) = 1          'January
ld(1) = fd(1) + 30
fd(2) = ld(1) + 1  'February
ld(2) = fd(2) + 27
fd(3) = ld(2) + 1  'March
ld(3) = fd(3) + 30
fd(4) = ld(3) + 1  'April
ld(4) = fd(4) + 29
fd(5) = ld(4) + 1  'May
ld(5) = fd(5) + 30
fd(6) = ld(5) + 1  'June
ld(6) = fd(6) + 29
fd(7) = ld(6) + 1  'July
ld(7) = fd(7) + 30
fd(8) = ld(7) + 1  'August
ld(8) = fd(8) + 30
fd(9) = ld(8) + 1  'September
ld(9) = fd(9) + 29
fd(10) = ld(9) + 1 'October
ld(10) = fd(10) + 30
fd(11) = ld(10) + 1 'November
ld(11) = fd(11) + 29
fd(12) = ld(11) + 1 'December
ld(12) = fd(12) + 30
```

convert_gal_ft = 0.1336806 'Conversion: 1 gallon to 0.1336806 cubic feet

row_num = 1

For days = fd(1) To ld(8)

For ToD_2hrs = 1 To 48

ToD = (ToD_2hrs - 1) / 2

'Cooling:

Flow_C = Worksheets("Cooling").Cells(row_num + 1, 2)

T_H = Worksheets("Cooling").Cells(row_num + 1, 3)

T_L = Worksheets("Cooling").Cells(row_num + 1, 4)

T_dif = T_H - T_L

qual_C = 0 'Quality of Saturated Liquid

T_L_val = Worksheets("Cooling").Cells(row_num + 1, 4)

Rem Debug.Print (T_L_val)

```
    If T_L_val = Empty Then GoTo 10
    rho_C = sttsat(T_L, qual_C, 3, 1)
    Cp_C = sttsat(T_L, qual_C, 11, 1)
```

```
    Cooling_Load = convert_gal_ft * Flow_C * rho_C * Cp_C * T_dif
```

```
10 Rem skip to here when data is missing
```

```
    row_num = row_num + 1
```

```
'Column Headings:
```

```
    Worksheets("Cooling").Cells(1, 8).Value = "Cooling Load (BTU/min)"
```

```
'Load Values to fill in Loads Tab Columns:
```

```
    Worksheets("Cooling").Cells(row_num, 8).Value = Cooling_Load
```

```
    Next ToD_2hrs
```

```
    Next days
```

```
End Sub
```

APPENDIX C: Outside Air Loads Code

Sub Calc_Air_Loads()

Dim fd(12), ld(12)

```
fd(1) = 1           'January
ld(1) = fd(1) + 30
fd(2) = ld(1) + 1   'February
ld(2) = fd(2) + 28
fd(3) = ld(2) + 1   'March
ld(3) = fd(3) + 30
fd(4) = ld(3) + 1   'April
ld(4) = fd(4) + 29
fd(5) = ld(4) + 1   'May
ld(5) = fd(5) + 30
fd(6) = ld(5) + 1   'June
ld(6) = fd(6) + 29
fd(7) = ld(6) + 1   'July
ld(7) = fd(7) + 30
fd(8) = ld(7) + 1   'August
ld(8) = fd(8) + 30
fd(9) = ld(8) + 1   'September
ld(9) = fd(9) + 29
fd(10) = ld(9) + 1  'October
ld(10) = fd(10) + 30
fd(11) = ld(10) + 1 'November
ld(11) = fd(11) + 29
fd(12) = ld(11) + 1 'December
ld(12) = fd(12) + 30
```

row_num = 1

For days = fd(1) To ld(12)

For ToD_2hrs = 1 To 48

ToD = (ToD_2hrs - 1) / 2

'Return Air Conditions & Calculations:

'AHUs 1 & 2:

T_RA12 = Worksheets("AHU 1&2").Cells(row_num + 1, 5)

RH_RA12 = Worksheets("AHU 1&2").Cells(row_num + 1, 4) / 100

omega_RA12 = matdbrh(T_RA12, RH_RA12, 11, , 1)

h_RA12 = matdbrh(T_RA12, RH_RA12, 19, , 1)

T_MA1 = Worksheets("AHU 1&2").Cells(row_num + 1, 2)

T_MA2 = Worksheets("AHU 1&2").Cells(row_num + 1, 3)

'AHU 3:

T_RA3 = Worksheets("AHU 3").Cells(row_num + 1, 2)

```

RH_RA3 = Worksheets("AHU 3").Cells(row_num + 1, 3) / 100
omega_RA3 = matdbrh(T_RA3, RH_RA3, 11, , 1)
h_RA3 = matdbrh(T_RA3, RH_RA3, 19, , 1)
'AHU 4:
T_RA4 = Worksheets("AHU 4").Cells(row_num + 1, 3)
RH_RA4 = Worksheets("AHU 4").Cells(row_num + 1, 4) / 100
omega_RA4 = matdbrh(T_RA4, RH_RA4, 11, , 1)
h_RA4 = matdbrh(T_RA4, RH_RA4, 19, , 1)
T_MA4 = Worksheets("AHU 4").Cells(row_num + 1, 2)

```

'Outside Air Conditions & Calculations:

```

T_OA = Worksheets("OA").Cells(row_num + 1, 2) * 1.8 + 32
RH_OA = Worksheets("OA").Cells(row_num + 1, 3) / 100
omega_OA = matdbrh(T_OA, RH_OA, 11, , 1)
h_OA = matdbrh(T_OA, RH_OA, 19, , 1)
h_MOA12 = h_OA - 0.72 * (h_OA - h_RA12)
h_MOA4 = h_OA - 0.72 * (h_OA - h_RA4)
specific_volume_OA = matdbrh(T_OA, RH_OA, 15, , 1)
rho_OA = 1 / specific_volume_OA

```

'Outside Air Volumetric Flow Calculations:

'Air Handler 1:

```

SP1 = 5.67
RPM_1 = 939
N_1 = Worksheets("AHU 1&2").Cells(row_num + 1, 7) * 60
N_1_val = Worksheets("AHU 1&2").Cells(row_num + 1, 7) * 60
Rem Debug.Print (N_1_val)
If N_1_val = Empty Then GoTo 12
C_01 = 7.6989
C_11 = 0.1011
C_21 = -0.002
a_1 = C_21
b_1 = C_11 * (N_1 / RPM_1)
c_1 = C_01 * (N_1 / RPM_1) ^ 2 - SP1
V_dot_SA1 = (-b_1 - Sqr(b_1 ^ 2 - 4 * a_1 * c_1)) / (2 * a_1) * 10^3

```

'Air Handler 2:

```

SP2 = 6.14
RPM_2 = 929
N_2 = Worksheets("AHU 1&2").Cells(row_num + 1, 8) * 60
N_2_val = Worksheets("AHU 1&2").Cells(row_num + 1, 8) * 60
Rem Debug.Print (N_2_val)
If N_2_val = 0 Then GoTo 13
If N_2_val = Empty Then GoTo 14
C_02 = 7.6989
C_12 = 0.1011
C_22 = -0.002

```

```

a_2 = C_22
b_2 = C_12 * (N_2 / RPM_2)
c_2 = C_02 * (N_2 / RPM_2) ^ 2 - SP2
V_dot_SA2 = (-b_2 - Sqr(b_2 ^ 2 - 4 * a_2 * c_2)) / (2 * a_2) * 10^3

```

- 12 Rem skip to here when data is missing
- 13 Rem skip to here when data is zero
- 14 Rem skip to here when data is missing

```

'Air Handler 3:
V_dot_SA3 = 22000    'Constant supply at 22000 CFM according to
                    drawings

```

```

'Air Handler 4:
SP4 = 6
RPM_4 = 921
N_4 = Worksheets("AHU 4").Cells(row_num + 1, 6) * 60
N_4_val = Worksheets("AHU 4").Cells(row_num + 1, 6) * 60
Rem Debug.Print (N_4_val)
    If N_4_val = Empty Then GoTo 15
C_04 = 7.1891
C_14 = 0.0934
C_24 = -0.002
a_4 = C_24
b_4 = C_14 * (N_4 / RPM_4)
c_4 = C_04 * (N_4 / RPM_4) ^ 2 - SP4
V_dot_SA4 = (-b_4 - Sqr(b_4 ^ 2 - 4 * a_4 * c_4)) / (2 * a_4) * 10^3

```

- 15 Rem skip to here when data is missing

```

If h_OA < h_RA12 And T_MA1 < T_OA Then
    h_OA1 = h_OA
Else
    h_OA1 = h_MOA12
End If
V_dot_OA1 = (V_dot_SA1 * (((((0.24 * T_MA1) / (0.444 * T_MA1 + 1061) + omega_RA12) * (h_OA1 - h_RA12) + h_RA12 * (omega_RA12 - omega_OA)) / ((h_OA1 - h_RA12) / (0.444 * T_MA1 + 1061) + omega_RA12 - omega_OA)) - h_RA12)) / (h_OA1 - h_RA12)

If h_OA < h_RA12 And T_MA2 < T_OA Then
    h_OA2 = h_OA
Else
    h_OA2 = h_MOA12
End If

```

$$V_dot_OA2 = (V_dot_SA2 * (((((0.24 * T_MA2) / (0.444 * T_MA2 + 1061) + \omega_RA12) * (h_OA2 - h_RA12) + h_RA12 * (\omega_RA12 - \omega_OA)) / ((h_OA2 - h_RA12) / (0.444 * T_MA2 + 1061) + \omega_RA12 - \omega_OA)) - h_RA12)) / (h_OA2 - h_RA12)$$

If h_OA < h_RA4 And T_MA4 < T_OA Then

$$h_OA4 = h_OA$$

Else

$$h_OA4 = h_MOA4$$

End If

$$V_dot_OA4 = (V_dot_SA4 * (((((0.24 * T_MA4) / (0.444 * T_MA4 + 1061) + \omega_RA4) * (h_OA4 - h_RA4) + h_RA4 * (\omega_RA4 - \omega_OA)) / ((h_OA4 - h_RA4) / (0.444 * T_MA4 + 1061) + \omega_RA4 - \omega_OA)) - h_RA4)) / (h_OA4 - h_RA4)$$

$$OA_Load1 = V_dot_OA1 * \rho_OA * h_OA1$$

$$OA_Load2 = V_dot_OA2 * \rho_OA * h_OA2$$

$$OA_Load3 = V_dot_SA3 * \rho_OA * h_OA$$

$$OA_Load4 = V_dot_OA4 * \rho_OA * h_OA4$$

$$OA_Load = OA_Load1 + OA_Load2 + OA_Load4$$

$$RA_Load1 = V_dot_OA1 * \rho_OA * h_RA12$$

$$RA_Load2 = V_dot_OA2 * \rho_OA * h_RA12$$

$$RA_Load3 = V_dot_SA3 * \rho_OA * h_RA3$$

$$RA_Load4 = V_dot_OA4 * \rho_OA * h_RA4$$

$$RA_Load = RA_Load1 + RA_Load2 + RA_Load4$$

$$Air_Load1 = V_dot_OA1 * \rho_OA * (h_OA1 - h_RA12)$$

$$Air_Load2 = V_dot_OA2 * \rho_OA * (h_OA2 - h_RA12)$$

$$Air_Load3 = V_dot_SA3 * \rho_OA * (h_OA - h_RA3)$$

$$Air_Load4 = V_dot_OA4 * \rho_OA * (h_OA4 - h_RA4)$$

$$Air_Load = Air_Load1 + Air_Load2 + Air_Load3 + Air_Load4$$

row_num = row_num + 1

'Column Headings:

Worksheets("AHU 1&2").Cells(1, 11).Value = "OA Load1 (BTU/min)"

Worksheets("AHU 1&2").Cells(1, 12).Value = "RA Load1 (BTU/min)"

Worksheets("AHU 1&2").Cells(1, 13).Value = "Air Load1 (BTU/min)"

Worksheets("AHU 1&2").Cells(1, 14).Value = "OA Load2 (BTU/min)"

Worksheets("AHU 1&2").Cells(1, 15).Value = "RA Load2 (BTU/min)"

Worksheets("AHU 1&2").Cells(1, 16).Value = "Air Load2 (BTU/min)"

Worksheets("AHU 1&2").Cells(1, 18).Value = "Total Air Load (BTU/min)"

```
Worksheets("AHU 3").Cells(1, 6).Value = "OA Load (BTU/min)"
Worksheets("AHU 3").Cells(1, 7).Value = "RA Load (BTU/min)"
Worksheets("AHU 3").Cells(1, 8).Value = "Air Load (BTU/min)"
Worksheets("AHU 3").Cells(1, 10).Value = "Total Air Load (BTU/min)"
Worksheets("AHU 4").Cells(1, 9).Value = "OA Load (BTU/min)"
Worksheets("AHU 4").Cells(1, 10).Value = "RA Load (BTU/min)"
Worksheets("AHU 4").Cells(1, 11).Value = "Air Load (BTU/min)"
Worksheets("AHU 4").Cells(1, 13).Value = "Total Air Load (BTU/min)"
```

'Load Values to fill in Loads Tab Columns:

```
Worksheets("AHU 1&2").Cells(row_num, 11).Value = OA_Load1
Worksheets("AHU 1&2").Cells(row_num, 12).Value = RA_Load1
Worksheets("AHU 1&2").Cells(row_num, 13).Value = Air_Load1
Worksheets("AHU 1&2").Cells(row_num, 14).Value = OA_Load2
Worksheets("AHU 1&2").Cells(row_num, 15).Value = RA_Load2
Worksheets("AHU 1&2").Cells(row_num, 16).Value = Air_Load2
Worksheets("AHU 1&2").Cells(row_num, 18).Value = Air_Load
Worksheets("AHU 3").Cells(row_num, 6).Value = OA_Load3
Worksheets("AHU 3").Cells(row_num, 7).Value = RA_Load3
Worksheets("AHU 3").Cells(row_num, 8).Value = Air_Load3
Worksheets("AHU 3").Cells(row_num, 10).Value = Air_Load
Worksheets("AHU 4").Cells(row_num, 9).Value = OA_Load4
Worksheets("AHU 4").Cells(row_num, 10).Value = RA_Load4
Worksheets("AHU 4").Cells(row_num, 11).Value = Air_Load4
Worksheets("AHU 4").Cells(row_num, 13).Value = Air_Load
```

Next ToD_2hrs

Next days

End Sub

APPENDIX D: Outside Air Load Flow Calculations

Start with 4 equations with 4 unknowns:

$$\dot{m}_{OA} + \dot{m}_{RA} = \dot{m}_{MA} \quad (1)$$

$$\dot{m}_{OA} h_{OA} + \dot{m}_{RA} h_{RA} = \dot{m}_{MA} h_{MA} \quad (2)$$

$$\dot{m}_{OA} \omega_{OA} + \dot{m}_{RA} \omega_{RA} = \dot{m}_{MA} \omega_{MA} \quad (3)$$

$$h_{MA} = C_{P,DA} T_{MA} + \omega_{MA} (C_{P,WV} T_{MA} + h_{WV@0°F}) \quad (4)$$

Combine the first three equations to be 1 equation with 2 unknowns:

$$\frac{h_{OA} - h_{RA}}{\omega_{OA} - \omega_{RA}} = \frac{h_{MA} - h_{RA}}{\omega_{MA} - \omega_{RA}} \quad (5)$$

Now equations 4 & 5 allow for 2 equations with 2 unknowns. In order to solve for \dot{m}_{OA} , the real unknown, one must first solve equation 1 for \dot{m}_{RA} such that it can be placed into equation 2 leaving only 2 unknowns, \dot{m}_{OA} & h_{MA} (to be solved for next):

$$\dot{m}_{RA} = \dot{m}_{MA} - \dot{m}_{OA} \quad (6)$$

$$\dot{m}_{OA} h_{OA} + (\dot{m}_{MA} - \dot{m}_{OA}) h_{RA} = \dot{m}_{MA} h_{MA} \quad (7)$$

$$\dot{m}_{OA} (h_{OA} - h_{RA}) + \dot{m}_{MA} h_{RA} = \dot{m}_{MA} h_{MA} \quad (8)$$

$$\dot{m}_{OA} = \frac{\dot{m}_{MA} (h_{MA} - h_{RA})}{(h_{OA} - h_{RA})} \quad (9)$$

Next, rearrange equation 5 to solve for ω_{MA} to then place into equation 4 leaving only 1 unknown (h_{MA}):

$$\omega_{MA} - \omega_{RA} = \frac{(h_{MA} - h_{RA})(\omega_{OA} - \omega_{RA})}{(h_{OA} - h_{RA})} \quad (10)$$

$$\omega_{MA} = \frac{(h_{MA} - h_{RA})(\omega_{OA} - \omega_{RA})}{(h_{OA} - h_{RA})} + \omega_{RA} \quad (11)$$

Now placing equation 11 into equation 4, one gets:

$$h_{MA} = C_{P,DA} T_{MA} + \left(\frac{(h_{MA} - h_{RA})(\omega_{OA} - \omega_{RA})}{(h_{OA} - h_{RA})} + \omega_{RA} \right) (C_{P,WV} T_{MA} + h_{WV@0^{\circ}F}) \quad (12)$$

$$h_{MA} = C_{P,DA} T_{MA} + \left(\frac{h_{MA}(\omega_{OA} - \omega_{RA}) + h_{RA}(\omega_{RA} - \omega_{OA})}{(h_{OA} - h_{RA})} + \omega_{RA} \right) (C_{P,WV} T_{MA} + h_{WV@0^{\circ}F}) \quad (13)$$

$$\frac{h_{MA}}{C_{P,WV} T_{MA} + h_{WV@0^{\circ}F}} = \frac{C_{P,DA} T_{MA}}{C_{P,WV} T_{MA} + h_{WV@0^{\circ}F}} + \frac{h_{MA}(\omega_{OA} - \omega_{RA}) + h_{RA}(\omega_{RA} - \omega_{OA})}{(h_{OA} - h_{RA})} + \omega_{RA} \quad (14)$$

$$\frac{h_{MA}(h_{OA} - h_{RA})}{C_{P,WV} T_{MA} + h_{WV@0^{\circ}F}} = \left(\frac{C_{P,DA} T_{MA}}{C_{P,WV} T_{MA} + h_{WV@0^{\circ}F}} + \omega_{RA} \right) (h_{OA} - h_{RA}) + h_{MA}(\omega_{OA} - \omega_{RA}) + h_{RA}(\omega_{RA} - \omega_{OA}) \quad (15)$$

$$h_{MA} \left(\frac{h_{OA} - h_{RA}}{C_{P,WV} T_{MA} + h_{WV@0^{\circ}F}} + \omega_{RA} - \omega_{OA} \right) = \left(\frac{C_{P,DA} T_{MA}}{C_{P,WV} T_{MA} + h_{WV@0^{\circ}F}} + \omega_{RA} \right) (h_{OA} - h_{RA}) + h_{RA}(\omega_{RA} - \omega_{OA}) \quad (16)$$

$$h_{MA} = \frac{\left(\frac{C_{P,DA} T_{MA}}{C_{P,WV} T_{MA} + h_{WV@0^{\circ}F}} + \omega_{RA} \right) (h_{OA} - h_{RA}) + h_{RA} (\omega_{RA} - \omega_{OA})}{\left(\frac{h_{OA} - h_{RA}}{C_{P,WV} T_{MA} + h_{WV@0^{\circ}F}} + \omega_{RA} - \omega_{OA} \right)} \quad (17)$$

Replace h_{MA} in equation 9 with the h_{MA} found above in equation 17 to obtain an equation to find \dot{m}_{OA} using only known variables as shown below:

$$\dot{m}_{MA} = \frac{\left(\left(\frac{C_{P,DA} T_{MA}}{C_{P,WV} T_{MA} + h_{WV@0^{\circ}F}} + \omega_{RA} \right) (h_{OA} - h_{RA}) + h_{RA} (\omega_{RA} - \omega_{OA}) \right) (-h_{RA})}{(h_{OA} - h_{RA})} \quad (18)$$

This, ultimately, also gives the outside air volumetric flow rate:

$$\dot{V}_{MA} \left(\frac{\rho_{OA}}{\rho_{MA}} \right) = \frac{\left(\left(\frac{C_{P,DA} T_{MA}}{C_{P,WV} T_{MA} + h_{WV@0^{\circ}F}} + \omega_{RA} \right) (h_{OA} - h_{RA}) + h_{RA} (\omega_{RA} - \omega_{OA}) \right) (-h_{RA})}{(h_{OA} - h_{RA})} \quad (19)$$

Sample EES Code to Verify Outside Air Flow Calculations:

```
//test of adiabatic mixing calculation
//assuming m_dot_OA known find correct T_MA
//using correct T_MA as a measured datum, recompute m_dot_OA
//see that recalculated value = assumed value
//
//assume a value for m_dot_OA (cannot be measured in practice)
m_dot_OA = 0.05[lbm/sec]
// measured or inferred MA flow = SA flow usually available
m_dot_RA=1.0[lbm/sec]

// OA conditions
// measured OA props available
T_OA=95[F]
W_OA = 0.022
P_0=14.7[psia]

h_OA=enthalpy(airH2O, T=T_OA, W=W_OA, P=P_0)

// measured RA props available
T_RA=75[F]
RH_RA=0.5

h_RA=enthalpy(airH2O, T=T_RA, R=RH_RA, P=P_0)
W_RA=HUMRAT(airH2O, T=T_RA, R=RH_RA, P=P_0)

// ideal adiabatic mixing process to determine correct MA temp
m_dot_MA=m_dot_RA+m_dot_OA
h_MA=(m_dot_RA*h_RA+m_dot_OA*h_OA)/m_dot_MA
W_MA=(m_dot_RA*W_RA+m_dot_OA*W_OA)/m_dot_MA

T_MA=temperature(airH2O, H=h_MA, W=W_MA, P=P_0)

// recompute (RC) m_dot_OA by Valade-Gao calculation

m_dot_MA=m_dot_RA_RC+m_dot_OA_RC
h_MA_RC=(m_dot_RA*h_RA+m_dot_OA_RC*h_OA)/m_dot_MA
W_MA_RC=(m_dot_RA_RC*W_RA+m_dot_OA*W_OA)/m_dot_MA
h_MA_RC=enthalpy(airH2O, T=T_MA, W=W_MA_RC, P=P_0)
```

APPENDIX E: Clear Sky Model Code

```

Function G_T(LTZ, Latitude, Longitude, Time_of_day, day_of_year, G_BN_AM0, _
    B_CS, F_CS, Beta, rho_FG) "Total irradiation in W/m2
    declination_angle = 23.45 * Sin((Application.pi() / 180) * 360 * ((284 + _
        day_of_year) / 365))
    BBB = 360 * (day_of_year - 81) / 364 * (Application.pi() / 180)
    EOT = 9.87 * Sin(2 * BBB) - 7.53 * cos(BBB) - 1.5 * Sin(BBB)
    Solar_Time = (Time_of_day + EOT + 4 * (LTZ - Longitude)) / 60
    Solar_Hour_Angle = 15 * (Solar_Time - 12)
    Solar_Altitude_Angle = Application.Asin(Sin(Latitude * (Application.pi() / 180)) * _
        Sin(declination_angle * (Application.pi() / 180)) + cos(Latitude * _
        (Application.pi() / 180)) * cos(declination_angle * (Application.pi() / 180)) * _
        cos(Solar_Hour_Angle * (Application.pi() / 180))) / (Application.pi() / 180)
    G_BN = G_BN_AM0 * Exp(-B_CS / Sin(Solar_Altitude_Angle * _
        (Application.pi() / 180)))
        If Solar_Altitude_Angle < 0 Then
            G_BN = 0
        End If
    G_SD = F_CS * G_BN
    Theta_B = Application.Acos(Sin(Solar_Altitude_Angle * (Application.pi() / 180))) /
        (Application.pi() / 180)
    G_T = G_BN * cos(Theta_B * (Application.pi() / 180)) + G_SD * ((1 + cos(Beta *
        (Application.pi() / 180))) / 2) + rho_FG * (G_BN * Sin(Solar_Altitude_Angle *
        (Application.pi() / 180)) + G_SD) * ((1 - cos(Beta * (Application.pi() / 180))) / 2)
End Function

```

```

Sub Calculate_Total_Solar_Radiation()

```

```

Worksheets("CSM").Cells(1, 1).Value = "Day of the Year"
Worksheets("CSM").Cells(1, 2).Value = "Time of Day"
Worksheets("CSM").Cells(1, 3).Value = "G_T"
Worksheets("CSM").Cells(2, 1).Value = "--"
Worksheets("CSM").Cells(2, 2).Value = "(minutes)"
Worksheets("CSM").Cells(2, 3).Value = "(W/m^2)"

```

```

Dim fd(12), ld(12)
    fd(1) = 1           'January
    ld(1) = fd(1) + 30
    fd(2) = ld(1) + 1  'February
    ld(2) = fd(2) + 27
    fd(3) = ld(2) + 1  'March
    ld(3) = fd(3) + 30
    fd(4) = ld(3) + 1  'April
    ld(4) = fd(4) + 29

```

$fd(5) = ld(4) + 1$ 'May
 $ld(5) = fd(5) + 30$
 $fd(6) = ld(5) + 1$ 'June
 $ld(6) = fd(6) + 29$
 $fd(7) = ld(6) + 1$ 'July
 $ld(7) = fd(7) + 30$
 $fd(8) = ld(7) + 1$ 'August
 $ld(8) = fd(8) + 30$
 $fd(9) = ld(8) + 1$ 'September
 $ld(9) = fd(9) + 29$
 $fd(10) = ld(9) + 1$ 'October
 $ld(10) = fd(10) + 30$
 $fd(11) = ld(10) + 1$ 'November
 $ld(11) = fd(11) + 29$
 $fd(12) = ld(11) + 1$ 'December
 $ld(12) = fd(12) + 30$

Dim bcs(12), fcs(12), gbnamo(12)

$bcs(1) = 0.142$ 'January
 $fcs(1) = 0.058$
 $gbnamo(1) = 390$
 $bcs(2) = 0.144$ 'February
 $fcs(2) = 0.06$
 $gbnamo(2) = 385$
 $bcs(3) = 0.156$ 'March
 $fcs(3) = 0.071$
 $gbnamo(3) = 376$
 $bcs(4) = 0.18$ 'April
 $fcs(4) = 0.097$
 $gbnamo(4) = 360$
 $bcs(5) = 0.196$ 'May
 $fcs(5) = 0.121$
 $gbnamo(5) = 350$
 $bcs(6) = 0.205$ 'June
 $fcs(6) = 0.134$
 $gbnamo(6) = 345$
 $bcs(7) = 0.207$ 'July
 $fcs(7) = 0.136$
 $gbnamo(7) = 344$
 $bcs(8) = 0.201$ 'August
 $fcs(8) = 0.122$
 $gbnamo(8) = 351$
 $bcs(9) = 0.177$ 'September
 $fcs(9) = 0.092$
 $gbnamo(9) = 365$
 $bcs(10) = 0.16$ 'October

```

fcs(10) = 0.073
gbnamo(10) = 378
bcs(11) = 0.149      'November
fcs(11) = 0.063
gbnamo(11) = 387
bcs(12) = 0.142      'December
fcs(12) = 0.057
gbnamo(12) = 391

row_num = 1
For Days = fd(1) To ld(12)
  For ToD_hrs = 1 To 24
    ToD = ToD_hrs - 1
    row_num = row_num + 1
    'Change these variables per location:
    LTZ = 75      'Local Time Zone (degrees)
    lat = 33.7    'Latitude of location (degrees)
    lon = 84.4    'Longitude of location (degrees)
    ToDm = 0      'Time of Day (in minutes!)
    doy = 1       'Day of the Year (1 = January 1st ...)
    gr = 1353     'Global Radiation Constant (W/m2)
    Beta = 0      'Tilt (degrees)
    rho = 0.2     'Foreground reflectance

    For iMonth = 1 To 12
      If fd(iMonth) < Days < ld(iMonth) Then
        bcsm = bcs(iMonth)
        fcsm = fcs(iMonth)
        gbnamos = gbnamo(iMonth)
      End If

      tsr = G_T(LTZ, lat, lon, ToD * 60, Days, gbnamos, bcsm, fcsm, Beta, rho)
      If tsr < 0 Then
        Worksheets("CSM").Cells(row_num + 1, 3).Value = 0
      Else
        Worksheets("CSM").Cells(row_num + 1, 3).Value = tsr
      End If

      Worksheets("CSM").Cells(row_num + 1, 2).Value = ToD * 60
      Worksheets("CSM").Cells(row_num + 1, 1).Value = Days

    Next iMonth
  Next ToD_hrs
Next Days
End Sub

```

APPENDIX F: Combined Skin Load Code

```
Function Linterp(r As Range, x As Double) As Double
    ' linear interpolator / extrapolator
    ' R is a two-column range containing known x, known y
    Dim IR As Long, I1 As Long, I2 As Long
    Dim nR As Long
    'If x = 1.5 Then Stop
    nR = r.Rows.Count
    If nR < 2 Then Exit Function
    If x < r(1, 1) Then ' x < xmin, extrapolate
        I1 = 1: I2 = 2: GoTo Interp
    ElseIf x > r(nR, 1) Then ' x > xmax, extrapolate
        I1 = nR - 1: I2 = nR: GoTo Interp
    Else
        ' a binary search would be better here
        For IR = 1 To nR
            If r(IR, 1) = x Then ' x is exact from table
                Linterp = r(IR, 2)
                Exit Function
            ElseIf r(IR, 1) > x Then ' x is between tabulated values, interpolate
                I1 = IR: I2 = IR - 1: GoTo Interp
            End If
        Next
    End If
    Interp:
    Linterp = r(I1, 2) _
        + (r(I2, 2) - r(I1, 2)) _
        * (x - r(I1, 1)) _
        / (r(I2, 1) - r(I1, 1))
End Function

Sub Calculate_Skin_Loads()

Application.Calculation = xlCalculationManual

Dim theta_B_S As Double
Dim theta_B_SW As Double
Dim theta_B_W As Double
Dim theta_B_NW As Double
Dim theta_B_N As Double
Dim theta_B_NE As Double
Dim theta_B_E As Double
```

Dim theta_B_SE As Double

Dim fd(12), ld(12)

fd(1) = 1 'January
ld(1) = fd(1) + 30
fd(2) = ld(1) + 1 'February
ld(2) = fd(2) + 28
fd(3) = ld(2) + 1 'March
ld(3) = fd(3) + 30
fd(4) = ld(3) + 1 'April
ld(4) = fd(4) + 29
fd(5) = ld(4) + 1 'May
ld(5) = fd(5) + 30
fd(6) = ld(5) + 1 'June
ld(6) = fd(6) + 29
fd(7) = ld(6) + 1 'July
ld(7) = fd(7) + 30
fd(8) = ld(7) + 1 'August
ld(8) = fd(8) + 30
fd(9) = ld(8) + 1 'September
ld(9) = fd(9) + 29
fd(10) = ld(9) + 1 'October
ld(10) = fd(10) + 30
fd(11) = ld(10) + 1 'November
ld(11) = fd(11) + 29
fd(12) = ld(11) + 1 'December
ld(12) = fd(12) + 30

Dim bcs(12), fcs(12), gbname(12)

bcs(1) = 0.142 'January
fcs(1) = 0.058
gbname(1) = 390
bcs(2) = 0.144 'February
fcs(2) = 0.06
gbname(2) = 385
bcs(3) = 0.156 'March
fcs(3) = 0.071
gbname(3) = 376
bcs(4) = 0.18 'April
fcs(4) = 0.097
gbname(4) = 360
bcs(5) = 0.196 'May
fcs(5) = 0.121
gbname(5) = 350
bcs(6) = 0.205 'June
fcs(6) = 0.134

gbnamo(6) = 345
 bcs(7) = 0.207 'July
 fcs(7) = 0.136
 gbnamo(7) = 344
 bcs(8) = 0.201 'August
 fcs(8) = 0.122
 gbnamo(8) = 351
 bcs(9) = 0.177 'September
 fcs(9) = 0.092
 gbnamo(9) = 365
 bcs(10) = 0.16 'October
 fcs(10) = 0.073
 gbnamo(10) = 378
 bcs(11) = 0.149 'November
 fcs(11) = 0.063
 gbnamo(11) = 387
 bcs(12) = 0.142 'December
 fcs(12) = 0.057
 gbnamo(12) = 391

Dim gamma_sur(8)

gamma_sur(1) = 0 'South Wall (degrees)
 gamma_sur(2) = 45 'South-West Wall (degrees)
 gamma_sur(3) = 90 'West Wall (degrees)
 gamma_sur(4) = 135 'North-West Wall (degrees)
 gamma_sur(5) = 180 'North Wall (degrees)
 gamma_sur(6) = -135 'North-East Wall (degrees)
 gamma_sur(7) = -90 'East Wall (degrees)
 gamma_sur(8) = -45 'South-East Wall (degrees)

Dim CAB(9)

CAB(1) = 0
 CAB(2) = 7.178049038916E-04
 CAB(3) = 0.02972517920018
 CAB(4) = 0.2490303701482
 CAB(5) = 0.9466134865964
 CAB(6) = 1.477191594315
 CAB(7) = 1.56801154
 CAB(8) = 2.077319493401
 CAB(9) = 1.377810138749

Dim XO(10)

XO(1) = 0
 XO(2) = 0.05
 XO(3) = 0.15
 XO(4) = 0.25

XO(5) = 0.35
 XO(6) = 0.45
 XO(7) = 0.55
 XO(8) = 0.65
 XO(9) = 0.75
 XO(10) = 0.85

Dim YO(9)

YO(1) = 0
 YO(2) = YO(1) + CAB(1) * (XO(2) - XO(1))
 YO(3) = YO(2) + CAB(2) * (XO(3) - XO(2))
 YO(4) = YO(3) + CAB(3) * (XO(4) - XO(3))
 YO(5) = YO(4) + CAB(4) * (XO(5) - XO(4))
 YO(6) = YO(5) + CAB(5) * (XO(6) - XO(5))
 YO(7) = YO(6) + CAB(6) * (XO(7) - XO(6))
 YO(8) = YO(7) + CAB(7) * (XO(8) - XO(7))
 YO(9) = YO(8) + CAB(8) * (XO(9) - XO(8))

row_num = 0

For days = fd(1) To ld(12)

For ToD_hrs = 1 To 24

ToD = ToD_hrs - 1

row_num = row_num + 1

'Change these variables per location:

LTZ = 75 'Local Time Zone (degrees)
 Lat = 33.7 'Latitude of location (degrees)
 lon = 84.4 'Longitude of location (degrees)
 ToDm = 0 'Time of Day (in minutes!)
 doy = 1 'Day of the Year (1 = January 1st ...)
 gr = 1353 'Global Radiation Constant (W/m2)
 Beta = 90 '0 for roof, 90 for walls (degrees)
 rho = 0.2 'Foreground reflectance

For iMonth = 1 To 12

If fd(iMonth) < days < ld(iMonth) Then

bcss = bcs(iMonth)

fcsc = fcs(iMonth)

End If

SR = Worksheets("Skin Loads").Cells(row_num + 1, 4)

G_SC = 1367 'Solar Constant (W/m2)

declination_angle = 23.45 * Sin((Application.Pi() / 180) * 360 * ((284 + _
days) / 366))

BBB = 360 * (days - 81) / 364 * (Application.Pi() / 180)

EOT = 9.87 * Sin(2 * BBB) - 7.53 * Cos(BBB) - 1.5 * Sin(BBB)

Solar_Time = (ToD * 60 + EOT + 4 * (LTZ - lon)) / 60

```

Solar_Hour_Angle = 15 * (Solar_Time - 12)
Solar_Altitude_Angle = Application.Asin(Sin(Lat * (Application.Pi() / 180)) * Sin(declination_angle * (Application.Pi() / 180)) + Cos(Lat * (Application.Pi() / 180)) * Cos(declination_angle * (Application.Pi() / 180)) * Cos(Solar_Hour_Angle * (Application.Pi() / 180))) / (Application.Pi() / 180)
k_t = SR / (G_SC * Sin(Solar_Altitude_Angle * (Application.Pi() / 180)))

If k_t < 0 Or k_t > 0.8 Then
    k_t = 0
End If

If k_t < 0.05 Then
    tau = YO(1) + (k_t - XO(1)) * CAB(1)
ElseIf k_t < 0.15 Then
    tau = YO(2) + (k_t - XO(2)) * CAB(2)
ElseIf k_t < 0.25 Then
    tau = YO(3) + (k_t - XO(3)) * CAB(3)
ElseIf k_t < 0.35 Then
    tau = YO(4) + (k_t - XO(4)) * CAB(4)
ElseIf k_t < 0.45 Then
    tau = YO(5) + (k_t - XO(5)) * CAB(5)
ElseIf k_t < 0.55 Then
    tau = YO(6) + (k_t - XO(6)) * CAB(6)
ElseIf k_t < 0.65 Then
    tau = YO(7) + (k_t - XO(7)) * CAB(7)
ElseIf k_t < 0.75 Then
    tau = YO(8) + (k_t - XO(8)) * CAB(8)
Else
    tau = YO(9) + (k_t - XO(9)) * CAB(9)
End If

G_BN = tau * SR
G_SD = SR - G_BN * Sin(Solar_Altitude_Angle * (Application.Pi() / 180))

sine_gamma_s = (Cos(declination_angle * (Application.Pi() / 180)) * Sin(Solar_Hour_Angle * (Application.Pi() / 180)) / Cos(Solar_Altitude_Angle * (Application.Pi() / 180)))
cosine_gamma_s = (Cos(declination_angle * (Application.Pi() / 180)) * Cos(Solar_Hour_Angle * (Application.Pi() / 180)) * Sin(Lat * (Application.Pi() / 180)) - (Sin(declination_angle * (Application.Pi() / 180)) * Cos(Lat * (Application.Pi() / 180)))) / Cos(Solar_Altitude_Angle * (Application.Pi() / 180))

gamma_s = Application.Atan2(cosine_gamma_s, sine_gamma_s) / (Application.Pi() / 180)

```


$$G_{T_SE} = G_{BN} * \cos_theta_B_SE + G_{SD} * ((1 + \cos(\text{Beta} * \frac{\text{Application.Pi}()}{180}))) / 2 + \rho * (G_{BN} * \sin(\text{Solar_Altitude_Angle} * \frac{\text{Application.Pi}()}{180}) + G_{SD}) * ((1 - \cos(\text{Beta} * \frac{\text{Application.Pi}()}{180}))) / 2$$

If G_T_S < 0 Then
 G_T_S = 0
 End If

If G_T_SW < 0 Then
 G_T_SW = 0
 End If

If G_T_W < 0 Then
 G_T_W = 0
 End If

If G_T_NW < 0 Then
 G_T_NW = 0
 End If

If G_T_N < 0 Then
 G_T_N = 0
 End If

If G_T_NE < 0 Then
 G_T_NE = 0
 End If

If G_T_E < 0 Then
 G_T_E = 0
 End If

If G_T_SE < 0 Then
 G_T_SE = 0
 End If

'Variables needed for T_sol-air calculations:

T_OA_SI = Worksheets("Skin Loads").Cells(row_num + 1, 3)

T_OA = 1.8 * T_OA_SI + 32 'Convert to oF

alpha_abs_ls = 0.45 'absorptance for a light surface

alpha_abs_ds = 0.9 'absorptance for a dark surface

h_0 = 3 'BTU / (hr*ft^2*oF)

delta_T_IR_h = 7 '7oF for a horizontal surface

delta_T_IR_v = 0 '0oF for a vertical surface

G_T_convert = 0.31696 'Converts W/m2 to BTU/(hr*ft^2)

Window_NE = 11400 'ft^2
 Window_E = 2900 'ft^2
 Window_SE = 665 'ft^2
 CW_S = 4700 'ft^2
 CW_SW = 2800 'ft^2
 CW_W = 5500 'ft^2
 CW_NW = 3185 'ft^2
 CW_N = 3150 'ft^2
 CW_NE = 11000 'ft^2
 CW_E = 2565 'ft^2
 CW_SE = 2600 'ft^2
 BW_S = 3125 'ft^2
 BW_SW = 1200 'ft^2
 BW_W = 3650 'ft^2
 BW_NW = 2125 'ft^2
 BW_N = 0 'ft^2
 BW_NE = 0 'ft^2
 BW_E = 5985 'ft^2
 BW_SE = 300 'ft^2

'R values for the 4 wall types

Rv_roof = 53.65 '(oF*hr*ft^2)/BTU
 Rv_CW = 16.44 '(oF*hr*ft^2)/BTU
 Rv_BW = 23.05 '(oF*hr*ft^2)/BTU

'Skin Load Calculations

SL_roof = Roof_area / Rv_roof * (T_sol_air_roof - T_zone)
 SL_CW_S = CW_S / Rv_CW * (T_sol_air_ls_S - T_zone)
 SL_CW_SW = CW_SW / Rv_CW * (T_sol_air_ls_SW - T_zone)
 SL_CW_W = CW_W / Rv_CW * (T_sol_air_ls_W - T_zone)
 SL_CW_NW = CW_NW / Rv_CW * (T_sol_air_ls_NW - T_zone)
 SL_CW_N = CW_N / Rv_CW * (T_sol_air_ls_N - T_zone)
 SL_CW_NE = CW_NE / Rv_CW * (T_sol_air_ls_NE - T_zone)
 SL_CW_E = CW_E / Rv_CW * (T_sol_air_ls_E - T_zone)
 SL_CW_SE = CW_SE / Rv_CW * (T_sol_air_ls_SE - T_zone)
 SL_BW_S = BW_S / Rv_BW * (T_sol_air_ds_S - T_zone)
 SL_BW_SW = BW_SW / Rv_BW * (T_sol_air_ds_SW - T_zone)
 SL_BW_W = BW_W / Rv_BW * (T_sol_air_ds_W - T_zone)
 SL_BW_NW = BW_NW / Rv_BW * (T_sol_air_ds_NW - T_zone)
 SL_BW_N = BW_N / Rv_BW * (T_sol_air_ds_N - T_zone)
 SL_BW_NE = BW_NE / Rv_BW * (T_sol_air_ds_NE - T_zone)
 SL_BW_E = BW_E / Rv_BW * (T_sol_air_ds_E - T_zone)
 SL_BW_SE = BW_SE / Rv_BW * (T_sol_air_ds_SE - T_zone)

'Window Variables:

alpha = 0.9 'Suggested by Dr. Jeter to have a high absorbtivity

SC = 0.43 'Taken from DOE document

```
theta_B_S = Application.Acos(cos_theta_B_S) * 180 / Application.Pi()
  If theta_B_S < 0 Or theta_B_S > 90 Then
    theta_B_S = 90
  End If
theta_B_SW = Application.Acos(cos_theta_B_SW) * 180 / Application.Pi()
  If theta_B_SW < 0 Or theta_B_SW > 90 Then
    theta_B_SW = 90
  End If
theta_B_W = Application.Acos(cos_theta_B_W) * 180 / Application.Pi()
  If theta_B_W < 0 Or theta_B_W > 90 Then
    theta_B_W = 90
  End If
theta_B_NW = Application.Acos(cos_theta_B_NW) * 180 / Application.Pi()
  If theta_B_NW < 0 Or theta_B_NW > 90 Then
    theta_B_NW = 90
  End If
theta_B_N = Application.Acos(cos_theta_B_N) * 180 / Application.Pi()
  If theta_B_N < 0 Or theta_B_N > 90 Then
    theta_B_N = 90
  End If
theta_B_NE = Application.Acos(cos_theta_B_NE) * 180 / Application.Pi()
  If theta_B_NE < 0 Or theta_B_NE > 90 Then
    theta_B_NE = 90
  End If
theta_B_E = Application.Acos(cos_theta_B_E) * 180 / Application.Pi()
  If theta_B_E < 0 Or theta_B_E > 90 Then
    theta_B_S = 90
  End If
theta_B_SE = Application.Acos(cos_theta_B_SE) * 180 / Application.Pi()
  If theta_B_SE < 0 Or theta_B_SE > 90 Then
    theta_B_SE = 90
  End If
```

Linterp_range = Worksheets("Skin Load Input").[A2:B20]

```
tau_ref_S = Linterp(Worksheets("Skin Load Input").[A2:B20], theta_B_S)
tau_ref_SW = Linterp(Worksheets("Skin Load Input").[A2:B20], _
  theta_B_SW)
tau_ref_W = Linterp(Worksheets("Skin Load Input").[A2:B20], theta_B_W)
tau_ref_NW = Linterp(Worksheets("Skin Load Input").[A2:B20], _
  theta_B_NW)
tau_ref_N = Linterp(Worksheets("Skin Load Input").[A2:B20], theta_B_N)
tau_ref_NE = Linterp(Worksheets("Skin Load Input").[A2:B20], _
  theta_B_NE)
```


tau_ref_E = Linterp(Worksheets("Skin Load Input").[A2:B20], theta_B_E)
tau_ref_SE = Linterp(Worksheets("Skin Load Input").[A2:B20], _
theta_B_SE)

If tau_ref_S < 0 Or tau_ref_S > 0.875 Then
tau_ref_S = 0
End If

If tau_ref_SW < 0 Or tau_ref_SW > 0.875 Then
tau_ref_SW = 0
End If

If tau_ref_W < 0 Or tau_ref_W > 0.875 Then
tau_ref_W = 0
End If

If tau_ref_NW < 0 Or tau_ref_NW > 0.875 Then
tau_ref_NW = 0
End If

If tau_ref_N < 0 Or tau_ref_N > 0.875 Then
tau_ref_N = 0
End If

If tau_ref_NE < 0 Or tau_ref_NE > 0.875 Then
tau_ref_NE = 0
End If

If tau_ref_E < 0 Or tau_ref_E > 0.875 Then
tau_ref_E = 0
End If

If tau_ref_SE < 0 Or tau_ref_SE > 0.875 Then
tau_ref_SE = 0
End If

'Window Calculations:

SL_Window_S = alpha * G_T_S * SC * Window_S * tau_ref_S
SL_Window_SW = alpha * G_T_SW * SC * Window_SW * tau_ref_SW
SL_Window_W = alpha * G_T_W * SC * Window_W * tau_ref_W
SL_Window_NW = alpha * G_T_NW * SC * Window_NW * tau_ref_NW
SL_Window_N = alpha * G_T_N * SC * Window_N * tau_ref_N
SL_Window_NE = alpha * G_T_NE * SC * Window_NE * tau_ref_NE
SL_Window_E = alpha * G_T_E * SC * Window_E * tau_ref_E
SL_Window_SE = alpha * G_T_SE * SC * Window_SE * tau_ref_SE

Skin_Load_CW = SL_CW_S + SL_CW_SW + SL_CW_W +
SL_CW_NW + SL_CW_N + SL_CW_NE + SL_CW_E +
SL_CW_SE

Skin_Load_BW = SL_BW_S + SL_BW_SW + SL_BW_W +
SL_BW_NW + SL_BW_N + SL_BW_NE + SL_BW_E +
SL_BW_SE

Skin_Load_Window = SL_Window_S + SL_Window_SW +
SL_Window_W + SL_Window_NW + SL_Window_N +
SL_Window_NE + SL_Window_E + SL_Window_SE

Conduction_Skin_Load = SL_roof + Skin_Load_CW + Skin_Load_BW
Solar_Gain_Skin_Load = Skin_Load_Window
Total_Skin_Load = Conduction_Skin_Load + Solar_Gain_Skin_Load

Worksheets("Skin Loads").Cells(1, 6).Value = "Roof"
Worksheets("Skin Loads").Cells(1, 7).Value = "CW"
Worksheets("Skin Loads").Cells(1, 8).Value = "BW"
Worksheets("Skin Loads").Cells(1, 9).Value = "Conduction"
Worksheets("Skin Loads").Cells(1, 10).Value = "Window SG"
Worksheets("Skin Loads").Cells(1, 11).Value = "Skin Load"

Worksheets("Skin Loads").Cells(row_num + 1, 6).Value = SL_roof
Worksheets("Skin Loads").Cells(row_num + 1, 7).Value = Skin_Load_CW
Worksheets("Skin Loads").Cells(row_num + 1, 8).Value = Skin_Load_BW
Worksheets("Skin Loads").Cells(row_num + 1, 9).Value =
Conduction_Skin_Load
Worksheets("Skin Loads").Cells(row_num + 1, 10).Value =
Skin_Load_Window
Worksheets("Skin Loads").Cells(row_num + 1, 11).Value =
Total_Skin_Load

Next iMonth
Next ToD_hrs
Next days
Application.Calculate
Application.Calculation = xlCalculationAutomatic

End Sub

APPENDIX G: Transfer Function Conduction Skin Loads Code

Sub Calculate_Transfer_Conduction_Skin_Loads()

Dim fd(12), ld(12)

```
fd(1) = 1          'January
ld(1) = fd(1) + 30
fd(2) = ld(1) + 1  'February
ld(2) = fd(2) + 27
fd(3) = ld(2) + 1  'March
ld(3) = fd(3) + 30
fd(4) = ld(3) + 1  'April
ld(4) = fd(4) + 29
fd(5) = ld(4) + 1  'May
ld(5) = fd(5) + 30
fd(6) = ld(5) + 1  'June
ld(6) = fd(6) + 29
fd(7) = ld(6) + 1  'July
ld(7) = fd(7) + 30
fd(8) = ld(7) + 1  'August
ld(8) = fd(8) + 30
fd(9) = ld(8) + 1  'September
ld(9) = fd(9) + 29
fd(10) = ld(9) + 1 'October
ld(10) = fd(10) + 30
fd(11) = ld(10) + 1 'November
ld(11) = fd(11) + 29
fd(12) = ld(11) + 1 'December
ld(12) = fd(12) + 30
```

```
row_num = 0
```

```
For days = fd(1) To ld(12)
```

```
  For ToD_hrs = 1 To 24
```

```
    ToD = ToD_hrs - 1
```

```
    row_num = row_num + 1
```

```
  'Zone Temperature:
```

```
    T_zone = 72    'oF
```

```
  'Wall Compositions (Area):
```

```
    Roof_area = 6060 'ft^2
```

```
    CW_S = 4700    'ft^2
```

```
    CW_SW = 2800   'ft^2
```

```
    CW_W = 5500    'ft^2
```

```
    CW_NW = 3185   'ft^2
```

CW_N = 3150 'ft^2
CW_NE = 11000 'ft^2
CW_E = 2565 'ft^2
CW_SE = 2600 'ft^2
BW_S = 3125 'ft^2
BW_SW = 1200 'ft^2
BW_W = 3650 'ft^2
BW_NW = 2125 'ft^2
BW_N = 0 'ft^2
BW_NE = 0 'ft^2
BW_E = 5985 'ft^2
BW_SE = 300 'ft^2

'Transfer Coefficients:

bn_roof_0 = 0
bn_roof_1 = 0.00003
bn_roof_2 = 0.00035
bn_roof_3 = 0.00056
bn_roof_4 = 0.00018
bn_roof_5 = 0.00025
cn_roof = 0.00114
dn_roof_1 = -0.24424
dn_roof_2 = 0.12954
dn_roof_3 = -0.0256
dn_roof_4 = 0.0017
dn_roof_5 = -0.00003
bn_brick_0 = 0
bn_brick_1 = 0.00056
bn_brick_2 = 0.00208
bn_brick_3 = 0.00104
bn_brick_4 = 0.00009
cn_brick = 0.00378
dn_brick_1 = -0.25101
dn_brick_2 = 0.1021
dn_brick_3 = -0.01258
dn_brick_4 = 0.00041
bn_cw_0 = 0.00382
bn_cw_1 = 0.01985
bn_cw_2 = 0.00629
bn_cw_3 = 0.00008
cn_cw = 0.03003
dn_cw_1 = -0.44738
dn_cw_2 = 0.06573
dn_cw_3 = -0.00002

'Sol-Air Temperatures:

T_sol_air_roof_5 = Worksheets("Sol-Air Temps").Cells(row_num - 5, 19)
T_sol_air_roof_4 = Worksheets("Sol-Air Temps").Cells(row_num - 4, 19)
T_sol_air_roof_3 = Worksheets("Sol-Air Temps").Cells(row_num - 3, 19)
T_sol_air_roof_2 = Worksheets("Sol-Air Temps").Cells(row_num - 2, 19)
T_sol_air_roof_1 = Worksheets("Sol-Air Temps").Cells(row_num - 1, 19)
T_sol_air_roof_0 = Worksheets("Sol-Air Temps").Cells(row_num, 19)
T_sol_air_ls_S_3 = Worksheets("Sol-Air Temps").Cells(row_num - 3, 3)
T_sol_air_ls_S_2 = Worksheets("Sol-Air Temps").Cells(row_num - 2, 3)
T_sol_air_ls_S_1 = Worksheets("Sol-Air Temps").Cells(row_num - 1, 3)
T_sol_air_ls_S_0 = Worksheets("Sol-Air Temps").Cells(row_num, 3)
T_sol_air_ls_SW_3 = Worksheets("Sol-Air Temps").Cells(row_num - 3, 5)
T_sol_air_ls_SW_2 = Worksheets("Sol-Air Temps").Cells(row_num - 2, 5)
T_sol_air_ls_SW_1 = Worksheets("Sol-Air Temps").Cells(row_num - 1, 5)
T_sol_air_ls_SW_0 = Worksheets("Sol-Air Temps").Cells(row_num, 5)
T_sol_air_ls_W_3 = Worksheets("Sol-Air Temps").Cells(row_num - 3, 7)
T_sol_air_ls_W_2 = Worksheets("Sol-Air Temps").Cells(row_num - 2, 7)
T_sol_air_ls_W_1 = Worksheets("Sol-Air Temps").Cells(row_num - 1, 7)
T_sol_air_ls_W_0 = Worksheets("Sol-Air Temps").Cells(row_num, 7)
T_sol_air_ls_NW_3 = Worksheets("Sol-Air Temps").Cells(row_num - 3, 9)
T_sol_air_ls_NW_2 = Worksheets("Sol-Air Temps").Cells(row_num - 2, 9)
T_sol_air_ls_NW_1 = Worksheets("Sol-Air Temps").Cells(row_num - 1, 9)
T_sol_air_ls_NW_0 = Worksheets("Sol-Air Temps").Cells(row_num, 9)
T_sol_air_ls_N_3 = Worksheets("Sol-Air Temps").Cells(row_num - 3, 11)
T_sol_air_ls_N_2 = Worksheets("Sol-Air Temps").Cells(row_num - 2, 11)
T_sol_air_ls_N_1 = Worksheets("Sol-Air Temps").Cells(row_num - 1, 11)
T_sol_air_ls_N_0 = Worksheets("Sol-Air Temps").Cells(row_num, 11)
T_sol_air_ls_NE_3 = Worksheets("Sol-Air Temps").Cells(row_num - 3, 13)
T_sol_air_ls_NE_2 = Worksheets("Sol-Air Temps").Cells(row_num - 2, 13)
T_sol_air_ls_NE_1 = Worksheets("Sol-Air Temps").Cells(row_num - 1, 13)
T_sol_air_ls_NE_0 = Worksheets("Sol-Air Temps").Cells(row_num, 13)
T_sol_air_ls_E_3 = Worksheets("Sol-Air Temps").Cells(row_num - 3, 15)
T_sol_air_ls_E_2 = Worksheets("Sol-Air Temps").Cells(row_num - 2, 15)
T_sol_air_ls_E_1 = Worksheets("Sol-Air Temps").Cells(row_num - 1, 15)
T_sol_air_ls_E_0 = Worksheets("Sol-Air Temps").Cells(row_num, 15)
T_sol_air_ls_SE_3 = Worksheets("Sol-Air Temps").Cells(row_num - 3, 17)
T_sol_air_ls_SE_2 = Worksheets("Sol-Air Temps").Cells(row_num - 2, 17)
T_sol_air_ls_SE_1 = Worksheets("Sol-Air Temps").Cells(row_num - 3, 17)
T_sol_air_ls_SE_0 = Worksheets("Sol-Air Temps").Cells(row_num, 17)
T_sol_air_ds_S_4 = Worksheets("Sol-Air Temps").Cells(row_num - 4, 4)
T_sol_air_ds_S_3 = Worksheets("Sol-Air Temps").Cells(row_num - 3, 4)
T_sol_air_ds_S_2 = Worksheets("Sol-Air Temps").Cells(row_num - 2, 4)
T_sol_air_ds_S_1 = Worksheets("Sol-Air Temps").Cells(row_num - 1, 4)
T_sol_air_ds_S_0 = Worksheets("Sol-Air Temps").Cells(row_num, 4)
T_sol_air_ds_SW_4 = Worksheets("Sol-Air Temps").Cells(row_num - 4, 6)
T_sol_air_ds_SW_3 = Worksheets("Sol-Air Temps").Cells(row_num - 3, 6)
T_sol_air_ds_SW_2 = Worksheets("Sol-Air Temps").Cells(row_num - 2, 6)

T_sol_air_ds_SW_1 = Worksheets("Sol-Air Temps").Cells(row_num - 1, 6)
 T_sol_air_ds_SW_0 = Worksheets("Sol-Air Temps").Cells(row_num, 6)
 T_sol_air_ds_W_4 = Worksheets("Sol-Air Temps").Cells(row_num - 4, 8)
 T_sol_air_ds_W_3 = Worksheets("Sol-Air Temps").Cells(row_num - 3, 8)
 T_sol_air_ds_W_2 = Worksheets("Sol-Air Temps").Cells(row_num - 2, 8)
 T_sol_air_ds_W_1 = Worksheets("Sol-Air Temps").Cells(row_num - 1, 8)
 T_sol_air_ds_W_0 = Worksheets("Sol-Air Temps").Cells(row_num, 8)
 T_sol_air_ds_NW_4=Worksheets("Sol-Air Temps").Cells(row_num - 4, 10)
 T_sol_air_ds_NW_3=Worksheets("Sol-Air Temps").Cells(row_num - 3, 10)
 T_sol_air_ds_NW_2=Worksheets("Sol-Air Temps").Cells(row_num - 2, 10)
 T_sol_air_ds_NW_1=Worksheets("Sol-Air Temps").Cells(row_num - 1, 10)
 T_sol_air_ds_NW_0 = Worksheets("Sol-Air Temps").Cells(row_num, 10)
 T_sol_air_ds_N_4 = Worksheets("Sol-Air Temps").Cells(row_num - 4, 12)
 T_sol_air_ds_N_3 = Worksheets("Sol-Air Temps").Cells(row_num - 3, 12)
 T_sol_air_ds_N_2 = Worksheets("Sol-Air Temps").Cells(row_num - 2, 12)
 T_sol_air_ds_N_1 = Worksheets("Sol-Air Temps").Cells(row_num - 1, 12)
 T_sol_air_ds_N_0 = Worksheets("Sol-Air Temps").Cells(row_num, 12)
 T_sol_air_ds_NE_4 = Worksheets("Sol-Air Temps").Cells(row_num - 4, 14)
 T_sol_air_ds_NE_3 = Worksheets("Sol-Air Temps").Cells(row_num - 3, 14)
 T_sol_air_ds_NE_2 = Worksheets("Sol-Air Temps").Cells(row_num - 2, 14)
 T_sol_air_ds_NE_1 = Worksheets("Sol-Air Temps").Cells(row_num - 1, 14)
 T_sol_air_ds_NE_0 = Worksheets("Sol-Air Temps").Cells(row_num, 14)
 T_sol_air_ds_E_4 = Worksheets("Sol-Air Temps").Cells(row_num - 4, 16)
 T_sol_air_ds_E_3 = Worksheets("Sol-Air Temps").Cells(row_num - 3, 16)
 T_sol_air_ds_E_2 = Worksheets("Sol-Air Temps").Cells(row_num - 2, 16)
 T_sol_air_ds_E_1 = Worksheets("Sol-Air Temps").Cells(row_num - 1, 16)
 T_sol_air_ds_E_0 = Worksheets("Sol-Air Temps").Cells(row_num, 16)
 T_sol_air_ds_SE_4 = Worksheets("Sol-Air Temps").Cells(row_num - 4, 18)
 T_sol_air_ds_SE_3 = Worksheets("Sol-Air Temps").Cells(row_num - 3, 18)
 T_sol_air_ds_SE_2 = Worksheets("Sol-Air Temps").Cells(row_num - 2, 18)
 T_sol_air_ds_SE_1 = Worksheets("Sol-Air Temps").Cells(row_num - 1, 18)
 T_sol_air_ds_SE_0 = Worksheets("Sol-Air Temps").Cells(row_num, 18)

Prior Skin Load Values:

SL_roof_5 = Worksheets("TFCSL - Roof").Cells(row_num - 5, 2)
 SL_roof_4 = Worksheets("TFCSL - Roof").Cells(row_num - 4, 2)
 SL_roof_3 = Worksheets("TFCSL - Roof").Cells(row_num - 3, 2)
 SL_roof_2 = Worksheets("TFCSL - Roof").Cells(row_num - 2, 2)
 SL_roof_1 = Worksheets("TFCSL - Roof").Cells(row_num - 1, 2)
 SL_CW_S_3 = Worksheets("TFCSL - GACW").Cells(row_num - 3, 3)
 SL_CW_S_2 = Worksheets("TFCSL - GACW").Cells(row_num - 2, 3)
 SL_CW_S_1 = Worksheets("TFCSL - GACW").Cells(row_num - 1, 3)
 SL_CW_SW_3 = Worksheets("TFCSL - GACW").Cells(row_num - 3, 4)
 SL_CW_SW_2 = Worksheets("TFCSL - GACW").Cells(row_num - 2, 4)
 SL_CW_SW_1 = Worksheets("TFCSL - GACW").Cells(row_num - 1, 4)
 SL_CW_W_3 = Worksheets("TFCSL - GACW").Cells(row_num - 3, 5)

SL_CW_W_2 = Worksheets("TFCSL - GACW").Cells(row_num - 2, 5)
SL_CW_W_1 = Worksheets("TFCSL - GACW").Cells(row_num - 1, 5)
SL_CW_NW_3 = Worksheets("TFCSL - GACW").Cells(row_num - 3, 6)
SL_CW_NW_2 = Worksheets("TFCSL - GACW").Cells(row_num - 2, 6)
SL_CW_NW_1 = Worksheets("TFCSL - GACW").Cells(row_num - 1, 6)
SL_CW_N_3 = Worksheets("TFCSL - GACW").Cells(row_num - 3, 7)
SL_CW_N_2 = Worksheets("TFCSL - GACW").Cells(row_num - 2, 7)
SL_CW_N_1 = Worksheets("TFCSL - GACW").Cells(row_num - 1, 7)
SL_CW_NE_3 = Worksheets("TFCSL - GACW").Cells(row_num - 3, 8)
SL_CW_NE_2 = Worksheets("TFCSL - GACW").Cells(row_num - 2, 8)
SL_CW_NE_1 = Worksheets("TFCSL - GACW").Cells(row_num - 1, 8)
SL_CW_E_3 = Worksheets("TFCSL - GACW").Cells(row_num - 3, 9)
SL_CW_E_2 = Worksheets("TFCSL - GACW").Cells(row_num - 2, 9)
SL_CW_E_1 = Worksheets("TFCSL - GACW").Cells(row_num - 1, 9)
SL_CW_SE_3 = Worksheets("TFCSL - GACW").Cells(row_num - 3, 10)
SL_CW_SE_2 = Worksheets("TFCSL - GACW").Cells(row_num - 2, 10)
SL_CW_SE_1 = Worksheets("TFCSL - GACW").Cells(row_num - 1, 10)
SL_BW_S_4 = Worksheets("TFCSL - Brick").Cells(row_num - 4, 3)
SL_BW_S_3 = Worksheets("TFCSL - Brick").Cells(row_num - 3, 3)
SL_BW_S_2 = Worksheets("TFCSL - Brick").Cells(row_num - 2, 3)
SL_BW_S_1 = Worksheets("TFCSL - Brick").Cells(row_num - 1, 3)
SL_BW_SW_4 = Worksheets("TFCSL - Brick").Cells(row_num - 4, 4)
SL_BW_SW_3 = Worksheets("TFCSL - Brick").Cells(row_num - 3, 4)
SL_BW_SW_2 = Worksheets("TFCSL - Brick").Cells(row_num - 2, 4)
SL_BW_SW_1 = Worksheets("TFCSL - Brick").Cells(row_num - 1, 4)
SL_BW_W_4 = Worksheets("TFCSL - Brick").Cells(row_num - 4, 5)
SL_BW_W_3 = Worksheets("TFCSL - Brick").Cells(row_num - 3, 5)
SL_BW_W_2 = Worksheets("TFCSL - Brick").Cells(row_num - 2, 5)
SL_BW_W_1 = Worksheets("TFCSL - Brick").Cells(row_num - 1, 5)
SL_BW_NW_4 = Worksheets("TFCSL - Brick").Cells(row_num - 4, 6)
SL_BW_NW_3 = Worksheets("TFCSL - Brick").Cells(row_num - 3, 6)
SL_BW_NW_2 = Worksheets("TFCSL - Brick").Cells(row_num - 2, 6)
SL_BW_NW_1 = Worksheets("TFCSL - Brick").Cells(row_num - 1, 6)
SL_BW_N_4 = Worksheets("TFCSL - Brick").Cells(row_num - 4, 7)
SL_BW_N_3 = Worksheets("TFCSL - Brick").Cells(row_num - 3, 7)
SL_BW_N_2 = Worksheets("TFCSL - Brick").Cells(row_num - 2, 7)
SL_BW_N_1 = Worksheets("TFCSL - Brick").Cells(row_num - 1, 7)
SL_BW_NE_4 = Worksheets("TFCSL - Brick").Cells(row_num - 4, 8)
SL_BW_NE_3 = Worksheets("TFCSL - Brick").Cells(row_num - 3, 8)
SL_BW_NE_2 = Worksheets("TFCSL - Brick").Cells(row_num - 2, 8)
SL_BW_NE_1 = Worksheets("TFCSL - Brick").Cells(row_num - 1, 8)
SL_BW_E_4 = Worksheets("TFCSL - Brick").Cells(row_num - 4, 9)
SL_BW_E_3 = Worksheets("TFCSL - Brick").Cells(row_num - 3, 9)
SL_BW_E_2 = Worksheets("TFCSL - Brick").Cells(row_num - 2, 9)
SL_BW_E_1 = Worksheets("TFCSL - Brick").Cells(row_num - 1, 9)
SL_BW_SE_4 = Worksheets("TFCSL - Brick").Cells(row_num - 4, 10)

SL_BW_SE_3 = Worksheets("TFCSL - Brick").Cells(row_num - 3, 10)
 SL_BW_SE_2 = Worksheets("TFCSL - Brick").Cells(row_num - 2, 10)
 SL_BW_SE_1 = Worksheets("TFCSL - Brick").Cells(row_num - 1, 10)

'Skin Load Calculations:

SL_roof = Roof_area * ((bn_roof_5 * T_sol_air_roof_5 + _
 bn_roof_4 * T_sol_air_roof_4 + _
 bn_roof_3 * T_sol_air_roof_3 + _
 bn_roof_2 * T_sol_air_roof_2 + _
 bn_roof_1 * T_sol_air_roof_1 + _
 bn_roof_0 * T_sol_air_roof_0) - _
 (dn_roof_5 * SL_roof_5 / Roof_area + _
 dn_roof_4 * SL_roof_4 / Roof_area + _
 dn_roof_3 * SL_roof_3 / Roof_area + _
 dn_roof_2 * SL_roof_2 / Roof_area + _
 dn_roof_1 * SL_roof_1 / Roof_area) - _
 (T_zone * cn_roof))

SL_CW_S = CW_S * ((bn_cw_3 * T_sol_air_ls_S_3 + _
 bn_cw_2 * T_sol_air_ls_S_2 + _
 bn_cw_1 * T_sol_air_ls_S_1 + _
 bn_cw_0 * T_sol_air_ls_S_0) - _
 (dn_cw_3 * SL_CW_S_3 / CW_S + _
 dn_cw_2 * SL_CW_S_2 / CW_S + _
 dn_cw_1 * SL_CW_S_1 / CW_S) - _
 (T_zone * cn_cw))

SL_CW_SW = CW_SW * ((bn_cw_3 * T_sol_air_ls_SW_3 + _
 bn_cw_2 * T_sol_air_ls_SW_2 + _
 bn_cw_1 * T_sol_air_ls_SW_1 + _
 bn_cw_0 * T_sol_air_ls_SW_0) - _
 (dn_cw_3 * SL_CW_SW_3 / CW_SW + _
 dn_cw_2 * SL_CW_SW_2 / CW_SW + _
 dn_cw_1 * SL_CW_SW_1 / CW_SW) - _
 (T_zone * cn_cw))

SL_CW_W = CW_W * ((bn_cw_3 * T_sol_air_ls_W_3 + _
 bn_cw_2 * T_sol_air_ls_W_2 + _
 bn_cw_1 * T_sol_air_ls_W_1 + _
 bn_cw_0 * T_sol_air_ls_W_0) - _
 (dn_cw_3 * SL_CW_W_3 / CW_W + _
 dn_cw_2 * SL_CW_W_2 / CW_W + _
 dn_cw_1 * SL_CW_W_1 / CW_W) - _
 (T_zone * cn_cw))

SL_CW_NW = CW_NW * ((bn_cw_3 * T_sol_air_ls_NW_3 + _
 bn_cw_2 * T_sol_air_ls_NW_2 + _
 bn_cw_1 * T_sol_air_ls_NW_1 + _
 bn_cw_0 * T_sol_air_ls_NW_0) - _
 (dn_cw_3 * SL_CW_NW_3 / CW_NW + _

$$\begin{aligned}
& \text{dn_cw_2} * \text{SL_CW_NW_2} / \text{CW_NW} + _ \\
& \text{dn_cw_1} * \text{SL_CW_NW_1} / \text{CW_NW}) - _ \\
& (\text{T_zone} * \text{cn_cw})) \\
\text{SL_CW_N} = & \text{CW_N} * ((\text{bn_cw_3} * \text{T_sol_air_ls_N_3} + _ \\
& \text{bn_cw_2} * \text{T_sol_air_ls_N_2} + _ \\
& \text{bn_cw_1} * \text{T_sol_air_ls_N_1} + _ \\
& \text{bn_cw_0} * \text{T_sol_air_ls_N_0}) - _ \\
& (\text{dn_cw_3} * \text{SL_CW_N_3} / \text{CW_N} + _ \\
& \text{dn_cw_2} * \text{SL_CW_N_2} / \text{CW_N} + _ \\
& \text{dn_cw_1} * \text{SL_CW_N_1} / \text{CW_N}) - _ \\
& (\text{T_zone} * \text{cn_cw})) \\
\text{SL_CW_NE} = & \text{CW_NE} * ((\text{bn_cw_3} * \text{T_sol_air_ls_NE_3} + _ \\
& \text{bn_cw_2} * \text{T_sol_air_ls_NE_2} + _ \\
& \text{bn_cw_1} * \text{T_sol_air_ls_NE_1} + _ \\
& \text{bn_cw_0} * \text{T_sol_air_ls_NE_0}) - _ \\
& (\text{dn_cw_3} * \text{SL_CW_NE_3} / \text{CW_NE} + _ \\
& \text{dn_cw_2} * \text{SL_CW_NE_2} / \text{CW_NE} + _ \\
& \text{dn_cw_1} * \text{SL_CW_NE_1} / \text{CW_NE}) - _ \\
& (\text{T_zone} * \text{cn_cw})) \\
\text{SL_CW_E} = & \text{CW_E} * ((\text{bn_cw_3} * \text{T_sol_air_ls_E_3} + _ \\
& \text{bn_cw_2} * \text{T_sol_air_ls_E_2} + _ \\
& \text{bn_cw_1} * \text{T_sol_air_ls_E_1} + _ \\
& \text{bn_cw_0} * \text{T_sol_air_ls_E_0}) - _ \\
& (\text{dn_cw_3} * \text{SL_CW_E_3} / \text{CW_E} + _ \\
& \text{dn_cw_2} * \text{SL_CW_E_2} / \text{CW_E} + _ \\
& \text{dn_cw_1} * \text{SL_CW_E_1} / \text{CW_E}) - _ \\
& (\text{T_zone} * \text{cn_cw})) \\
\text{SL_CW_SE} = & \text{CW_SE} * ((\text{bn_cw_3} * \text{T_sol_air_ls_SE_3} + _ \\
& \text{bn_cw_2} * \text{T_sol_air_ls_SE_2} + _ \\
& \text{bn_cw_1} * \text{T_sol_air_ls_SE_1} + _ \\
& \text{bn_cw_0} * \text{T_sol_air_ls_SE_0}) - _ \\
& (\text{dn_cw_3} * \text{SL_CW_SE_3} / \text{CW_SE} + _ \\
& \text{dn_cw_2} * \text{SL_CW_SE_2} / \text{CW_SE} + _ \\
& \text{dn_cw_1} * \text{SL_CW_SE_1} / \text{CW_SE}) - _ \\
& (\text{T_zone} * \text{cn_cw})) \\
\text{SL_BW_S} = & \text{BW_S} * ((\text{bn_brick_4} * \text{T_sol_air_ds_S_4} + _ \\
& \text{bn_brick_3} * \text{T_sol_air_ds_S_3} + _ \\
& \text{bn_brick_2} * \text{T_sol_air_ds_S_2} + _ \\
& \text{bn_brick_1} * \text{T_sol_air_ds_S_1} + _ \\
& \text{bn_brick_0} * \text{T_sol_air_ds_S_0}) - _ \\
& (\text{dn_brick_4} * \text{SL_BW_S_4} / \text{BW_S} + _ \\
& \text{dn_brick_3} * \text{SL_BW_S_3} / \text{BW_S} + _ \\
& \text{dn_brick_2} * \text{SL_BW_S_2} / \text{BW_S} + _ \\
& \text{dn_brick_1} * \text{SL_BW_S_1} / \text{BW_S}) - _ \\
& (\text{T_zone} * \text{cn_brick})) \\
\text{SL_BW_SW} = & \text{BW_SW} * ((\text{bn_brick_4} * \text{T_sol_air_ds_SW_4} + _
\end{aligned}$$

$$\begin{aligned}
& \text{bn_brick_3} * T_{\text{sol_air_ds_SW_3}} + _ \\
& \text{bn_brick_2} * T_{\text{sol_air_ds_SW_2}} + _ \\
& \text{bn_brick_1} * T_{\text{sol_air_ds_SW_1}} + _ \\
& \text{bn_brick_0} * T_{\text{sol_air_ds_SW_0}}) - _ \\
& (\text{dn_brick_4} * \text{SL_BW_SW_4} / \text{BW_SW} + _ \\
& \text{dn_brick_3} * \text{SL_BW_SW_3} / \text{BW_SW} + _ \\
& \text{dn_brick_2} * \text{SL_BW_SW_2} / \text{BW_SW} + _ \\
& \text{dn_brick_1} * \text{SL_BW_SW_1} / \text{BW_SW}) - _ \\
& (T_{\text{zone}} * \text{cn_brick}) \\
\text{SL_BW_W} = & \text{BW_W} * ((\text{bn_brick_4} * T_{\text{sol_air_ds_W_4}} + _ \\
& \text{bn_brick_3} * T_{\text{sol_air_ds_W_3}} + _ \\
& \text{bn_brick_2} * T_{\text{sol_air_ds_W_2}} + _ \\
& \text{bn_brick_1} * T_{\text{sol_air_ds_W_1}} + _ \\
& \text{bn_brick_0} * T_{\text{sol_air_ds_W_0}}) - _ \\
& (\text{dn_brick_4} * \text{SL_BW_W_4} / \text{BW_W} + _ \\
& \text{dn_brick_3} * \text{SL_BW_W_3} / \text{BW_W} + _ \\
& \text{dn_brick_2} * \text{SL_BW_W_2} / \text{BW_W} + _ \\
& \text{dn_brick_1} * \text{SL_BW_W_1} / \text{BW_W}) - _ \\
& (T_{\text{zone}} * \text{cn_brick}) \\
\text{SL_BW_NW} = & \text{BW_NW} * ((\text{bn_brick_4} * T_{\text{sol_air_ds_NW_4}} + _ \\
& \text{bn_brick_3} * T_{\text{sol_air_ds_NW_3}} + _ \\
& \text{bn_brick_2} * T_{\text{sol_air_ds_NW_2}} + _ \\
& \text{bn_brick_1} * T_{\text{sol_air_ds_NW_1}} + _ \\
& \text{bn_brick_0} * T_{\text{sol_air_ds_NW_0}}) - _ \\
& (\text{dn_brick_4} * \text{SL_BW_NW_4} / \text{BW_W} + _ \\
& \text{dn_brick_3} * \text{SL_BW_NW_3} / \text{BW_NW} + _ \\
& \text{dn_brick_2} * \text{SL_BW_NW_2} / \text{BW_NW} + _ \\
& \text{dn_brick_1} * \text{SL_BW_NW_1} / \text{BW_NW}) - _ \\
& (T_{\text{zone}} * \text{cn_brick}) \\
\text{SL_BW_N} = & \text{BW_N} * ((\text{bn_brick_4} * T_{\text{sol_air_ds_N_4}} + _ \\
& \text{bn_brick_3} * T_{\text{sol_air_ds_N_3}} + _ \\
& \text{bn_brick_2} * T_{\text{sol_air_ds_N_2}} + _ \\
& \text{bn_brick_1} * T_{\text{sol_air_ds_N_1}} + _ \\
& \text{bn_brick_0} * T_{\text{sol_air_ds_N_0}}) - _ \\
& (\text{dn_brick_4} * \text{SL_BW_N_4} / \text{BW_N} + _ \\
& \text{dn_brick_3} * \text{SL_BW_N_3} / \text{BW_N} + _ \\
& \text{dn_brick_2} * \text{SL_BW_N_2} / \text{BW_N} + _ \\
& \text{dn_brick_1} * \text{SL_BW_N_1} / \text{BW_N}) - _ \\
& (T_{\text{zone}} * \text{cn_brick}) \\
\text{SL_BW_NE} = & \text{BW_NE} * ((\text{bn_brick_4} * T_{\text{sol_air_ds_NE_4}} + _ \\
& \text{bn_brick_3} * T_{\text{sol_air_ds_NE_3}} + _ \\
& \text{bn_brick_2} * T_{\text{sol_air_ds_NE_2}} + _ \\
& \text{bn_brick_1} * T_{\text{sol_air_ds_NE_1}} + _ \\
& \text{bn_brick_0} * T_{\text{sol_air_ds_NE_0}}) - _ \\
& (\text{dn_brick_4} * \text{SL_BW_NE_4} / \text{BW_NE} + _ \\
& \text{dn_brick_3} * \text{SL_BW_NE_3} / \text{BW_NE} + _
\end{aligned}$$

```

dn_brick_2 * SL_BW_NE_2 / BW_NE + _
dn_brick_1 * SL_BW_NE_1 / BW_NE) - _
(T_zone * cn_brick))
SL_BW_E = BW_E * ((bn_brick_4 * T_sol_air_ds_E_4 + _
bn_brick_3 * T_sol_air_ds_E_3 + _
bn_brick_2 * T_sol_air_ds_E_2 + _
bn_brick_1 * T_sol_air_ds_E_1 + _
bn_brick_0 * T_sol_air_ds_E_0) - _
(dn_brick_4 * SL_BW_E_4 / BW_E + _
dn_brick_3 * SL_BW_E_3 / BW_E + _
dn_brick_2 * SL_BW_E_2 / BW_E + _
dn_brick_1 * SL_BW_E_1 / BW_E) - _
(T_zone * cn_brick))
SL_BW_SE = BW_SE * ((bn_brick_4 * T_sol_air_ds_SE_4 + _
bn_brick_3 * T_sol_air_ds_SE_3 + _
bn_brick_2 * T_sol_air_ds_SE_2 + _
bn_brick_1 * T_sol_air_ds_SE_1 + _
bn_brick_0 * T_sol_air_ds_SE_0) - _
(dn_brick_4 * SL_BW_SE_4 / BW_SE + _
dn_brick_3 * SL_BW_SE_3 / BW_SE + _
dn_brick_2 * SL_BW_SE_2 / BW_SE + _
dn_brick_1 * SL_BW_SE_1 / BW_SE) - _
(T_zone * cn_brick))

Skin_Load_CW = SL_CW_S + SL_CW_SW + SL_CW_W + _
SL_CW_NW + SL_CW_N + SL_CW_NE + SL_CW_E + _
SL_CW_SE
Skin_Load_BW = SL_BW_S + SL_BW_SW + SL_BW_W + _
SL_BW_NW + SL_BW_N + SL_BW_NE + SL_BW_E + _
SL_BW_SE

Conduction_Skin_Load = SL_roof + Skin_Load_CW + Skin_Load_BW

Worksheets("TFCSL - Roof").Cells(row_num + 1, 2).Value = SL_roof
Worksheets("TFCSL - GACW").Cells(row_num + 1, 3).Value = SL_CW_S
Worksheets("TFCSL - GACW").Cells(row_num + 1, 4).Value = _
SL_CW_SW
Worksheets("TFCSL - GACW").Cells(row_num + 1, 5).Value = SL_CW_W
Worksheets("TFCSL - GACW").Cells(row_num + 1, 6).Value = _
SL_CW_NW
Worksheets("TFCSL - GACW").Cells(row_num + 1, 7).Value = SL_CW_N
Worksheets("TFCSL - GACW").Cells(row_num + 1, 8).Value = _
SL_CW_NE
Worksheets("TFCSL - GACW").Cells(row_num + 1, 9).Value = SL_CW_E
Worksheets("TFCSL - GACW").Cells(row_num + 1, 10).Value = _
SL_CW_SE

```

```
Worksheets("TFCSL - Brick").Cells(row_num + 1, 3).Value = SL_BW_S
Worksheets("TFCSL - Brick").Cells(row_num + 1, 4).Value = SL_BW_SW
Worksheets("TFCSL - Brick").Cells(row_num + 1, 5).Value = SL_BW_W
Worksheets("TFCSL - Brick").Cells(row_num + 1, 6).Value = SL_BW_NW
Worksheets("TFCSL - Brick").Cells(row_num + 1, 7).Value = SL_BW_N
Worksheets("TFCSL - Brick").Cells(row_num + 1, 8).Value = SL_BW_NE
Worksheets("TFCSL - Brick").Cells(row_num + 1, 9).Value = SL_BW_E
Worksheets("TFCSL - Brick").Cells(row_num + 1, 10).Value = SL_BW_SE
```

```
Worksheets("Comparison").Cells(1, 3).Value = "Roof"
Worksheets("Comparison").Cells(1, 5).Value = "CW"
Worksheets("Comparison").Cells(1, 4).Value = "BW"
Worksheets("Comparison").Cells(1, 7).Value = "Transfer Function"
```

```
Worksheets("Comparison").Cells(row_num + 1, 6).Value = SL_roof
Worksheets("Comparison").Cells(row_num + 1, 7).Value = Skin_Load_CW
Worksheets("Comparison").Cells(row_num + 1, 8).Value = Skin_Load_BW
Worksheets("Comparison").Cells(row_num + 1, 9).Value = _
Conduction_Skin_Load
```

```
Next ToD_hrs
Next days
End Sub
```

APPENDIX H: Electrical Loads Code

Sub Calc_Electrical_Loads()

Dim fd(12), ld(12)

```
fd(1) = 1           'January
ld(1) = fd(1) + 30
fd(2) = ld(1) + 1  'February
ld(2) = fd(2) + 28
fd(3) = ld(2) + 1  'March
ld(3) = fd(3) + 30
fd(4) = ld(3) + 1  'April
ld(4) = fd(4) + 29
fd(5) = ld(4) + 1  'May
ld(5) = fd(5) + 30
fd(6) = ld(5) + 1  'June
ld(6) = fd(6) + 29
fd(7) = ld(6) + 1  'July
ld(7) = fd(7) + 30
fd(8) = ld(7) + 1  'August
ld(8) = fd(8) + 30
fd(9) = ld(8) + 1  'September
ld(9) = fd(9) + 29
fd(10) = ld(9) + 1 'October
ld(10) = fd(10) + 30
fd(11) = ld(10) + 1 'November
ld(11) = fd(11) + 29
fd(12) = ld(11) + 1 'December
ld(12) = fd(12) + 30
```

row_num = 1

For days = fd(1) To ld(12)

For ToD_2hrs = 1 To 48

ToD = (ToD_2hrs - 1) / 2

'Electrical:

Power_and_Lights = Worksheets("Electrical").Cells(row_num + 1, 2)

Emerg_Power_and_Lights = Worksheets("Electrical").Cells(row_num + 1, 3)

Bus_A = Worksheets("Electrical").Cells(row_num + 1, 4)

Bus_B = Worksheets("Electrical").Cells(row_num + 1, 5)

Electrical_Load = Bus_A + Bus_B

Building_Load = (Power_and_Lights + Emerg_Power_and_Lights) / 100

row_num = row_num + 1

'Column Headings:

Worksheets("Electrical").Cells(1, 6).Value = "Electrical Load (kW)"

Worksheets("Electrical").Cells(1, 7).Value = "Building Load (kW)"

'Load Values to fill in Columns:

Worksheets("Electrical").Cells(row_num, 6).Value = Electrical_Load

Worksheets("Electrical").Cells(row_num, 7).Value = Building_Load

Next ToD_2hrs

Next days

End Sub

APPENDIX I: Metasys Sensor Identification Numbers

Chilled Water:

B153.NAE-6.T1.P1132.DX14 (CHW).BLDG-F.Trend (gpm)
B153.NAE-6.T1.P1132.DX14 (CHW).CHWR-T.Trend (deg F)
B153.NAE-6.T1.P1132.DX14 (CHW).CHWS-T.Trend (deg F)
B153.NAE-6.T1.P1132.DX14 (CHW).BCHWR-P.Trend (psi)
B153.NAE-6.T1.P1132.DX14 (CHW).BCHWS-P.Trend (psi)

Hot Water / Steam / Condensate:

B153.NAE-6.T1.P1132.DX16 (HW).HWS-T.Trend (deg F)
B153.NAE-6.T1.P1132.DX16 (HW).HWR-T.Trend (deg F)
B153.NAE-6.T1.P1132.DX16 (HW).STM-P.Trend (psi)
B153.NAE-6.T1.P1132.DX14 (CHW).COND-F.Present Value.Trend (Gal)

Outside Air Conditions:

B153.NAE-5.T2.R4302.DX52 (AHU-1&2).OA-T.Trend (deg F)
B153.NAE-5.T2.R4302.DX52 (AHU-1&2).OA-CO2.Trend (ppm)
B153.NAE-5.T2.R4302.DX52 (AHU-1&2).OA-H.Trend (%RH)

Return Air Conditions:

B153.NAE-5.T2.R4302.DX52 (AHU-1&2).RA-H.Trend (%RH)
B153.NAE-5.T2.R4302.DX52 (AHU-1&2).RA-T.Trend (deg F)
B153.NAE-5.T2.R4302.DX52 (AHU-1&2).RA-CO2.Trend (ppm)
B153.NAE-5.T2.R4302.DX54 (AHU-3).RA-T.Trend (deg F)
B153.NAE-5.T2.R4302.DX54 (AHU-3).RA-H.Trend (%RH)
B153.NAE-5.T2.R4302.DX54 (AHU-3).RA-CO2.Trend (ppm)
B153.NAE-6.T2.R3450.DX145 (AHU-4).RA-T.Trend (deg F)
B153.NAE-6.T2.R3450.DX145 (AHU-4).RA-H.Trend (%RH)
B153.NAE-6.T2.R3450.DX145 (AHU-4).RA-CO2.Trend (ppm)

Mixed Air Conditions:

B153.NAE-5.T2.R4302.DX52 (AHU-1&2).SF1-MAT.Trend (deg F)
B153.NAE-5.T2.R4302.DX52 (AHU-1&2).SF2-MAT.Trend (deg F)
B153.NAE-6.T2.R3450.DX145 (AHU-4).MA-T.Trend (deg F)

Static Pressure:

B153.NAE-5.T2.R4302.DX52 (AHU-1&2).SA-SP.Trend (in wc)
B153.NAE-6.T2.R3450.DX145 (AHU-4).SA-SP.Trend (in wc)

Fan Frequency:

B153.NAE-5.T2.R4302.VND200 (AHU-1 VFD).FREQ.Trend (Hz)
B153.NAE-5.T2.R4302.VND201 (AHU-2 VFD).FREQ.Trend (Hz)
B153.NAE-6.T2.R3450.VND204 (AHU-4 SF VFD).FREQ.Trend (Hz)

Electrical:

B153.NAE-5.T1.P1305.VND97 (BLDL-PWR).POWER.Trend (W)
B153.NAE-5.T1.P1305.VND97 (BLDL-PWR).PWR-DEM.Trend (W)
B153.NAE-5.T1.P1305.VND97 (BLDL-PWR).ENERGY.Trend (Wh)
B153.NAE-5.T1.R4301.VND99 (EMRL1PWR).POWER.Trend (W)
B153.NAE-5.T1.R4301.VND99 (EMRL1PWR).PWR-DEM.Trend (W)
B153.NAE-5.T1.R4301.VND99 (EMRL1PWR).ENERGY.Trend (Wh)
B153.NAE-5.T1.P1305.VND102 (SWBD-A).POWER.Trend (kW)
B153.NAE-5.T1.P1305.VND102 (SWBD-A).PWR-DEM.Trend (kW)
B153.NAE-5.T1.P1305.VND102 (SWBD-A).ENERGY.Trend (kWh)
B153.NAE-5.T1.P1305.VND102 (SWBD-B).POWER.Trend (kW)
B153.NAE-5.T1.P1305.VND102 (SWBD-B).PWR-DEM.Trend (kW)
B153.NAE-5.T1.P1305.VND102 (SWBD-B).ENERGY.Trend (kWh)

APPENDIX J: UGA Weather Data

COLUMN #	FIELD DESCRIPTION	UNITS
1	Site Id	-
2	Year	-
3	Julian day of the year	-
4	time of day	-
5	Julian day of the year+hour/2400	-
6	Air Temperature	°C
7	Humidity	%
8	Dewpoint	°C
9	Vapor Pressure	kPa
10	Vapor Pressure Deficit	kPa
11	Barometric Pressure	kPa
12	Wind Speed	m/s
13	Wind Direction	0°-360°
14	Standard Deviation	0°-360°
15	Maximum wind speed	m/s
16	Time of maximum wind speed	-
17	Soil Temperature 2cm	°C
18	Soil Temperature 5cm	°C
19	Soil Temperature 10cm	°C
20	Soil Temperature 20cm	°C
21	Soil Temperature A (Duluth, Nahunta)	°C
22	Soil Temperature B (Duluth, Nahunta)	°C
23	Soil Moisture	%
24	Pan	mm
25	Evap	n/a
26	Water Temperature(Floyd County Only)	°C
27	Solar Radiation	W/m ²
28	Total Solar Radiation	KJ/m ²
29	Par	umole/(m ² *s)
30	Total Par	Einstein/m ²
31	Net Radiation	W/m ²
32	Total Net Radiation	KJ/m ²

COLUMN #	FIELD DESCRIPTION	UNITS
33	Rainfall	mm
34	Rainfall #2	mm
35	Max Rainfall	mm
36	Time of Max Rainfall	-
37	Max Rainfall #2	mm
38	Time Max Rainfall #2	-
39	Leaf Wetness	-
40	Wetness Frequency	%

APPENDIX K: Creating a Mock-TMY Data File

The information provided in this appendix was used to create the mock-TMY file used in this research. The knowledge acquired to create this file was found through the National Renewable Energy Laboratory's (NREL) Renewable Resource Data Center (RReDC), (NREL, 2008).

A TMY file contains one year of hourly solar radiation, illuminance, and meteorological data. Each hourly record not only contains the solar radiation, illuminance, or meteorological value, but also a two-character source and uncertainty flag which indicates whether the data value was measured, modeled, or missing, and to provide an estimated uncertainty. The mock-TMY file used for this research was created in Microsoft Excel, converted to a text file (.txt) and then, finally, converted to a binary (.bin) file.

The first line of the TMY file is known as the file header. This line describes the location of the weather station. The positioning of all of the numbers, letters, and symbols is very important for the entire TMY file, in particular this header section. The station's Weather Bureau Army Navy (WBAN) number is predetermined. For example, Atlanta, Georgia is number 13874. This five digit number is placed in field positions 002-006 of the file header. Next, the name of the city (e.g. Atlanta) is placed in positions 008-029, followed by the two letter state abbreviation (e.g. GA) in positions 031-032. Then the time zone number which is determined by the number of hours which the local standard time is ahead of or behind the Universal Time is in positions 034-036. Next is the latitude location of the weather station in positions 038-044 with 038 as either "N" or

“S” (North or South of the equator), 040-041 is the degrees and 043-044 is the minutes. Similarly, the longitude of the weather station is in positions 046-053 with 046 as either “W” or “E” (West or East), 048-050 is the degrees, and 052-053 is the minutes. Finally, elevation of the station (in meter above sea level) is the last part of the header in positions 056-059.

Following the file header are 8760 rows of hourly data records are provided for solar radiation, illuminance, and meteorological data, along with their source and uncertainty flags. Unfortunately, the TMY files do not account for leap years, and therefore February 29th must be removed. Each line begins with the year (position 002-003), followed by the month (004-005), day (006-007), and hour (008-009). After filing in these known values are the radiation, illuminance, zenith luminance, sky cover, temperature, humidity, pressure, wind, visibility, ceiling height, present weather, precipitable water, aerosol optical depth, and snow data, respectively.

The radiation data is placed into positions 010-035. In positions 010-013 is the extraterrestrial horizontal radiation which is the amount of solar radiation (0-1415) in Wh/m^2 received on a horizontal surface at the top of the atmosphere during the 60 minutes preceding the hour indicated. Then, in positions 014-017 is the extraterrestrial direct normal radiation which is the amount of solar radiation (0-1415) in Wh/m^2 received on a surface normal to the sun at the top of the atmosphere during the 60 minutes preceding the hour indicated. Next, in positions 018-023 is the global horizontal radiation which is the amount of direct and diffuse solar radiation (0-1200) in Wh/m^2 received on a horizontal surface during the 60 minutes preceding the hour indicated, while position 022 is the flag for data source (A-H, ?), and position 023 is the flag for

data uncertainty (0-9). This is followed by the direct normal radiation in positions 024-029 which is the amount of solar radiation (0-1100) in Wh/m^2 received within a 5.7° field of view centered on the sun during the 60 minutes preceding the hour indicated, while position 028 is the flag for data source (A-H, ?), and position 029 is the flag for data uncertainty (0-9). And, finally, in positions 030-035 is the diffuse horizontal radiation which is the amount of solar radiation (0-700) in Wh/m^2 received from the sky (excluding the solar disk) on a horizontal surface during the 60 minutes preceding the hour indicated, while position 034 is the flag for data source (A-H, ?), and position 035 is the flag for data uncertainty (0-9).

Next, the illuminance data is placed into positions 036-053. In positions 036-041 is the global horizontal illuminance which is the average total amount of direct and diffuse illuminance in hundreds of lux (0 to 1300 = 0 to 130,000 lux) received on a horizontal surface during the 60 minutes preceding the hour indicated, while position 040 is the flag for data source (I, ?), and position 041 is the flag for data uncertainty (0-9). Next, in positions 042-047 is the direct normal illuminance which is the average amount of direct normal illuminance in hundreds of lux (0 to 1100 = 0 to 110,000 lux) received within a 5.7° field of view centered on the sun during the 60 minutes preceding the hour indicated, while position 046 is the flag for data source (I, ?), and position 047 is the flag for data uncertainty (0-9). And, finally, in position 048-053 is the diffuse horizontal illuminance which is the average amount of illuminance in hundreds of lux (0 to 800 = 0 to 80,000 lux) received from the sky (excluding the solar disk) on a horizontal surface during the 60 minutes preceding the hour indicated, while position 052 is the flag for data source (I, ?), and position 053 is the flag for data uncertainty (0-9).

The zenith luminance is then in positions 054-059 which is the average amount of luminance at the sky's zenith in tens of Cd/m^2 (0 to 7,000 = 0 to 70, 000 Cd/m^2) during the 60 minutes preceding the hour indicated, while position 058 is the flag for data source (I, ?), and position 059 is the flag for data uncertainty (0-9).

Next, the sky cover data is placed in positions 060-067. In positions 060-063 is the total sky cover which is the amount of sky dome in tenths (0-10) covered by clouds or obscuring phenomena at the hour indicated, with position 062 as the flag for data source (A-F), and position 063 as the flag for data uncertainty (0-9). Next, in positions 064-067 is the opaque sky cover which is the amount of sky dome in tenths (0-10) covered by clouds or obscuring phenomena that prevent observing the sky or higher cloud layers as the hour indicated, with position 066 as the flag for data source (A-F), and position 067 as the flag for data uncertainty (0-9).

Next, temperature data is placed in positions 068-079. In positions 068-073 is dry bulb temperature in tenths of $^{\circ}\text{C}$ (-500 to 500 = -50.0 to 50.0 $^{\circ}\text{C}$) at the hour indicated, followed by the flag for data source (A-F) in position 072, and the flag for data uncertainty (0-9) in position 073. Then, in positions 074-079 is dew point temperature in tenths of $^{\circ}\text{C}$ (-600 to 300 = -60.0 to 30.0 $^{\circ}\text{C}$) at the hour indicated, followed by the flag for data source (A-F) in position 078, and the flag for data uncertainty (0-9) in position 079.

The percent relative humidity data (0-100) is then in positions 080-082 with the flag for data source (A-F) in position 083 and the flag for data uncertainty (0-9) in position 084. This is then followed by the atmospheric pressure in millibars (700-1100)

in positions 085-088 with the flag for data source (A-F) in position 089 and the flag for data uncertainty (0-9) in position 090.

Next, the wind data is placed in positions 091-100. In positions 091-095 is the wind direction in degrees (0-360) at the hour indicated where 0° (or 360°) is North, 90° is East, 180° is South, and 270° is West, with position 094 as the flag for the data source (A-F), and position 095 as the flag for data uncertainty (0-9). Next, in positions 096-100 is the wind speed in tenths of meters per second (0 to 400 = 0 to 40.0 m/s) with position 099 as the flag for the data source (A-F), and position 100 as the flag for data uncertainty (0-9).

Next, the visibility data is in positions 101-104 which is the horizontal visibility in tenths of kilometers (0 to 1609 = 0.0 to 160.9 km) with 7777 = unlimited visibility and 9999 = missing data, also position 105 is the flag for data source (A-F, ?), and position 106 is the flag for data uncertainty (0-9).

Then, the ceiling height is in positions 107-111 which is the ceiling height in meters (0-30450) at the hour indicated with 77777 = unlimited ceiling height, 88888 = cirroform, and 99999 = missing data, also position 112 is the flag for data source (A-F, ?), and position 113 is the flag for data uncertainty (0-9).

A 10-digit present weather condition code is then placed in positions 114-123. This is followed by precipitable water in millimeters (0-100) at the hour indicated in positions 124-126 with position 127 as the flag for data source (A-F), and position 128 as the flag for data uncertainty (0-9). Next, the aerosol optical depth is placed in positions 129-133 where the broadband aerosol optical depth (broad-band turbidity) in thousandths

(0-240) fills positions 129-131, the flag for data source (A-F) is position 132, and the flag for data uncertainty (0-9) is position 133.

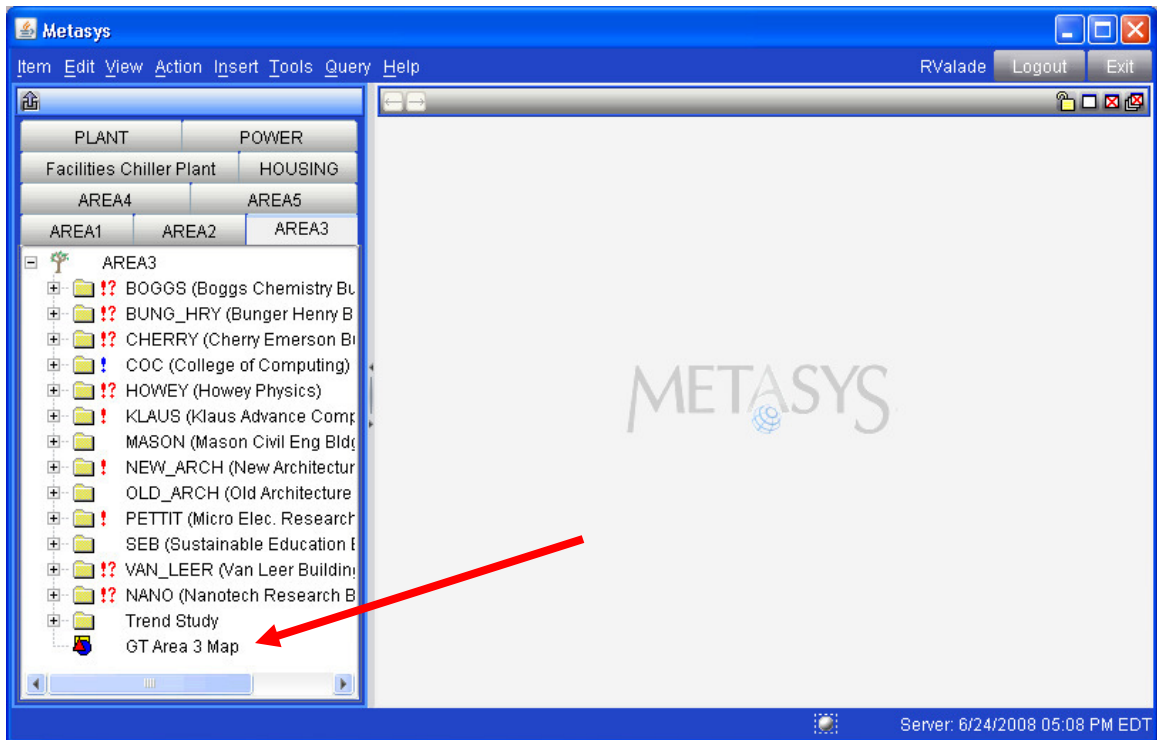
Finally, the last data to add are the snow values in positions 134-142. In positions 134-136 are the snow depth values (0-150) in centimeters on the day indicated with position 137 as the flag for data source (A-F, ?) and position 138 as the flag for data uncertainty (0-9). Last are the days since last snowfall (0-88) where 88 = 88 or more days since the last snow fall in positions 139-140 with position 141 as the flag for data source (A-F, ?) and position 142 as the flag for data uncertainty (0-9).

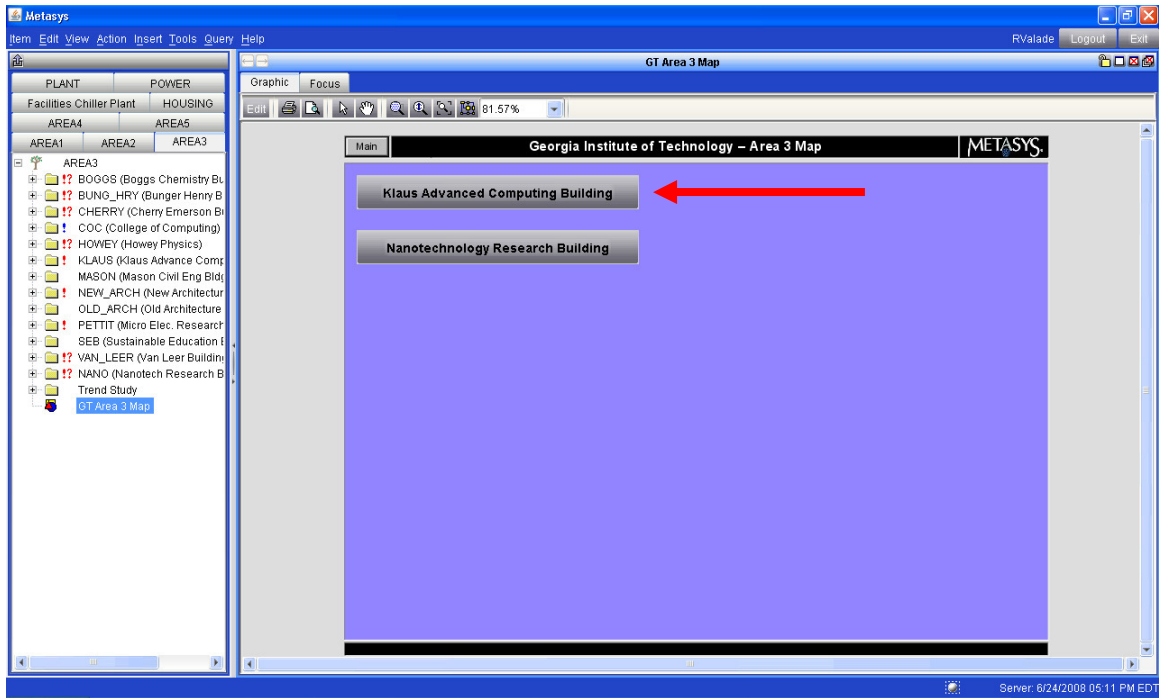
As a side note, any time data is missing, the data positions are filled with 9's, the data source positions are filled with ?'s and the flag for data uncertainties positions are filled with 0's.

After the header file and the 142 positions for 8760 hours had been filled in on the Excel spreadsheet, they were transferred to a text document (.txt) before being converted to a binary document (.bin) which is the necessary weather file format for the DOE-2 and eQUEST computer simulation programs.

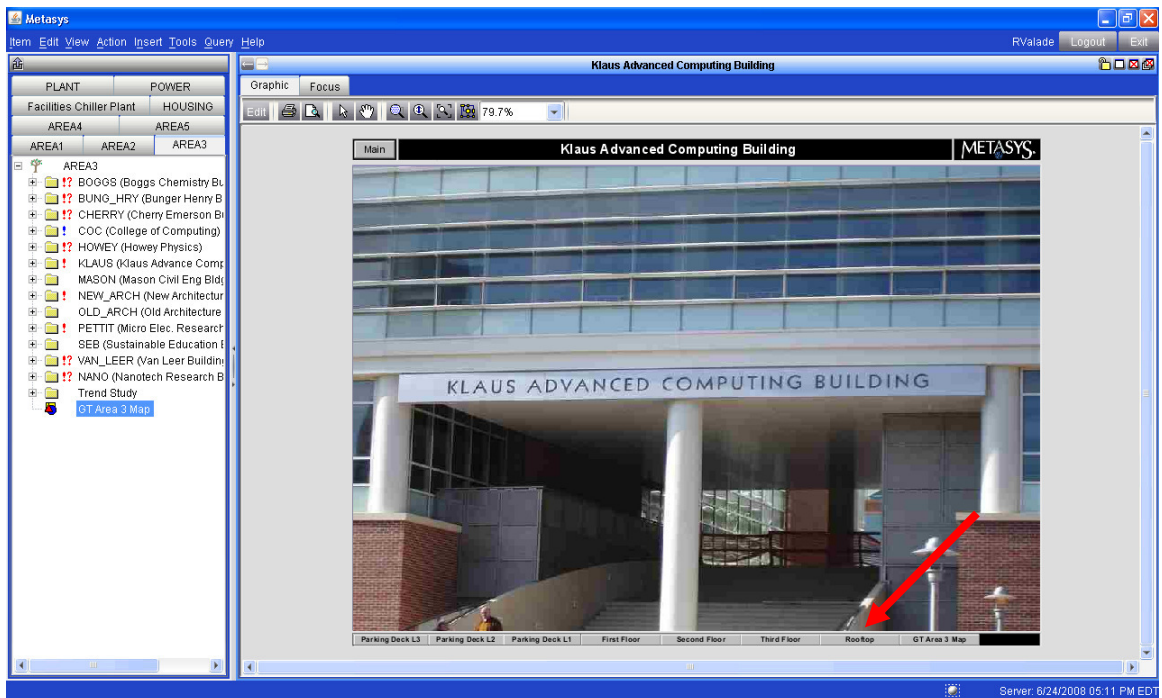
APPENDIX L: Directions for Metasys Data Collection

In order to retrieve collected data from JCI's Metasys program, one either needs to be logged on to a Facilities Department computer or virtually connect through the GT Controls Network before even logging onto Metasys. After in the Metasys program, one must choose the area of campus the building of interest is located in before choosing the building. For the KACB, one must choose "GT Area 3 Map" and then "Klaus Advanced Computing Building" as illustrated below.

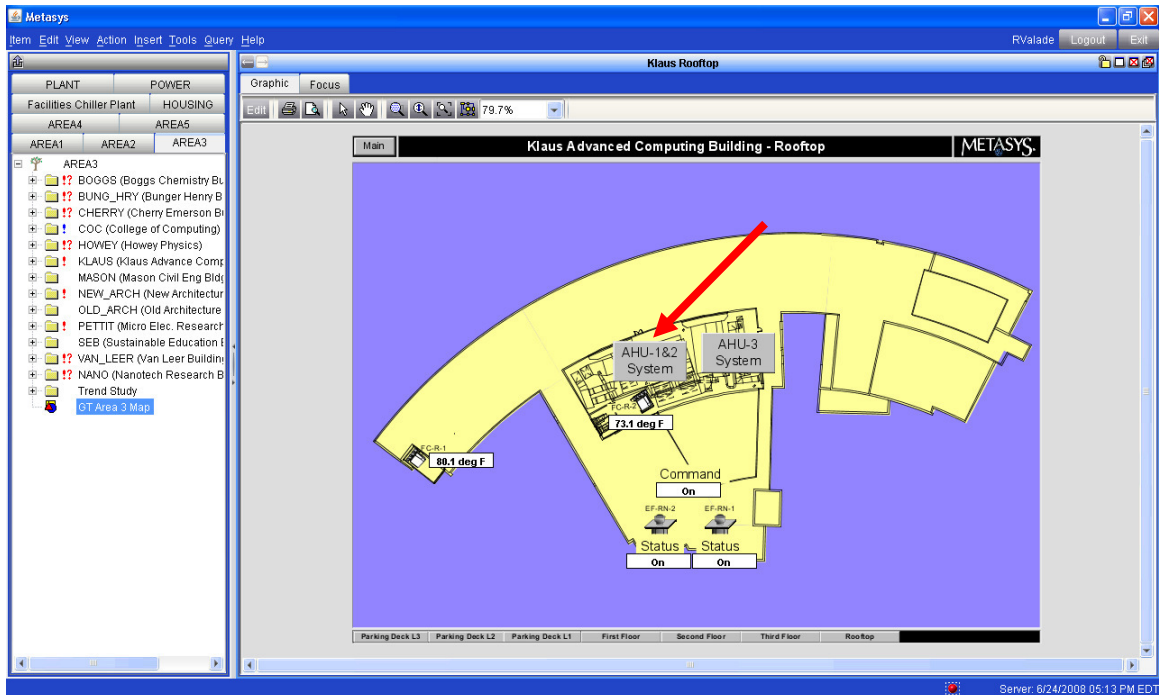




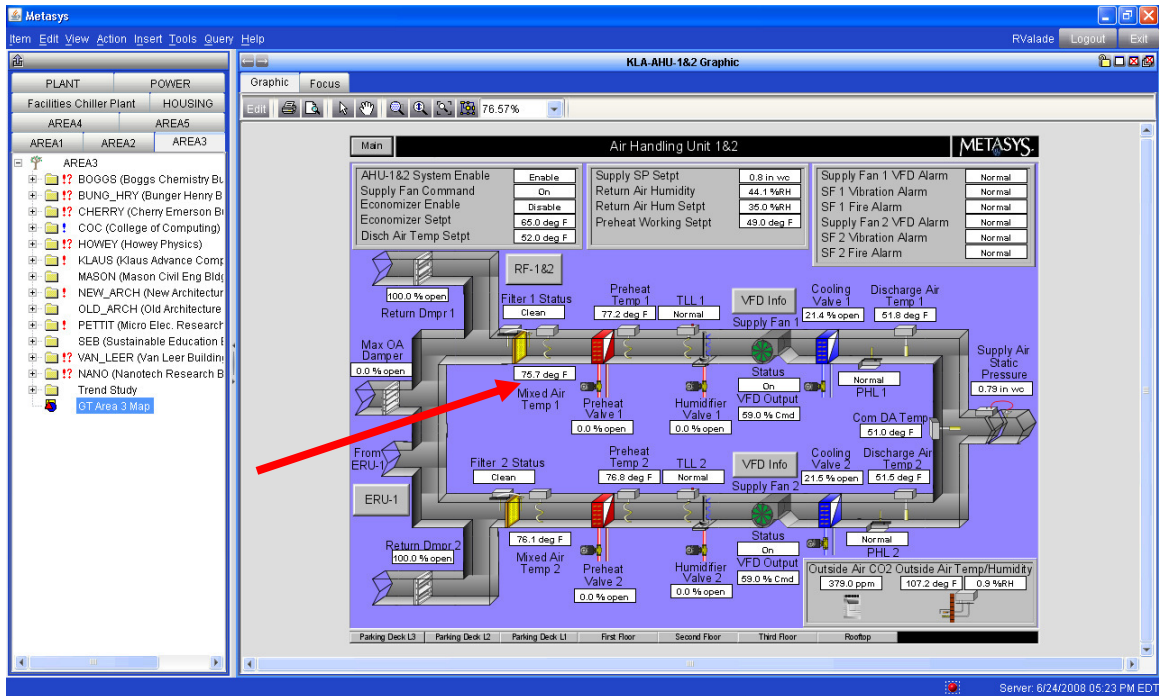
After choosing the building, options as to what part of the building to collect data from will appear:



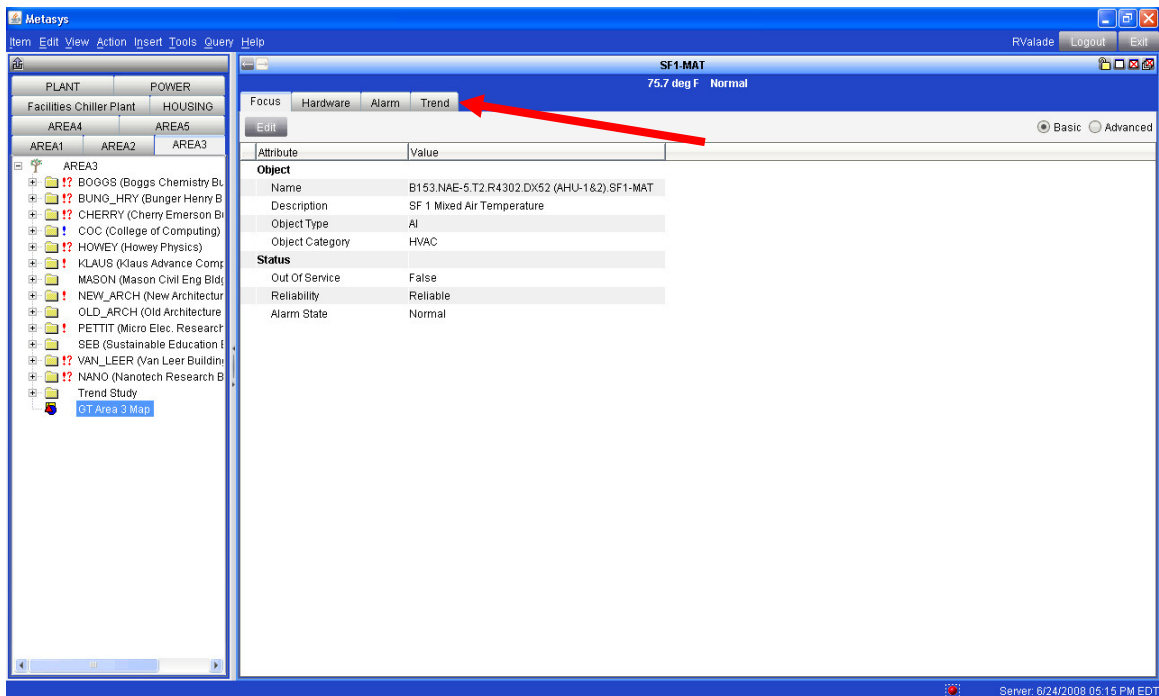
To better understand how data was collected, a step-by-step example for the Mixed Air Temperature 1 (MAT 1) of Air Handling Unit 1 (AHU 1) will be followed. Since AHU 1 is found in the penthouse on the roof of KACB, first choose “Rooftop” as specified above. Once the “Rooftop” is selected, the following screen appears as illustrated below.



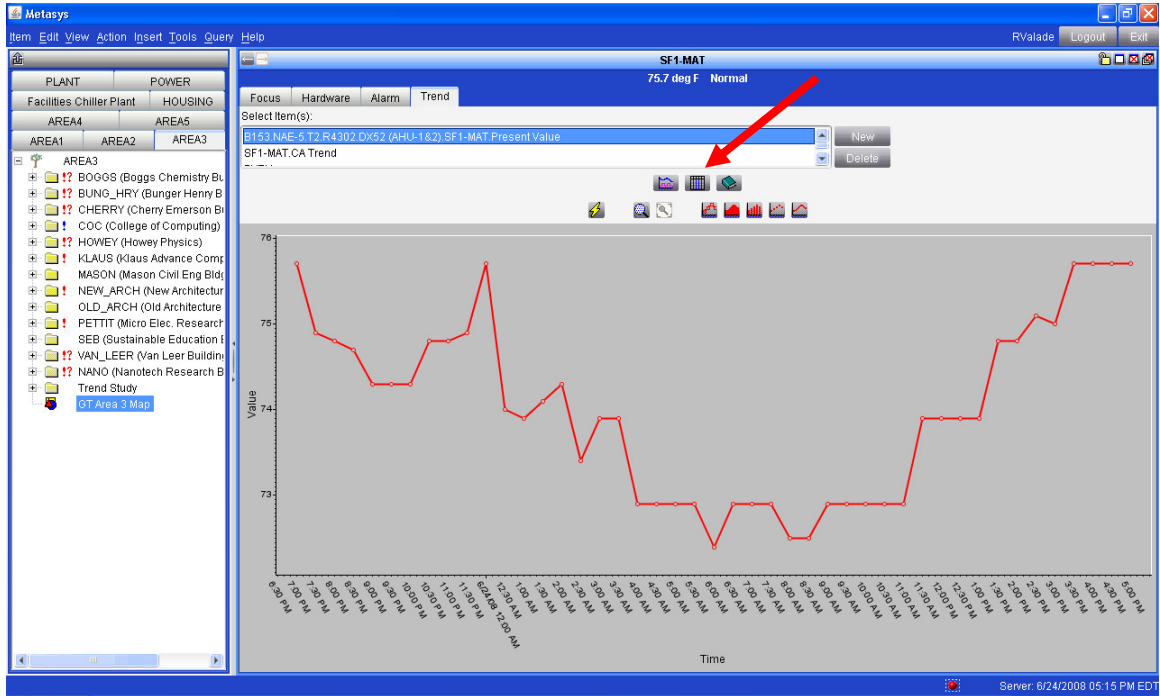
Since MAT 1 is found in AHU 1, the next step is to choose the button labeled “AHU-1 & 2 System” as pointed out above by the arrow. This then produces the next screen as shown below which illustrates what is happening within AHUs 1 & 2. Next, select the temperature button located directly above the “Mixed Air Temp 1” label.



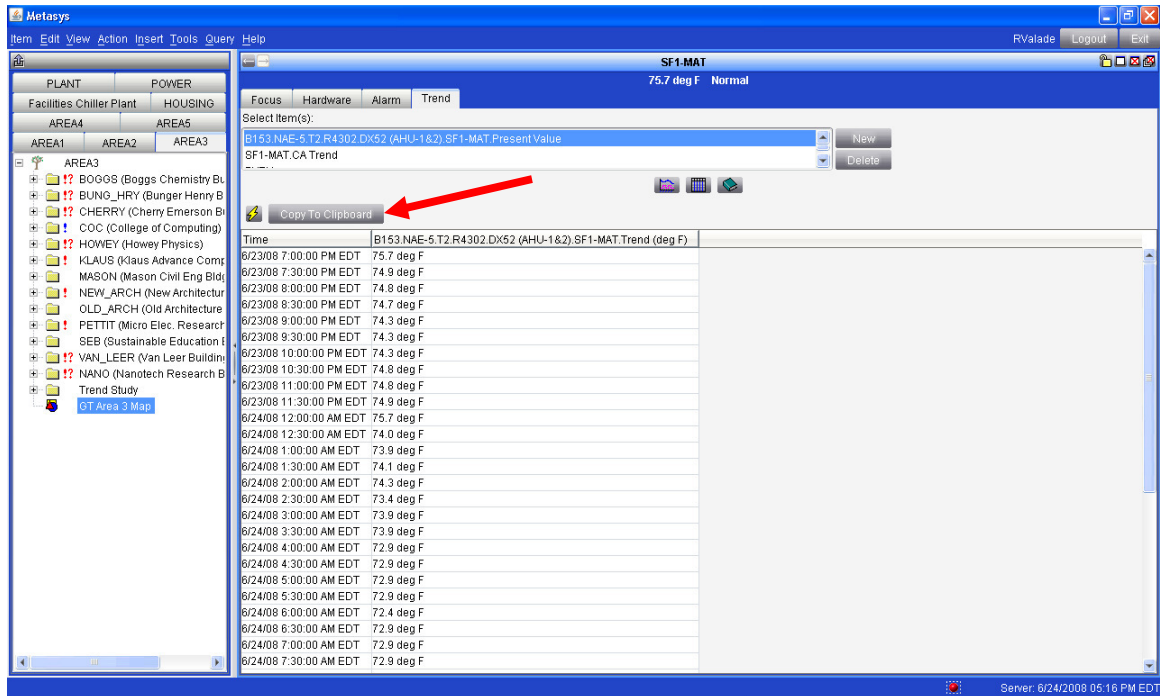
Once “Mixed Air Temp 1” has been selected, four option tabs appear. Choose the right most tab labeled “Trend” to be able to collect the most recently trended data.



A chart appears illustrating the mixed air temperatures which had occurred in the past 20ish hours.



Although the chart gives a clear overview of the trended data, there is also button which allows for a table view of the data. Choose this “Table View” button, as illustrated above, which then produces the table shown below.



The table allows users to view the actual numbers, in this case temperatures, for each data point as they were portrayed in the chart view. This includes the past 20ish hours of data as well as any erroneous data which has been further discussed in Section 4.1.2: Processing the Raw Data. Since, unfortunately, the collected data is only for the 20 hours or so prior to collection, this process must be completed at least once a day for all 41 data samples as to avoid gaps within the data.

The last step within Metasys to conclude collecting the MAT 1 data would be to select the “Copy To Clipboard” icon as illustrated above. Now that the data has been copied from the Metasys program, it can easily be pasted into any desired document like Microsoft Word, Microsoft Excel, Notepad or the like. In order to expedite future data processing and calculations, all of the data collected from Metasys has been place in Microsoft Excel.

APPENDIX M: Directions for NOAA Data Collection

First of all, in order to retrieve *free* weather data from NOAA, one needs to be connected to the internet from a .edu address or computer. Next, access the following website: <http://cdo.ncdc.noaa.gov/ulcd/ULCD>. Choose “Click here for data 01/2005 of after” as illustrated below.

The screenshot shows the NOAA NCDC website interface for selecting a state. At the top, it says "NCDC / Locate Station / Select State". On the left, there is a section titled "Unedited Local Climatological Data" with the text "Your Access is Free (.edu)". Below this, there is a list of links: "Documentation/Decode", "Pricing/Description", "NWS Wind Chill Chart", "Samples", "Daily Summary, ASCII", "Hourly Observations, ASCII", "Hourly Precipitation, ASCII", and "Important Notes". In the center, there is a map of the United States with the text "Select using map" below it. To the right of the map, there is a "Select State" section with the text "Where Desired Station is Located" and a dropdown menu showing "Alabama", "Alaska", "Arizona", "Arkansas", and "California". Below the dropdown menu is a "Continue" button. At the bottom, there is a link that says "Click here for data 01/2005 or after" with a red arrow pointing to it.

Next, choose the desired state in which the necessary weather data is located. In this case, scroll down and choose “Georgia” as shown below.

February 2008 Data Alert:

Data for February 2008 ASOS and AWOS stations were potentially erroneous if you accessed them prior to March 12, 2008. Data have now been corrected.

**Quality Controlled
Local
Climatological
Data**

**Your Access is Free
(lawn-128-61-28-58.lawn.gatech.edu)**

- [Updates/Differences](#)
- [Documentation/Decode](#)
- [Station Type Descriptions](#)
- [Frequently Asked Questions](#)
- [Pricing/Description](#)
- [LCD Serial Publication System](#)
- [NWS Wind Chill Chart](#)
- [US Climate Reference Network \(CRN\)](#)
- **Samples**
 - [Daily Summary, ASCII](#)
 - [Hourly Observations, ASCII](#)
 - [Hourly Remarks, ASCII](#)
 - [Hourly Precipitation, ASCII](#)
- [Important Notes](#)








• [Search by Map](#)

Delaware
District of Columbia
Florida
Georgia
Hawaii
Idaho
Illinois
Indiana
Iowa
Kansas

Continue

After choosing the desired state, there appears a list of stations within that state.

Even though there are five different stations located in Atlanta, GA, the only one of interest is the one at Hartsfield-Jackson Atlanta International Airport, labeled “***Atlanta: Hartsfield-Jackson Atlanta Intl AP (13874/ALT).” Choose that station as indicated below.

[NCDC](#) / [Locate Station](#) / [Select State](#) / [Select Station](#)

February 2008 Data Alert:
 Data for February 2008 ASOS and AWOS stations were potentially erroneous if you accessed them prior to March 12, 2008. Data have now been corrected.

**Quality Controlled
Local
Climatological
Data**

Your Access is Free
 (lawn-128-61-28-58.lawn.gatech.edu)

- [Updates/Differences](#)
- [Documentation/Decode](#)
- [Station Type Descriptions](#)
- [Frequently Asked Questions](#)
- [Pricing/Description](#)
- [LCD Serial Publication System](#)
- [NWS Wind Chill Chart](#)
- [US Climate Reference Network \(CRN\)](#)
- **Samples**
 - [Daily Summary, ASCII](#)
 - [Hourly Observations, ASCII](#)
 - [Hourly Remarks, ASCII](#)
 - [Hourly Precipitation, ASCII](#)
- [Important Notes](#)

State: GA

Select Desired Station

ALBANY : SW GEORGIA REGIONAL ARPT (13869/ABY)

*** ALMA : BACON COUNTY AIRPORT (13870/AMG)

*** ATHENS : ATHENS/BEN EPPS AIRPORT (13873/AHN)

*** ATLANTA : HARTSFIELD-JACKSON ATLANTA INTL AP (13874/ATL)

ATLANTA : PCHTRE CTY-FALCON FLD ARPT (53819/FFC)

ATLANTA : FULTON CO-BROWN FLD ARPT (03888/FTY)

ATLANTA : DEKALB-PEACHTREE AIRPORT (53863/PDK)

ATLANTA : COBB CO-MC COLLUM FLD ARPT (63813/RYY)

*** AUGUSTA : AUGUSTA REGIONAL AT BUSH FIELD AP (03820/AGS)

AUGUSTA : DANIEL FIELD AIRPORT (13837/DNL)

*** Contain final edited (VER3) data.
 ### HOURLY DATA available, summarized daily data will *NOT* be available.

CRN stations contain **hourly observations** of dry bulb temperature, wind speed (at 1.5 meters), and precipitation only.

Each data set can only be obtained on a monthly basis. Therefore, the next step is to select the desired year and month.

February 2008 Data Alert:

Data for February 2008 ASOS and AWOS stations were potentially erroneous if you accessed them prior to March 12, 2008. Data have now been corrected.

**Quality Controlled
Local
Climatological
Data**

Your Access is Free
(lawn-128-61-28-58.lawn.gatech.edu)

- [Updates/Differences](#)
- [Documentation/Decode](#)
- [Station Type Descriptions](#)
- [Frequently Asked Questions](#)
- [Pricing/Description](#)
- [LCD Serial Publication System](#)
- [NWS Wind Chill Chart](#)
- [US Climate Reference Network \(CRN\)](#)
- **Samples**
 - [Daily Summary, ASCII](#)
 - [Hourly Observations, ASCII](#)
 - [Hourly Remarks, ASCII](#)
 - [Hourly Precipitation, ASCII](#)
- [Important Notes](#)

**Data Months with Quality Control Version
Number represent QC'ed Data**

Select Desired YearMonth

2008 06 (13874/ATL) ATLANTA: HARTSFIELD-JACKSON ATLANTA INTL AP VER2
2008 05 (13874/ATL) ATLANTA: HARTSFIELD-JACKSON ATLANTA INTL AP VER2
2008 04 (13874/ATL) ATLANTA: HARTSFIELD-JACKSON ATLANTA INTL AP VER3
2008 03 (13874/ATL) ATLANTA: HARTSFIELD-JACKSON ATLANTA INTL AP VER3
2008 02 (13874/ATL) ATLANTA: HARTSFIELD-JACKSON ATLANTA INTL AP VER3
2008 01 (13874/ATL) ATLANTA: HARTSFIELD-JACKSON ATLANTA INTL AP VER3
2007 12 (13874/ATL) ATLANTA: HARTSFIELD-JACKSON ATLANTA INTL AP VER3
2007 11 (13874/ATL) ATLANTA: HARTSFIELD-JACKSON ATLANTA INTL AP VER3
2007 10 (13874/ATL) ATLANTA: HARTSFIELD-JACKSON ATLANTA INTL AP VER3
2007 09 (13874/ATL) ATLANTA: HARTSFIELD-JACKSON ATLANTA INTL AP VER3

Detailed Station Description

Product date range for this station is

19960701 to 20080625

Data gaps may exist

Continue

Each day can be viewed individually, but to be able to view hourly observations for the entire month, select “E” followed by “LCD Hourly Obs (10A)” as shown below.

[NCDC](#) / [Locate Station](#) / [Select State](#) / [HARTSFIELD-JACKSON ATLANTA INT](#) / [Select Year/Month](#)

February 2008 Data Alert

Data for February 2008 ASOS and AWOS stations were potentially erroneous if you accessed them prior to March 12, 2008. Data have now been corrected.

**Quality Controlled
Local
Climatological
Data**

Your Access is Free
(lawn-128-61-28-58.lawn.gatech.edu)

- [Updates/Differences](#)
- [Documentation/Decode](#)
- [Station Type Descriptions](#)
- [Frequently Asked Questions](#)
- [Pricing/Description](#)
- [LCD Serial Publication System](#)
- [NWS Wind Chill Chart](#)
- [US Climate Reference Network \(CRN\)](#)
- **Samples**
 - [Daily Summary, ASCII](#)
 - [Hourly Observations, ASCII](#)
 - [Hourly Remarks, ASCII](#)
 - [Hourly Precipitation, ASCII](#)
- [Important Notes](#)

13874/ATL
ATLANTA:
HARTSFIELD-JACKSON ATLANTA INT
05 / 2008

Select Day or Entire Month (E)

E

- 01
- 02
- 03
- 04
- 05
- 06
- 07
- 08
- 09
- 10
- 11

←

LCD Daily Summary (10B)

LCD Hourly Obs (10A)

LCD Hourly Remarks

LCD Hourly Precip

ASCII Download (Daily Summ.) (10B)

ASCII Download (Hourly Obs.) (10A)

ASCII Download (Hourly Rmks.)

ASCII Download (Hourly Precip.)

The hourly observations for the selected month (and day) will now open in a new window as demonstrated below.

**QUALITY CONTROLLED LOCAL
CLIMATOLOGICAL DATA
(may be updated)
HOURLY OBSERVATIONS TABLE
HARTSFIELD-JACKSON ATLANTA INTL AP
(13874)
ATLANTA, GA
(05/2008)**

Elevation: 998 ft. above sea level
Latitude: 33.640
Longitude: -84.427
Data Version: VER2

Date	Time (LST)	Station Type	Sky Conditions	Visibility (SM)	Weather Type	Dry Bulb Temp		Wet Bulb Temp		Dew Point Temp		Rel Humd %	Wind Speed (MPH)	Wind Dir	Wind Gusts (MPH)	Station Pressure (in. hg)	Press Tend	Net 3-hr Chg (mb)	Sea Level Pressure (in. hg)	Report Type	Precip. Total (in)	Alti-meter (in. hg)
						(F)	(C)	(F)	(C)	(F)	(C)											
1	2	3	4	5	6	7	8	9	10	11	12	13	14	15	16	17	18	19	20	21	22	23
01	0052	11	FEW250	10.00		57	13.9	51	10.4	45	7.2	64	5	180		28.98	8	001	30.06	AA		30.08
01	0152	11	FEW250	10.00		57	13.9	50	10.2	44	6.7	62	7	190		28.96			30.05	AA		30.06
01	0252	11	SCT250	10.00		56	13.3	49	9.6	43	6.1	62	0	000		28.96			30.04	AA		30.06
01	0352	11	SCT250	10.00		56	13.3	50	9.9	44	6.7	64	3	180		28.97	5	003	30.05	AA		30.07
01	0452	11	BKN250	10.00		56	13.3	49	9.6	43	6.1	62	3	150		28.98			30.07	AA		30.08
01	0552	11	SCT250	10.00		55	12.8	49	9.4	43	6.1	64	0	000		29.00			30.09	AA		30.10
01	0652	11	SCT250	10.00		57	13.9	50	9.9	43	6.1	60	5	160		29.02	3	019	30.11	AA		30.12
01	0752	11	SCT250	10.00		62	16.7	52	11.2	43	6.1	50	10	180		29.04			30.12	AA		30.14
01	0852	11	FEW250	10.00		65	18.3	55	12.6	46	7.8	50	9	180		29.04			30.12	AA		30.14
01	0952	11	FEW200 SCT250 BKN300	10.00		69	20.6	56	13.3	45	7.2	42	11	180		29.04	1	005	30.12	AA		30.14

Select all/desired data. Once selected, the last step with the website would be to copy it before pasting it into the desired document. As with the Metasys data, in order to expedite future data processing and calculations, all of the data collected from NOAA has been place in Microsoft Excel.

The data collected, as described above, is actually from the National Climatic Data Center (NCDC), a subsidiary of NOAA.

REFERENCES

- Ahmed, O., J. W. Mitchell, and S. A. Klein, 1997, "Development of a Simulator for Laboratory HVAC Systems," University of Wisconsin – Madison, Madison, WI.
- Argiriou, A., S. Lykoudis, S. Kontoyiannidis, C. A. Balaras, D. Asimakopoulos, M. Petrakis, and P. Kassomenos, 1999, "Comparison of Methodologies for TMY Generation Using 20 Years Data for Athens, Greece," *Solar Energy*, Volume 66, pp. 33-45.
- ASHRAE, 1977, 1993, 1997 & 2001, *ASHRAE Handbook, 1977, (1993, 1997, 2001) Fundamentals Volume*, The American Society of Heating, Refrigeration and Air Conditioning Engineers, Atlanta, GA.
- ASHRAE, 1996 & 2000a, *ASHRAE Handbook, 1996 (2000) HVAC Systems and Equipment Volume*, The American Society of Heating, Refrigeration and Air Conditioning Engineers, Atlanta, GA.
- ASHRAE, 1999 & 2003, *ASHRAE Handbook, 1999 (2003) HVAC Applications Volume*, The American Society of Heating, Refrigeration and Air Conditioning Engineers, Atlanta, GA.
- ASHRAE, 2000b, *90.1 User's Manual, ASHRAE/IESNA Standard 90.1-1999: Energy Standard for Buildings Except Low-Rise Residential*, The American Society of Heating, Refrigeration and Air Conditioning Engineers, Atlanta, GA.
- ASHRAE, 2002, *ANSI/ASHRAE Standard 62-2001: Ventilation for Acceptable Indoor Air Quality*, The American Society of Heating, Refrigeration and Air Conditioning Engineers, Atlanta, GA.
- ASHRAE, 2002, *ASHRAE Handbook, 2002 Refrigeration Volume*, The American Society of Heating, Refrigeration and Air Conditioning Engineers, Atlanta, GA.
- ASHRAE, 2007, *ASHRAE Standard, 2007 Energy Standard for Buildings Except Low-Rise Residential Buildings, Standard 90.1-2007, I-P Edition*, The American Society of Heating, Refrigeration and Air Conditioning Engineers, Atlanta, GA.
- ASTM Standard D 6245, 2007, "Standard Guide for Using Indoor Carbon Dioxide Concentrations to Evaluate Indoor Air Quality of Ventilation," ASTM International, West Conshohocken, PA.

- Balaras, C. A., 1988, "An Investigation of the Relationship Between Beam and Global Irradiation with the Development of Numerical Solar Radiation Models," *PhD Dissertation*, The George W. Woodruff School of Mechanical Engineering, Georgia Institute of Technology, Atlanta, GA.
- Balaras, C. A., 1996, "The Role of Thermal Mass on the Cooling Load of Buildings. An Overview of Computational Methods," *Energy and Buildings*, Volume 24, pp. 1-10.
- Balaras, C. A., E. Dascalaki, and A. Gaglia, 2007a, "HVAC and Indoor Thermal Conditions in Hospital Operating Rooms," *Energy and Buildings*, Volume 39, pp. 454-470.
- Balaras, C. A., A. G. Gaglia, E. Georgopoulou, S. Mirasgedis, Y. Sarafidis, and D. P. Lalas, 2007b, "European Residential Buildings and Empirical Assessment of the Hellenic Building Stock, Energy Consumption, Emissions and Potential Energy Savings," *Building and Environment*, Volume 42, pp. 1298-1314.
- Barringer, C. G. and C. A. McGugan, 1988, "Investigation of Enthalpy Residential Air-to-Air Heat Exchangers," Final Report for ASHRAE Research Project, Atlanta, GA.
- Barringer, C. G. and C. A. McGugan, 1989a, "Development of a Dynamic Model for Simulating Indoor Air Temperature and Humidity," *ASHRAE Transactions*, Volume 95, pp. 449-460.
- Barringer, C. G. and C. A. McGugan, 1989b, "Effect of Residential Air-to-Air Heat and Moisture Exchangers on Indoor Humidity," *ASHRAE Transactions*, Volume 95, pp. 461-474.
- Carriere, M., G. J. Schoenau, and R. W. Besant, 1999, "Investigation of Some Large Building Energy Conservation Opportunities Using the DOE-2 Model," *Energy Conversion and Management*, Volume 40, pp. 861-872.
- Cengel, Y. A. and M. A. Boles, 2002, *Thermodynamics: An Engineering Approach*, 4th Edition, McGraw-Hill, New York, NY.
- ChemicalLogic Corporation, 1998a, MoistAirTab Software, Burlington, MA.
- ChemicalLogic Corporation, 1998b, SteamTab Software, Burlington, MA.
- College of Computing Press Release, 2006, "Naming the Future" handout, Georgia Institute of Technology, Atlanta, GA.

- Crawley, D. B., 2001, "EnergyPlus: The Future of Building Energy Simulation: U.S. DOE replaces DOE-2 and BLAST," *HPAC Engineering*, November 2001, pp. 65-67.
- Dixon, S. L., 1998, *Fluid Mechanics: Thermodynamics of Turbomachinery*, 4th Edition, Butterworth-Heinemann Ltd., Woburn, MA.
- EnerLogic, J.J. Hirsch, and Associates, 2006, www.doe2.com, Camarillo, CA.
- Gaglia, A. G., C. A. Balaras, S. Mirasgedis, E. Georgopoulou, Y. Sarafidis, and D. P. Lalas, 2007, "Emperical Assessment of the Hellenic Non-Residential Building Stock, Energy Consumption, Emissions and Potential Energy Savings," *Energy Conversion and Management*, Volume 48, pp. 1160-1175.
- Google, 2008, Google Earth 4.3 Software, <http://earth.google.com>, Last Accessed: November 17, 2008, Mountain View, CA.
- Goswami, D. Y., F. Kreith, and J. F. Kreider, 2000, *Principles of Solar Engineering*, 2nd Edition, Taylor and Francis, Philadelphia, PA.
- Gugliermetti, F., G. Passerini, and F. Bisegna, 2004, "Climate Models for the Assessment of Office Buildings Energy Performance," *Building and Environment*, Volume 39, pp. 39-50.
- Hansen, S. M, 2004, *Mastering Excel 2003 Programming with VBA*, SYBEC Inc., Alameda, CA.
- Hatamipour, M. S., H. Mahiyar, and M. Taheri, 2007, "Evaluation of Existing Cooing Systems for Reducing Cooling Power Consumption," *Energy and Buildings*, Volume 39, pp. 105-112.
- Hirsch, J. J., S. D. Gates, S. A. Criswell, M. S. Addison, F. C. Winkelmann, W. F. Buhl, and K. L. Ellington, 1998, "DOE-2.2 and PowerDOE[®]: The New Generation in DOE-2 Building Energy Analysis," <http://www.doe2.com>, Camarillo, CA.
- Hirsch, J. J., and Associates, 2006a, *Building Energy Use and Cost Analysis Program*, DOE-2.2 Software, Camarillo, CA.
- Hirsch, J. J., and Associates, 2006b, *Building Energy Use and Cost Analysis Program*, eQUEST Software, Camarillo, CA.
- Howell, R. H., H. J. Sauer, Jr., and W. J Coad, 2005, *Principles of Heating, Ventilating and Air Conditioning*, The American Society of Heating, Refrigeration and Air Conditioning Engineers, Atlanta, GA.

- Hui, S. C. M. and K. P. Cheung, 1998. Application of Building Energy Simulation to Air-Conditioning Design, *Proc. of the Mainland-Hong Kong HVAC Seminar '98*, 23-25 March 1998, pp. 12-20, (in both English and Chinese) Beijing, China.
- Incropera, F. P., D. P. DeWitt, T. L. Bergman, and A. S. Lavine, 2007, *Fundamentals of Heat and Mass Transfer*, 6th Edition, John A. Wiley & Sons, Inc., Hoboken, NJ.
- Irving, A. D., 1988, "Validation of Dynamic Thermal Models," *Energy and Buildings*, Volume 10, pp. 213-220.
- Jensen, S. O., 1995, "Validation of Building Energy Simulation Programs: A Methodology," *Energy and Buildings*, Volume 22, pp. 133-144.
- Jeter, S. M. and C. A. Balaras, 1986, "A Regression Model for the Beam Transmittance of the Atmosphere Based on Data for Shenandoah, Georgia, U.S.A.," *Solar Energy*, Volume 37, pp. 7-14.
- Jeter, S. M. and C. A. Balaras, 1990, "Development of Improved Solar Radiation Models for Predicting Beam Transmittance," *Solar Energy*, Volume 44, pp. 149-156.
- Johnson Controls, Inc., 2007, "Operations and Maintenance Manuals," Project: J-11, Roswell, GA.
- Judkoff, R. D., 1988, "Validation of Building Energy Analysis Simulation Programs at the Solar Energy Research Institute," *Energy and Buildings*, Volume 10, pp. 221-239.
- Katipamula, S. and D. E. Claridge, 1993, "Use of Simplified System Models to Measure Retrofit Energy Savings," *Journal of Solar Energy Engineering*, Volume 115, pp. 57-68.
- Kreider, J. F., P.S. Curtiss, and A. Rabl, 2002, *Heating and Cooling of Buildings: Design for Efficiency*, 2nd Edition, McGraw-Hill, New York, NY.
- Larsen, S. F., C. Filippin, A. Beascochea, and G. Lesino, 2008, "An Experience on Integrating Monitoring and Simulation Tools in the Design of Energy-Saving Buildings," *Energy and Buildings*, Volume 40, pp. 987-997.
- Leadership in Energy and Environmental Design (LEED), 2003, *LEED Reference Guide: For New Construction and Major Renovations, Version 2.1*, 2nd Edition, U.S. Green Building Council, Washington, D.C.
- Lee, S. U., F. L. Painter, and D. E. Claridge, 2007, "Whole-Building Commercial HVAC System Simulation for Use in Energy Consumption Fault Detection," *ASHRAE Transactions*, Volume 113, Part 2.

- Loutzenhiser, P. G., and G. M. Maxwell, 2006, "A Comparison of DOE-2.1E Daylighting and HVAC System Interactions to Actual Building Performance," *ASHRAE Transactions*, Volume 112, pp. 409-417.
- Lu, L., W. Cai, Y. S. Chai, and L. Xie, 2005a, "Global Optimization for Overall HVAC Systems – Part I Problem Formulation and Analysis," *Energy Conversion and Management*, Volume 46, pp. 999-1014.
- Lu, L., W. Cai, Y. S. Chai, and L. Xie, 2005b, "Global Optimization for Overall HVAC Systems – Part II Problem Solution and Simulations," *Energy Conversion and Management*, Volume 46, pp. 1015-1028.
- Magnus, M., 2008, "Map Sources / GeoHack," <http://stable.toolserver.org/geohack/>, Cambridge, England.
- Meldem, R. and F. Winkelmann, 1998, "Comparison of DOE-2 with Temperature Measurements in the Pala Test Houses," *Energy and Buildings*, Volume 27, pp. 69-81.
- Neto, A. H., and F. A. S. Fiorelli, 2008, "Comparison Between Detailed Model Simulation and Artificial Neural Network for Forecasting Building Energy Consumption," *Energy and Buildings*, Volume 40, pp. 2169-2176.
- Norford, L. K., R. H. Socolow, E. S. Hsieh, and G. V. Spadaro, 1994, "Two-to-One Discrepancy Between Measured and Predicted Performance of a 'Low-Energy' Office Building: Insights from a Reconciliation Based on the DOE-2 Model," *Energy and Buildings*, Volume 21, 121-131.
- NREL, 2008, "National Renewable Energy Laboratory: Renewable Resource Data Center," <http://www.nrel.gov/rredc/>, Golden, CO.
- O'Sullivan, D. T. J., M. M. Keane, D. Kelliher, and R. J. Hitchcock, 2004, "Improving Building Operation by Tracking Performance Metrics Throughout the Building Lifecycle (BLC)," *Energy and Buildings*, Volume 36, pp. 1075-1090.
- Pan, Y., Z. Huang, and G. Wu, 2007, "Calibrated Building Energy Simulation and its Application in a High-Rise Commercial Building in Shanghai," *Energy and Buildings*, Volume 39, 651-657.
- Pasqualetto, L., R. Zmeureanu, and P. Fazio, 1998, "A Case Study of Validation of an Energy Analysis Program: MICRO-DOE2.1E," *Building and Environment*, Volume 33, pp. 21-41.
- Poel, B., G. van Cruchten, and C. A. Balaras, 2007, "Energy Performance Assessment of Existing Dwellings," *Energy and Buildings*, Volume 39, pp. 393-403.

- Poulos, Jim, Building Performance Engineers, INC., “LEED™ Energy and Atmosphere Credit 1: Optimize Energy Performance Narrative,” Atlanta, GA, June 3, 2003.
- Reddy, T. A., J. K. Lukes, and L. K. Norford, 2004, “Benefits of Multi-Building Electrical Load Aggregation: Actual and Simulation Case Studies,” *ASHRAE Transactions*, Volume 110, pp. 130-144.
- Salsbury, T. and R. Diamond, 2000, “Performance Validation and Energy Analysis of HVAC Systems Using Simulation,” *Energy and Buildings*, Volume 32, pp. 5-17.
- Stewart, M. E., “Validation of a Simplified Building Cooling Load Model Using a Complex Computer Simulation Model,” *Master’s Thesis*, Virginia Polytechnic Institute and State University, Blacksburg, VA, April 26, 2001.
- Sullivan, R., 1998, “Validation Studies of the DOE-2 Building Energy Simulation Program,” *Final Report*, Building Technologies Department, Lawrence Berkeley National Laboratory, Berkeley, CA.
- Taco, Inc., 2005, “Installation, Operation and Maintenance Instructions,” Form No. 302-013, Cranston, RI.
- Tester, J. W., E. M. Drake, M. J. Driscoll, M. W. Golay, and W. A. Peters, 2005, *Sustainable Energy: Choosing Among Options*, The Massachusetts Institute of Technology Press, Cambridge, MA, pp 777-795.
- Trane, Georgia, 2004, Literature #'s CAH-SVZ01A-EN, UNT-SVZ07A-EN, and VAV-SVX04A-EN, Atlanta, GA.
- Tronchin, L. and K. Fabbri, 2008, “Energy Performance Building Evaluation in Mediterranean Countries: Comparison Between Software Simulations and Operating Rating Simulation,” *Energy and Buildings*, Volume 40, pp. 1176-1187.
- Waltz, J. P., 1992, “Practical Experience in Achieving High Levels of Accuracy in Energy Simulations of Existing Buildings,” *ASHRAE Transactions*, Volume 98, pp. 606-617.
- Wang, S. and X. Xu, 2006a, “Parameter Estimation of Internal Thermal Mass of Building Dynamic Models Using Genetic Algorithm,” *Energy Conversion and Management*, Volume 47, pp. 1927-1941.
- Wang, S. and X. Xu, 2006b, “Simplified Building Model for Transient Thermal Performance Estimation Using GA-Based Parameter Identification,” *Intentional Journal of Thermal Sciences*, Volume 45, pp. 419-432.

- White, J. A., 1996, "Simplified Method for Predicting Building Energy Consumption Using Average Monthly Temperatures," *Proceedings of the International Conference on Energy Conversion*, August 1996, Washington, D.C.
- Xu, X. and S. Wang, 2008, "A Simplified Dynamic Model for Existing Buildings Using CTF and Thermal Network Models," *International Journal of Thermal Sciences*, Volume 47, pp. 1249-1262.
- Yao, R., N. Baker, and M. McEvoy, 2002, "A Simplified Thermal Resistance Network Model for Building Thermal Simulation," The Martin Centre for Architectural and Urban Studies, Department of Architecture, University of Cambridge, UK.
- Zeltser, A. A., 2007, "Energy Efficiency for Commercial Buildings: A Commitment by a Commercial Building Initiative," *Journal of Engineering and Public Policy*, Volume 11, Washington, D.C.
- Zhai, Z. J. and Q. Y. Chen, 2005, "Performance of Coupled Building Energy and CFD Simulation," *Energy and Buildings*, Volume 37, pp. 333-344.